Systematics and biogeography of the sawfly genus *Pristiphora* Latreille (Hymenoptera: Tenthredinidae) in North America

Spencer K. Monckton

A DISSERTATION SUBMITTED TO THE FACULTY OF GRADUATE STUDIES IN PARTIAL FULFILLMENT OF THE REQUIREMENTS FOR THE DEGREE OF DOCTOR OF PHILOSOPHY

GRADUATE PROGRAM IN BIOLOGY

YORK UNIVERSITY

TORONTO, ONTARIO

AUGUST 2022

Abstract

Sawflies in the subfamily Nematinae (Hymenoptera: Tenthredinidae) are cold-adapted insects that reach their greatest species richness in temperate, boreal, and arctic/subarctic regions of the Northern Hemisphere – a pattern that runs counter to that of most other organisms. The reasons for this pattern remain unclear, just as the full extent of the subfamily's diversity remains unknown. This dissertation addresses these gaps in knowledge in the genus *Pristiphora* Latreille: first, by revising the Nearctic representatives of three species groups: the *Pristiphora litura* group, *P. ruficornis* group, and *P. rufipes* group (23 species out of 57 total known from the Nearctic); second, by inferring a molecular phylogeny for the genus using DNA sequence data from one mitochondrial and three nuclear loci – obtained from specimens from across the Holarctic region – which is subsequently used to reconstruct the genus' biogeographic history; and third, by investigating the recent phylogeographic history of the common and widespread Holarctic species *Pristiphora cincta* Newman. In this dissertation, thorough descriptions and diagnoses are provided for all Nearctic species, two species are newly described, four new synonymies are proposed, and two formerly Palaearctic species are newly reported for the Nearctic. The genus boundaries of *Pristiphora* are discussed in light of new morphological and molecular evidence. Biogeographic reconstructions suggest a relatively recent radiation within the most speciose groups of *Pristiphora*, corresponding to the establishment of cool-temperate, boreal, and arctic/subarctic biotas across the northern hemisphere, beginning in the later half of the Miocene (ca. 15 Ma). Ancestral range reconstructions also indicate numerous geodispersals between the Palaearctic and Nearctic over the last ca. 110 million years. Finally, phylogeographic results suggest that climatic cycles during the Pleistocene led to the diversification of lineages within *P. cincta*, populations of which may have survived glaciations

in numerous isolated refugia, including in remote parts of the High Arctic. Taken together, the results suggest a complex and rich biogeographic history for the genus throughout the northern hemisphere. Important progress is made towards understanding the evolutionary history, biogeography, and taxonomy of the genus *Pristiphora* – and thereby of sawflies and northern hemisphere biogeography more broadly.

Acknowledgments

The following people are due thanks for their help in making this work a reality, and the list is by no means exhaustive. Laurence Packer for his unerring kindness, support, and mentorship over the past decade, for being a fierce advocate of his trainees, and for all the opportunities he has opened up. Liam Graham for his continued support in the Packer Lab, and for keeping everything running smoothly. Tom Onuferko and Rafael Ferrari for their kindness, friendship, and collaborative spirit, and for many productive conversations – on topics of entomology or otherwise. Terry Wheeler for his infectious enthusiasm, and for igniting a passion for Northern biodiversity. Henri Goulet and David R. Smith for their love of sawflies, and encouragement in pursuing symphytology. Marko Prous, Andreas Taeger, and Stephan Blank for their guidance and generosity with their time, data, access to literature, and opportunities for collaboration. Marko Prous especially for his enthusiastic support and collaborative spirit in the study of nematine sawflies. Amro Zayed, Roberto Quinlan, Sandra Rehan, and Joel Shore for their guidance and feedback. Amro Zayed and Sandra Rehan additionally for the use of their lab facilities, and to their respective lab members for making molecular lab work possible, including Ida Conflitti, Mateus Pepinelli, Jesse Huisken, Michael Mikát, Katherine Odanaka, and Evan Kelemen. Bridget Stutchbury, Dharti Patel, Cristalina Del Biondo, and Henrietta Erabhahiemen, for help navigating rules, regulations, paperwork, and countless other stressful administrative matters. CUPE 3903 executive members, staff, and other representatives for fiercely advocating on behalf of York's graduate students, and for keeping the interests of their membership top of mind. For assistance with molecular work: Karen Ho, Bhooma Thiruz, and Sergio Pereira at the Centre for Advanced Genomics in Toronto; David Carter at the London Regional Genomics Centre; Mrinal Pal at New England Biolabs; Tomasz Suchan for guidance with the hyRAD

protocol; Robin Bagley, Brock Harpur, and Miles Zhang for help troubleshooting high-throughput sequencing results. For assistance with fieldwork: Syd Cannings for his help with logistics and planning, and for collecting Yukon sawflies; Bruce Bennett for the same; Syd and Bruce both for arranging successful and memorable Yukon BioBlitz events; Kate Perez at the Centre for Biodiversity Genomics for arranging the use of Malaise traps; Carrie Mierau of Yukon Parks, Cavan Harpur of Parks Canada, and Brooke Bays of Ontario Parks for arranging permits; Kirsten Scott and Adam Thom of the Tr'ondëk Hwëch'in First Nation for permitting fieldwork in their traditional territories, and for sharing useful GPS data; LeeAnn Fishback of the Churchill Northern Studies Centre; Brooke Michell at Kawartha Highlands Provincial Park; and Phil Careless at QEII Wildlands Provincial Park. For providing access to their collections and arranging loans: Dave Langor, Daryl Williams and especially Greg Pohl at the Northern Forestry Centre for providing generous assistance and unfettered access to H. R. Wong's sawfly material; Henri Goulet, Andy Bennett, and John Huber at the Canadian National Collection of Insects; David R. Smith at the Smithsonian National Museum of Natural History; Allison Brown, Jayme Sones, and Jeremy deWaard at the Centre for Biodiversity Genomics; Stéphanie Boucher at the Lyman Museum, McGill (and Anna Solecki for providing field notes for the Northern Biodiversity Program); Joel Gibson and Rob Cannings at the Royal B.C. Museum; Steve Paiero at the University of Guelph Insect Collection; Peter Oboyski and Casey Hubble at the Essig Museum; Bob Zuparko at the Essig Museum and California Academy of Sciences; Elijah Talamas at the Florida State Collection of Arthropods; Shawn Kelly at the insect collection of the University of Central Florida; and Tommy McElrath at the Illinois Natural History Survey. For assistance labelling and databasing specimens and performing lab work, the following people are thanked for contributing their time and skills: Shane Abernethy, Sara Atherley,

Apoorva Chopra, Kushal Gandhi, Taylor Kerekes, Shammi Pereira, and Aimal Rahmati. Finally, I thank my family and family-in-law, for their unconditional love and support – and above all, my partner Katie, to whom this dissertation is dedicated, but who can never be thanked enough for all she has done to sustain, encourage, and motivate me: you are my lighthouse.

Dedication

This dissertation is dedicated to Katie, whose companionship, devotion, emotional and financial support, and whose sacrifices may as well form the very pages upon which it is written. Fittingly, there is far more white space than text – and yet if pages were weeks, the length of this document would not even come close to the credit she is due. And as for the text itself: her love and encouragement, her capacity for empathy and kindness, and her patience and understanding are the reasons that there is anything to read at all.

Disclaimer

All names and nomenclatural acts in this document are hereby disclaimed for nomenclatural purposes and shall not be considered available upon dissemination of this thesis. This disclaimer is included in accordance with Article 8.3 of the International Code of Zoological Nomenclature and is pursuant to the author’s intent to publish these names and nomenclatural acts in a widely distributed and peer-reviewed scientific journal.

Table of Contents

List of Tables

List of Figures

Chapter 2

CHAPTER 1: Introduction

Sawflies are herbivorous insects belonging the paraphyletic grouping Symphyta, in the order Hymenoptera. The majority of Symphyta (collectively called sawflies and woodwasps) are primarily external leaf feeders belonging to the superfamily Tenthredinoidea (hereafter simply called sawflies). Globally, this superfamily is represented by more than 7450 species (Taeger et al. 2018), inhabiting all parts of the world except Antarctica and most isolated oceanic islands. In contrast to most living groups (Wallace 1878, Hillebrand 2004), sawflies are more diverse in northern regions, with species richness declining toward the tropics (Marlatt 1896, Kouki et al. 1994, Kouki 1999). This pattern is in part driven by the diverse subfamily Nematinae (Tenthredinidae), which includes about 1250 species, mostly distributed in northern temperate, boreal, and subarctic regions. Larval Nematinae feed on a variety of host plants found in northern forests and on the tundra, particularly in wet and mesic habitats (Nyman et al. 2006a). As herbivores, nematine sawflies represent an important part of northern food webs, serving as hosts to a hyperdiverse assemblage of parasitoid wasps (Timms et al. 2016) and as food for vertebrates and invertebrates alike. Sawflies are particularly important in the diets of wetland passerine birds, both for nestlings (McDermott 2017, Tanneberger et al. 2017) and adults (Hagar et al. 2007). However, herbivore communities are also particularly sensitive to climatic changes (Danks 1992, Brodo 2000, Dollery et al. 2006, Høye and Forchhammer 2008, Høye and Sikes 2013), which are more severe in the Arctic (ACIA 2004, Parmesan 2006, J. E. Walsh 2014, Richter-Menge et al. 2017, Collier et al. 2018, Myers-Smith et al. 2018, Moon et al. 2021).

Unfortunately, Nearctic sawflies are relatively poorly known. The last catalogue of North American species was published 40 years ago (D. R. Smith 1979) and systematics work since

then has focused either on restricted subsets of nearctic species (e.g. Smith 1994, 2006, 2008, Looney et al. 2016), or on predominantly palaearctic species (Lacourt 1999, Haris 2006, Nyman et al. 2006a, Prous et al. 2016, 2017). Moreover, in many cases, species boundaries – and even some generic boundaries – are not well-defined (Prous et al. 2014). Thus, systematic work in this group is badly needed, especially in the species-rich Nematinae, of which there are nearly 400 species in the Nearctic (Table 1; Goulet 1992, Taeger et al. 2018).

Table 1 Estimated numbers of species of *Pristiphora* and higher-level taxa in the world, the Palaearctic, and the Nearctic. Data from ECatSym (Taeger et al. 2018).

	World	Palaearctic	Nearctic
Tenthredinoidea	7457	4014	1113
Tenthredinidae	5721	3445	940
Nematinae	1251	788	393
Pristiphora	221	151	57

Their high northern diversity and sensitivity to climate change as herbivores make sawflies potentially excellent indicators of northern habitat change. Besides advances in their taxonomy, one important key to studying them for this purpose is an improved understanding of the processes underlying changes in their diversity, and in particular the forces that give rise to and maintain diversity in this group. Their 'inverse' diversity gradient has been documented in Europe (Gauld and Bolton 1988, Kouki et al. 1994) and North America (Haack and Mattson 1993), where the Nematinae notably dominate high-latitude sawfly diversity (Marlatt 1896, D. R. Smith 1979, Gauld and Bolton 1988, Stahlhut et al. 2013). One explanation that has been put forward to explain the pattern – but not tested – is that sawfly diversity is the result a high-latitude speciation machine (HLSM; hypothesized by Nyman et al. 2010 and discussed in more detail in Chapter 3) powered by past periods of oscillating climatic conditions. As ranges

contract and expand, populations diverge in isolation and mix upon secondary contact, generating new diversity with each cycle (Ross 1972, Esselstyn et al. 2009).

It is necessary to make simultaneous progress along these different lines of inquiry, as they are mutually informative and equally important to unlocking the potential of sawflies as a model system for northern biodiversity science. Using the genus *Pristiphora* Latreille as a focal taxon, the objectives of this dissertation were to do just that, by conducting a partial revision of Nearctic species, inferring an updated phylogeny for the entire genus, and conducting historical biogeographic analyses of the genus plus a phylogeographic analysis of the common and widespread species *Pristiphora cincta* Newman.

The first major chapter of this dissertation (Chapter 2) presents a revision of three species groups for the Nearctic: the *P. litura* group, the *P. ruficornis* group, and the *P. rufipes* group. The early-diverging *P. litura* group holds evidence about the generic boundaries for *Pristiphora*, which are important to solidify for the sake of taxonomic stability. The *P. ruficornis* group is the most speciose, and its species are mainly northern in distribution (boreo-montane and arctic-alpine). The *P. rufipes* group includes *P. cincta* and its close relatives; this is perhaps the most commonly encountered species of *Pristiphora* in the Nearctic (and the focal species for Chapter 4), such that clarified species boundaries in this group are desirable to aid in the identification of specimens. As part of the revision, details are presented about species distributions, host plant associations, and genetic data for each species, as well as an assessment of genus boundaries, including supporting morphological characters and potential changes to the taxonomy of the genus.

In Chapter 3, molecular data from four mitochondrial and nuclear loci are used to infer a phylogeny for the entire genus, including representatives from the Nearctic, West Palaearctic, and East Palaearctic (past analyses have sampled primarily West Palaearctic species). This

phylogeny is used to assess taxonomic boundaries of species groups and to test elements of the HLSM hypothesis, including an historical biogeographic analysis with a dated phylogeny, calibrated using new fossil data for the subfamily Nematinae.

In Chapter 4, genome-wide sequence data from the widespread species *P. cincta* are obtained from decades-old museum specimens and used to study the phylogeographic history of this species, particularly in the context of the Pleistocene glaciations. Patterns in genetic diversity and population genetic structure are presented alongside model-based tests of population history scenarios. These results are used to assess elements of the HLSM hypothesis on smaller time scales (i.e. intraspecific), and to infer the use of glacial refugia and postglacial recolonization across North America.

By addressing some of the substantial taxonomic impediment in this group, and by shedding some initial light on the processes that give rise to sawfly diversity, this dissertation takes important steps forward in the study of North American sawflies.

References

ACIA (2004) ACIA Overview report Impacts of a Warming Arctic: Arctic Climate Impact Assessment. Cambridge University Press doi: 10.2277/0521617782

Brodo F (2000) The insects, mites and spiders of Hot Weather Creek, Ellesmere Island, Nunavut. In: Garneau M, Alt TB (Eds), Environmental Response to Climate Change in the Canadian High Arctic. Geological Survey of Canada Bulletin 529, 145–173.

Collier LS, Bjorkman AD, Frei ER, Onoda Y, Speed JDM, Thomas HJD, Ozinga WA, Eskelinen A, Hik DS, Campetella G, Sheremetev S, Lamarque LJ, Soudzilovskaia NA, Hülber K, Blok D, Myers-Smith IH, Tape KD, Berner L, Elmendorf SC, Ordoñez JC, Gould WA,

Alexander HD, Anadon-Rosell A, Jónsdóttir IS, Little CJ, Angers-Blondin S, Schamp B, Chapin FS, Hermanutz L, Jørgensen RH, Hofgaard A, Iversen CM, Tremblay M, Weiher E, Hollister RD, Rüger N, Grogan P, Jaroszynska F, Vellend M, Díaz S, Treier UA, Petraglia A, Enquist BJ, Beest M te, Kuleza S, Blach-Overgaard A, Tweedie C, Dullinger S, Nielsen SS, Cerabolini BEL, Blonder B, Kulonen A, Shetti R, Suding KN, Harper KA, Goetz SJ, Kaarlejärvi E, Dainese M, Rixen C, Vowles T, Zamin T, Street LE, Buras A, Lantz T, Molau U, Weijers S, Björk RG, Jorgenson J, Wookey PA, de Vries FT, Bond-Lamberty B, Cooper EJ, Elberling B, Bahn M, Craine J, Magnusson B, Beck PSA, Ninot JM, Karger DN, Niinemets Ü, Schaepman-Strub G, Michelsen A, Onipchenko VG, Reich PB, Green W, Wipf S, Cornwell WK, Guay KC, Sandel B, Johnstone JF, Manning P, Semenchuk P, Rumpf SB, Tremblay J-P, van Bodegom PM, Penuelas J, HilleRisLambers J, Nabe-Nielsen J, Henry GHR, Olofsson J, Poschlod P, Kattge J, Oberbauer SF, Alatalo JM, Buchwal A, Klein J, Boulanger-Lapointe N, Poorter H, Milla R, Hudson J, Grau O, Milbau A, Lévesque E, Christie K, Georges D, Hallinger M, Trant A, Prevéy JS, Carbognani M, Heijmans MMPD, Wilmking M, Normand S, Tomaselli M, Iturrate-Garcia M, Venn S, Klady R, Forbes BC, Spasojevic MJ, Cornelissen JHC (2018) Plant functional trait change across a warming tundra biome. Nature 562: 57–62. doi: 10.1038/s41586-018-0563-7

Danks H V (1992) Arctic insects as indicators of environmental change. Arctic 45: 159–166.

Dollery R, Hodkinson ID, Jónsdóttir IS, Spencer J (2006) Impact of Warming and Timing of Snow Melt on Soil Microarthropod Assemblages Associated with *Dryas*-Dominated Plant Communities on Svalbard. Ecography 29: 111–119.

Esselstyn JA, Timm RM, Brown RM (2009) Do geological or climatic processes drive speciation in dynamic archipelagos? The tempo and mode of diversification in southeast asian shrews.

Evolution 63: 2595–2610. doi: 10.1111/j.1558-5646.2009.00743.x

Gauld ID, Bolton B (1988) The Hymenoptera. Oxford University Press, Oxford, 332 pp.

Goulet H (1992) The Insects and Arachnids of Canada, Part 20 The Genera and Subgenera of Sawflies of Canada and Alaska: Hymenoptera: Symphyta. 1–235 pp. Available from: http://esc-sec.ca/aafcmonographs/insects_and_arachnids_part_20.pdf.

Haack RA, Mattson WJ (1993) Life History Patterns of North American Tree-Feeding Sawflies. In: Wagner MR, Raffa KF (Eds), Sawfly Life History Adaptations to Woody Plants. Academic Press, 503–545.

Hagar JC, Dugger KM, Starkey EE (2007) Arthropod prey of Wilson's Warblers in the understory of Douglas-fir forests. The Wilson Journal of Ornithology 119: 533–546. doi: 10.1676/06-056.1

Haris A (2006) Study on the Palaearctic *Pristiphora* species (Hymenoptera: Tenthredinidae). Natura Somogyiensis 9: 201–277. Available from: http://www.smmi.hu/termtud/ns/ns9/haris2 kicsi.pdf.

Hillebrand H (2004) On the Generality of the Latitudinal Diversity Gradient. The American Naturalist 163: 192–211. doi: 10.1086/381004

Høye TT, Forchhammer MC (2008) Phenology of High-Arctic Arthropods: Effects of Climate on Spatial, Seasonal, and Inter-Annual Variation. Advances in Ecological Research 40: 299–324. doi: 10.1016/S0065-2504(07)00013-X

Høye TT, Sikes DS (2013) Arctic entomology in the 21st century. The Canadian Entomologist 145: 125–130. doi: 10.4039/tce.2013.14

Kouki J (1999) Latitudinal Gradients in Species Richness in Northern Areas: Some Exceptional Patterns. Ecological Bulletins: 30–37. Available from: http://www.jstor.org/stable/20113224.

Kouki J, Niemela P, Viitasaari M (1994) Reversed latitudinal gradient in species richness of sawflies (Hymenoptera, Symphyta). Ann. Zool. Fennici 31: 83–88.

Lacourt J (1999) Répertoire des Tenthredinidae ouest-paléarctiques (Hymenoptera: Symphyta). Mémoires de la Société Entomologique de France 3: 1–432.

Looney C, Smith DR, Collman SJ, Langor DW, Peterson MA (2016) Sawflies (Hymenoptera, Symphyta) newly recorded from Washington State. Journal of Hymenoptera Research 159: 129–159. doi: 10.3897/JHR.49.7104

Marlatt CL (1896) Revision of the Nematinae of North America. Bulletin of the United States Department of Agriculture, Division of Entomology, Technical Series 3: 1–135. Available from: http://www.biodiversitylibrary.org/item/106469.

McDermott MT (2017) Arthropod Communities and Passerine Diet: Effects of Shrub Expansion in Western Alaska. University of Alaska Fairbanks doi: 10.13140/RG.2.2.20107.80161

Moon TA, Druckenmiller ML, Thoman RL eds. (2021) Arctic Report Card 2021. doi: 10.25923/5S0F-5163

Myers-Smith IH, Thomas HJD, Bjorkman AD (2018) Plant traits inform predictions of tundra responses to global change. New Phytologist: 1742–1748. doi: 10.1111/nph.15592

Nyman T, Farrell BD, Zinovjev AG, Vikberg V (2006) Larval habits, host-plant associations, and speciation in nematine sawflies (Hymenoptera: Tenthredinidae). Evolution 60: 1622–

1637. doi: 10.1111/j.0014-3820.2006.tb00507.x

Nyman T, Vikberg V, Smith DR, Boevé J-L (2010) How common is ecological speciation in plant-feeding insects? A “Higher” Nematinae perspective. BMC evolutionary biology 10: 266.

Parmesan C (2006) Ecological and Evolutionary Responses to Recent Climate Change. Annual of Ecology, Evolution and Systematics 37: 637–669. doi: 10.2307/annurev.ecolsys.37.091305.30000024

Prous M, Blank SM, Goulet H, Heibo E, Liston A, Malm T, Nyman T, Schmidt S, Smith DR, Vårdal H, Viitasaari M, Vikberg V, Taeger A (2014) The genera of Nematinae (Hymenoptera, Tenthredinidae). Journal of Hymenoptera Research 40: 1–69. doi: 10.3897/JHR.40.7442

Prous M, Kramp K, Vikberg V, Liston A (2017) North-Western Palaearctic species of *Pristiphora* (Hymenoptera, Tenthredinidae). Journal of Hymenoptera Research 59: 1–190. doi: 10.3897/jhr.59.12656

Prous M, Vikberg V, Liston A, Kramp K (2016) North-Western Palaearctic species of the *Pristiphora ruficornis* group (Hymenoptera, Tenthredinidae). Journal of Hymenoptera Research 51: 1–54. doi: 10.3897/jhr.51.9162

Richter-Menge J, Overland JE, Mathis JT, Osborne E eds. (2017) Arctic Report Card 2017. Available from: http://www.arctic.noaa.gov/Report-Card.

Ross HH (1972) The Origin of Species Diversity in Ecological Communities. Taxon 21: 253–259.

Smith DR (1979) Symphyta. In: Krombein K V., Hurd PDJ, Smith DR, Burks BD (Eds), Catalog of Hymenoptera in America North of Mexico. Volume 1. Smithsonian Institution Press, Washington D.C., 1–137.

Smith DR (1994) *Nepionema*, a nematine sawfly genus new to North America, and an unusual new species of *Nematus* (Hymenoptera: Tenthredinidae). Proceedings of The Entomological Society of Washington 96: 133–138.

Smith DR (2006) Review of the cypress and juniper sawflies of the genus *Susana* Rohwer and Middleton (Hymenoptera: Tenthredinidae). Proceedings of The Entomological Society of Washington 108: 62–75.

Smith DR (2008) The *abbotii* and *erythrogaster* groups of *Nematus* Panzer (Hymenoptera: Tenthredinidae) in North America. Proceedings of the Entomological Society of Washington 110: 647–667.

Stahlhut JK, Fernandez-Triana J, Adamowicz SJ, Buck M, Goulet H, Hebert PD, Huber JT, Merilo MT, Sheffield CS, Woodcock T, Smith MA (2013) DNA barcoding reveals diversity of hymenoptera and the dominance of parasitoids in a sub-arctic environment. BMC Ecology 13: 1–13. doi: 10.1186/1472-6785-13-2

Taeger A, Liston AD, Prous M, Groll EK, Gehroldt T, Blank SM (2018) ECatSym – Electronic World Catalog of Symphyta (Insecta, Hymenoptera). Available from: https://sdei.de/ecatsym/.

Tanneberger F, Flinks H, Arbeiter S, Minets M, Hegemann A (2017) Diet Analysis of Wetland Passerine Nestlings Using Neck Collars or Faecal Sampling Produces Similar Results. Ardea 105: 145–152. doi: 10.5253/arde.v105i2.a7

Timms LL, Schwarzfeld M, Sääksjärvi IE (2016) Extending understanding of latitudinal patterns in parasitoid wasp diversity Schonrogge K, Broad G (Eds). Insect Conservation and Diversity 9: 74–86. doi: 10.1111/icad.12144

Wallace AR (1878) Tropical Nature, and Other Essays. MacMillan and Co., London, 356 pp. doi: 10.1016/0003-6870(73)90259-7

Walsh JE (2014) Intensified warming of the Arctic: Causes and impacts on middle latitudes. Global and Planetary Change 117: 52–63. doi: 10.1016/j.gloplacha.2014.03.003

CHAPTER 2: Revision of the Nearctic species of the *Pristiphora litura*, *ruficornis*, and *rufipes* species groups, with comments on the taxonomy of the genus *Pristiphora* Latreille (Hymenoptera: Tenthredinidae)

Introduction

At present, the genus *Pristiphora* Latreille, as defined by Prous et al. (2014), includes 221 species worldwide (Taeger et al. 2018), of which 55 are known from the Nearctic, 151 from the Palaearctic, 23 from the Oriental Region, and 9 from the Neotropics. In the Nearctic, there are clear indications of undescribed species in need of taxonomic attention, particularly from remote regions of Northern North America (as is the case for many arctic arthropods; Høye and Sikes 2013)

The taxonomic literature on Nearctic *Pristiphora* is somewhat scattered, and there has not been a revision of the group for the region either in part or in whole in over 125 years, since the work of Marlatt (1896). Numerous species have since been described (Kincaid 1900, MacGillivray 1908, Rohwer 1908, 1911, Ross 1945, Wong and Ross 1960, Wong 1968a, 1968b, 1969, Smith 1994, Smith and Dolan 2016), and the definition of the genus was recently expanded to include species of the former, almost-exclusively-Nearctic genera *Neopareophora* MacGillivray (2 spp.), *Nepionema* Benson (2 spp.), *Melastola* Wong (3 spp.), and *Pristola* Ross (2 spp.) (Prous et al. 2014). As a result, identification of Nearctic *Pristiphora* species presently requires comparison to types, previously identified material, and/or descriptions from a variety of publications having

varying levels of detail (virtually none are sufficiently detailed nor adequately illustrated to permit identification on their own).

Besides its individual species, the genus itself is difficult to recognize, in part due to the synonymies mentioned above. Because the expanded definition of *Pristiphora* was based upon molecular data (Prous et al. 2014) and not accompanied by a thorough examination of morphological evidence from the Nearctic genera that were subsumed, there is good reason to re-consider the boundaries of the genus carefully. Therefore, a review of the Nearctic *Pristiphora* inclusive of those former genera is desirable to provide evidence for or against the definition of the genus as it currently stands.

The Canadian symphytologist Horne R. Wong worked for some time towards a worldwide revision of the genus, eventually leading to his revision of the Neotropical species (Wong 1976; later extended by Smith 2003) and recognition of the *Pristiphora abietina* group (Wong 1975) as a first step towards a subgeneric classification, which has since been built upon by Prous et al. (2017). The bulk of his remaining work, however, was unfinished and unpublished, and has sat more-or-less untouched in the collection of the Northern Forestry Centre in Edmonton, AB (H. Goulet and G. Pohl, pers. comm.). A cursory evaluation of Wong's material revealed the existence of new and undescribed species for the Nearctic, including manuscript names (epithets) and draft descriptions for putative species.

The objectives of this chapter are to make use of Wong's material, along with the detailed works of Prous et al. (2014, 2016, 2017, 2018, 2019) on the North-Western Palaearctic species, to revise a portion of the Nearctic *Pristiphora* – naming and describing those species that are new to science, and providing detailed re-descriptions of species present in our region, with fully differential diagnoses intended to clarify species boundaries and illustrated keys to enable the

identification of nearly half of the species in this diverse genus. There is also a need to bring Nearctic species into the species-group framework proposed for Palaearctic fauna (Prous et al. 2017) to work towards a more stable subgeneric classification. To that end, this chapter presents a revision of the *P. litura*, *P. ruficornis*, and *P. rufipes* species groups, each chosen to maximize impact per unit effort: the *P. litura* species group includes the former genera *Neopareophora* and *Nepionema*, providing an opportunity to carefully evaluate the morphological evidence for the revised genus boundaries; the *P. ruficornis* group is the largest, and particularly well-represented in the North; the *P. rufipes* group, as here expanded, includes perhaps the most common and widespread species in the Nearctic, *P. cincta* Newman, with which its less-common relatives are easily confused, such that there is a need to clarify species boundaries in this group. Together, these three groups represent 21 of the 55 species already known from the Nearctic, plus two newly described species for a total of 23. Included in this chapter are the first descriptions of males for the four species of the *litura* group, *P. aphanta* Wong & Ross, *P. nigra* Marlatt, *P. paloma* Wong & Ross, and of the female of *P. maura* Rohwer, as well as new synonymies for *P. bivittata* (Norton) (= *P. venatta* **n. syn.**), *P. cincta* (= *P. banksi*, **n. syn.**), and *P. sycophanta* Walsh (= *P. hyalina* **n. syn.**, *P. valvangula* **n. syn.**). A discussion of morphological characters as they relate to the definition of the genus is also included.

Methods

Studied material

An initial loan of 924 specimens from the Northern Forestry Centre, Edmonton, AB (NFRC) served as a reference collection, consisting of specimens studied and identified by H.R. Wong while working on his unfinished revision of *Pristiphora*. This loan also included 445 prepared slides, primarily of male genitalia and female ovipositors. Specimens from this loan were

databased, associated with slides where possible, and their identifications were checked against published descriptions and Wong's unpublished drawings of penis valves and lancets.

Additional specimens were collected during field trips to Yukon (2016, 2018), Churchill, MB (2016), and Ontario (2019), and borrowed from the following natural history collections: Biodiversity Institute of Ontario, University of Guelph, Guelph, ON (BIOUG); California Academy of Sciences, San Francisco, CA (CASC); UC Davis, Davis, CA (DAV); University of Guelph Insect Collection, Guelph, ON (DEBU); Essig Museum of Entomology, UC Berkeley, Berkeley, CA (EMEC); Florida State Collection of Arthropods, Gainesville, FL (FSCA); Lyman Entomological Museum, McGill University, Ste. Anne-de-Bellevue, QC (LEMU); Illinois Natural History Survey, Champaign, IL (INHS);Royal British Columbia Museum, Victoria, B.C. (RBCM); University of Central Florida, Orlando, FL (UCFC); U.S. National Museum of Natural History, Smithsonian Institution, Washington, DC (USNM). Newly collected specimens are deposited in the Packer Collection at York University, Toronto, ON (PCYU). Efforts were made to examine at least images of the type specimens of each species treated here (including synonymous types where available), however, due to protracted closures precipitated by the global COVID-19 pandemic, type specimens held at ANSP and USNM could not be examined. Type images available in ECatSym (Taeger et al. 2018) of thirteen types are from specimens stored at: Collection of Thierry Noblecourt, Quillan, France (CTN); Hungarian Natural History Museum, Budapest, Hungary (HNHM); Finnish Museum of Natural History, Helsinki, Finland (MZH); Swedish Museum of Natural History, Stockholm, Sweden (NHRS); Senckenberg German Entomological Institute, Müncheberg, Germany (SDEI); Russian Academy of Sciences, Zoological Institute, St. Petersburg, Russia (ZIN); Zoologische Staatssammlung, Munich, Germany (ZSM).

Wong's material was georeferenced using a combination of OpenStreetMap.org, Google Maps, the Canadian Geographical Names Database, and the Biological Survey of Canada's Canadian Locality Database. Georeferenced coordinates are indicated in italics. Specimens from parts of the Northwest Territories that are now Nunavut are recorded here as having been collected in Nunavut. Where appropriate, place names from Canada's North have been updated to reflect the name preferred by the local community, with the name from the label placed in square brackets.

Integrative taxonomy

Recently collected specimens were selected for DNA barcoding, for which one leg (usually a midleg) was removed and placed into a single well of a 96-well plate with 95% EtOH. Wells were alternatingly filled with legs from sawflies and bees to reduce the risk of undetected cross-contamination (none was observed). Extractions, PCR amplification, and sequencing of cytochrome *c* oxidase subunit I (COI) were performed at the Canadian Centre for DNA Barcoding (CCDB) in Guelph, ON. Barcodes were uploaded to the Barcode of Life Data System (Ratnasingham and Hebert 2007), clustered into molecular operational taxonomic units, and given Barcode Index Numbers (BINs) for each OTU (Ratnasingham and Hebert 2013). Neighbour-joining trees were constructed from DNA barcodes of all barcoded specimens (both newly-barcoded and borrowed from BIOUG) to investigate barcode sequence similarity within and among species. This analysis was done on the BOLD workbench using the BOLD Aligner and Kimura 2-parameter distance model for tree construction. Resulting trees were scrutinized for any mismatch between specimen identification and BIN and/or location on the tree: BINs spanning multiple species were investigated for any morphological evidence of their synonymy, and species recovered in multiple BINs were investigated for any morphological evidence of multiple species. Identifications were always based upon morphological comparison with

authoritatively identified material, published images and descriptions, and, where possible, type specimens. This integrative taxonomic approach has been used extensively in melittology (e.g. Gibbs 2009, Spencer K. Monckton 2016, Onuferko 2018, Ferrari 2019) and in previous studies of Nematinae (Prous et al. 2016, 2017, 2021) as well as among other taxa (Ferri et al. 2009, Pires and Marinoni 2010, Sheth and Thaker 2017).

Recently-collected, well-preserved specimens were also sampled for fragments of three nuclear regions for the purposes of phylogenetic analysis: sodium/potassium-transporting ATPase subunit alpha (NaK), DNA dependent RNA polymerase II subunit RPB1 (POL2), and triose-phosphate isomerase gene (TPI). Full methods and results are described in Chapter 3. Due to the slow rate of evolution in the mitochondrial genomes of sawflies, they can be prone to introgression between closely-related species (Tang et al. 2019, Prous et al. 2020). As a result, COI barcodes provide accurate species-level identification only about half of the time for *Pristiphora*, with nuclear markers providing better discrimination in many cases (Prous et al. 2017). Therefore, the maximum likelihood tree resulting from multi-locus analysis of COI, NaK, POL2, and TPI (Figs. 1–3, Chapter 3) was used to calculate average pairwise tree distances among and between species using the Species Delimitation plugin (Masters et al. 2011) in Geneious Prime 2022.1.1.

Terminology and descriptions

Terminology used in descriptions follows Viitasaari (2002) and the Hymenoptera Anatomy Ontology (Yoder et al. 2010), with additional considerations as follows: (I) For the paired valvulae 3, the term ‘sawsheath’ is used here to conveniently refer to the entire paired structure, with finer details described in relation to valvula 3. (II) The term ‘scopa’ has been used in previous sawfly literature to refer to one or more of: (i) a pair of posterior projections situated

laterad on the sawsheath (i.e. on either valvula 3; Ross 1937, D. R. Smith 1988, 1992); (ii) the invagination or concavity resulting from such projections as seen in dorsal view (Prous et al. 2017); (iii) a roughly or clearly defined, somewhat flattened, setose area on the posterior (or posteroventral) surface of the valves of the sawsheath – most conspicuous in Diprionidae (i.e. "scopal pad"; Ross 1955, D. R. Smith 1988). Indeed, all three may occur together, as apparently illustrated by Ross (1937: Figs 308 & 311), wherein distinctly setose surfaces run along the posterior lateral projections of the sawsheath, which in turn define a medial concavity of the sawsheath. To address the ambiguity of the term, Prous et al. (2018) suggested retiring the use of the word scopa in reference to sawflies, instead making explicit and separate reference to a pair of 'latero-posterior projections' (i.e. sensu (i) above) or to 'setose fields' (i.e. sensu (iii) above) as needed. For the former, here the term 'lateral posterior lobes' is used, because this portion of valvula 3 is not always especially produced (e.g. as in the *carinata* group). Instead, the lateral posterior lobes are described here as either produced or not. In *Pristiphora*, the lateral posterior lobes are distinctly setose, but not in the sense of meaning (iii) above; therefore, these are here referred to as 'setose areas', rather than 'setose fields'. (III) In addition to terminology for macrosculpture and microsculpture designated by Viitasaari (2002), here the common habit is adopted of describing the appearance of surfaces as either shiny or dull. Shiny surfaces normally have smooth or weak microsculpture, such that light sources produce tidy reflections, while dull surfaces normally have imbricate microsculpture or are otherwise more strongly sculptured (i.e. with strong macrosculpture), producing scattered reflections (Figs .2–4). Some surfaces may be shiny despite the presence of macrosculpture, such as widely spaced punctures; therefore, the sheen, microsculpture, and macrosculpture are described separately. Punctation is quite regular in *Pristiphora*, however, and does not carry much taxonomic value, so it is referred to only very

sparingly. (IV) For the male genitalia, the terms “dorsal” and “ventral” are used to refer to the actual dorsal and ventral surfaces; Tenthredinoidea are strophandrous, such that these are in fact the primary (i.e. morphological) ventral and dorsal surfaces, respectively (Viitasaari 2002). Selected morphological terminology is illustrated in Fig. 1.

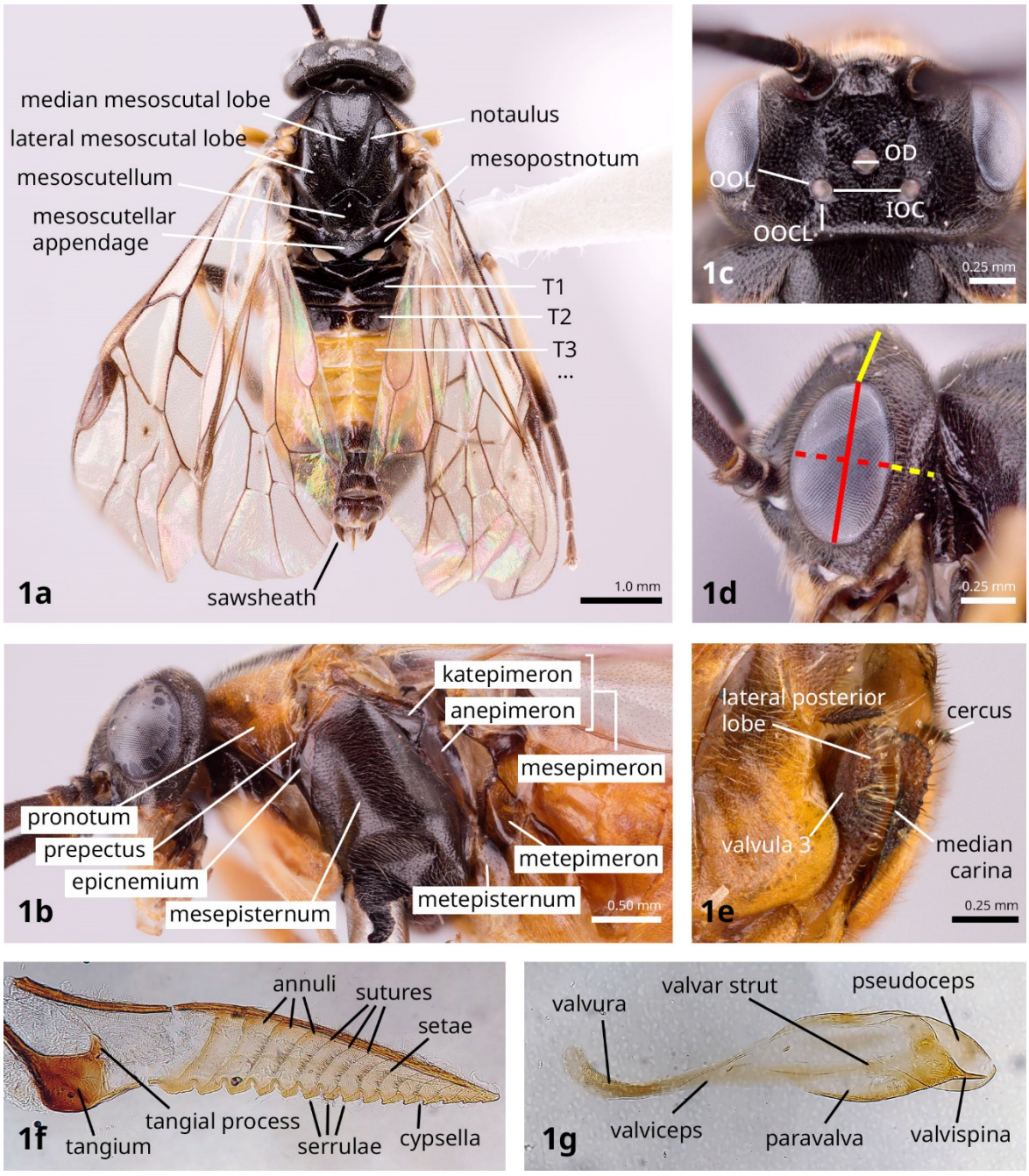

Figure 1. Selected morphological terms. **1a**. Body of female, dorsal view. **1b**. Thorax, lateral view. **1c**. Head, dorsal view, abbreviations as defined in text. **1d**. Head, lateral view; red lines indicate length (solid) and width (dotted) of eye, yellow lines indicate distance from dorsal margin of eye to back of head (solid) and width of gena (dotted). **1e**. Sawsheath, oblique posterior view. **1f**. Lancet of ovipositor, lateral view. **1g**. Penis valve, lateral view.

The following abbreviations are used: F = flagellomere; T = tergum ; S = sternum; OD = diameter of the median ocellus; LOD = lower interocular distance; IOC = interocellar distance; OOL = oculo-ocellar distance; OOCL = ocellar-occipital carina distance. The dimensions of the postocellar space are taken as IOC and OOCL for width and length, respectively.

Because specimen colour can vary, and because specimens may become discolored depending on age or preservation method, colour is described in relative terms as a range between pale and dark. For lack of more suitable terms, intermediate states are described as shades of yellow, orange, and brown (e.g. dark brown, yellow-brown).

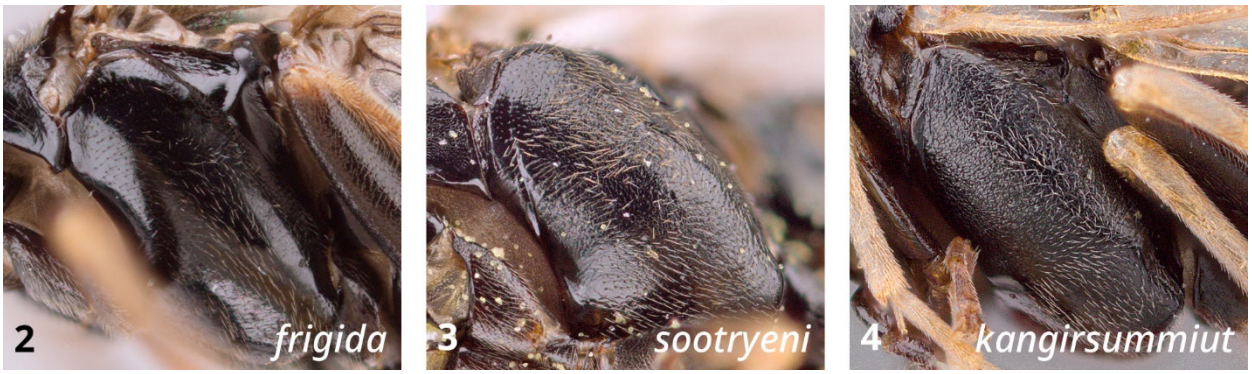

Figures 2–4. Examples of surface sculpture of mesepisternum. **2**. Shiny, microsculpture smooth (*P. frigida* Boheman). **3**. Dull, imbricate (*P. sootryeni* Lindqvist). **4**. Rough, coriaceous (*P. kangirsummiut* Monckton n. sp.).

Specimens were examined using a Nikon SMZ1000 stereomicroscope. Prepared slides and wet mounts of genitalia were viewed under a Leica CME compound microscope. Specimen images were taken primarily using a Google Pixel 6 Pro (Google LLC, Menlo Park, CA) mounted on a Nikon SMZ1000 stereomicroscope using a Celestron NexYZ 3-Axis Adapter (Celestron,

Torrance, CA). Where greater depth of field was required, images were taken using a Visionary Digital BK Plus Lab System with a Canon EOS 5D SR digital camera and Canon Macro MP-E 65mm lens, using the software P-51 Camlift Controller v2.9.4.0. Image slices were stacked using Helicon Focus v5.3.3. Surface sculpture was assessed with bright, diffuse light from a Fenix RC20 rechargeable LED flashlight (1000 lm, 21,100 cd; Fenix Lighting LLC, Littleton, CO); diffusion was achieved by wrapping the head of the flashlight in a lint-free task wipe and securing it with masking tape.

Results

Diagnosis of Pristiphora *found in the Nearctic*

Nearctic representatives of the genus *Pristiphora* can generally be recognized according to the definition set out by Prous et al. (2017) for those found in the North-Western Palaearctic region. That definition is slightly modified for the Nearctic as follows: in both sexes, mandibles asymmetrical (left mandible strongly constricted at mid-length, right mandible evenly tapered towards apex), clypeus usually truncate or only weakly emarginate, apex of forewing vein C swollen, width of cell C at vein Rs+M about half as wide as vein C or less (Fig. 5); forewing vein 2r-rs absent (except in species of the *P. litura* group); in females, valvula 3 with at least a raised setose area (usually with distinctly produced lateral posterior lobe), tangium of lancet with campaniform sensilla; in males, T8 lacking apical projection (except *P. aphanta* Wong & Ross, *P. chlorea* (Norton), and *P. litura* group), penis valve divided into pseudoceps and paravalva, with valvispina arising closer to ventral margin than dorsal margin of paravalva and usually at least very weakly bent dorsally. This combination of characters should differentiate most species of *Pristiphora* from the rest of the subfamily, and in particular from the genera *Nematus* and *Euura* (Prous et al. 2014), with which it is most likely to be confused. Members of the *macnabi*

group (formerly *Melastola*, *Pristola*) are most easily diagnosed separately: by the weakly outlined notauli, tarsal claw without subapical tooth, hindwing cell A either open at apex, or closed and at most as long as vein beyond its apex, and posterior margin of mesoscutellar appendage not raised above membrane between it and mesopostnotum.

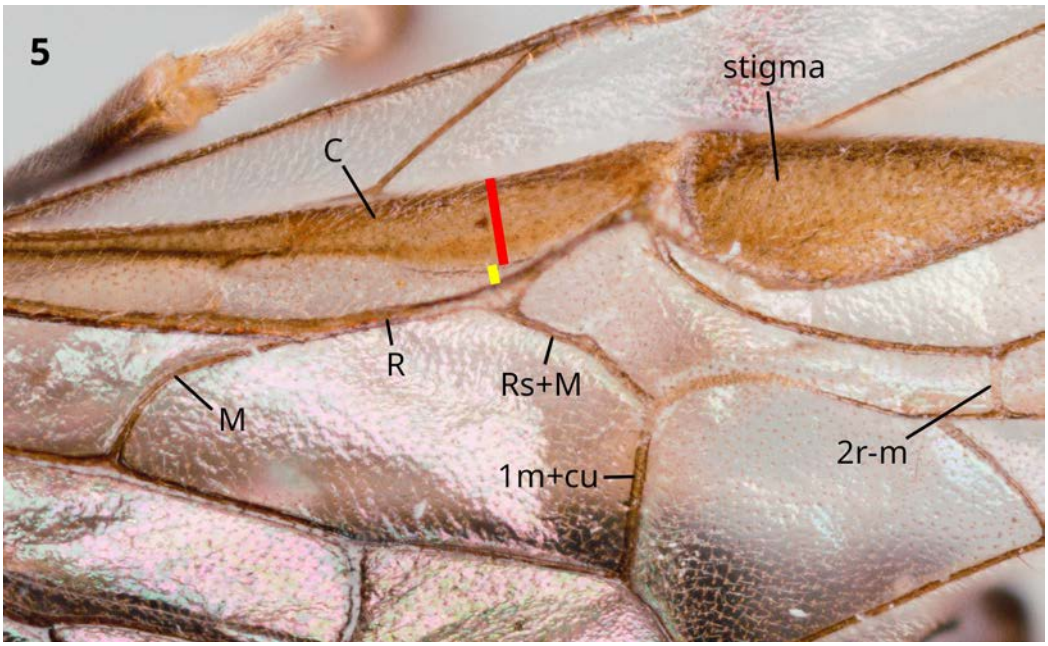

Figure 5. Expanded apex of vein C, a diagnostic character of *Pristiphora*. The width of cell C (yellow line) at the intersection of vein Rs+M is less than half as wide as vein C.

Taxonomy

***Pristiphora litura* group (formerly *Neopareophora*, *Nepionema*)**

This primarily Nearctic group includes the species of the former genera *Neopareophora* (*erythrothorax*, *flavipectus*, *litura*) and *Nepionema*, (*appalachiana*, *helvetica*). Although specimens of the Palaearctic species *P. helvetica* (Benson, 1960) were not examined, it is included in this group based on evidence from Benson's original description (1960), Smith's description of *P. appalachiana* (D. R. Smith 1994), photos published on ECatSym (Taeger et al. 2018), and phylogenetic results (see Chapter 3).

Diagnosis. Members of this group are easily distinguished by the presence of vein 2r-rs (absent in all other species of *Pristiphora*), tarsal claw simple, and absence of the prepectus (Fig. 6). In females, the lance (Figs. 51–54) and lancet (Figs. 55–58) are strongly sclerotized, narrow, and distinctly curved, and the setae of the lancet are spine-like, short and stout. Males have a distinct apical projection on the posterior margin of T8 (Figs. 45–48), similar to that of *Euura* spp., which is otherwise only present in *P. aphanta*, *P. chlorea*, and the Palaearctic *P. armata* group. Penis valves (Figs. 59–62) are also distinctive, with pseudoceps narrow, paravalva approximately rectangular, and valvispina long and slender. The host plants are known only for *P. litura*, which is recorded from *Vaccinium* L., particularly *V. angustifolium* Aiton (D. R. Smith 1979, D. R. Smith and Strazanac 2016). Genetic data strongly support monophyly of the *litura* group (see Chapter 3).

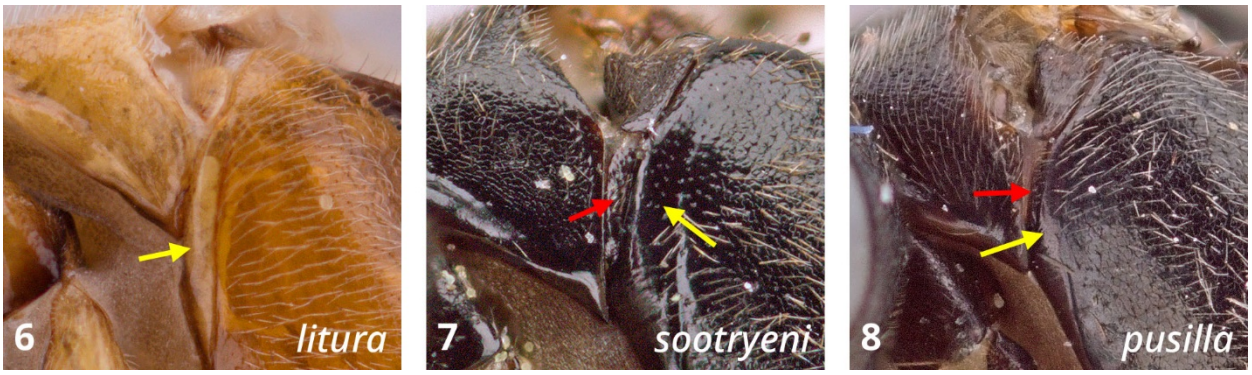

Figure 6–8. Anterior margin of mesepisternum and adjacent pronotum, showing prepectus (red arrows) and epicnemium (yellow arrows). **6**. Prepectus absent or indistinct (*P. litura* (Klug)). **7**. Prepectus present and distinct, similar in width to adjacent portion of epicnemium (*P. sootryeni*). **8**. Prepectus present and narrow, less than half width of adjacent portion of epicnemium (*P. pusilla* Malaise).

Key to species of the *P. litura* group

1. Vein 2r-m of forewing present; mesoscutellum with posterior depression distinct for its entire width (Fig. 41); mesoscutellar appendage with a median longitudinal groove present for its entire length, and a distinct posteromedial emargination (Fig. 41)..... 2

1'. Vein 2r-m of forewing almost always absent (but if present, then at least sternum of thorax entirely pale); mesoscutellum with posterior depression weak medially (Fig. 42–44); mesoscutellar appendage with median longitudinal groove absent or present only in posterior half, posterior margin notched medially or not (Figs. 42–44). 3

2. Female lancet with setae absent from annuli or reduced in number (Fig. 55); female femora mostly pale; male penis valve with valvispina long and slender, about twice as long as width of paravalva (Fig. 59). (Known only from the Eastern United States)..... P. appalachiana

2'. Female lancet with setae distinctly present for entire height of annuli (Fig. 3, Benson 1960); female femora mostly dark; male penis valve shorter, only about 1.2x as long as width of paravalva (Fig. 1, Benson 1960). (Known only from the European Alps; not revised here.)

..... *P. helvetica*

3. Female mesepisternum pale, always with posteroventral triangle of pectus pale; mesoscutellar appendage with median longtidunal groove in posterior half and posterior margin notched medially (Fig.43)..... *P. flavipectus*

3'. Female mesepisternum pale or dark, but always with posteroventral triangle of pectus dark; mesoscutellar appendage without median logitudinal groove, and posterior margin entire, or at most very weakly notched (Figs. 42, 44) 4

4 . Female thorax almost entirely orange-yellow, at most mesoscutellum slightly darkened (Figs. 17, 19); male trochanters and trochantelli dark; male penis valve with dorsal margin of pseudoceps distinctly concave at the level of base of paravalva (Fig. 60) .....

..... *P. erythrothorax*

4'. Female thorax with median lobe of mesonotum partly dark, mesoscutellum entirely dark (Figs. 33, 35); male trochanters and trochantelli pale; male penis valve with dorsal margin of pseudoceps linear or only weakly concave at the level of base of paravalva (Fig. 62) .....

.....*P. litura*

***Pristiphora appalachiana* (Smith, 1994)**

(Figs. 9–16, 41, 45, 51, 55, 59)

Nepionema appalachiana Smith, 1994: 134–135.

Diagnosis. Individuals of both sexes are easily distinguished from others in the group by: vein 2r-m of forewing absent (occasionally also absent in *P. flavipectus*); posterior meoscutellar depression present as distinct groove for entire width (weak medially in other species, Figs. 41-44); mesoscutellar appendage dull, coarsely imbricate and punctate (shiny and puncticulate in other species), with distinct median longitudinal groove present for entire length (present only in posterior half in *P. flavipectus*, absent in other species; Figs. 41-44), distinct posterior emargination medially (present also in *P. flavipectus*, other species with posterior margin entire or only weakly notched); protibia with two apical spurs (a single protibial spur in other species). These characters are shared with *P. helvetica* – known only from high altitudes in the European Alps – from which females of the present species differ by the reduced or absent setal bands on the lancet, present only in upper one-third to one-half of annuli (Fig. 55; present for full height on most annuli in *P. helvetica*), and mostly pale femora (mostly dark in *P. helvetica*); males may differ by the shape of the valvispina, which appears to be longer and slenderer in *P. appalachiana* (Fig. 59) than *P. helvetica* per Benson's illustrations of the latter species (Benson 1960).

Female. Length, 5.0–6.0 mm.

Colour: Antenna and head dark. Mouthparts dark to pale brownish apically, mandibles translucent brown. Thorax dark, epicnemium dark brown, posterior corner of pronotum narrowly pale, tegula pale. Legs pale except coxae extreme basolateral corner to basal third dark, femora

usually brownish basally and dorsally, hind tibia narrowly brownish apically, hind tarsus dark brown except basitarsus pale in basal half. Wings hyaline, veins dark, vein C and stigma brown, veins C and Sc pale near wing base. Abdomen dark, T9 pale medially, apicolateral spot brown or yellow-brown, T10 pale sometimes brownish centrally, valvifer 2 basal half to two-thirds pale.

Head: Antenna length 2.25–2.6x head width; F1 0.8–0.9x length of eye; F1 shorter than F2 (F1:F2 = 0.85–0.9x), subequal to or slightly shorter than F3 (F1:F3 = 0.9–1.0x), proceeding flagellomeres progressively shorter (F7:F1 = 0.8–0.85x). Clypeus truncate or shallowly emarginate. Malar space 0.8x OD. LOD 1.4–1.5x height of eye in frontal view. In dorsal view, length of eye 1.8–2.3x distance from dorsal margin of eye to back of head. IOC:OOL = 0.9–1.0x. IOC:OD = 2.75x. Postocellar area approximately twice as wide as long (IOC:OOCL = 1.8–2.0x). Head somewhat shiny, lower face and lower gena with microsculpture coarsely imbricate, frontal area smooth, vertexal area smooth to weakly imbricate.

Thorax: Pronotum dull, imbricate. Prepectus absent. Mesepisternum shiny, microsculpture smooth or very weakly imbricate. Mesepimeron shiny and smooth in anterior half, dull and costulate in posterior half. Mesonotum somewhat shiny, weakly imbricate, except mesoscutellum shiny and smooth; mesoscutellar appendage dull, coarsely imbricate and punctate, with distinct median longitudinal groove along its entire length, and posterior margin medially notched. Posterior mesoscutellar depression distinct for entire width, such that mesoscutellar appendage well delimited anteriorly. Parapsis shiny, microsculpture smooth to weakly costulate ventrally. Mesopostnotum rough, coarsely imbricate, except posteromedial corner shiny, smooth. Protibia with two apical spurs, anterior spur without velum, posterior spur about half as long as anterior spur. Metabasitarsus shorter than (0.77–0.8x) metatarsomeres 2–4 combined. Tarsal claw simple, without subapical tooth. Wing vein 2r-rs present, 2r-m absent.

Abdomen: Terga with microsculpture somewhat dull, imbricate, except marginal zones somewhat shiny, weakly imbricate. Sawsheath in dorsal view approximately triangular, drawn to a rounded apex medially, longest setae more than half as long as (0.6x) basal width of sawsheath, visible length of sawsheath about two-thirds as long as cerci. Sawsheath in lateral view approximately triangular, lower margin evenly rounded and meeting dorsal margin at a rounded, slightly acute angle. Valvula 3 not produced, but with oblique flattened setose area. In apical view, width of sawsheath 0.4x height of setose area. Lance tapering gradually for most of length, more strongly so for apical 9–10 annuli. Lancet with basal 2–3 sutures apically leaning with dorsal quarter basally recurved, proceeding sutures vertical to weakly recurved, apical 6–7 sutures dorsally apically curved; sclerora widened to a convex bump at approximate center of basal 4–5 annuli, not so widened on proceeding annuli.

Male. Length, 4.0–4.1 mm.

Darker than female, only legs partly pale: femora apical quarter to half, fore and mid tibia entirely, hind tibia except broad apical ring, and basitarsus ventrally pale. Structure and surface sculpture similar to female except: antenna with F1 shorter than F2 and F3 (F1:F2 = 0.85x; F1:F3 = 0.9x), proceeding flagellomeres progressively shorter (F7:F1 = 0.9–1.0x); anterior protibial spur with velum. T8 with distinct apical projection, weakly wedge-shaped and slightly wider apically, approximately 0.4x as long as total medial length. Penis valve with paravalva rounded-rectangular, valvispina long and slender, slightly dorsally curved at apex.

Material studied. **USA**: **GA**: Clarke Co., Athens-Whitehall, 6-13.iii.1979, R.H.Turnbow Jr., H.N.Greenbaum, insect flight trap, 1 ♀ (FSCA 00091528) 1 ♂ (FSCA 00091529) (FSCA); **NC**: Raleigh, 26.ii.1930, C.S.Brimley, 1 ♂ (USNM); **VA**: Fairfax Co., Dead Run, 23.iii.1916, R.C.Shannon, 1 ♂ (USNM); Prince William Co., Bull Run M. C., Jackson Hollow, campground,

far, 33.877° -77.689°, 8-23.iii.2016, D.R.Smith, O.S.Flint, Malaise trap, 1 ♀ (USNM); Prince William Co., Bull Run M. C., Jackson Hollow, campground, field, 38.879° -77.69°, 8-23.iii.2016, D.R.Smith, O.S.Flint, Malaise trap, 1 ♀ (USNM).

Distribution. This species occurs in the southern Great Appalachian Valley, and is recorded from West Virginia, Virginia, North Carolina, and Georgia.

Genetic data. Specimens of this species belong to a single BIN: BOLD:AED0663. Based on available genetic data (one specimen) the nearest neighbour (*P. helvetica*) is 8.6% different.

Hosts. Unknown.

Comments. All but one of the studied specimens were collected in March, and one was collected in late February, consistent with Smith's (1994) hypothesis that this early spring species likely oviposits into tough plant tissues such as twigs or buds, before leaves are available.

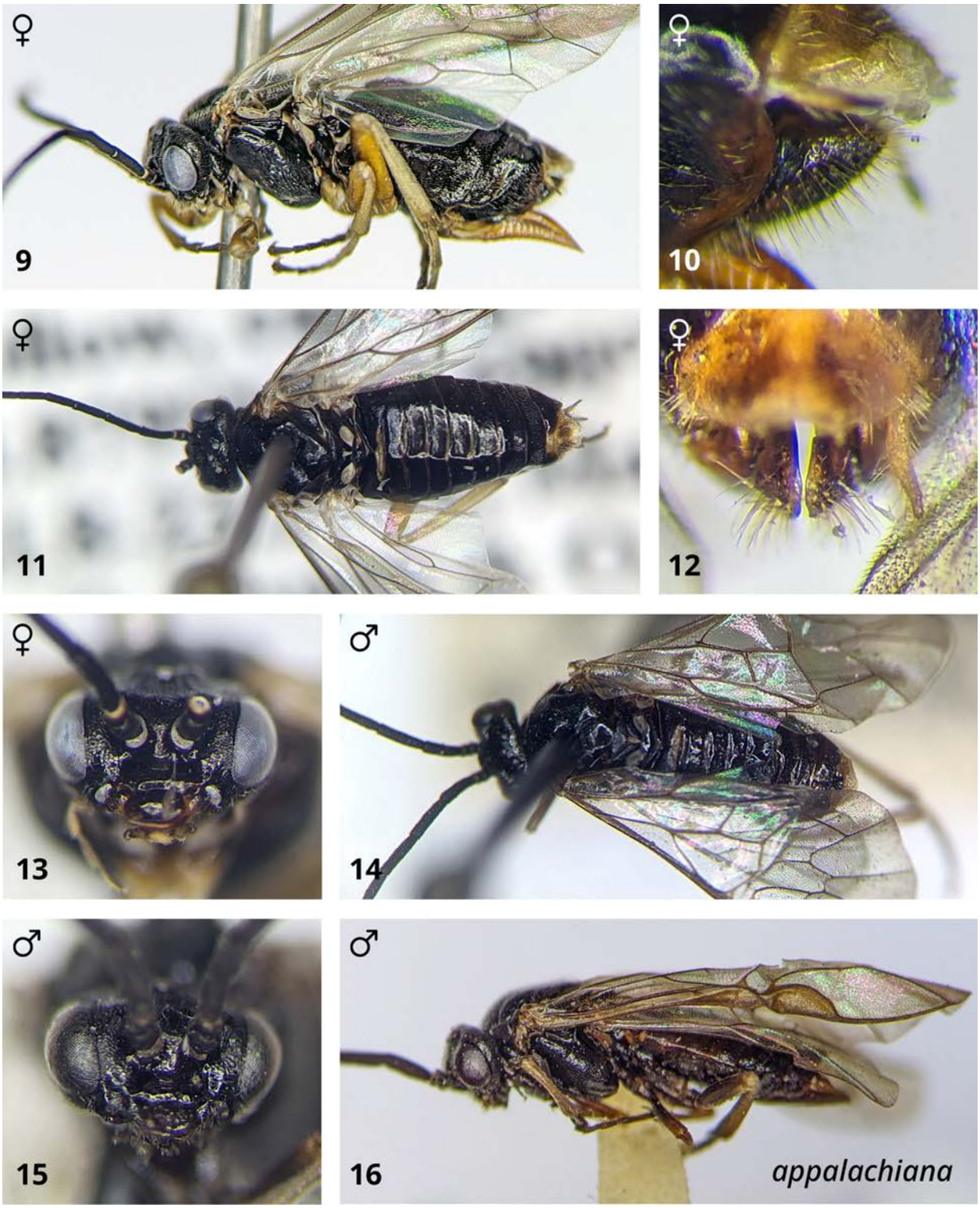

Figures 9–16. *Pristiphora appalachiana*. **9**. Female lateral view. **10**. Sawsheath lateral view. **11**. Female dorsal view. **12**. Sawsheath dorsal view. **13**. Female head. **14**. Male dorsal view. **15**. Male head. **16**. Male lateral view.

***Pristiphora erythrothorax* (Rohwer, 1911)**

(Figs. 17–24, 42, 46, 52, 56, 60)

Marlattia erythrothorax Rohwer, 1911: 385–386

Diagnosis. Females are easily distinguished from others in the *litura* group by the almost entirely orange-yellow thorax (Figs. 17, 19; median lobe of mesonotum at least partly and mesoscutellum entirely dark in other species) and dark abdomen (usually pale laterally and ventrally in other species, e.g. Figs. 33, 35). Males are less easily distinguished, but can be recognized by the darker leg colouration, with trochanters, trochantelli, and basal third to half of femora dark (usually pale in other species; darker specimens of *P. litura* may have femora with broad basal ring and most of ventral margin dark, but these can be distinguished by the pale trochanters and trochantelli). Penis valves differ only slightly: in this species, the dorsal margin of the pseudoceps is dinstinctly concave at the level of the base of the paravalva (in other species, the dorsal margin is approximately straight or only very weakly concave; Figs. 59–62).

Female. Length, 3.7–4.5 mm.

Colour: Antenna and head dark, mouthparts pale brownish, mandibles translucent brown with anterobasal corner and apex dark. Thorax mostly pale, following parts dark: posteromedial spot on mesoscutellum, mesoscutellar appendage, mesopostnotum medially, metascutellum except lateral corner, metapostnotum, posterior margin of mesothoracic katepimeron, and metapleuron. Legs pale except tarsomeres at least apically brownish, metacoxa basolateral third to entirely dark. Wings hyaline, veins brown, pale immediately adjacent to wing base. Abdomen dark, T9 either entirely dark or with broad basolateral spot pale, T10 and valvifer 2 entirely pale, valvula 3 either dark or pale with broadly dark margins.

Head: Antenna length 2.3x head width; F1 0.8x length of eye; first three flagellomeres subequal in length, proceeding flagellomeres progressively shorter (F7:F1 = 0.7x). Clypeus shallowly emarginate. Malar space 0.6x OD. LOD 1.4–1.5x height of eye in frontal view. In dorsal view, length of eye 1.2x distance from dorsal margin of eye to back of head. IOC:OOL = 0.9x. IOC:OD = 2.7–2.8x. Postocellar area less than twice as wide as long (IOC:OOCL = 1.7–2.0x). Head somewhat shiny, setigerous punctures slightly raised above surface, lower face and gena with microsculpture imbricate, frontal area smooth, vertexal area smooth to weakly imbricate.

Thorax: Pronotum dull, imbricate. Prepectus absent. Mesepisternum shiny, microsculpture smooth. Mesonotum somewhat dull, imbricate, except mesoscutellum and mesoscutellar appendage shiny, microsculpture smooth. Posterior mesoscutellar depression shallow, especially medially, such that mesoscutellar appendage is weakly delimited anteromedially. Parapsis shiny, microsculpture smooth to weakly imbricate posteroventrally. Mesopostnotum dull, imbricate, except posteromedial corner shiny, smooth. Protibia with single apical spur, without velum. Metabasitarsus shorter than (0.8–0.9x) metatarsomeres 2–4 combined. Tarsal claw simple, without subapical tooth. Wing vein 2r-rs present.

Abdomen: Terga somewhat dull, imbricate. Sawsheath in dorsal view emarginate, with distinct median carina, longest setae less than half as long as apical width of sawsheath, visible length of sawsheath about half as long as cerci or shorter. Sawsheath in lateral view short, lower margin evenly rounded and meeting dorsal margin at a rounded right angle. Valvula 3 lateral posterior lobe produced and narrow, slightly less produced than median carina. In apical view, width of sawsheath 0.85x height of setose area. Lance tapering only very weakly for most of length, more strongly so for apical 4–5 annuli. Lancet with basal 4–5 sutures dorsally apically

directed, proceeding sutures vertical to recurved; sclerora widened to a convex bump on each annulus, situated apically on annuli 1–3, approximately centred on annuli 4–onward.

Male. Length, 3.7–4.9 mm.

Darker than female: thorax entirely dark, at most posterolateral margins of pronotum narrowly pale, tegula partly pale; coxae dark, trochanters and trochantelli dark except on hind leg ventrally yellow-brown, femora basal third to half dark and apically pale, tibiae entirely pale, first two tarsomeres pale except narrowly brownish apically, proceeding tarsomeres brown; abdomen dark or brown. Structure and surface sculpture similar to female except: antenna with F1 shorter than F2 and F3 (F1:F2 = 0.85x; F1:F3 = 0.95x), proceeding flagellomeres progressively shorter (F7:F1 = 0.85x); head shiny, microsculpture weakly imbricate, smooth on frontal area; mesonotum shiny, weakly imbricate, except mesoscutellum and mesoscutellar appendage smooth; protibial spur with velum. T8 with distinct apical projection, wedge shaped and wider apically, approximately 0.35x as long as total medial length. Penis valve with paravalva apically concave due to produced apicoventral corner, valvispina 0.2–0.25x as wide at base as long.

Material studied. *Holotype* ♀—**USA**: **FL**: Jacksonville, Cat. No. 13993 (USNM). *Additional material*—**USA**: **FL**: Alachua Co, Austin Cary Forest, 15.i-4.iii.1977, coll. unknown, insect flight trap, FSCA 00091548, 1 ♂ (FSCA); Archbold Biol. Sta. Lk. Placid Highlands Co., 11.ii.1985, M.Deyrup, Malaise trap, FSCA 00091531, 1 ♂ (FSCA); idem except 21.iii.1984, 1 ♂ (USNM); idem except 25.ii.1985, FSCA 00091530, 1 ♀ (FSCA); Brevard Co., Malabar, Malabar Rd., 17-25.ii.2001, P.J.Russell, Z.Prusak, S.M.Fullerton, Malaise trap, UCFC 0 098 075, 1 ♀ (UCFC); Osceola Co., Kissimmee St. 2, TNC-Dis. Wild. Pres., 28.07° -81.26°, 67 ft, 15-22.iii.2002, TNC staff, Malaise trap, UCFC 0 167 536, 1 ♂ (UCFC); Sarasota Co., MCC-Venic

Campus, 2.iii.1997, K.J.Mahray, S.M.Fullerton, Malaise trap, UCFC 0 512 418, 1 ♀ (UCFC); **GA**: Clarke Co., Athens-Whitehall, 26.iii-2.iv.1979, R.H.Turnbow Jr., H.N.Greenbaum, insect flight trap, FSCA 00091533, 1 ♂ (FSCA); Stone Mt., 5.iv.1974, F.W.Fattig, 1 ♂ (USNM).

Distribution. This species is restricted to the Southeastern and Coastal Plain of Florida and Georgia.

Genetic data. None available.

Hosts. Unknown.

Comments. The association of males of this species is through shared collecting locality: one male was collected via Malaise trap at Lake Placid, FL, two weeks before a female was collected from the same trap. Adults of this species are active very early in the season, with most specimens being collected in February, and some in March; although soft tissues of various plants are available for oviposition year-round in Florida, the strongly sclerotized ovipositor of this species indicates that it probably oviposits into leaf buds like its near relative, *P. litura*.

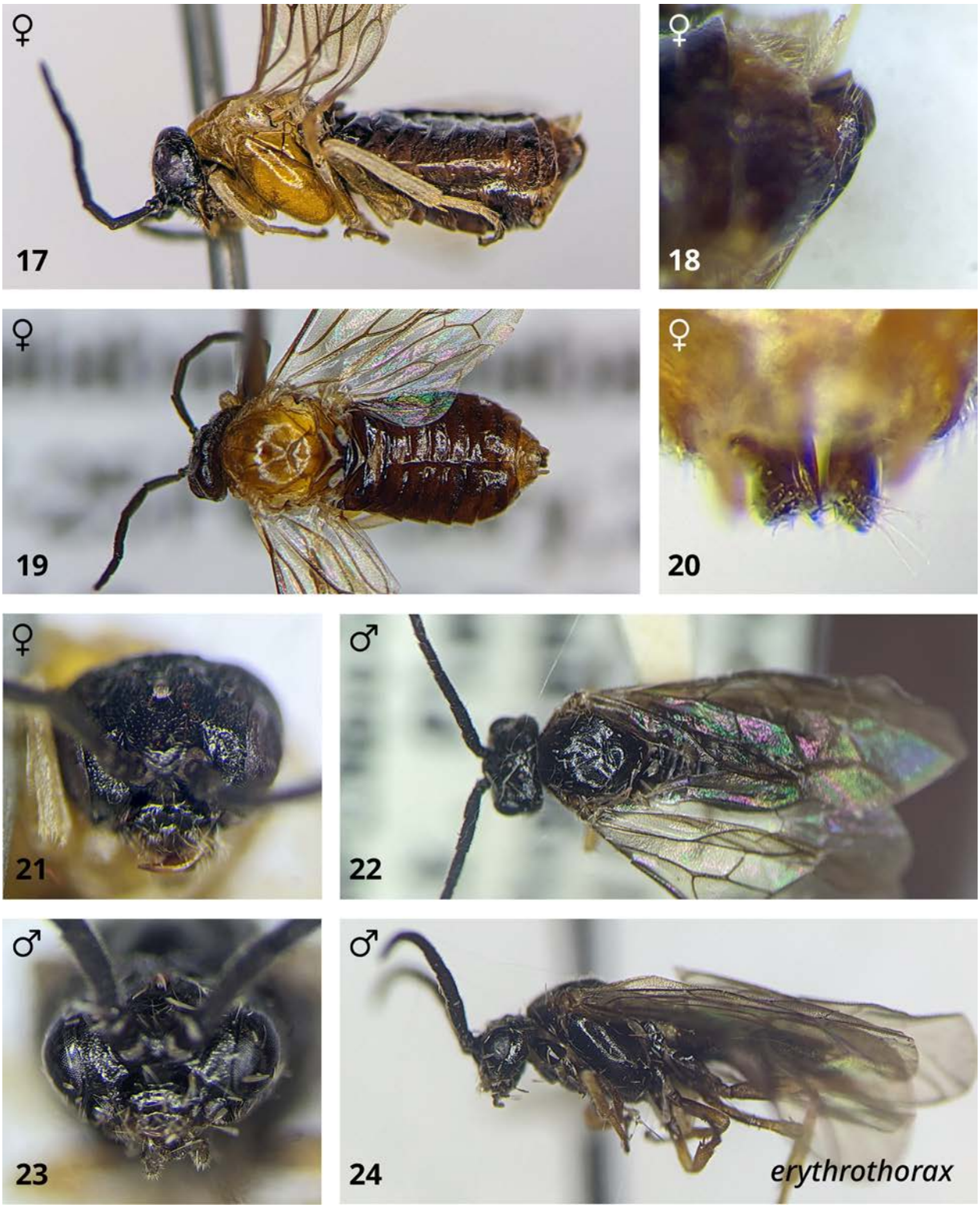

Figures 17–24. *Pristiphora erythrothorax*. **17**. Female lateral view. **18**. Sawsheath lateral view. **19**. Female dorsal view. **20**. Sawsheath dorsal view. **21**. Female head. **22**. Male dorsal view. **23**. Male head. **24**. Male lateral view.

***Pristiphora flavipectus* Monckton, n. sp.**

(Figs. 25–32, 43, 47, 53, 57, 61)

Diagnosis. Females can be differentiated from others in the *litura* group as follows: from *P. appalachiana* and *P. litura* by the pale mesepisternum with posteroventral triangle of pectus always pale (this portion of mesepisternum dark in *P. litura*, mesepisternum entirely dark in *P. appalachiana*); from *P. erythrothorax* by the long, pointed sawsheath in lateral view (Fig. 26; short and truncate in *P. erythrothorax*, Fig. 18) and by the darker thorax, usually with wide medial dark band occupying part of median lobe of mesonotum and entire mesoscutellum (Fig. 27; at most a posteromedial dark spot on mesoscutellum in *P. erythrothorax*, Fig. 19) – or if the thorax is nearly entirely pale, then so is the abdomen (abdomen always dark in *P. erythrothorax*). Males resemble *P. litura* in colouration, with legs more-or-less entirely pale (coxae, trochanters, trochantelli, and femora basally dark in *P. appalachiana* and *P. erythrothorax*), and may be differentiated by the structure of the mesoscutellar appendage, which has a median longitudinal groove in posterior half (absent in *P. litura*; e.g. as in Figs. 43, 44) and posterior margin notched (entire in *P. litura*), and by the paravalva with basoventral margin of sclerotized portion meeting pseudoceps in a distinct notch, such that basoventral corner of paravalva appears convexly produced (Fig. 61; margin of sclerotized portion appears linear in *P. litura*, meeting pseudoceps at a gradual oblique angle, Fig. 62).

Female. Length, 5.3 mm.

Colour: Antenna and head dark, mouthparts pale brownish, mandibles translucent brown with anterobasal corner and apex dark, labrum pale, clypeus yellow-brown in apical half,

supraclypeal area with diffuse brownish spot. Thorax pale, following parts dark: mesonotum median lobe in posterior third and medial corner of lateral lobe narrowly, mesoscutellum except lateral corner narrowly, mesoscutellar appendage except lateral quarter, metascutellum. Legs entirely pale, except apical two tarsomeres on fore leg and apical three tarsomeres on mid and hind leg brownish. Wings hyaline, veins brown except pale near wing base. Abdomen pale with medial brown band extending across T2-T5, no wider than exposed length of T3 and narrowing apically, darker apicomedially on T2; valvifer 1, adjacent margin of S7, and basal half of valvifer 2 dark; valvifer 2 otherwise irregularly brownish; valvula 3 dorsal and ventral margins dark, otherwise irregularly brownish.

Head: Antenna length 2.4x head width; F1 0.85x length of eye; F1 shorter than F2 (F1:F2 = 0.9x), approximately same length as F3, proceeding flagellomeres progressively shorter (F7:F1 = 0.75x). Clypeus shallowly, circularly emarginate. Malar space 0.75x OD. LOD 1.4x height of eye in frontal view. In dorsal view, length of eye 1.9x distance from dorsal margin of eye to back of head. IOC:OOL = 1.05x. IOC:OD = 2.5x. Postocellar area approximately twice as wide as long (IOC:OOCL = 2.1x). Head somewhat dull, setigerous punctures slightly raised above surface, face and gena with microsculpture coarsely imbricate, vertexal area imbricate, laterally somewhat weakly so.

Thorax: Pronotum dull, imbricate. Prepectus absent. Mesepisternum shiny, weakly imbricate. Mesepimeron shiny, microsculpture smooth. Mesonotum somewhat dull, weakly imbricate except mesoscutellum and mesoscutellar appendage shiny, smooth; mesoscutellar appendage shiny, smooth, with distinct median longitudinal groove in posterior half, posterior margin medially notched. Posterior mesoscutellar depression distinct for entire width, such that mesoscutellar depression is well delimited anteriorly. Parapsis shiny, microsculpture smooth to

weakly imbricate posteroventrally. Mesopostnotum dull, imbricate, except posteromedial corner shiny, smooth. Protibia with single apical spur, without velum. Metabasitarsus shorter than (0.9x) metatarsomeres 2–4 combined. Tarsal claw simple, without subapical tooth. Wing vein 2r-rs present.

Abdomen: Terga somewhat dull, imbricate, T2-T6 weakly imbricate and shiny medially. Sawsheath in dorsal view subtruncate, with distinct median carina, longest setae about as long as apical width of sawsheath, visible length of sawsheath about two-thirds as long as cerci. Sawsheath in lateral view drawn to a rounded acute apex, lower margin evenly rounded. Valvula 3 lateral posterior lobe weakly produced and narrow, distinctly less produced than median carina. In apical view, width of sawsheath 0.5x height of setose area. Lance tapering toward apex, more strongly so for apical 4–5 annuli. Lancet with basal 4 sutures dorsally apically directed, proceeding sutures vertical to recurved; setae bluntly rounded; sclerora widened to a convex bump on each annulus, situated apically on annuli 1–6, approximately centred on annuli 7–onward.

Male. Length, 4.5 mm.

Darker than female: thorax dark except lateral portion of pronotum mostly pale, tegula pale; legs pale as in female except coxae with basolateral third dark; abdomen entirely dark brown. Structure and surface sculpture similar to female except: antenna length 3.0x head width; F1 shorter than (0.85x) F2 and F3, the latter two approximately equal in length, proceeding flagellomeres progressively shorter (F7:F1 = 0.85x); protibial spur with velum; terga imbricate throughout. T8 with distinct apical projection, more-or-less triangular and distinctly wider apically, 0.3–0.4x as long as total medial length. Penis valve with paravalva apically deeply concave due to strongly produced apicoventral corner, basoventral sclerotized portion meeting

pseudoceps with a distinct notch, thus appearing basally convexly produced, valvispina 0.2x as wide at base as long, slightly widened at midlength.

Type material. *Holotype* ♀—**USA**: **MO**: Shannon Co., Current River Cons. Area, Comt 2, Stand 34, Trail 27, 10-26.iii.2007, R.J.Marquis, N.Schiff (USNM). *Allotype* ♂—Same data as holotype (USNM). *Paratypes* (8 ♀ 2 ♂)—**FL**: Alachua Co., 9 mi NW Gainesville UF Horticultural Unit, 24-28.ii.1977, H.Greenbaum, Malaise trap, FSCA 00091535, 1 ♀ (UCFC); Baker Co., Glen St. Mary, 30.3° -82.0153°, 22.iii.2007, E.Zoll, S.Fullerton, Malaise trap, UCFC 0 383 198, 1 ♀ (UCFC); Citrus Co., Withlacoochee St. For., Citrus Tract, 28.8498° -82.4337°, 2.iv.2010, J.Bradley, Malaise trap, UCFC 0 474 815, 1 ♂ (UCFC); idem except 8.iv.2010, UCFC 0 484 440, 1 ♀(UCFC); Orange Co., Orlando, 26.i.1997, K.J.Mahray, S.M.Fullerton, Malaise trap, UCFC 0 512 527, 1 ♀(UCFC); **GA**: Jones Co., 30.05° -83.7167°, 30.iii-6.iv.1993, J.Pickering, UGCA 027528, 1 ♀ (USNM); **MD**: Glen Echo, 1.v.1918, R.M.Fouts, 1 ♂ (USNM); **MO**: same data as holotype, 1 ♀ (USNM); **NY**: Orient, L.I., 9.vii.1949, Roy Latham, 1 ♀ (USNM); **VA**: Essex Co., 1 mi. SE Dunnsville, 37.8667° -76.8°, 1-19.iv.1993, D.R.Smith, O.S.Flint, Malaise trap, 1 ♀ (USNM); Prince William Co., Bull Run M. C., Jackson Hollow, campground, field, 38.879° -77.69°, 13.iv-1.v.2018, D.R.Smith, O.S.Flint, 1 ♀ (USNM).

Distribution. This species occurs from Long Island, NY, in the north, south to Florida, and west to Missouri. It is recorded from New York, Maryland, Virginia, Missouri, Georgia, and Florida.

Genetic data. Based on available genetic data (two specimens), within-species divergence is 1.4% and the nearest neighbour (*P. litura*) is 2.7% different.

Hosts. Unknown.

Etymology. The name of this species refers to its entirely pale pectus.

Comments. Female colouration varies, from thorax and abdomen entirely pale, to body mostly dark with only pronotum, tegula, mesonotum laterally, mesepisternum entirely, legs except basolateral corners of coxa, a lateral spot on T1, T9 medially, and T10 pale. Darker individuals thus closely resemble *P. litura*, but differ from that species by the entirely pale pectus and notched mesoscutellar appendage. In some female specimens, wing vein 2r-m is absent, which – along with the distinct posterior mesoscutellar depression and medially grooved, notched mesoscutellar appendage – is also seen in *P. appalachiana*.

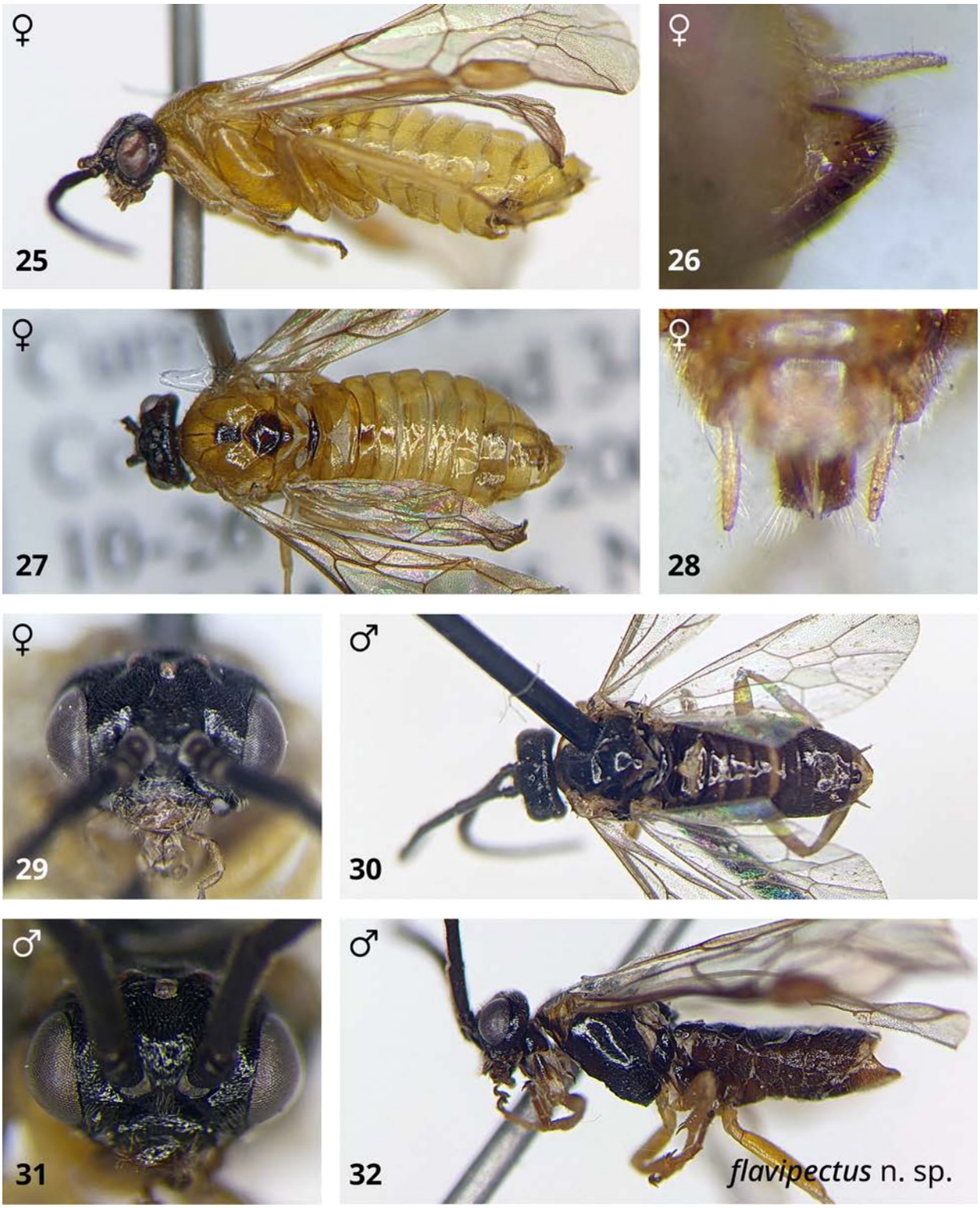

Figures 25–32. *Pristiphora flavipectus*. **25**. Female lateral view. **26**. Sawsheath lateral view. **27**. Female dorsal view. **28**. Sawsheath dorsal view. **29**. Female head. **30**. Male dorsal view. **31**. Male head. **32**. Male lateral view.

***Pristiphora litura* (Klug, 1816)**

(Figs. 6, 33–40, 41, 44, 48, 54, 58, 62)

Tenthredo litura Klug, 1816: 83.

Dineura lateralis Norton, 1867: 240.

Dineura linitus Norton, 1867: 240.

Dineura litura (Klug, 1816) – Dalla Torre, 1894: 279.

Neopareophora martini MacGillivray, 1908: 289

Neopareophora litura (Klug, 1816) – Ross, 1935: 205.

Pristiphora litura (Klug, 1816) – Prous et al., 2014: 50.

Diagnosis. Females can be differentiated from others in the *litura* group by the partly pale mesepisternum with posteroventral triangle of pectus dark (Fig. 33; mesepisternum more-or-less entirely pale in *P. erythrothorax* and *P. flavipectus*, Figs. 17, 25; entirely dark in *P. appalachiana*, Fig. 9), and from the similarly-coloured *P. flavipectus* by the mesoscutellar appendage without median longitudinal groove and posterior emargination (Fig. 44; both present in *P. flavipectus*, Fig. 43). Males can be differentiated thus: from *P. appalachiana* and *P. flavipectus* by the mesoscutellar appendage without median longitudinal groove (present for entire length in *P. appalachiana*, posterior half in *P. flavipectus*; e.g. Figs. 41, 43, 44) and posterior margin entire (notched in *P. appalachiana* and *P. flavipectus*); from *P. appalachiana* and *P. erythrothorax* by the usually entirely pale legs, with trochanters and trochantelli always entirely pale (dark in *P. erythrothorax* and *P. appalachianum*); from *P. flavipectus* by the

paravalva with basoventral margin of sclerotized portion meeting pseudoceps at a gradual oblique angle (Fig. 62; margin of sclerotized portion appears notched in *P. flavipectus* such that basoventral corner of paravalva appears convexly produced, Fig. 61). The most similar species is *P. flavipectus*, from which *P. litura* can be differentiated using the above characters.

Female. Length, 4.0–5.0 mm.

Colour: Colour variable. Antenna and head dark, mouthparts pale brownish, mandibles translucent brown with apex dark; spot on lower paraocular area, head behind eyes, apical ring of scape and pedicel, dark or brownish; following parts dark or pale: labrum, clypeus in part or in whole, spot on supraclypeal area. Thorax partly to mostly pale, at least following parts dark: mesonotum on medial half of median lobe and posteromedial margin of lateral lobe, mesoscutellum, mesoscutellar appendage medially, mesopostnotum, metascutellum, metapostnotum, ventral anterior margin of mespisternum narrowly, posteroventral triangle on mesepisternum (i.e. portion of pectus corresponding to mesosternum), anepimeron of mesepimeron; at least following parts pale: pronotum except narrowly on lateral portion of anterior margin, tegula, posterolateral margin of mesoscutellar appendage narrowly, mespisternum in dorsal half. Legs entirely pale except tarsi brown apically, coxae sometimes with basolateral corners narrowly brown. Wings hyaline, veins brown except pale near wing base, stigma lighter brown or pale. Abdomen variable from mostly dark to mostly pale: at least lateral recurved portions of T1–T8 somewhat lightened, usually more extensively pale, with as little as medial quarter of terga and apical margins narrowly dark, giving appearance of a dorsal longitudinal dark band that narrows posteriorly; sterna pale at least basally; T9 and T10 always entirely pale; valvifer 2 at least basal half pale; valvula 3 dark, sometimes brownish centrally.

Head: Antenna length 2.5x head width; F1 0.85–1.0x length of eye; first three flagellomeres subequal in length, proceeding flagellomeres progressively shorter (F7:F1 = 0.7–0.75x). Clypeus weakly to distinctly circularly emarginate. Malar space 0.67–0.8x OD. LOD 1.33–1.5x height of eye in frontal view. In dorsal view, length of eye 1.6–1.9x distance from dorsal margin of eye to back of head. IOC:OOL = 0.95–1.2x. IOC:OD = 2.4–3.0x. Postocellar area approximately twice as wide as long (IOC:OOCL = 1.8–2.3x). Head somewhat shiny, setigerous punctures slightly raised above surface, lower face, lower gena, and vertexal area with microsculpture coarsely imbricate, frontal area weakly imbricate.

Thorax: Pronotum dull, imbricate. Prepectus absent. Mesepisternum shiny, microsculpture smooth or weakly imbricate. Mesepimeron shiny, smooth, katepimeron with weak irregular horizontal lineations in posterior half. Mesonotum shiny, weakly imbricate except mesoscutellum and mesoscutellar appendage smooth. Posterior mesoscutellar depression shallow especially medially, such that mesoscutellar appendage is weakly delimited anteromedially. Parapsis shiny, microsculpture smooth to weakly imbricate posteroventrally. Mesopostnotum dull, imbricate, except posteromedial corner shiny, smooth. Protibia with single apical spur, with or without velum. Metabasitarsus approximately same length as metatarsomeres 2–4 combined. Tarsal claw simple, without subapical tooth. Wing vein 2r-rs present.

Abdomen: Terga somewhat dull, imbricate. Sawsheath with shape somewhat variable, both in actual structure and according to specimen posture and viewing angle: in dorsal view varyingly emarginate to subtruncate, with distinct median carina, longest setae longer than apical width of sawsheath, visible length of sawsheath half to two-thirds as long as cerci; in lateral view with lower margin variably rounded-obtuse to nearly linear, meeting dorsal margin at a rounded acute angle. Valvula 3 lateral posterior lobe produced and narrow, about equally as produced as

median carina. In apical view, width of sawsheath 0.5x height of setose area or less. Lance tapering toward apex, more strongly so for apical 2–3 annuli. Lancet with basal 3 sutures dorsally apically directed, proceeding sutures vertical to recurved; setae weakly pointed; sclerora widened to a convex bump approximately centred on each annulus, may be situated basally on annulus 1.

Male. Length, 3.6–4.2 mm.

Darker than female: head entirely dark, sometimes labrum pale; thorax entirely dark except tegula pale, pronotum either dark, pale along posterolateral margins, or mostly pale, mesepisternum rarely with irregular pale brownish spot at centre; legs pale as in female, except coxae may be partly to entirely dark, femora occasionally brown ventrally in basal half; abdomen dark or brown. Structure and surface sculpture similar to female except: antenna with F1 shorter than F2 and F3 (F1:F2 = 0.85x; F1:F3 = 0.9x), proceeding flagellomeres progressively shorter (F7:F1 = 0.8–0.9x); protibial spur always with velum. T8 with distinct apical projection, rounded-triangular and distinctly wider apically, 0.4x as long as total medial length. Penis valve with paravalva apically deeply concave due to strongly produced apicoventral corner, which is gently curved up apically, valvispina 0.2–0.25x as wide at base as long (but see comments).

Material studied. *Holotype* ♀ (images)—USA: GA: Georgia, Klug (SDEI). *Holotype* (♀) of *martini*—USA: MA: Hampden, West Springfield. 42.10694°, -72.62083°, 07.v.1898, J.O.Martin (INHS). *Additional material*—**USA**: **IL**: Pope Co., Eddyville, 37.49889° -88.58778°, date unknown, E.Ray, Insect Collection 639925, 1 ♀ (INHS); **MO**: Pulaski Co., Devil's Elbow, 36.9953° -91.0145°, date unknown, R.C.Froeschner, Insect Collection 175666, 1 ♀ (INHS); **FL**: Alachua Co, Austin Cary Forest, 15.i-4.iii.1977, coll. unknown, insect flight trap, FSCA 00091548, 1 ♀ (FSCA); **FL**: Alachua Co., 9 mi NW Gainesville UF Horticultural Unit, 24-

28.ii.1977, H.Greenbaum, Malaise trap, FSCA 00091535, 1 ♀ (FSCA); **GA**: Clarke Co., Athens-Whitehall, 13-19.iii.1979, R.H.Turnbow Jr., H.N.Greenbaum, insect flight trap, 1 ♀ (FSCA 00091547) 1 ♂ (FSCA 00091546) (FSCA); idem except 19-26.iii.1979, 1 ♀ (FSCA 00091545) 1 M (FSCA 00091544) (FSCA); idem except 26.iii-2.iv.1979, 7 ♀ (FSCA 00091533, FSCA 00091536, FSCA 00091537, FSCA 00091538, FSCA 00091539, FSCA 00091540, FSCA 00091541) (FSCA); idem except 26-29.iii.1974, FSCA 00091534, 1 ♀ (FSCA); idem except 2-9.iv.1979, FSCA 00091532, 1 ♀ (FSCA); idem except 6-13.iii.1979, 1 ♀ (FSCA 00091542) 1 M (FSCA 00091543) (FSCA).

Distribution. This species occurs from northern Canadian Shield forest in Ontario and Québec, east to New Brunswick, south to Florida, and west to Arkansas and Lousiana. It is recorded from Ontario, Québec, New Brunswick, Michigan, New York, New Hampshire, Maine, Massachusetts, Pennsylvania, Maryland, West Virginia, Virginia, Arkansas, Louisiana, Alabama, and Florida (D. R. Smith 1979, Goulet and Bennett 2021).

Genetic data. Based on available genetic data (two specimens), within-species divergence is 1.3% and the nearest neighbour (P. *flavipectus*) is 2.7% different.

Hosts. *Vaccinium* spp., *Vaccinium angustifolium* Aiton (D. R. Smith 1979, D. R. Smith and Strazanac 2016).

Comments. This species is quite variable in colouration and in the shape of the sawsheath, which in lateral view may appear obliquely truncate or else evenly tapering to an acute point. Variation between the extremes appears to be continuous and does not apparently coincide with variation in any other characters, nor with geographic distribution. All studied specimens are thus considered to be conspecific. The shape of the valvispina also appears to vary with viewing

angle, and in particular may appear much broader from an oblique ventral angle than in lateral view. One specimen (SKM.NAPr.232) has the valvispina broad as seen from all angles, but is consistent in all other respects with *P. litura*. Though not examined, the types of *linitus* and *lateralis* are most likely conspecific with *litura*, not *flavipectus*, as MacGillivray's (1867) descriptions indicate that both have a dark pectus.

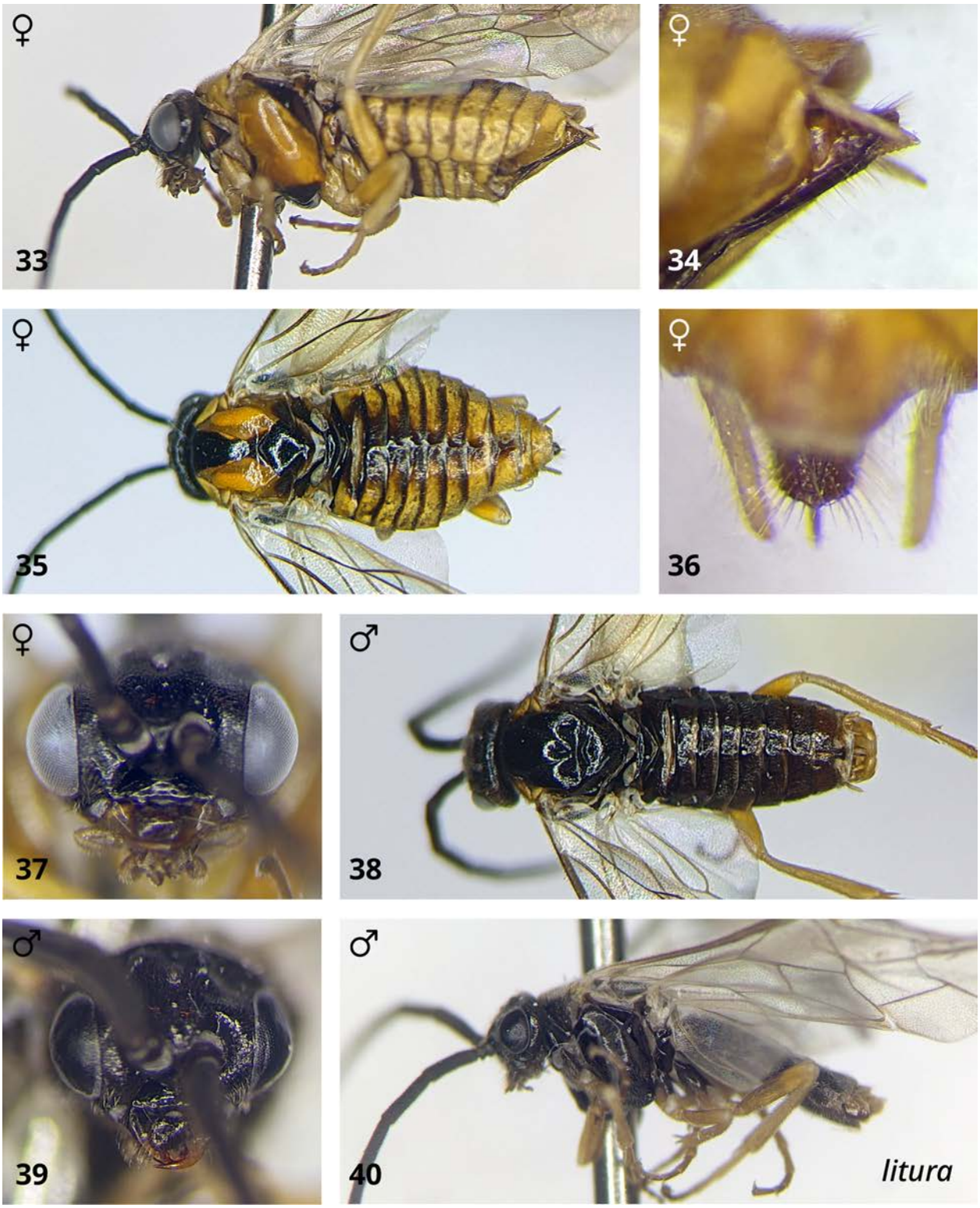

Figures 33–40. *Pristiphora litura*. **33**. Female lateral view. **34**. Sawsheath lateral view. **35**. Female dorsal view. **36**. Sawsheath dorsal view. **37**. Female head. **38**. Male dorsal view. **39**. Male head. **40**. Male lateral view.

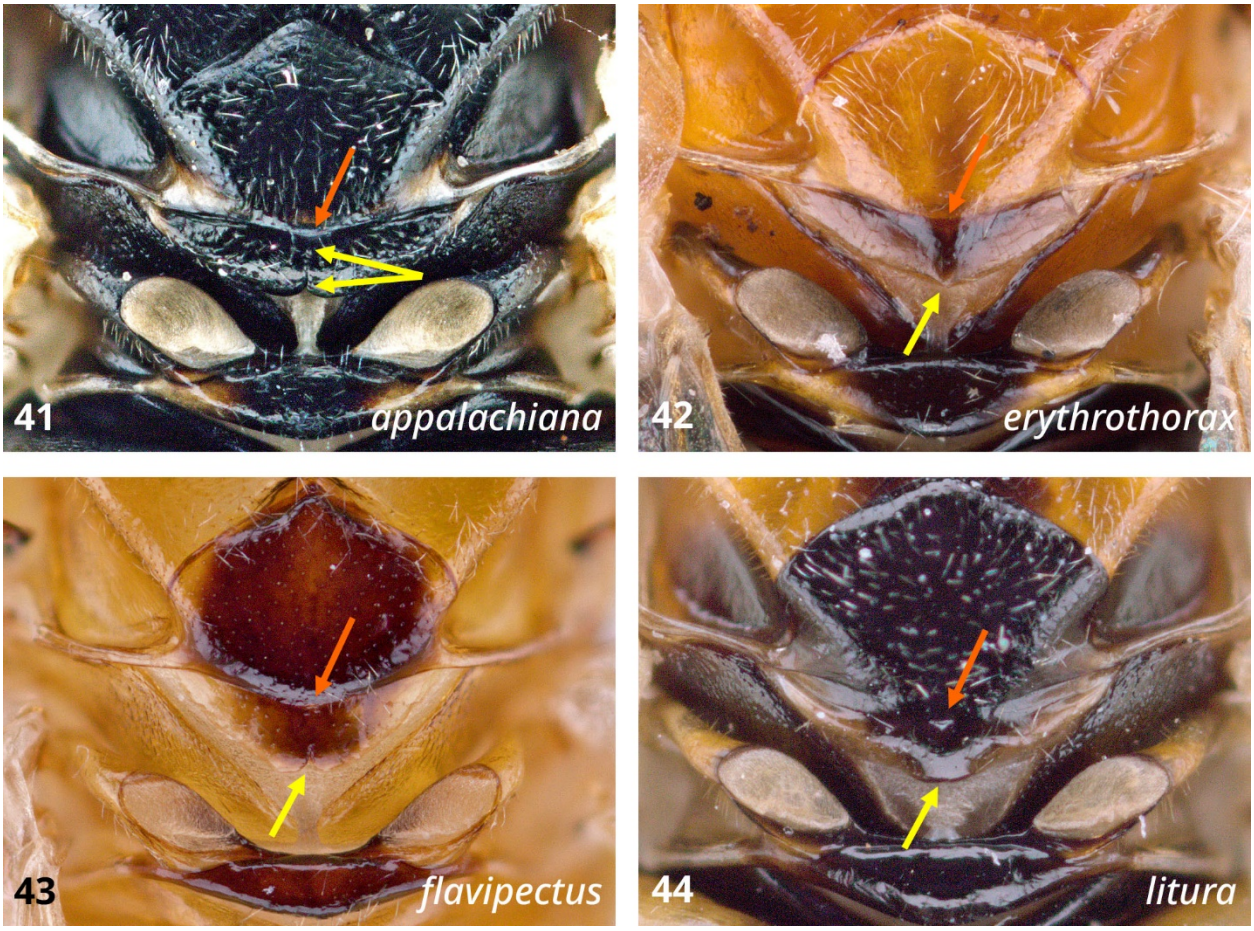

Figures 41-44. Mesoscutellum and mesoscutellar appendage of *Pristiphora litura* group. **41**. *P. appalachiana*. **42**. *P. erythrothorax*. **43**. *P. flavipectus*. **44**. *P. litura*.

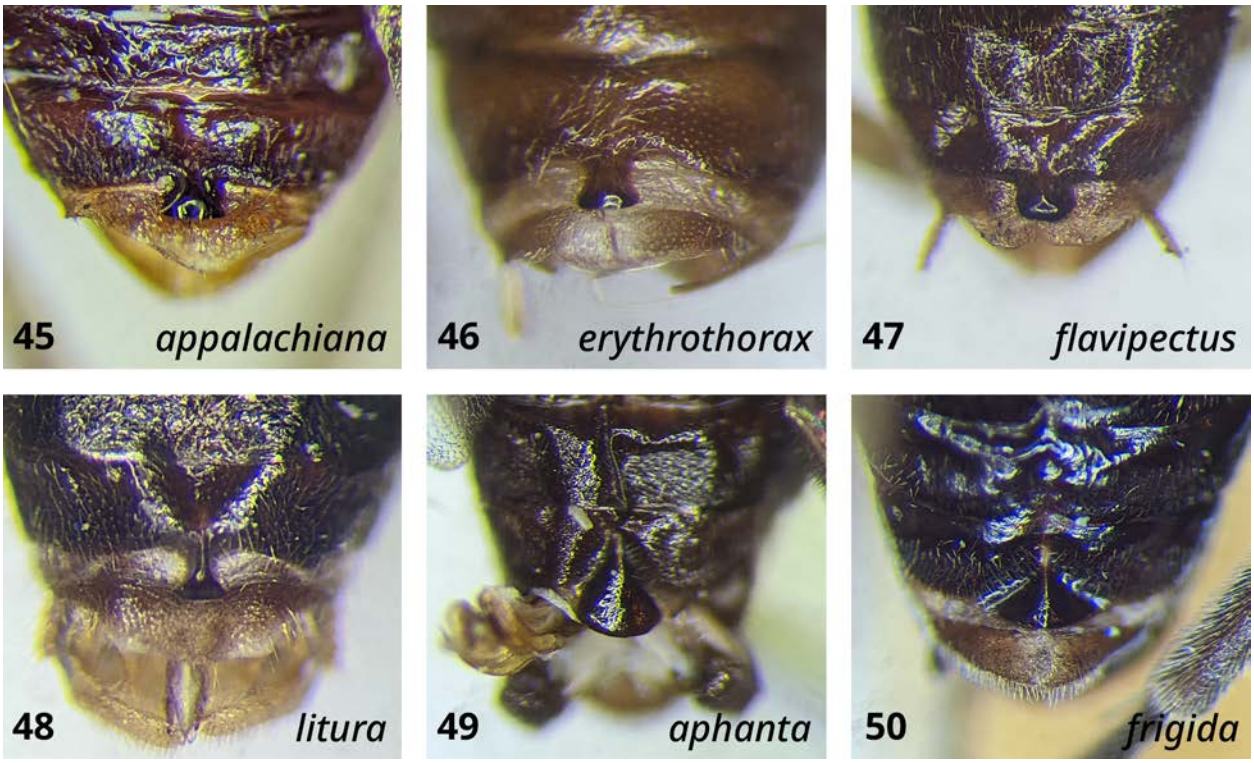

Figures 45–50. Male T8, with projection present (45–49) or absent (50). **45**. *P. appalachiana*. **46**. *P. erythrothorax*. **47**. *P. flavipectus*. **48**. *P. litura*. **49**. *P. aphanta*. **50**. *P. frigida*.

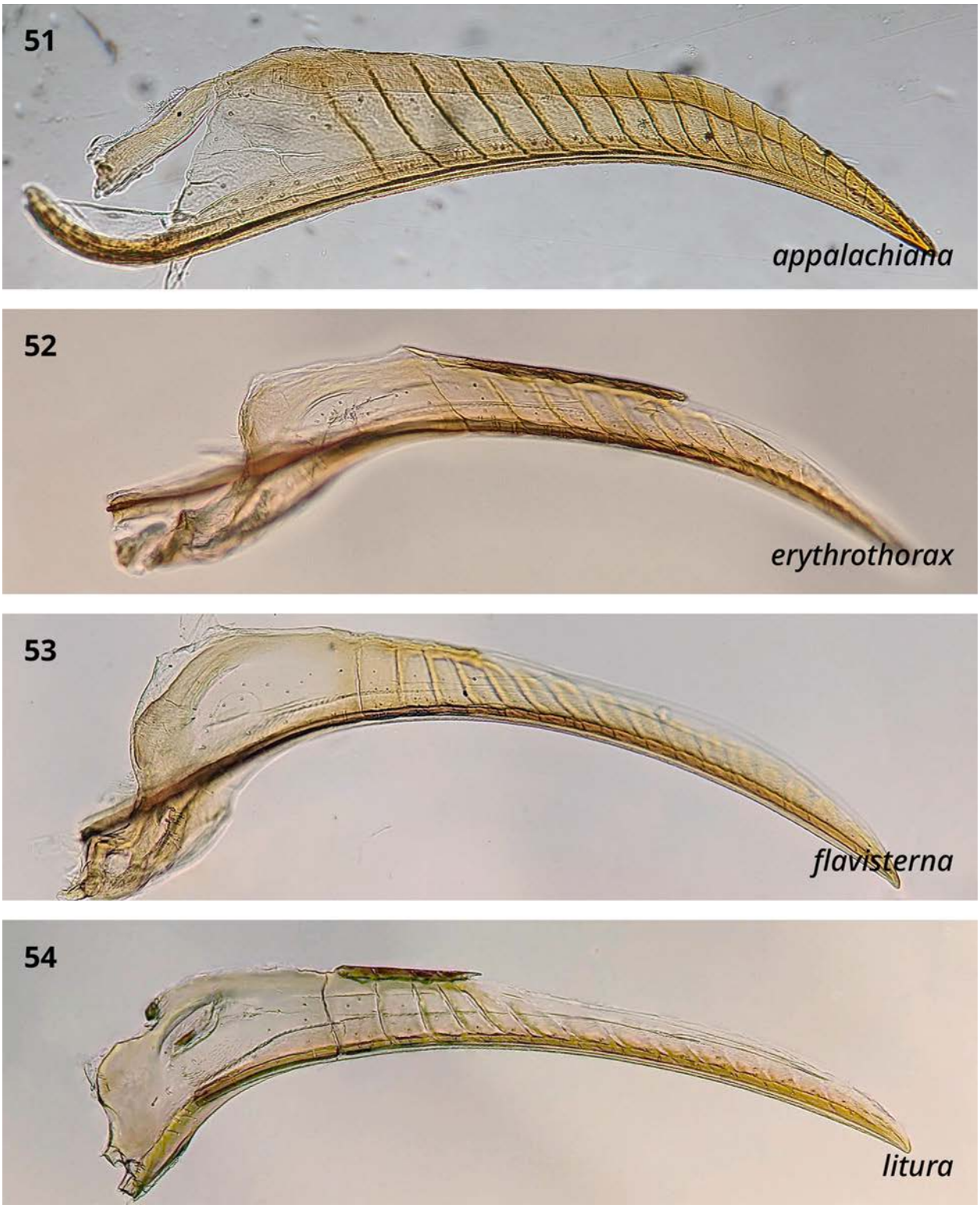

Figures 51–54. Lances of *Pristiphora litura* group (lateral view). **51**. *P. appalachiana*. **52**. *P. erythrothorax*. **53**. *P. flavipectus*. **54**. *P. litura*.

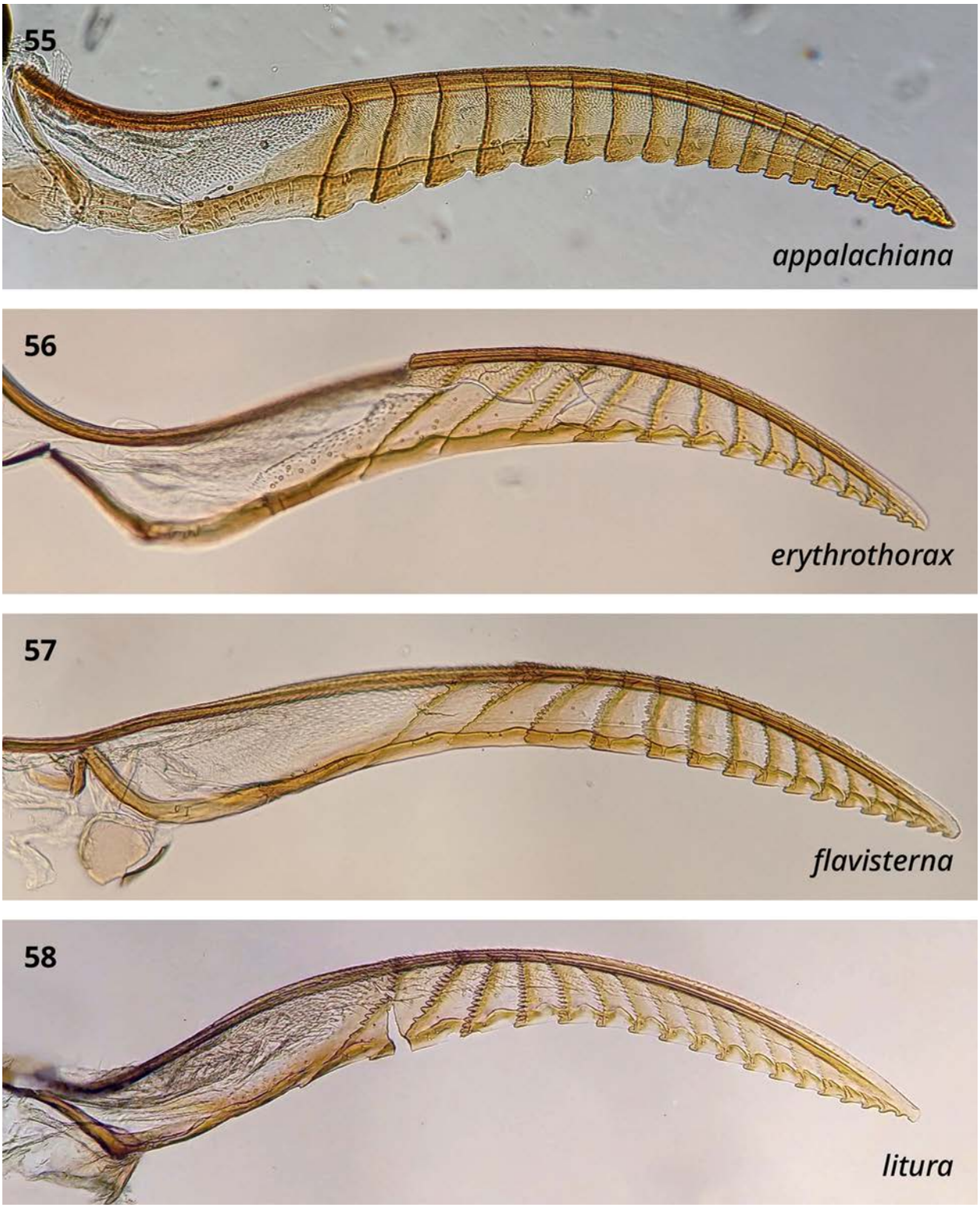

Figures 55–58. Lancets of *Pristiphora litura* group (lateral view). **55**. *P. appalachiana*. **56**. *P. erythrothorax*. **57**. *P. flavipectus*. **58**. *P. litura*.

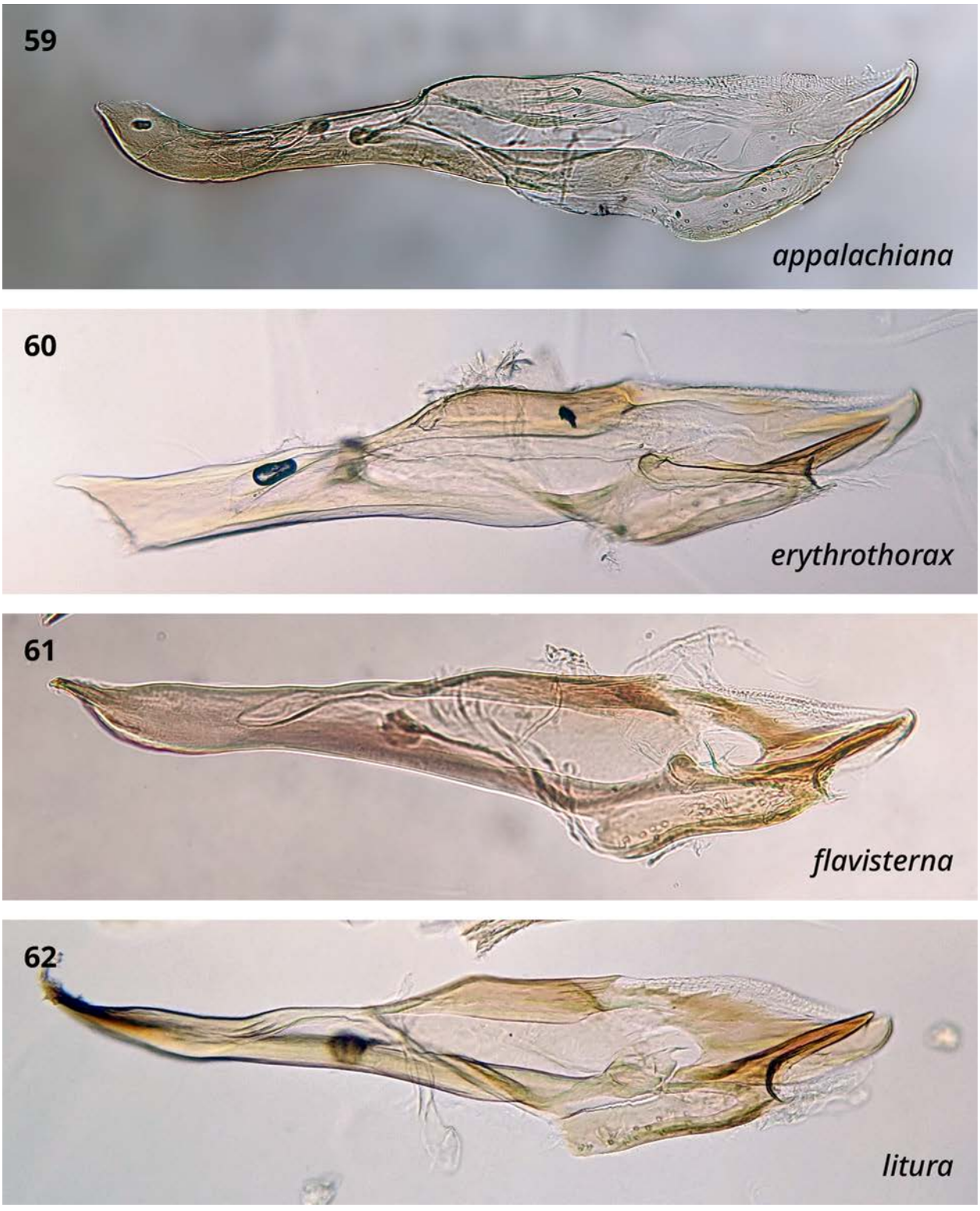

Figures 59–62. Penis valves of *Pristiphora litura* group (lateral view). **59**. *P. appalachiana*. **60**. *P. erythrothorax*. **61**. *P. flavipectus*. **62**. *P. litura*.

***Pristiphora ruficornis* group**

In the Nearctic, this group is represented by the following subgroups and species: *albitibia* subgroup (*P. sootryeni*), *aphantoneura* subgroup (*P. elaphita*, *P. hucksena*, *P. kangirsummiut*, *P. nigra*, *P. pusilla*, *P. staudingeri*, *P. sycophanta*), *appendiculata* subgroup (*P. appendiculata*), *ruficornis* subgroup (*P. melanocarpa*, *P. siskiyouensis*), and *P. aphanta* (not assigned to a subgroup, but possibly a representative of the Palaearctic *armata* subgroup). Species in the *ruficornis* group are best characterized by the structure of the male penis valve, which has a large and usually distinctly bent valvispina that takes up most or all of the paravalva (Figs. 192–204). Females can be recognized by the shape of the annuli on the lancets, most of which are usually distinctly sigmoid and dorsally strongly apically curved (Figs. 178–191). The above subgroups were originally described by Prous et al. (2016), but the inclusion of certain Nearctic species requires some further comment: *P. elaphita* and *P. hucksena* are assigned to the *aphantoneura* subgroup on the basis of the tangium of the lancet (Figs. 180 & 182), which is similar in size and shape to that of *P. staudingeri*; *P. aphanta* is not assigned to any subgroup, and although males have a distinct apical projection on T8 similar to that of the Palaearctic *armata* subgroup (Fig. 49), the penis valve (Fig. 192) differs considerably in structure.

Diagnosis. Externally, this group can generally be recognized by their dark colouration, with at most the labrum, ventral surface of antennae, posterior corner of the pronotum, and some parts of the legs yellow (all femora mostly or entirely dark in all species but *P. aphanta*, *P. appendiculata*, and *P. hucksena*). Females have the lateral posterior lobe of valvula 3 distinctly produced, and in all Nearctic species but *P. aphanta* and *P. appendiculata*, these lobes extend along the posterodorsal margins to meet in the middle. As a result, the sawsheath may appear either truncate or emarginate in dorsal view, depending on the angle at which it is viewed.

Species in this group can usually be differentiated from the *rufipes* group by the short postocellar space, which in dorsal view is at least twice as wide as long (IOC:OOCL ≥ 2.0x in *ruficornis* group; ≤ 1.9x in *rufipes* group) except in *P. appendiculata* (*ruficornis* group, 1.6–1.8x) and *P. cincta* (*rufipes* group, 1.8–2.0x). As well, in the *ruficornis* group, the medial surface of the head between the antennal sockets is usually raised as a distinct ridge, appearing at least weakly convex in dorsal view; in the *rufipes* group, it is only weakly raised, appearing weakly concave in dorsal view. Known host plants include *Ribes* L., *Salix* L., and *Betula* L., while *Oxytropis campestris* (L.) DC. is a recorded host plant for *P. sootryeni* in the Palaearctic region (Prous et al. 2017). Genetic data strongly support monophyly of the *ruficornis* group and all subgroups except the *aphantoneura* subgroup (see Chapter 3).

Key to species of the *P. ruficornis* group

Females

1. Mesepisternum shiny, smooth (Fig. 2) 2

1'. Mesepisternum dull, imbricate (Fig. 3) or rough, coriaceous (Fig. 4) 8

2. Tarsal claw medium or large (Figs. 173, 174) 3

2'. Tarsal claw small (Fig. 172) or absent 5

3. Pronotum shiny, microsculpture smooth (Fig. 2); tangium of lancet large and broad, about half as high as lancet and almost as high as wide (Fig. 194) .....*P. frigida*

3'. Pronotum dull, imbricate (Fig. 3); tangium of lancet smaller, at most one-quarter as high as lancet, and rectangular, twice as long as high or longer (Figs. 178, 184) 4

4. Lateral posterior lobe of valvula 3 produced and continuing medially along posterodorsal margin as a carinate ridge; tangium of lancet elongate, rectangular, at least four times longer than high (Fig. 184); lamnium with small spiny pectines that reach the sclerora (Fig. 184).....

..... *P. maura*

4'. Lateral posterior lobe of valvula 3 produced, but not continuing dorsomedially; tangium of lancet shorter, approximately twice as long as high (Fig. 178); lancet with small spiny pectines absent from sclerora (Fig. 178) .....*P. aphanta*

5. Middle and hind femora mostly pale (Figs. 74, 95; may be mostly brown, but clearly lighter in colour than dark parts of body) 6

5'. Middle and hind femora mostly dark (Fig. 116) 7

6. Lateral posterior lobe of valvula 3 produced and continuing medially along posterodorsal margin as a carinate ridge; subapical tooth of tarsal claw present but small, less than half as long as apical tooth (e.g. Fig. 172); mesopostnotum rough, coarsely imbricate (e.g. Figs. 3–4); tangium of lancet broad, approximately rectangular but somewhat tapering apically, tangial process clearly arising from tangium (Fig. 182) .....*P. hucksena*

6'. Lateral posterior lobe of valvula 3 produced, but not continuing dorsomedially; subapical tooth of tarsal claw absent; mesopostnotum shiny, microsculpture smooth (e.g. Fig. 2); tangium of lancet triangular, strongly tapering apically, tangial process separated from rest of tangium (Fig. 179) .....*P. appendiculata*

7. Coxae entirely or almost entirely dark, hind coxa at most with narrow apical ring pale; hindfemur entirely dark, or at most with a small apicodorsal spot pale; flagellum uniformly dark or at most slightly paler below (Fig. 65); tangium of lancet ventrally produced into a distinct lobe (Fig. 185), or if only weakly produced then with distal edge of basoventral corner approximately flat; serrulae distinctly slanted and sharply pointed, especially apically (Fig. 185)...*P. melanocarpa*

7'. Forecoxa with at least a narrow apical ring pale, middle and hind coxae with at least apical one-quarter pale; hindfemur with narrow basal and apical ring pale; flagellum paler ventrally at least in apical half (e.g. Fig. 64); tangium of lancet at most convexly produced ventrally and always evenly rounded (Fig. 188); serrulae less strongly slanted, less sharply pointed (Fig. 201) ....*P. siskiyouensis*

8. Coxae with narrow apical ring to as much as apical half pale; trochanters and trochantelli entirely pale 9

8'. Coxae at most with small apicoventral spot pale; trochanters and trochantelli at most with narrow apical ring pale on fore and midleg, sometimes entirely pale on hindleg 10

9. Lower face shiny, microsculpture smooth; sawsheath narrow, in apical view about 0.6-0.7x as wide as height of setose area; tangium of lancet long and slender, at least four times longer than high (Fig. 191)..... *P. sycophanta*

9'. Lower face dull, imbricate; sawsheath wider, in apical view about 0.9x as wide as height of setose area; tangium of lancet large and broad, about twice as long as high (Fig. 180)..... .....*P. elaphita*

10. Tangium of lancet large and broad, at most twice as long as high (Figs. 183, 190)..... 11

10'. Tangium of lancet rectangular, clearly more than twice as long as high (Figs. 186, 187, 189) 12

11. Sawsheath in lateral view with lower margin evenly rounded, appearing broadly rounded in profile (Fig. 149); lancet with first and second suture approximately straight (Fig. 190); serrulae somewhat sharply pointed, cypsellae present between apical-most serrulae; setae on annuli one-third to one-half as long as corresponding annulus..... *P. staudingeri*

11'. Sawsheath in lateral view more slender, lower margin straighter (Fig. 101); lancet with first and usually second suture distinctly recurved dorsally (Fig. 183); serrulae of lancet less sharply pointed, cypsellae absent between apical-most serrulae; setae on annuli one-third width of corresponding annulus or less .....*P. kangirsummiut*

12. Subapical tooth of tarsal claw medium to large, at least half as long as apical tooth and longer on hindleg (e.g. Figs. 173, 174); tangium of lancet long and slender, at least four times longer than high (Fig. 189); lamnium with small spiny pectines that reach the sclerora (Fig. 189)..... .....*P. sootryeni*

12'. Subapical tooth of tarsal claw small, less than half as long as apical tooth (e.g. Fig. 172), or absent; tangium of lancet at most three times as long as high (Figs. 186, 187); lamnium with small spiny pectines absent from sclerora (Figs. 186, 187) 13

13. Parapsis dull, imbricate throughout; lancet with very few small setae on annuli, or with setae apparently absent (Fig. 186); tangial process small, present only for dorsal half of tangium, without a membranous fold (Fig. 186).....*P. nigra*

13'. Parapsis shiny, microsculpture smooth at least in ventral half; lancet with well-developed setae on annuli one-quarter to one-third width of corresponding annulus (Fig. 187); tangial process distinctly sclerotized, with well-developed membranous fold (Fig. 187).....*P. pusilla*

Males

1. Antenna pale ventrally (Fig. 63) at least in apical half (Fig. 64) 2

1'. Antenna uniformly dark (Fig. 65), or at most only slightly paler ventrally (dark dorsally, brownish ventrally) 5

2. Apex of T8 with large medial projection (Fig. 49).....*P. aphanta*

2'. Apical margin of T8 at most weakly produced and convex medially (Fig. 50)..... 3

3. Mesopostnotum shiny, microsculpture smooth; penis valve (Fig. 193) with valvispina large and bent dorsally, about as long as and forming an acute angle with apical margin of paravalva; pseudoceps without membranous fold near tip of valvispina .....*P. appendiculata*

3'. Mesopostnotum dull, coarsely imbricate; penis valve (Figs. 197, 201) with valvispina long and slender, bent dorsally near midlength, and occupying entire paravalva; pseudoceps with distinct membranous fold near tip of valvispina..... 4

4. Penis valve (Fig. 197) with valvispina long and slender, dorsally bent apical portion about half as wide as basal portion; dorsal margin of pseudoceps evenly rounded near base.....
.....*P. melanocarpa*

4'. Penis valve (Fig. 201) with valvispina broader, apical portion similar in width to basal portion; dorsal margin of pseudoceps distinctly produced to an obtuse angle near base .....
.....*P. siskiyouensis*

5. Hind tarsal claw with subapical tooth large, more than half as long as apical tooth (Figs. 173, 174) 6

5'. Hind tarsal claw with subapical tooth small, less than half as long as apical tooth (Fig. 172).. 7

6. Pronotum and mesepisternum shiny, microsculpture smooth (e.g. Fig. 2); eye relatively small, F1 about 1.3x as long as eye in lateral view, LOD 1.5-1.7x length of eye in frontal view; pseudoceps of penis valve (Fig.) with distinct membranous fold near tip of valvispina .....*P. frigida*

6'. Pronotum and mesepisternum dull, imbricate or coarsely imbricate (e.g. Figs. 3, 4); Eye not especially small, F1 at most 0.9x as long as eye in lateral view, LOD about 1.4x length of eye in frontal view; peusodceps of penis valve (Fig. 202) without membranous fold near tip of valvispina .....*P. sootryeni*

7. Penis valve with valvispina broad throughout its length, or broadest in apical half, tapering abruptly near apex (Figs. 199–201) 8

7'. Penis valve with valvispina broadest basally, tapering more-or-less evenly towards apex (Figs. 196, 195, 203, 204) 9

8. Penis valve (Fig. 199) with valvispina strongly dorsally bent and semicircular, apical portion at acute angle relative to basal portion; pseudoceps with dorsal margin convex, semicircular, deeply concave near base .....*P. nigra*

8'. Penis valve (Figs. 200–201) with valvispina less strongly bent, apical portion at obtuse angle relative to basal portion (on right penis valve; Fig. 199) or at most forming a right angle (on left penis valve; Fig. 200); pseudoceps with dorsal margin straighter, at most weakly concave near base.....*P. pusilla*

9. Penis valve (Fig. 196) with valvispina very strongly bent, apical portion forming acute angle with basal portion, which arises at a near-perpendicular angle from valviceps..... *P. maura*

9'. Penis valve (Figs. 195, 203, 204) less strongly bent, apical portion forming approximately obtuse or at most a right angle with basal portion, which arises more-or-less in line with valviceps..... 10

10. Pseudoceps of penis valve (Fig. 204) distinctly dorsally bent at an obtuse angle relative to valvura; ergot absent indistinct ..... *P. sycophanta*

10'. Pseudoceps of penis valve (Fig. 203) not dorsally bent, approximately in line with valvura and longitudinal axis of penis valve; ergot usually well-developed and distinctly produced 11

11. Valvispina of penis valve with a distinct, bulbous, enlarged section where it bends dorsally (Fig. 195).....*P. kangirsummiut*

11'. Valvispina of penis valve at most widened where it bends dorsally, lacking distinct bulbous section (Fig. 203) ..... *P. staudingeri*

Figures 63–65. Male antenna colouration. **63**. Pale ventrally (*P. appendiculata*). **64**. Paler ventrally only in apical half of antenna (*P. siskiyouensis*). **65**. Entirely dark (*P. sycophanta*).

***Pristiphora aphanta* Wong & Ross, 1960**

(Figs. 49, 66–73, 160, 178, 192)

Pristiphora aphanta Wong & Ross, 1960: 196.

Diagnosis. Females of this species can be differentiated from most other Nearctic species in the *ruficornis* group by their relatively slender sawsheath, in apical view about two-thirds as wide as height of setose area (wider in most other species), with lateral posterior lobe of valvula 3 small and narrow (in other species it is wider and produced a greater distance); mesepisternum shiny, microsculpture smooth (e.g. Fig. 2; in other species with this combination of characters, it is dull, imbricate to rough, coriaceous, e.g. Figs. 3–4); tarsal claw with medium subapical tooth, about

half as long as apical tooth (Fig. 173; in other species with this combination of characters, it is small, less than half as long as apical tooth, e.g. Fig. 172). This combination of characters differentiates females of *P. aphanta* from all but *P. hucksena*, *P. maura*, *P. melanocarpa*, and *P. siskiyouensis*, from which it can be differentiated by its lancet, which has an approximately rectangular tangium, about twice as long as high (Fig. 178; in *P. maura* tangium rectangular and much longer, Fig. 184; in *P. hucksena* tangium rectangular and larger, less than twice as long as high, Fig. 182; in *P. melanocarpa* and *P. siskiyouensis* tangium large, ventrally rounded or produced, and about as long as high or less so, Figs. 185, 188). The tangial process of *P. aphanta* rises above the tangium by about half the height of the latter and is weakly sclerotized, appearing membranous (distinctly sclerotized in the other four species). Males of *P. aphanta* are readily differentiated by the large apical projection of T8 (Fig. 49), which is absent from all other Nearctic species.

Female. Length, 4.4–5.5 mm.

Colour: Antenna dark; head dark; mouthparts dark brown, mandible apical half translucent brown except dark apex; labrum brown, apical margin translucent yellow-brown. Thorax dark; tegula variable, dark brown to translucent yellow. Legs dark, except coxae narrow apical ring pale, trochanters and trochantelli pale, foreleg with femur apical half, tibia, and tarsus pale except apical two to three tarsomeres often brown, midleg with femur narrow basal and apical ring, tibia, and tarsus pale, except narrow apical ring of tibia and tarsomeres yellow-brown, apical one to two tarsomeres brown, hindleg with femur narrow basal and apical ring and tibia basal two-thirds pale, tarsus dark brown. Abdomen dark or dark brown, apical margins of terga often broadly yellow-brown medially, cerci dark.

Head: Antenna length 2.9–3.1x head width; F1 1.05–1.1x length of eye; F1 subequal to or slightly shorter than F2 (F1:F2 = 0.95–1.0x), subequal to or slightly longer than F3 (F1:F3 = 1.05x), proceeding flagellomeres progressively shorter (F7:F1 = 0.67–0.75x). Clypeus truncate. Malar space 0.9–1.0x OD. LOD 1.2–1.3x height of eye in frontal view. IOC:OOL = 1.2–1.4x. Head somewhat shiny, weakly imbricate.

Thorax: Pronotum dull, imbricate. Prepectus distinct & pitted, setose. Mesepisternum shiny, microsculpture smooth, epicnemium shiny, microsculpture smooth with weak horizontal lineations. Mesepimeron shiny, microsculpture smooth. Mesonotum shiny, microsculpture smooth, except somewhat dull, weakly imbricate medially on median lobe and laterally on lateral lobe; mesoscutellum shiny, microsculpture smooth; mesoscutellar appendage shiny, weakly imbricate, rougher around posterlateral edges. Parapsis shiny, weakly costulate/puncticulate. Mesopostnotum dull, imbricate. Metabasitarsus approximately same length as metatarsomeres 2–4 combined. Subapical tooth of tarsal claw medium, about half as long as apical tooth.

Abdomen: Terga somewhat dull, imbricate. Sawsheath in dorsal view emarginate, with distinct median carina, longest setae about two-thirds as long as apical width of sawsheath, visible length of sawsheath about the same length as cerci. Sawsheath in lateral view with lower margin evenly rounded, meeting dorsal margin at a sub-quadrate apex. Valvula 3 lateral posterior lobe produced. In apical view, width of sawsheath 0.6-0.7x height of setose area. Tangium of lancet rectangular and somewhat small, about twice as long as high; tangial process extending above 1.5x as high as tangium and weakly sclerotized. Lancet with three sutures approximately straight, proceeding sutures weakly sigmoid; annuli with very short setae; serrulae protruding and somewhat sharply pointed, basoventral angle rounded-acute; small spiny pectines absent from sclerora.

Male. Length, 5.5–5.7 mm.

Colour as in female except as follows. Antenna dark, pale ventrally, with stout black setae. Legs dark, except coxae narrow apical ring brown, trochanters and trochantelli variable, narrowly pale apically to more extensively pale and suffused with brown, foreleg with femur more extensively pale, with apical half to three-quarters dorsally pale, midleg with femur more extensively pale, with apical quarter of anterior surface pale. Abdomen dark or dark brown. Structure and sculpture similar to female, except: antenna 3.1–3.3x head width; F1 1–1.1x length of eye, F1 subequal to or slightly longer than F2 (F1:F2 = 1.05x), longer than F3 (F1:F3 = 1.1–1.2x), proceeding flagellomeres progressively shorter (F7:F1 = 0.75–0.85x); LOD 1.4–1.5x height of eye in frontal view; IOC:OD 2.3–2.7x; head somewhat dull, weakly imbricate, gena dull, imbricate; mesonotum shiny, microsculpture smooth, mesoscutellar appendage somewhat dull, deeply pitted, weakly rugulose laterally, mesopostnoum rough, rugose. T8 with distinct apical projection, slightly wider apically, approximately 0.5-0.6x as long as total medial length. Penis valve with valvispina large, very broad, moderately bent at a rounded obtuse angle; pseudoceps with distinctly produced ventroapical lobe, dorsal margin widely notched with large membranous fold; valvura with large ergot.

Material studied. *Holotype* ♀—**USA**: **NY**: Cortland, Labrador Lake, 16.vi.1937, D.T.Ries, M.E.Davis, slide prep: ovipositor (INHS). *Additional material*—**CANADA**: **ON**: Bruce Pen. Jct Hwy 6 & Dyer B. Rd., pavement alvar, 2.vi.1997, P.Bouchard, flight int., 1 ♂ (LEMU); Carden Twp., 7.5km E Seabright, shrubland alvar, 3.vi.1997, P.Bouchard, Malaise trap, 1 ♂ (LEMU); Carden Twp., N North Quarter Line, shrubland alvar, 11.ix.1997, P.Bouchard, Malaise trap, 1 ♀ 2 ♂ (LEMU); Manitoulin Is., 10km S Gore Bay, burt-oak alvar, 20.viii.1996, P.Bouchard, Malaise trap, 1 ♀ (LEMU); Ottawa, date unknown, W.B.Harrington, 1 ♀ (CNC); **QC**:

Kazabazua, *45.949*° *-76.015*°, 7.vi.1937, F.A.Urquhart, slide prep: ovipositor, 1 ♀ (NFRC); **USA**: **NY**: Tompkins Co., McLean Bogs, *42.550*° *-76.275*°, 29.v.1915, coll. unknown, slide prep: penis valves, 1 ♂ (NFRC).

Distribution. This species is primarily known from alvar habitats in Ontario, and may be associated with nutrient-poor soils (one specimen is from a kettle bog in New York). It has a relatively small distribution in the Eastern Mixed Woods of Ontario, Québec, and New York.

Genetic data. None available.

Host. Unknown, but given its restricted distribution and association with habitats characterized by nutrient-poor soils, this species may feed on a plant with similar habitat preferences, such as *Astragalus neglectus* (Torr. & Gray) Sheld., *Waldsteinia fragarioides* (Michx.) Tratt., *Salix lucida* Muhl., or *S. serissima* (L.H. Bailey) Fernald (all belonging to known host genera for *Pristiphora*).

Comments. Males of *P. aphanta* are associated with females based on collecting data: only the female from Carden shares a collecting event with a male of this species and is assumed therefore to be conspecific. As well, both the apical projection on male T8 and the structure of the female lancet (small rectangular tangium, reduced setae on sutures) are similar to those of the Palaearctic *armata* subgroup, suggesting they represent either the only Nearctic representative of that subgroup or a close relative.

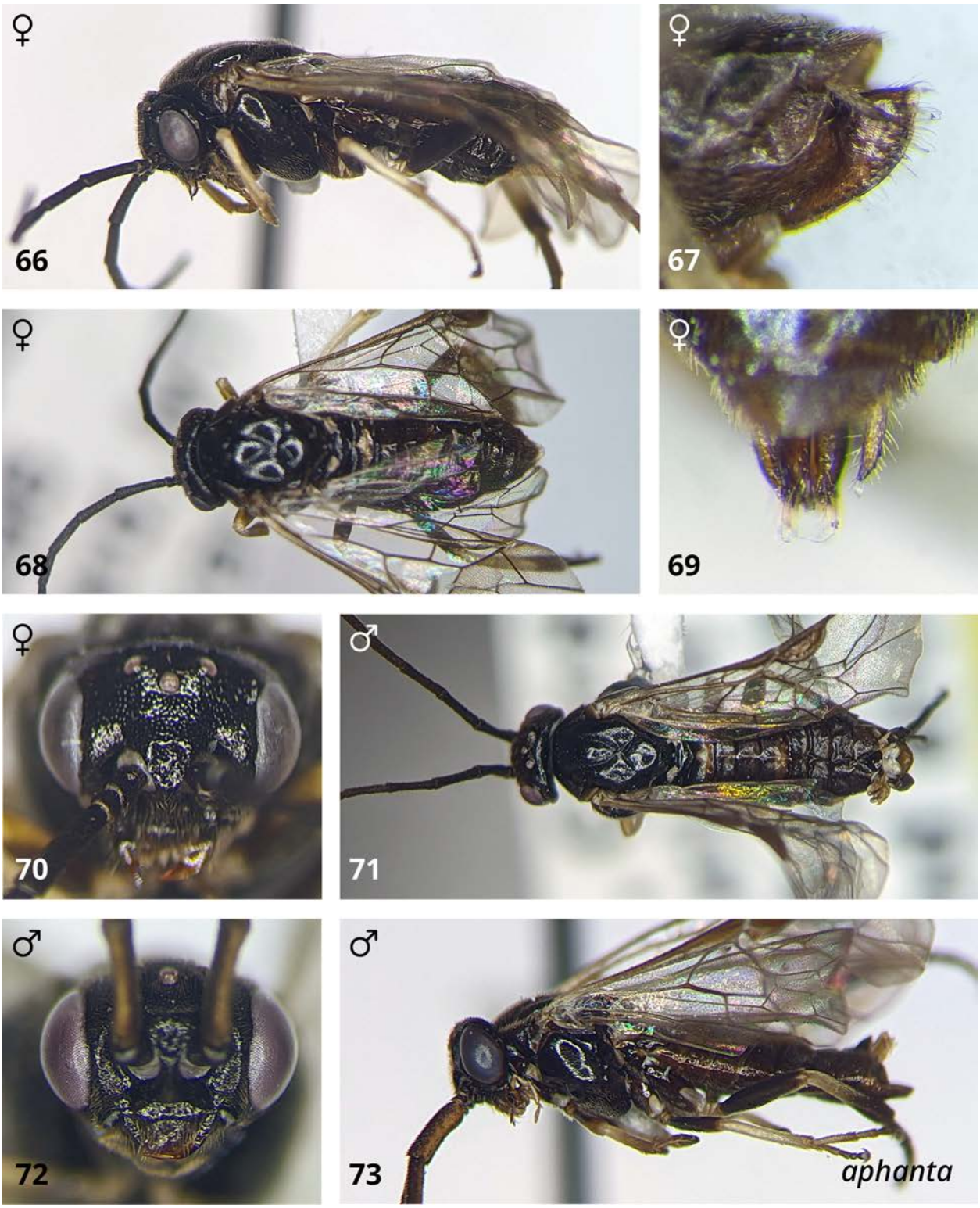

Figures 66–73. *Pristiphora aphanta*. **66**. Female lateral view. **67**. Sawsheath lateral view. **68**. Female dorsal view. **69**. Sawsheath dorsal view. **70**. Female head. **71**. Male dorsal view. **72**. Male head. **73**. Male lateral view.

***Pristiphora appendiculata* (Hartig, 1837)**

(Figs. 63, 74–81, 179, 193)

Pristiphora pallipes Serville, 1823: 75.

Pristiphora pallipes Lepeletier, 1823: 60.

Tenthredo pallicornis T.W. Harris, 1835: 583.

Tenthredo labrata T.W. Harris, 1835: 583.

Nematus flavipes Dahlbom, 1835: 25-26.

Nematus appendiculatus Hartig, 1837: 202-203.

Nematus fuscicornis Hartig, 1837: 225.

Diphadnus fuscicornis (Hartig, 1837) – Hartig, 1840: 28.

Nematus enervis Herrich-Schäffer, 1840: 176.

Nematus cathoraticus Förster, 1854: 325-326.

Nematus pallicornis Norton, 1861: 160.

Pristiphora grossulariae Walsh, 1866: 123.

Nematus peletieri André, 1880a: 111.

Cryptocampus fuscicornis (Hartig, 1837) – André, 1880b: 87.

Nematus hypobalius Zaddach in Brischke, 1884: 154.

Nematus pumilus Zaddach in Brischke, 1884: 172.

Amauronematus hypobalius (Zaddach, 1884) – Konow, 1890: 246.

Nematus ghilianii Costa, 1894: 73.

Pontania pallicornis (Norton, 1861) – Konow, 1905: 53.

Nematus pallipes (Lepeletier, 1823) – Zhelochovtsev and Zinovjev, 1988: 157.

Pristiphora anivskiensis Haris, 2006: 194-195.

Diagnosis. The shiny, smooth mespostnotum (e.g. Fig. 2) distinguishes both sexes of this species from all other Nearctic species in the *ruficornis* group. The following combination of characters should additionally permit females to be easily distinguished from all other Nearctic species of *Pristiphora*: antennae relatively pale (flagellum brown dorsally and pale ventrally), head dark, hindfemur either entirely brown or pale in apical half, mesepisternum shiny and smooth, and sawsheath very wide in apical view (width 0.9x height of setose area), deeply emarginate in dorsal view (Fig. 77), and with lateral posterior lobe considerably more produced than median carina. Males are easily recognized by the structure of the penis valve, with large, bent valvispina that is about as long as the apical margin of paravalva, with which it forms an acute angle (Fig. 193).

Female. Length, 5.0–6.0 mm.

Colour: Antenna dark; head dark; mouthparts pale brownish, mandible translucent brown except dark near base and apex; labrum pale except brown basomedially. Thorax dark; pronotum posterior corner sometimes with margins broadly pale; tegula yellow. Legs pale, except coxae brown except narrow apical ring (fore coxa) to apical third (middle and hind coxa) pale, foreleg with basal half of femur ventrally yellow-brown, first three tarsomeres with narrow apical ring and apical two tarsomeres entirely brown, midleg with as on foreleg, hindleg with femur variable, entirely pale, basal half dark ventrally, or entirely dark except narrow apical ring pale,

tibia usually with narrow dorsoapical spot dark. Abdomen dark or dark brown, valvifer 2 brown or yellow-brown, cerci yellow-brown.

Head: Antenna length 2.0–2.3x head width; F1 0.8–0.9x length of eye; F1 longer than F2 (F1:F2 = 1.1–1.2x), longer than F3 (F1:F3 = 1.2x), proceeding flagellomeres progressively shorter (F7:F1 = 0.7x). Clypeus truncate. Malar space 0.8–1.0x OD. LOD 1.4–1.5x height of eye in frontal view. IOC:OOL = 1.2–1.4x. Head shiny, microsculpture smooth.

Thorax: Pronotum somewhat dull, weakly imbricate. Prepectus distinct, but weakly sclerotized, weakly pitted/rough texture; glabrous, or at most with a few setae. Mesepisternum shiny, microsculpture smooth, epicnemium shiny, microsculpture smooth, sometimes with weak horizontal lineations. Mesepimeron shiny, smooth. Mesonotum shiny, microsculpture smooth. Parapsis shiny, weakly costulate/puncticulate. Mesopostnotum shiny, microsculpture smooth to shallowly/weakly puncticulate. Metabasitarsus approximately same length as metatarsomeres 2–4 combined. Tarsal claw simple, without subapical tooth.

Abdomen: Terga somewhat dull, imbricate. Sawsheath in dorsal view emarginate deeply, with distinct median carina, longest setae about two-thirds as long as apical width of sawsheath, visible length of sawsheath about the same length as cerci. Sawsheath in lateral view with lower margin weakly rounded, sometimes appearing linear or weakly concave at level of setose area, meeting dorsal margin at rounded apex. Valvula 3 lateral posterior lobe produced. In apical view, width of sawsheath about 0.9x height of setose area. Tangium of lancet approximately triangular, narrowing apically; tangial process present as an oblique sclerotized band apparently distinct from tangium. Lancet with basal one or two sutures weakly sigmoid, proceeding sutures sigmoid to approximately straight; annuli without or with only a few setae; serrulae protruding, basoventral angle rounded-right; small spiny pectines absent from sclerora.

Male. Length, 4.1–5.0 mm.

Colour as in female except as follows. Antenna brown, pale ventrally, with stout setae; labrum brown apical margin. Legs variable, pale as in female to much darker, except coxae entirely dark, foreleg with basal half of femur dark, midleg with basal half of femur dark, hindleg with femur with all but apical one-quarter to broad apical ring pale. Abdomen dark or dark brown. Structure and sculpture similar to female, except: F1 0.8–0.9x length of eye, F1 longer than F2 (F1:F2 = 1.05–1.1x), longer than F3 (F1:F3 = 1.1x), proceeding flagellomeres progressively shorter (F7:F1 = 0.85x); head variable, from shiny, microsculpture smooth to dull, imbricate; mesonotum variable, from shiny, microsculpture smooth to dull, imbricate, mesoscutellar appendage variable, from shiny, microsculpture smooth to dull, imbricate. T8 apical margin weakly produced and convex medially. Penis valve with paravalva broad apically, valvispina large, broad, very strongly bent, about as long as apical margin of paravalva, with which it forms an acute angle; pseudoceps simple; valvura without ergot.

Material studied. *Lectotype* ♀ (images)—**GERMANY**: Germany (ZSM). *Holotype* (♂) of *anivskiensis* (images)—**RUSSIA**: Sakhalin Oblast, Anivsky District, Novo-Alekszandrovsk (HNHM,). *Lectotype* (♀) of *cathoraticus* (images)—**GERMANY**: North Rhine-Westphalia, Aachen (ZSM). *Additional material*—**CANADA**: **AB**: Miette Rd, J.N.P., *53.170° -117.820°*, 13.vii.1950, coll. unknown, A556A, 1 ♀ (NFRC); **BC**: Agassiz, *49.233° -121.767°*, 6.vi.1921, R.Glendenning, 1 ♀ (NFRC); Vancouver, *49.250° -123.117°*, 3.vii.1933, H.B.Leech, 1 ♀ (CNC); **ON**: Kearney, *45.556° -79.225°*, 2-9.vii.1909, M.C.VanDuzee, 1 ♂ (CASC); Leeds and Grenville, Elizabethtown-Kitley, 4452 Rowsome Rd., 44.621° -75.773°, 112m, 14-16.vii.2010, James Sones, Malaise trap, BIOUG01093-B05, 1 ♀ (BIOUG); Leeds and Grenville, Elizabethtown-Kitley, 4452 Rowsome Rd., 44.621° -75.773°, 112m, 22.iv.2010, James Sones,

Malaise trap, BIOUG01022-B06, 1 ♀ (BIOUG); Milton, Craig Kielburger Secondary School, 43.5142° -79.83°, 196m, 22.iv-5.v.2014, Scott Cates, Malaise trap, BIOUG13128-A01, 1 ♀ (BIOUG); **QC**: Oka, 22.vi.1980, A.T.Finnamore, 1 ♀ (LEMU); Ste. Anne de Bellevue, 10.vii.1963, V.R.Vickery, 1 ♀ (LEMU); **USA**: **CO**: Ft. Collins, *40.585*° *-105.084*°, 17.v.1901, coll. unknown, gooseberry, 1 ♀ (USNM); Ft. Collins, *40.585*° *-105.084*°, 8.vi.1899, coll. unknown, 2 ♀ (USNM); Green Mt. Falls, *38.935*° *-105.017*°, 8.viii.1943, H.H.Ross, 1 ♀ (NFRC); **ID**: Parma, *43.785*° *-116.943*°, 678m, 1.vi.1928, C.Wakeland, slide prep: penis valves, 1 ♂ (NFRC); **IL**: Rock Island, *41.509*° *-90.579*°, 3.vi.1930, Frison, Ross, 1 ♀ (NFRC); **MI**: Dickinson Co., Channing, 13.vi.1983, R.L.Fischer (USNM); **NM**: Sandoval County, Valles Caldera Nat'l Preserve, N. of Alamo Cnyon, E. side, "The Grotto", VC08, 35.92888° -106.5939°, 22.vii.2008, Parmenter et al., SEL Hym unit, Malaise trap, 2 ♀ 3 ♂ (USNM); idem except 9.vii.2008, 1 ♂ (USNM); idem except 30.vii.2008, 2 ♀ (USNM); idem except 26.vi.2009, 1 ♀ (USNM); idem except 27.viii.2009, 1 ♂ (USNM); **TN**: Sevier Co., GRSM ATBI plot, Clingmans Dome, 35.56028° -83.41194°, Malaise trap, 16.iv.2001, I.C.Stocks, MT1620010524, 1 ♂ (USNM); **WV**: Tucker Co., Fernow Expt. Forest, 39.05° -79.667°, 29.vii-7.viii.1992, E.M.Barrows, Malaise trap, 1 ♀ (USNM); **WY**: Albany Co., Medicine Bow Ntl. For., Curtis Gulch Campgrnd., T28N–R73W–Sec. 8, 8-10.vii.1974, R.L. Fischer, 1 ♀ (USNM).

Distribution. Holarctic. In the Nearctic, this species is found across cool-temperate parts of Canada and the United States, extending south along the Rocky Mountains in the West and the Appalachians in the East. It is recorded from British Columbia, Alberta, Saskatchewan (Goulet and Bennett 2021), Ontario, Quebec, Idaho, Wyoming, New Mexico, Michigan, Illinois, Tennessee and West Virginia.

Genetic data. Specimens of this species are divided among two BINs: BOLD:AAG7866 and BOLD:AAU8684. Based on available genetic data (two Palaearctic and one Nearctic specimen), maximum within-species divergence is 3.1% and the nearest neighbour (*P. luteipes*) is 8.4% different.

Hosts. *Ribes* spp. (D. R. Smith and Strazanac 2016). In the Palaearctic, this species is additionally recorded from *Ribes alpinum* L., *R. aureum* Pursh, *R. nigrum* L., *R. rubrum* L., *R. sanguineum* Pursh, *R. spicatum* Robs., and *R. uva-crispa* L. emend. Lam. (Prous et al. 2017).

Comments. Females of this species are easily differentiated from all other *Pristiphora* by their ventrally pale antennae, shiny and smooth mesepisternum, and wide and deeply emarginate sawsheath. The only other nematine associated with *Ribes* in the Nearctic is *Euura ribesii* (D. R. Smith and Strazanac 2016), which is easily differentiated as follows: adults with inner orbits and area behind eyes brownish or pale, all femora mostly or entirely pale, female abdomen mostly pale, male abdomen ventrally pale (same parts dark in *P. appendiculata*); larvae with black spots covering body, otherwise bluish green with contrasting yellow rings near anterior and posterior ends (body more-or-less uniformly green in *P. appendiculata*).

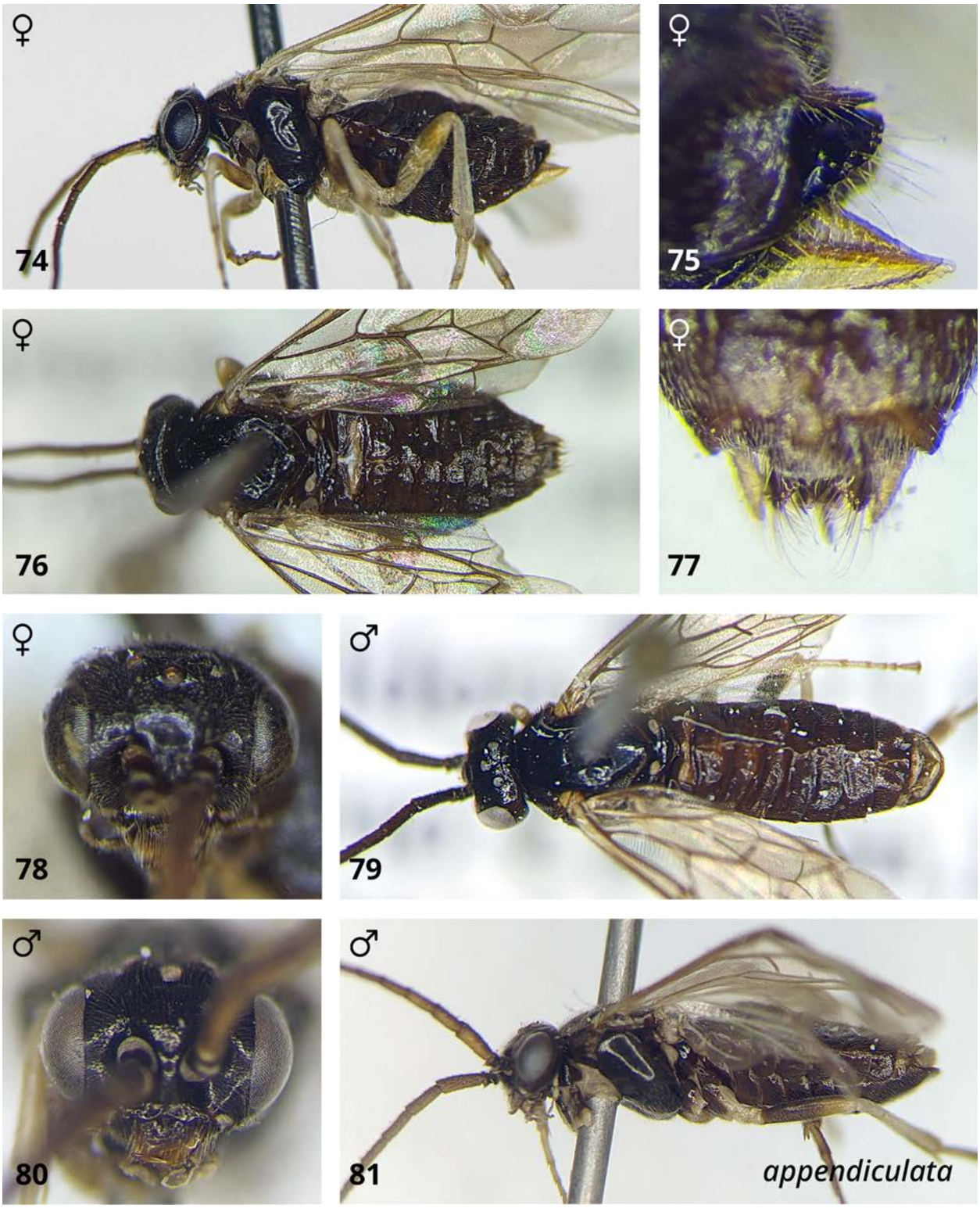

Figures 74–81. *Pristiphora appendiculata*. **74**. Female lateral view. **75**. Sawsheath lateral view. **76**. Female dorsal view. **77**. Sawsheath dorsal view. **78**. Female head. **79**. Male dorsal view. **80**. Male head. **81**. Male lateral view.

***Pristiphora elaphita* Wong & Ross, 1960**

(Figs. 82–86, 180)

Pristiphora elaphita Wong & Ross, 1960: 194.

Diagnosis. Females of this species can be differentiated from most other Nearctic species in the *ruficornis* group by their rough surface sculpture with head dull, imbricate and mesepisternum and mesonotum rough, coarsely imbricate to scabrous-coriaceous (e.g. Figs. 3–4;one or more of these body areas shiny, microsculpture smooth or weakly imbricate in other species, e.g. Fig. 2), and tarsal claw with small subapical tooth, less than half as long as apical tooth (e.g. Fig. 172; at least half as long as apical tooth in others, e.g. Figs. 173–174). This combination of characters differentiates females of *P. elaphita* from all but *P. kangirsummiut*, *P. nigra*, *P. sootryeni*, and *P. staudingeri*, from which it can be differentiated by its lancet, with large tangium about twice as long as high (Fig. 180; in *P. nigra* and *P. sootryeni* tangium smaller, at least three times longer than high, Figs. 186, 189), and large tangial process, extending twice as high as tangium (only extending slightly higher than tangium in *P. kangirsummiut* and *P. staudingeri*, Figs. 183, 190). The lancet is very similar to that of *P. hucksena*, but *P. elaphita* has a less robustly sclerotized tangial process (more strongly sclerotized and folded back on itself in *P. hucksena*, Fig. 182), rough mesepisternum with microsculpture coarsely imbricate to scabrous-coriaceous (shiny, microsculpture smooth in *P. hucksena*) and dark femora (mostly pale in *P. hucksena*). Males are unknown.

Female. Length, 5.4–6.5 mm.

Colour: Antenna dark, slightly paler ventrally; head dark; mouthparts dark brown, mandible translucent brown except dark near base and apex; labrum translucent brown. Thorax dark;

tegula translucent dark brown. Legs dark, except coxae narrow apical ring (fore and middle coxa) to as much as apical half (hind coxa) pale, trochanters and trochantelli pale, foreleg with femur apical one-third, tibia, and tarsus pale, except apical half of apical tarsomere brown and sometimes tibia with narrow apical ring brown, midleg with femur narrow apical ring, tibia, and tarsus pale, except apical tarsomere brown, hindleg with tibia pale except broad apical ring dark brown, basal half of first tarsomere pale. Abdomen dark or dark brown, cerci yellow-brown.

Head: Antenna length 2.3–2.4x head width; F1 0.85–0.95x length of eye; F1 subequal to F2 (F1:F2 = 1.0x), longer than F3 (F1:F3 = 1.1x), proceeding flagellomeres progressively shorter (F7:F1 = 0.7x). Clypeus truncate/shallowly widely emarginate. Malar space 1.1–1.2x OD. LOD 1.5x height of eye in frontal view. IOC:OOL = 1.25–1.3x. Head dull, imbricate.

Thorax: Pronotum rough, coarsely imbricate. Prepectus distinct & pitted, setose. Mesepisternum rough, coarsely imbricate to scabrous-coriaceous, epicnemium shiny, microsculpture smooth with few weak horizontal lines. Mesepimeron shiny, microsculpture smooth. Mesonotum rough, coarsely imbricate to scabrous-coriaceous. Parapsis shiny, weakly costulate/puncticulate. Mesopostnotum rough, coarsely imbricate. Metabasitarsus shorter than metatarsomeres 2–4 combined. Subapical tooth of tarsal claw small, less than half as long as apical tooth.

Abdomen: Terga dull, imbricate. Sawsheath in dorsal view emarginate or truncate depending on angle, with distinct median carina, longest setae about two-thirds as long as apical width of sawsheath, visible length of sawsheath about the same length as cerci. Sawsheath in lateral view with lower margin evenly rounded, meeting dorsal margin at a sub-quadrate apex. Valvula 3 lateral posterior lobe produced & continuing medially along posterodorsal margin as a carinate ridge, which is shorter submedially. In apical view, width of sawsheath about 0.9x height of

setose area. Tangium of lancet large, basally almost as high as radix, subapically about twice as long as high; tangial process tall, extending twice as high as tangium and somewhat weakly sclerotized. Lancet with basal one or two sutures straight or weakly sigmoid, proceeding sutures distinctly sigmoid; annuli with numerous setae, one-third to half width of corresponding annulus; serrulae somewhat protruding, basoventral angle rounded-right; small spiny pectines absent from sclerora.

Material studied. *Holotype* ♀ (images)—CANADA: SK: Glaslyn, 28.vi.1952, F.I.S.: W-1367 (CNC). *Additional material*—**USA**: **AK**: Unalakleet, *63.873° -160.788°*, 28.vi.1961, B.S.Heming, slide prep: ovipositor, 1 ♀ (CNC); **CA**: Upper Santa Ana River, 25.vi.1948, A.L.Melander, 1 ♀ (USNM); **NM**: Beulah, 8000', date unknown, Cockerell, 1 ♀ (USNM).

Distribution. This species occurs from Alaska south along the Western Cordillera to California and New Mexico, as well as in Saskatchewan. It is recorded from Alaska, British Columbia, Alberta, Saskatchewan, California, and New Mexico (D. R. Smith 1979, Goulet and Bennett 2021).

Genetic data. None available.

Host. Unknown.

Comments. Males of this species are unknown, but a single male apparently belonging to the same subgroup – but markedly different from any other described male in the *ruficornis* group – is known from British Columbia. The male of the co-distributed species *P. hucksena* is also unknown but given that species' close relationship to *P. luteipes* it is perhaps more likely that the undescribed male is either conspecific with *P. elaphita* or represents a separate, undescribed species.

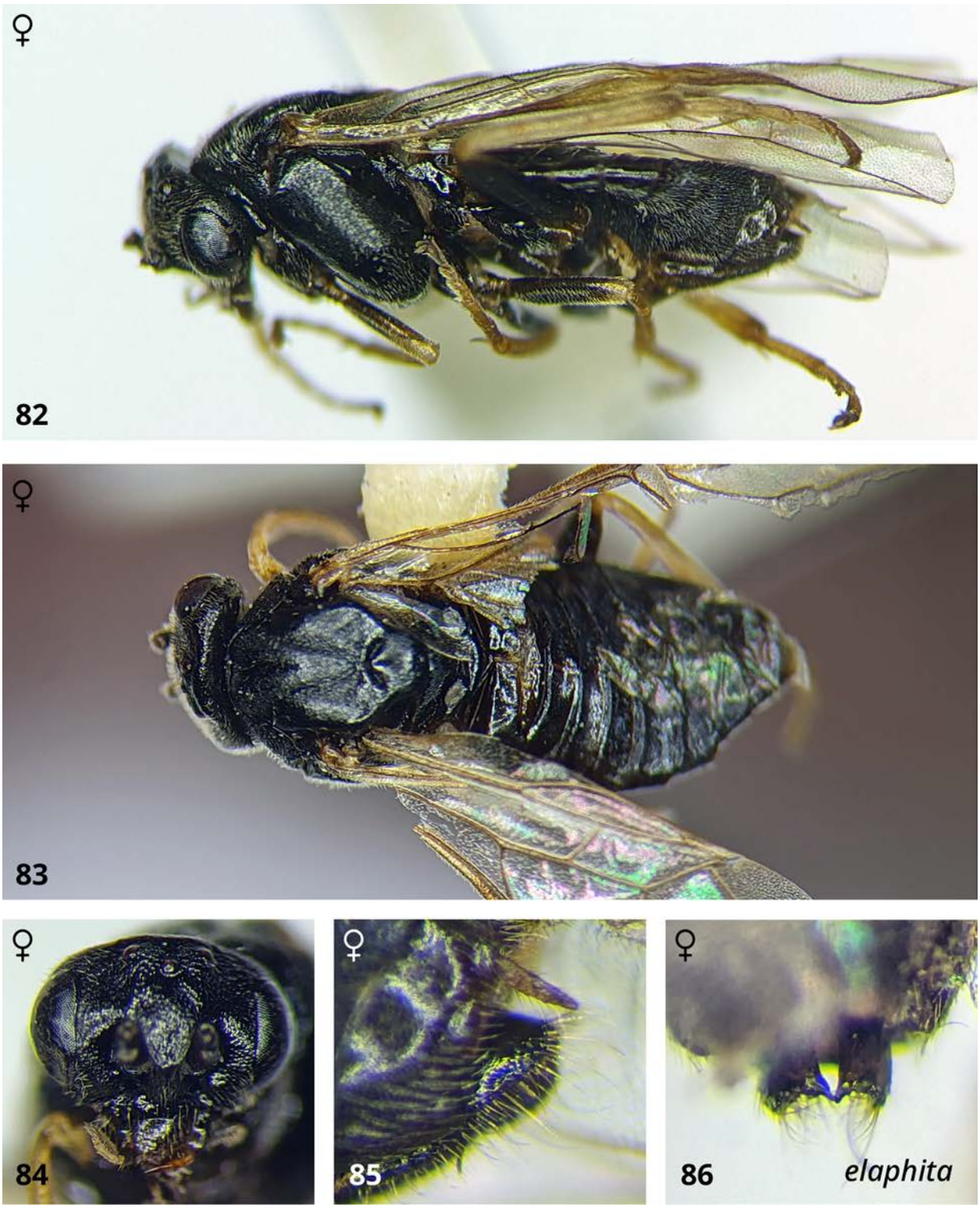

Figures 82–86. *Pristiphora elaphita*. **82**. Female lateral view. **83**. Female dorsal view. **84**. Female head. **85**. Sawsheath lateral view. **86**. Sawsheath dorsal view.

***Pristiphora frigida* (Boheman, 1865)**

(Figs. 2, 50, 87–94, 174, 181, 194)

Nematus frigidus Boheman, 1865: 568-569.

Pristiphora adelungi Konow, 1902: 167-168.

Pristiphora gelida Wong, 1968b: 185.

Diagnosis. Individuals of both sexes of *P. frigida* can be differentiated from all other Nearctic species in the *ruficornis* group by their smooth surface sculpture with head, mesepisternum, and mesonotum shiny, microsculpture smooth (Fig. 2; one or more of these body areas dull, imbricate or rough, scabrous-coriaceous in other species, e.g. Figs. 3–4), and large subapical tooth of tarsal claw, which is wider and about two-thirds as long as apical tooth (Fig. 174; at most about half as long as apical tooth in other species, e.g. Figs. 172–173). This combination of characters should reliably distinguish *P. frigida* from all but *P. aphanta* and *P. maura*, which have tarsal claws with subapical tooth about half as long as apical tooth. From these two, females of *P. frigida* can be differentiated by the shiny pronotum, microsculpture smooth (dull, imbricate in *P. aphanta* and *P. maura*); males can be differentiated from *P. aphanta* by the entirely dark antennae (pale ventrally in *P. aphanta*), and from *P. maura* by F1 approximately 1.3x height of eye in lateral view (0.8–0.9x in *P. maura*). The lancet of *P. frigida* (Fig. 181) is most similar to *P. melanocarpa* and *P. siskiyouensis* (Figs. 185, 188), with broad tangium, distinct tangial process, and rounded basoventral angle, but *P. frigida* has more and longer setae on the annuli, one-quarter to one-third width of annulus (few very short setae in *P. melanocarpa* and *P. siskiyouensis*). The penis valve of *P. frigida* (Fig. 194) also resembles those of *P. melanocarpa* and *P. siskiyouensis* (Figs. 197, 201), with all three species having a membranous fold on the

pseudoceps near the tip of the valvispina, but in *P. frigida* the pseudoceps lacks a convex bump on its ventral margin (present in *P. melanocarpa* and *P. siskiyouensis*), and the valvispina is less strongly curved compared to the other two species and intermediate in width (narrower in *P. melanocarpa*, broader in *P. siskiyouensis*).

Female. Length, 4.0–5.5 mm.

Colour: Antenna dark, sometimes slightly paler ventrally; head dark; mouthparts dark brown, mandible apical half translucent brown except dark apex; labrum brown; head behind eyes sometimes with dark brown areas behind eyes. Thorax dark; tegula sometimes translucent brown. Legs dark, except, trochanters and trochantelli apical margins narrowly brown, foreleg with femur broad apical ring to apical one-third, tibia basal three-quarters, basal half of first tarsomere pale, remainder of tarsus yellow-brown ventrally, midleg with femur narrow apical ring and tibia with at least basal quarter pale, tibia otherwise pale-infuscate with apical quarter brown, hindleg with femur narrow apical ring and tibia basal two-thirds to three-quarters pale, tibia sometimes pale-infuscate. Abdomen dark or dark brown, cerci brown or yellow-brown.

Head: Antenna length 2.4–2.5x head width; F1 0.75x length of eye; F1 subequal to or slightly shorter than F2 (F1:F2 = 0.95–1.0x), subequal to or slightly shorter than F3 (F1:F3 = 0.95–1.0x), proceeding flagellomeres progressively shorter (F7:F1 = 0.9x). Clypeus truncate. Malar space 1.0–1.4x OD. LOD 1.5–1.7x height of eye in frontal view. IOC:OOL = 1.2–1.4x. Head shiny, microsculpture smooth.

Thorax: Pronotum shiny, smooth. Prepectus distinct & pitted, setose, may be weakly sclerotized and light in colour. Mesepisternum shiny, microsculpture smooth, epicnemium shiny, microsculpture smooth, sometimes with weak horizontal lineations. Mesepimeron shiny,

microsculpture smooth. Mesonotum shiny, microsculpture smooth or very weakly imbricate. Parapsis shiny, weakly imbricate/puncticulate ventrally, mostly smooth dorsally. Mesopostnotum somewhat dull, imbricate. Metabasitarsus shorter than metatarsomeres 2–4 combined. Subapical tooth of tarsal claw large, about two-thirds as long as and wider than apical tooth.

Abdomen: Terga shiny, weakly imbricate. Sawsheath in dorsal view emarginate, not especially carinate medially, longest setae about as long as apical width of sawsheath, visible length of sawsheath less than cerci. Sawsheath in lateral view with lower margin evenly rounded, meeting dorsal margin at a broadly rounded apex. Valvula 3 lateral posterior lobe produced & continuing medially along posterodorsal margin as a carinate ridge, which is shorter submedially. In apical view, width of sawsheath about 0.8x height of setose area. Tangium of lancet large, almost as high as wide with rounded basoventral angle; tangial process extending above tangium by one-third of its height. Lancet with basal one to three sutures approximately straight, at most first suture weakly recurved, proceeding sutures approximately sigmoid; annuli with numerous setae, one-quarter to one-third width of corresponding annulus; basal serrulae not especially protruding, basoventral angle rounded-obtuse, apical serrulae flat, basoventral angle rounded-acute; small spiny pectines absent from sclerora.

Male. Length, 4.2–5.0 mm.

Colour as in female except as follows. Antenna dark, without stout black setae (some setae appear slightly thicker, darker, but these are very difficult to discern). Legs as in female, except mid and hind tibiae dark yellow-brown, except. Structure and sculpture similar to female, except: F1 1.3x length of eye , gena at least somewhat dull, imbricate; pronotum at least somewhat dull, imbricate; , mesopostnoum dull, imbricate. T8 apical margin weakly produced and convex medially. Penis valve with valvispina long, somewhat slender, strongly bent, apex nearly

perpendicular to longitudinal axis of penis valve; pseudoceps weakly produced apically, dorsal margin with distinct fold of membrane near apex of valvispina; valvura without ergot.

Material studied. *Lectotype* ♂ (images)—NORWAY: Svalbard, Spitsbergen Island, Middel Hook in Belsund, 19.vi.1899 (NHRS). *Lectotype* (♀) of *adelungi* (images)—NORWAY: Svalbard, Spitsbergen Island, Hornsund, 19.vi.1899 (ZIN). *Paralectotype* (♂) of *adelungi* (images): Same data as lectotype, slide prep: genitalia (ZIN). *Holotype* (♂) of *gelida*—**USA**: **AK**: Pt. Barrow, 6.vii.1952, P.D.Hurd (USNM). *Allotype* (♀) of *gelida*—Same data as holotype, except 30.vi.1952 (USNM). *Paratypes* (1 ♂ 2 ♀) of *gelida*—Same data as holotype, except 27.vi.1953, 1 ♂ (USNM); idem, 1 ♂ 1 ♀ (CNC). *Additional material*—**CANADA**: **AB**: Sunshine Lodge, Banff, 24-27.vii.1962, Mason, Malaise trap, 1 ♂ (CNC); **BC**: Finlay - Russel P.P. & Protected Area, base camp area, 57.35282° -125.93591°, 1771m, 29.vii.2014, R.Bennett, C. & D.Copley, ENT014-013891, 1 ♂ (RBCM); Mt Simpson, unnamed peak nearby, 59.7282° -131.2887°, 1702m, 5.vii.2017, R.Bennett, C. & D.Copley, ENT017-006231, 1 ♀ (RBCM); **NU**: Kanngiqtugaapik [Clyde, Baffin Is.], 4.vii.1958, J.E.H.Martin, 1 ♂ (CNC); **USA**: **AK**: Atkasook, Meade River, 30.467° -157.4167°, 24.vi.1977, T.S.Jensen, 1 ♀ (USNM); idem except 29.vi.1976, 1 ♀ (USNM).

Distribution. Holarctic. In the Nearctic, this species has an arctic-alpine distribution in the North and along the Western Cordillera. It is recorded from Alaska, Yukon, Northwest Territories, Nunavut, Alberta, and Colorado (D. R. Smith 1979, Goulet and Bennett 2021).

Genetic data. Specimens of this species belong to a single BIN: BOLD:AAY6900. Based on available genetic data (one Nearctic specimen) the nearest neighbour (*P. luteipes*) is 4.3% different.

Host. Unknown.

Comments. The slide-mounted penis valves of the holotype of *gelida* look quite different from those typical of *P. frigid*a, but examination of the paratypes of *gelida* and additional Nearctic specimens of *P. frigida* makes it clear that this is an artifact of slide preparation, resulting from the normally folded pseudoceps being flattened out and the valvispina slightly rotated about its longitudinal axis.

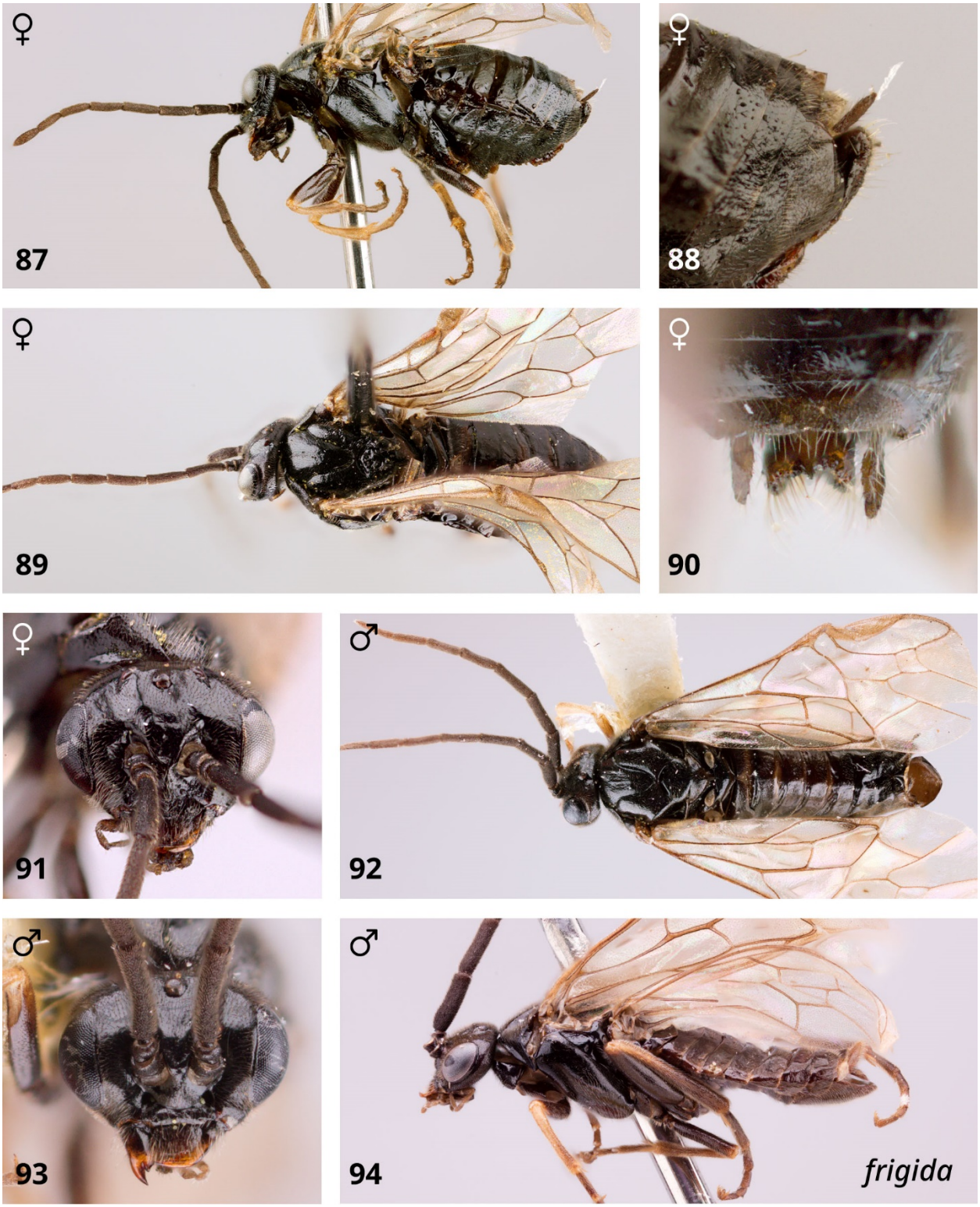

Figures 87–94. *Pristiphora frigida*. **87**. Female lateral view. **88**. Sawsheath lateral view. **89**. Female dorsal view. **90**. Sawsheath dorsal view. **91**. Female head. **92**. Male dorsal view. **93**. Male head. **94**. Male lateral view.

***Pristiphora hucksena* Wong & Ross, 1960**

(Figs. 95–99, 182)

Pristiphora hucksena Wong & Ross, 1960: 194.

Diagnosis. Females of this species can usually be separated from other Nearctic species in the *ruficornis* group by colouration: legs entirely pale except base of coxae, apex of hind tibia, hind tarsus (dark colouration more extensive in all others except *P. appendiculata*), labrum usually pale, scape usually mostly pale brown. Specimens with a darker labrum and scape may be confused with *P. appendiculata* but can be differentiated by the sawsheath with lateral posterior lobe continuing medially along posterodorsal margin (absent dorsomedially in *P. appendiculata*) and roughly textured mesopostnotum (e.g. Fig. 4; shiny, microsculpture smooth in *P. appendiculata*, e.g. Fig. 2). The lancet is very similar to that of *P. elaphita*, but *P. hucksena* has a more robustly sclerotized tangial process, which is folded back on itself (Fig. 182; less strongly sclerotized and not appearing folded in *P. elaphita*, Fig. 180), shiny mesepisternum with microsculpture smooth (rough and coarsely imbricate to scabrous-coriaceous in *P. elaphita*) and extensively pale femora (mostly dark in *P. elaphita*). Males are unknown.

Female. Length, 5.0–6.0 mm.

Colour: Antenna dark, scape usually pale apically; head dark; mouthparts pale brownish, mandible translucent brown except dark near base and apex; labrum variable: pale, dark, or dark with apical margin translucent brown. Thorax dark; tegula translucent yellow. Legs pale, except coxae basolateral corner with margins narrowly dark, foreleg with usually with apical two to three tarsomeres brown, midleg with apical two to three tarsomeres brown, hindleg with tibia

narrow apical ring and tarsus brown or dark, except basal half of first tarsomere pale. Abdomen dark or dark brown, cerci often yellow-brown, sometimes dark.

Head: Antenna length 2.5x head width; F1 0.95–1x length of eye; F1 longer than F2 (F1:F2 = 1.05–1.2x), longer than F3 (F1:F3 = 1.1–1.3x), proceeding flagellomeres progressively shorter (F7:F1 = 0.65x). Clypeus shallowly widely emarginate. Malar space 1.3–1.5x OD. LOD 1.4–1.5x height of eye in frontal view. IOC:OOL = 1.1–1.2x. Head shiny, microsculpture smooth to somewhat dull, imbricate, vertexal area shiny, weakly imbricate medially; dull and more strongly imbricate laterally.

Thorax: Pronotum dull, imbricate. Prepectus distinct & pitted, setose. Mesepisternum shiny, microsculpture smooth, epicnemium shiny, microsculpture smooth with few weak, confused lineations. Mesepimeron anepimeron dull, rugulose, except somewhat shiny and weakly imbricate in anteroventral corner; katepimeron mostly shiny, weakly imbricate, except for a somewhat dull, weakly ruguloe posteromedial spot. Mesonotum somewhat dull, weakly imbricate; mesoscutellum shiny to somewhat dull, microsculpture weakly imbricate to roughly imbricate around posterior & posterolateral edges; mesoscutellar appendage dull, pitted and rugulose. Parapsis shiny, weakly costulate/puncticulate. Mesopostnotum rough, coarsely imbricate. Metabasitarsus approximately same length as or slightly longer than metatarsomeres 2–4 combined. Subapical tooth of tarsal claw small, less than half as long as apical tooth.

Abdomen: Terga somewhat dull, imbricate. Sawsheath in dorsal view emarginate or truncate depending on angle, with distinct median carina, longest setae 0.8-0.9x as long as apical width of sawsheath, visible length of sawsheath less. Sawsheath in lateral view with lower margin evenly rounded, meeting dorsal margin at a sub-quadrate apex. Valvula 3 lateral posterior lobe produced & continuing medially along posterodorsal margin as a carinate ridge. In apical view, width of

sawsheath 0.6-0.7x height of setose area. Tangium of lancet large, 1.6-1.8x as long as high; tangial process large and robust, with distinct membranous fold. Lancet with basalmost one or two sutures approximately straight, proceeding sutures distinctly sigmoid; annuli with numerous setae, one-quarter to half width of corresponding annulus; serrulae somewhat protruding, basoventral angle rounded-right; small spiny pectines absent from sclerora.

Material studied. *Holotype* ♀—**CANADA**: **BC**: Vancouver, 49.25, -123.13333, 24.iv.1931, H.H. Ross, slide prep: ovipositor (INHS). *Additional material*—**CANADA**: **BC**: Hatzic Lake, 24.vii.1953, W.R.M.Mason, 1 ♀ (CNC); Mission City, 18.vii.1953, W.R.M.Mason, 1 ♀ (CNC); Vancouver I., Saanich, Mt. Newton, 6-13.viii.1993, D.Blades, Malaise trap, ENT93-2232, 1 ♀ (RBCM); **NU**: Taloyoak [Spence Bay], *69.533° -93.536°*, 30.vi.1951, A.E.R.Downe, slide prep: ovipositor, 1 ♀ (CNC).

Distribution. This specimen has a restricted arctic-alpine distribution. It is known only from the mountains of British Columbia and from Nunavut.

Genetic data. Based on available genetic data (one specimen) the nearest neighbour (*P. luteipes*) is 0.6% different.

Host. Unknown.

Comments. Based on genetic data, *P. hucksena* may be synonymous with the Palaearctic species *P. luteipes*. Available images in ECatSym (Taeger et al. 2018) show that the two species have near-identical lancets, and both have a shiny mesepisternum, shiny to somewhat dull head, and extensively pale legs. Males of *P. hucksena* are unknown, but the penis valve of *P. luteipes* closely resembles that of *P. staudingeri*, so one might expect the same for this species.

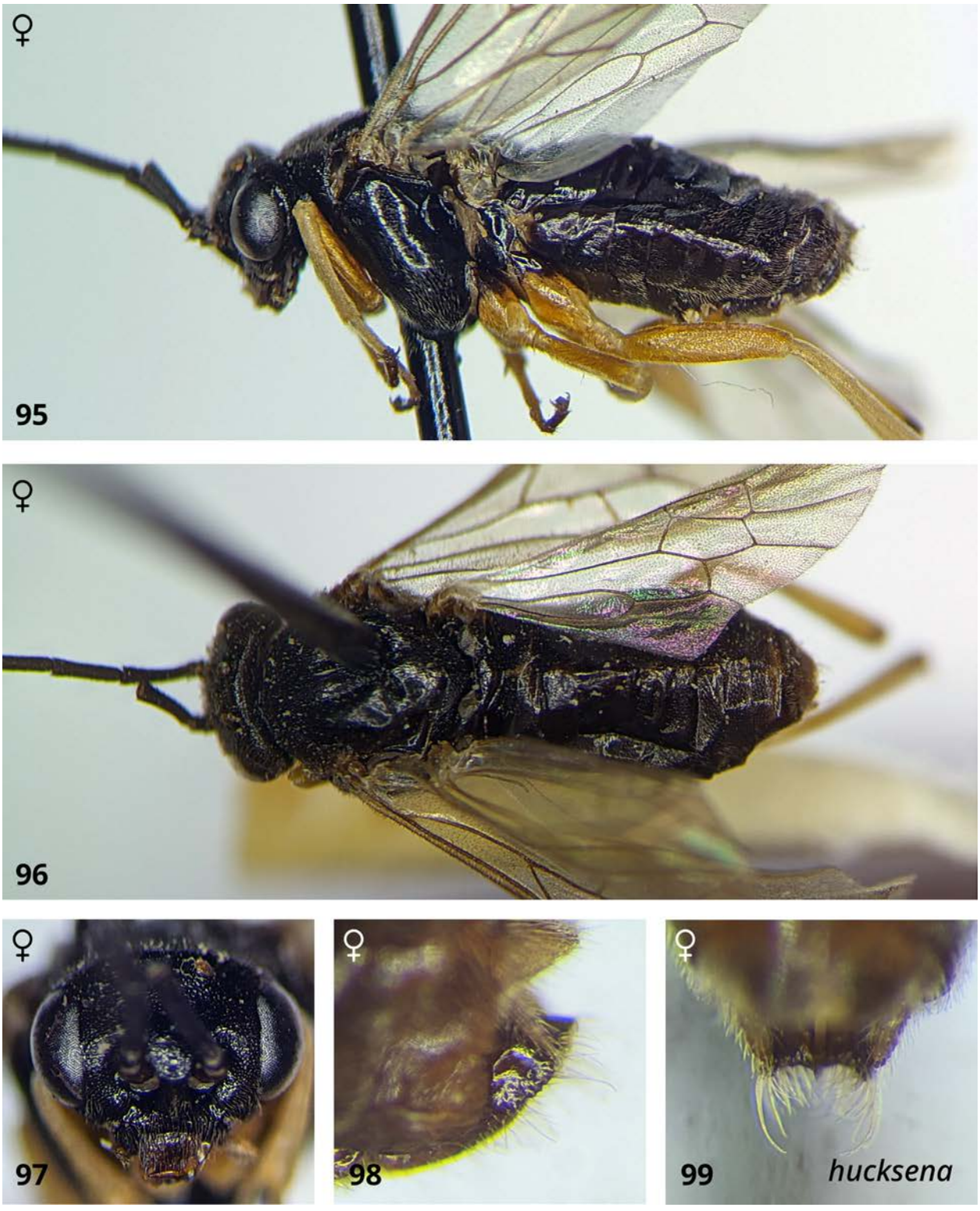

Figures 95–99. *Pristiphora hucksena*. **95**. Female lateral view. **96**. Female dorsal view. **97**. Female head. **98**. Sawsheath lateral view. **99**. Sawsheath dorsal view.

***Pristiphora kangirsummiut* Monckton, n. sp.**

(Figs. 4, 100–107, 175, 183, 195)

Diagnosis. Females are most similar to *P. staudingeri*, with which they share: head rough, coarsely imbricate, mesepisternum rough, coriaceous (e.g. Fig. 4; head and mesepisternum dull, imbricate or shiny, microsculpture smooth in most other species, e.g. Figs. 2–3), tangium of lancet large, about twice as long as high (Fig. 183; longer and shorter in most other species), and tangial process extending only slightly higher than tangium (*P. elaphita* has a similarly-shaped tangium, but its tangial process extends twice as high as tangium, Fig. 180). Compared to *P. staudingeri*, the lancet of *P. kangirsummiut* has shorter setae on annuli, one-third width of annulus or less (one-third to half as long as annulus in *P. staudingeri*, Fig. 190), and the first and usually second suture are distinctly recurved dorsally (approximately straight in *P. staudingeri*). As well, compared to *P. staudingeri*, the lancet of *P. kangirsummiut* has less sharply pointed serrulae, with cypsellae absent between apical-most serrulae (present in *P. staudingeri*), and the sawsheath appears more slender in lateral view, with the lower margin straighter (lower margin evenly rounded in *P. staudingeri*, giving sawsheath broadly rounded appearance in lateral view). Males can be separated from all but *P. nigra*, *P. sootryeni*, and *P. staudingeri* by the rough sculpturing of the head and mesepisternum as in female; *P. kangirsummiut* and *P. staudingeri* can be separated from *P. nigra* and *P. sootryeni* by the harpes of the genital capsule, which are relatively long and rectangular, overlapping medially at rest (Figs. 172–173; at most meeting medially in other species, Fig. 174) and by the penis valve, with valvispina less strongly curved (Fig. 195; semicircular in *P. nigra*, Fig. 198; more abruptly curved in *P. sootryeni*, Fig. 202), and pseudoceps more rectangular in shape with dorsal margin weakly rounded (in *P. nigra* and *P. sootryeni* rounder with dorsal margin broadly rounded). The valvispina of *P. kangirsummiut* has

a distinct, bulbous, enlarged section where it bends dorsally (at most widened in *P. staudingeri*, lacking bulbous shape, Fig. 203).

Female. Length, 4.3–4.8 mm.

Colour: Antenna dark; head dark; mouthparts dark brown, mandible translucent brown except dark near base and apex; labrum apical margin dark brown. Thorax dark; tegula apical margin narrowly brown. Legs dark, except, foreleg with femur apical quarter, tibia, and tarsus pale, except apical two to three tarsomeres dark brown, midleg with femur narrow apical ring, tibia, and tarsus pale, except apical two to three tarsomeres dark brown, hindleg with femur narrow apical ring yellow-brown, tibia pale except narrow apical ring to apical quarter dark, tarsus dark brown except basal half of first tarsomere pale at least ventrally pale. Abdomen dark or dark brown, cerci dark, or sometimes yellow-brown.

Head: Antenna length 2.3–2.4x head width; F1 0.8–0.85x length of eye; F1 longer than F2 (F1:F2 = 1.05–1.1x), longer than F3 (F1:F3 = 1.1–1.2x), proceeding flagellomeres progressively shorter (F7:F1 = 0.8x). Clypeus very weakly irregularly emarginate. Malar space 1.1–1.4x OD. LOD 1.4–1.5x height of eye in frontal view. IOC:OOL = 1.3–1.4x. Head rough, coarsely imbricate.

Thorax: Pronotum rough, coarsely imbricate. Prepectus distinct & pitted, setose. Mesepisternum rough, coriaceous, epicnemium shiny, microsculpture smooth with few weak oblique/horizontal lineations. Mesepimeron anepimeron rough, rugulose, except somewhat shiny and weakly imbricate in anteroventral corner; katepimeron dull, imbricate anteriorly to costulate posteriorly. Mesonotum rough, coarsely imbricate; mesoscutellum dull, coarsely imbricate, may be somewhat shiny and weakly imbricate along margins. Parapsis shiny to somewhat dull,

surfacy bumpy and weakly imbricate ventrally, less so dorsally. Mesopostnotum rough, coarsely imbricate. Metabasitarsus approximately same length as or slightly shorter than metatarsomeres 2–4 combined. Subapical tooth of tarsal claw small, less than half as long as apical tooth.

Abdomen: Terga somewhat dull, imbricate. Sawsheath in dorsal view emarginate or truncate depending on angle, with distinct median carina, longest setae about 0.6x as long as apical width of sawsheath, visible length of sawsheath about the same length as cerci. Sawsheath in lateral view with lower margin weakly rounded, meeting dorsal margin at a sub-quadrate apex. Valvula 3 lateral posterior lobe produced & continuing medially along posterodorsal margin as a carinate ridge, which is shorter submedially. In apical view, width of sawsheath 0.85-0.9x height of setose area. Tangium of lancet large, about twice as long as high; tangial process extending only slightly above tangium. Lancet with basal one or two sutures recurved, proceeding sutures weakly to more-or-less sigmoid; annuli with numerous short setae, one-third width of corresponding annulus or less; somewhat protruding and blunt, basoventral angle rounded-obtuse to rounded-right; small spiny pectines absent from sclerora.

Male. Length, 4.2–4.8 mm.

Colour as in female except as follows. Antenna dark, with indistinct stout black setae.; tegula dark. Structure and sculpture similar to female, except: F1 0.85–0.9x length of eye, F1 subequal to F2 (F1:F2 = 1–1.05x), subequal to or slightly longer than F3 (F1:F3 = 1.05–1.1x), proceeding flagellomeres progressively shorter (F7:F1 = 0.9x); malar space 1.1x OD; LOD 1.3–1.5x height of eye in frontal view , parapsis shiny to somewhat dull, or entirely dull - surfacy bumpy and weakly imbricate, sometimes weakly so and shiny dorsally; metabasitarsus shorter than metatarsomeres 2–4 combined; subapical tooth of tarsal claw smaller than in female, apical tooth moderately bent. T8 apical margin weakly produced and convex medially. Harpes of

genital capsule long and rectangular, overlapping medially at rest. Penis valve with valvispina large, broad, moderately bent at a rounded obtuse angle, with distinct, bulbous, enlarged section at middle of bend; pseudoceps approximately rectangular and weakly produced apically; valvura with large ergot.

Type material. *Holotype* ♀—**CANADA**: **QC**: Kangirsuk [Payne Bay], *60.025° -69.997°*, 11.viii.1958, W.R.M.Mason, slide prep: ovipositor (CNC). *Allotype* ♂—Same data as holotype, except E.E.MacDougall, 19.vii.1958, slide prep: ovipositor (CNC). *Paratypes* (3 ♀ 8 ♂)—***QC***: Same data as holotype, 1 ♀; idem except 7.vii.1958, slide prep: penis valves, 1 ♀ 1 ♂ (CNC); idem except 9.vii.1958, slide prep: penis valves, 1 ♂ (CNC); idem except 19.viii.1958, slide prep: penis valves, 1 ♂ (CNC); idem except 21.vii.1958, 1 ♂ (CNC); idem except 25.vii.1958, slide prep: penis valves, 1 ♂ (CNC); idem except 10.vii.1958, E.E.MacDougall, slide prep: penis valves, 1 ♂ (CNC); idem except 11.vii.1958, slide prep: penis valves, 1 ♂ (CNC); James Bay Hwy Km 335, 8-19.vi.1985, H.Goulet, D.R.Smith, Malaise trap, 1 ♂ (USNM); James Bay Hwy Km 68, 4-19.vi.1985, H.Goulet, D.R.Smith, Malaise trap, 1 ♂ (USNM).

Genetic data. None available.

Distribution. This species is found in boreal and arctic parts of Northern Quebec.

Host. Unknown.

Etymology. The name of this species comes from the Inuktut word ‘Kangirsummiut’ meaning, “someone from Kangirsuk” (Pirurvik Centre 2022). It is a noun in apposition.

Comments. Among those specimens previously examined by Wong, this species was labeled with the epithet ‘paynensis’ (those specimens were collected at Kangirsuk [Payne Bay], QC in July 1958). Although very similar to *P. staudingeri*, the males have a distinctly swollen

valvispina, which is interpreted here as outside of the range of variation in valvispina shape for *P. staudingeri*, and the females are sufficiently different to warrant recognition as a separate species.

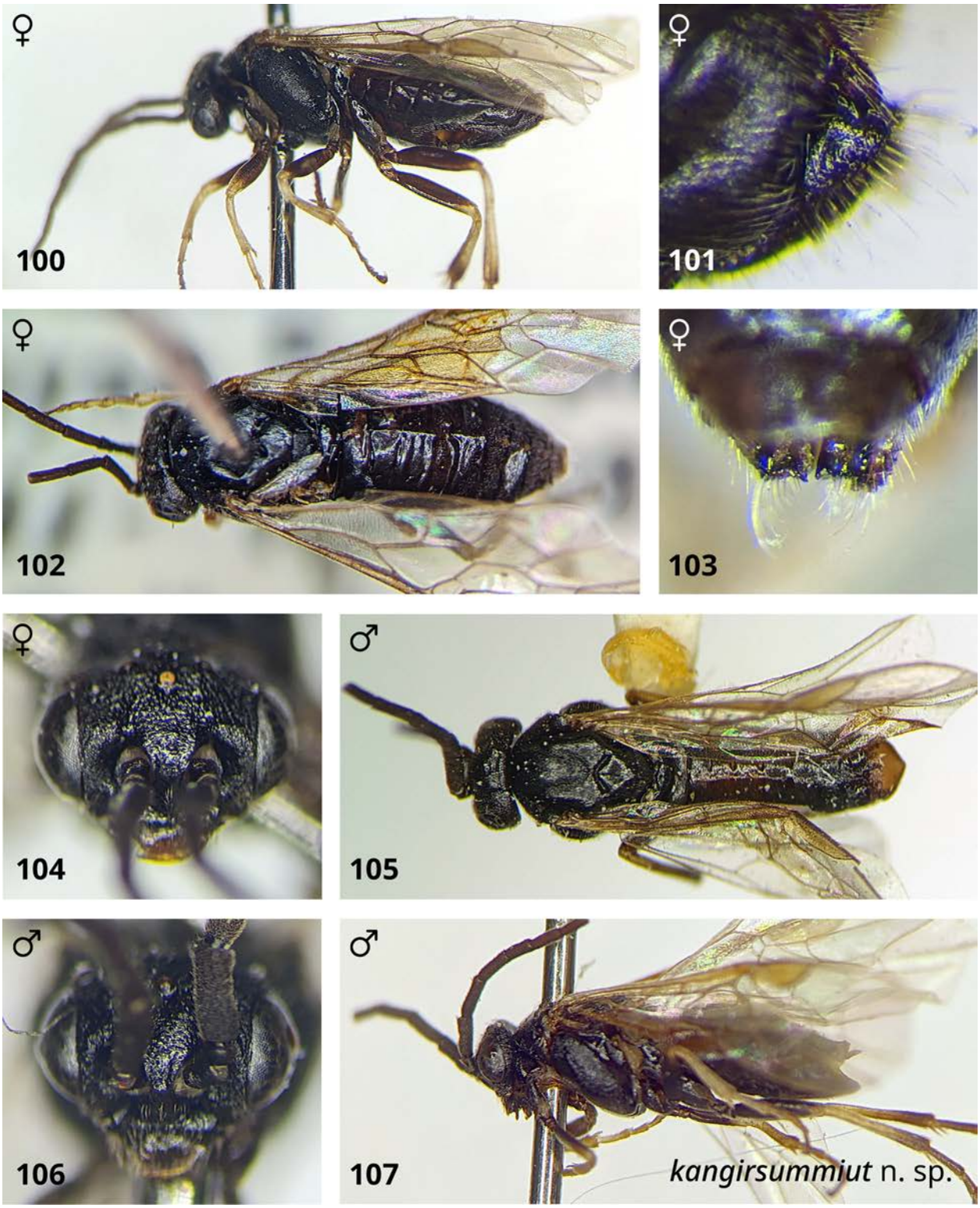

Figures 100–107. *Pristiphora kangirsummiut*. **100**. Female lateral view. **101**. Sawsheath lateral view. **102**. Female dorsal view. **103**. Sawsheath dorsal view. **104**. Female head. **105**. Male dorsal view. **106**. Male head. **107**. Male lateral view.

***Pristiphora maura* Rohwer, 1908**

(Figs. 3, 108–115, 184, 196)

Pristiphora maura Rohwer, 1908: 109.

Diagnosis. Females can be differentiated from most other Nearctic species in the ruficornis group by the shiny mesepisternum, microsculpture smooth (e.g. Fig. 2; dull, imbricate or rough, scabrous-coriaceous in other species, e.g. Figs. 3–4) and tarsal claw with medium to large subapical tooth, at least half as long as apical tooth (e.g. Figs. 173–174; smaller, less than half as long as apical tooth in other species, e.g. Fig. 172), which separates *P. maura* from all but *P. aphanta* and *P. frigida*. From these two species, *P. maura* can be separated by its lancet, with slender rectangular tangium at least three times longer than tall (Fig. 184; in *P. aphanta* about twice as wide as tall, Fig. 178; in *P. frigida* only slightly wider than tall, Fig. 181) and first two or three sutures distinctly recurved dorsally (in *P. aphanta* straight to dorsally apically curved, in *P. frigida* at most first suture weakly recurved). The lancet is most similar to *P. sootryeni*: both species have small spiny pectines that reach the sclerora (Figs. 184, 189; absent from sclerora in all other species) with a similarly shaped tangium. *P. maura* can be differentiated by the smaller tangial process, present only for dorsal half of tangium (well-developed and about one-and-a-half times the height of the tangium in *P. sootryeni*, Fig. 189), the evenly rounded basoventral angle of the tangium (at least weakly concave in *P. sootryeni*, resulting in a slightly produced basoventral angle), and by the shinier mesepisternum, with microsculpture smooth (dull, coarsely imbricate in *P. sootryeni*). Males of *P. maura* are only readily differentiated by examining the penis valve (Fig. 196), which has a distinctive shape that differs from all but *P. sootryeni*: both species have a very strongly dorsally curved valvispina tapering to a sharp point, apicodorsal corner of pseudoceps darkly sclerotized, and a large ergot. Differences between males of these

two species are minute: *P. maura* has a more weakly-sculptured mesepisternum, shiny or only somewhat dull (dull, imbricate in *P. sootryeni*), valvispina slenderer, tapering evenly to point (Fig. 196; in *P. sootryeni* tapering more abruptly near apex, Fig. 202), and pseudoceps more rectangular in shape, with apical and dorsal margins flatter (in *P. sootryeni* the apical and dorsal margins are more evenly rounded).

Female. Length, 4.3–5.4 mm.

Colour: Antenna dark; head dark; mouthparts dark brown, mandible apical half translucent brown except dark apex; labrum dark brown. Thorax dark; pronotum posterior corner sometimes with margins very narrowly yellow-brown; tegula sometimes translucent yellow. Legs dark, except coxae with apicoventral spot pale, trochanters and trochantelli on fore and midleg sometimes narrow apical ring pale, on hindleg pale-infuscate, foreleg with femur apical third to half, tibia, and tarsus pale, except apical tarsomere brown, midleg with as on foreleg, hindleg with femur narrow apical ring yellow-brown, tibia pale except broad apical ring brown, tarsus brown except basal half of first tarsomere pale. Abdomen dark or dark brown.

Head: Antenna length 2.4–2.5x head width; F1 0.9x length of eye; F1 longer than F2 (F1:F2 = 1.05–1.1x), longer than F3 (F1:F3 = 1.1–1.2x), proceeding flagellomeres progressively shorter (F7:F1 = 0.75x). Clypeus shallowly widely emarginate. Malar space 1.0–1.1x OD. LOD 1.4x height of eye in frontal view. IOC:OOL = 1.2–1.3x. Head shiny, microsculpture smooth, lower face somewhat dull, weakly imbricate adjacent to eye, gena dull imbricate dorsal half, vertexal area somewhat dull, weakly imbricate, duller and more strongly imbricate laterally.

Thorax: Pronotum dull, imbricate. Prepectus narrow, pitted (often hidden beneath pronotum), setose. Mesepisternum shiny, microsculpture smooth, epicnemium shiny,

microsculpture smooth. Mesepimeron anepimeron shiny, microsculpture smooth in anterior half to dull, imbricate posterior half; katepimeron shiny, microsculpture smooth. Mesonotum shiny, microsculpture smooth, except median lobe somewhat dull and minutely imbricate medially; mesoscutellar appendage shiny, microsculpture smooth or weakly imbricate. Parapsis somewhat dull, imbricate, more weakly so dorsally. Mesopostnotum dull, coarsely imbricate. Metabasitarsus approximately same length as or slightly shorter than metatarsomeres 2–4 combined. Subapical tooth of tarsal claw medium, about half as long as apical tooth, usually slightly longer on hindleg.

Abdomen: Terga dull, imbricate. Sawsheath in dorsal view emarginate or truncate depending on angle, with distinct median carina, longest setae about two-thirds as long as apical width of sawsheath, visible length of sawsheath less than cerci. Sawsheath in lateral view with lower margin weakly rounded, meeting dorsal margin at a sub-acute apex. Valvula 3 lateral posterior lobe produced & continuing medially along posterodorsal margin as a carinate ridge. In apical view, width of sawsheath 0.7-0.8x height of setose area. Tangium of lancet long and slender, approximately rectangular, at least four times longer than high; tangial process small, present only for dorsal half of tangium. Lancet slender, with basal two to three sutures distinctly recurved, proceeding sutures weakly to distinctly sigmoid; annuli with few very short setae, may appear absent; serrulae somewhat sharply pointed, basoventral angle rounded-acute; small spiny pectines present at level of sclerora.

Male. Length, 4.0–6.7 mm.

Colour as in female except as follows. Antenna dark brown, with stout black setae. Abdomen. Structure and sculpture similar to female, except: F1 0.8–0.9x length of eye, F1 subequal to F2 (F1:F2 = 0.95–1.05x), subequal to F3 (F1:F3 = 0.95–1.05x), proceeding

flagellomeres progressively shorter (F7:F1 = 0.9x); malar space 1.0–1.1x OD; LOD 1.3–1.4x height of eye in frontal view; mesepisternum shiny to somewhat dull, weakly imbricate; subapical tooth of tarsal claw smaller than in female, half as long as apical tooth or less. T8 apical margin weakly produced and convex medially. Penis valve with valvispina long, strongly bent, approximately semicircular, broad basally and gradually tapering to a slender, finely pointed apex; pseudoceps somewhat rectangular, weakly produced ventroapically; valvura with large ergot.

Material studied. **CANADA**: **AB**: 8 mi. East, Morley, 22.vi.1962, W.R.M.Mason, slide prep: ovipositor, 2 ♀ (CNC); 8 mi. East, Morley, *51.188°* -*114.690°*, 22.vi.1962, W.R.M.Mason, slide prep: ovipositor, 1 ♀ (CNC); Johnston Canyon, *51.250°* -*115.835°*, 1433m, 30-31.vii.1962, K.C.Herrmann, slide prep: ovipositor, 1 ♀ (CNC); **BC**: Liard Hot Spg., Mi496 Alaska Hwy, *59.400°* -*126.067°*, 457m, 9-10.vii.1959, R.E.Leech, slide prep: ovipositor, 1 ♀ (CNC); **MB**: 30 m. N. Roblin, *51.576°* -*101.163°*, 14.vii.1954, Brooks-Wallis, slide prep: ovipositor, 1 ♀ (CNC); **NT**: Norman Wells, *65.282°* -*126.833°*, 17.vii.1949, W.R.M.Mason, slide prep: ovipositor, 2 ♀ (CNC); **NU**: Baker Lake, *64.325°* -*96.029°*, 25.vii.1947, T.N.Freeman, slide prep: ovipositor, 1 ♀ (CNC); **QC**: Kangirsuk [Payne Bay], *60.025°* -*69.997°*, 11.viii.1958, W.R.M.Mason, slide prep: ovipositor, 1 ♀ (CNC); **YT**: Ross River, 61.9333° -132.5000°, 19.vi.1960, E.W.Rockburne, slide prep: ovipositor, 1 ♀ (CNC); N of Whitehorse, Nilsson-Lammers Research Forest, 60.841° -135.208°, 682m, 27.vi-6.vii.2014, Mary Whitley, Malaise trap, BIOUG25365-B05, 1 ♂ (BIOUG); **USA**: **CO**: Doolittle Ranch, Mt. Evans, *39.675°* -*105.601°*, 2987m, 17.vii.1961, W.R.M.Mason, slide prep: ovipositor, 1 ♀ (CNC); idem except 23.vii.1961, J.G.Chillcott, slide prep: penis valves, 1 ♀ 1 ♂ (CNC); idem except 31.vii.1961, S.M.Clark, slide prep: ovipositor, 1 ♀ (CNC).

Distribution. This species has an arctic-alpine distribution, being found across the North (including Northern Quebec) and along the Western Cordillera. It is recorded from Alaska, Yukon, Northwest Territories, Nunavut, British Columbia, Alberta, Manitoba, Colorado, and Quebec (D. R. Smith 1979, Goulet and Bennett 2021).

Genetic data. Specimens of this specimens belong to a single BIN: BOLD:ADA5136. Based on available genetic data (two specimens), within-species divergence is 6.4% and the nearest neighbour (*P. astragali*) is 4.4% different.

Host. Unknown.

Comments. Genetic data suggest that there may be two species under this name, with *P. sootryeni* nested among them, but there appears to be no morphological evidence for recognizing a difference between the two genetically divergent individuals. Females of this species from the North were labeled by Wong with the epithet ‘masoni’, but they do not show any consistent morphological differences from this species, and can moreover be differentiated from the closely-related *P. sootryeni* in the same way. They are therefore considered conspecific.

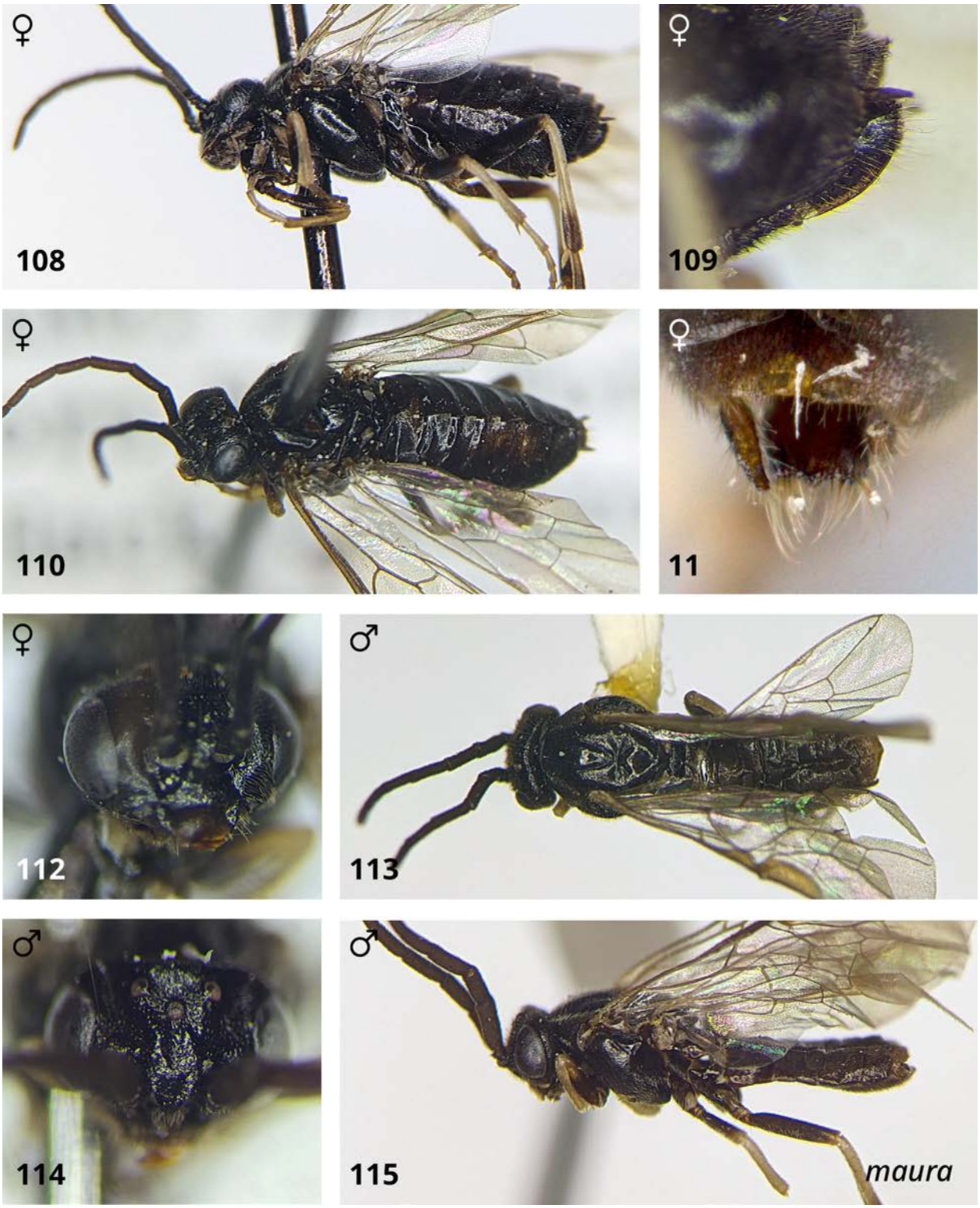

Figures 108–115. *Pristiphora maura*. **108**. Female lateral view. **109**. Sawsheath lateral view. **110**. Female dorsal view. **111**. Sawsheath dorsal view. **112**. Female head. **113**. Male dorsal view. **114**. Male head. **115**. Male lateral view.

***Pristiphora melanocarpa* (Hartig, 1840)**

(Figs. 116–123, 172, 185, 197)

Nematus melanocarpus Hartig, 1840: 27.

Nematus funerulus Costa, 1859: 20–21.

Nematus wuestneii Stein, 1885: 304.

Pristiphora ortinga Kincaid, 1900: 349-350.

Diagnosis. Individuals of both sexes of *P. melanocarpa* can be differentiated from most other Nearctic species in the *ruficornis* group by the shiny mesepisternum, microsculpture smooth (e.g. Fig. 2; at least somewhat dull, imbricate in other species, e.g. Figs. 3–4) and small subapical tooth of tarsal claw, less than half as long as apical tooth (Fig. 172; more than half as long as apical tooth or absent in other species, e.g. Figs. 173-174). This combination of characters separates females from all but *P. hucksena* and *P. siskiyouensis*, and males from all but *P. maura* and *P. siskiyouensis*. Females can be differentiated from *P. hucksena* and *P. siskiyouensis* by the darker leg colouration, with coxae entirely or almost entirely dark, hind coxa at most with narrow apical ring pale (in *P. hucksena* almost entirely pale; in *P. siskiyouensis* fore coxa at least narrow apical ring, middle and hind coxa at least apical one-quarter pale) and hind femur entirely dark, or at most with a small apicodorsal spot pale (in *P. hucksena* entirely pale; in *P. siskiyouensis* narrow basal and apical ring pale). The lancet closely resembles that of *P. siskiyouensis*, but *P. melanocarpa* usually differs by having the tangium ventrally produced into a distinct lobe (Fig. 185; at most convexly produced ventrally and rounded in *P. siskiyouensis*, Fig. 188); in some individuals the tangium is only weakly produced, as in *P. siskiyouensis*, but in these cases the distal edge of the basoventral corner is approximately flat (always evenly rounded

in *P. siskiyouensis*); additionally, the serrulae are more strongly slanted and more sharply pointed, especially apically (less strongly slanted, less sharply pointed in *P. siskiyouensis*). Males can be differentiated from *P. maura* by the penis valve with membranous fold on the pseudoceps near the tip of the valvispina, a character which it shares with *P. siskiyouensis* (Figs. 197, 201; absent in *P. maura*, Fig. 193); from the latter, *P. melanocarpa* can be differentiated by the slenderer, more strongly bent valvispina (Fig. 197; broader, more robust, less strongly bent in *P. siskiyouensis*, Fig. 201) and dorsal margin of pseudoceps evenly rounded near base (distinctly produced to an obtuse angle in *P. siskiyouensis*).

Female. Length, 4.0–5.5 mm.

Colour: Antenna dark; head dark; mouthparts pale brownish, mandible translucent brown except dark near base and apex; labrum sometimes apical margin translucent brown. Thorax dark; tegula apical margin narrowly translucent brown to pale. Legs dark, except coxae yellow-brown apicoventral spot on hind coxa, sometimes with yellow-brown apicoventral spot on fore and middle cox and apical margin of hind coxa narrowly pale, trochanters and trochantelli variable, narrow apical ring pale to entirely pale except narrow basal ring dark, foreleg with femur apical third to half, tibia, and tarsus pale, except apical two to three tarsomeres brown, midleg with femur apical narrow ring to apical quarter, tibia, and tarsus pale, except apical two to three tarsomeres brown, hindleg with femur sometimes with small apicodorsal spot, tibia except broad apical ring, and first tarsomere at least ventrally pale. Abdomen dark or dark brown, cerci dark.

Head: Antenna length 2.4–2.5x head width; F1 0.75–0.9x length of eye; F1 subequal to F2 (F1:F2 = 1.0x), subequal to F3 (F1:F3 = 1–1.05x), proceeding flagellomeres progressively shorter (F7:F1 = 0.8x). Clypeus truncate. Malar space 1.2–1.3x OD. LOD 1.4x height of eye in

frontal view. IOC:OOL = 1.3–1.5x. Head shiny, microsculpture smooth to very weakly imbricate, gena somewhat dull, weakly imbricate, vertexal area somewhat dull imbricate laterally.

Thorax: Pronotum dull, imbricate. Prepectus narrow, pitted, setose. Mesepisternum shiny, microsculpture smooth, epicnemium shiny, microsculpture smooth. Mesepimeron anepimeron mostly dull, shiny smooth along anterior margin, otherwise imbricate; katepimeron shiny smooth to very weakly imbricate posteriorly. Mesonotum shiny, weakly imbricate. Parapsis somewhat dull, imbricate. Mesopostnotum dull, coarsely imbricate. Metabasitarsus shorter than metatarsomeres 2–4 combined. Subapical tooth of tarsal claw small, less than half as long as apical tooth.

Abdomen: Terga somewhat dull, imbricate. Sawsheath in dorsal view emarginate or truncate depending on angle, with distinct median carina, longest setae about as long as apical width of sawsheath, visible length of sawsheath longer than cerci. Sawsheath in lateral view with lower margin evenly rounded, meeting dorsal margin at a broadly rounded apex. Valvula 3 lateral posterior lobe produced & continuing medially along posterodorsal margin as a carinate ridge. In apical view, width of sawsheath about 0.7x height of setose area. Tangium of lancet large, broad, usually ventrally produced into a distinct lobe, if only weakly produced then distal edge of basoventral corner approximately flat; tangial process extending slightly higher than tangium, not usually distinctly sclerotized. Lancet with basal one or two sutures approximately straight, proceeding sutures weakly to distinctly sigmoid; annuli with few very short setae, may appear absent; serrulae somewhat sharply pointed, basoventral angle rounded-acute; small spiny pectines absent from sclerora.

Male. Length, 3.9–5.5 mm.

Colour as in female except as follows. Antenna dark, paler ventrally, with stout black setae. Abdomen. Structure and sculpture similar to female, except: antenna 2.6x head width; F1 0.7–0.85x length of eye; malar space 1.0–1.5x OD; LOD 1.2–1.3x height of eye in frontal view; IOC:OD 3.2–3.3x , parapsis shiny, weakly imbricate/puncticulate; subapical tooth of tarsal claw smaller than in female, minute. T8 apical margin weakly produced and convex medially. Penis valve with valvispina long, slender, strongly bent, apex nearly perpendicular to longitudinal axis of penis valve; pseudoceps with distinct fold of membrane surrounding apex of valvispina; valvura without ergot.

Material studied. *Lectotype* ♀ (images)—**GERMANY**: North Germany (ZSM). *Paralectotype* ♂ (images)—Same data as holotype, except 16.vi.1837 (ZSM). *Additional material*—**CANADA**: **AB**: Elk Island National Park, Astotin Lake, The Point, near administration/warden office, 53.685° -112.86°, 719m, 8-15.vi.2012, Stephanie Church, Malaise trap, BIOUG03397-G05, 1 ♂ (BIOUG); **NT**: Gros Cap, date unknown, coll. unknown, Insect Collection 180813, 1 ♀ (INHS); **NU**: Bathurst Inlet, *66.839°* -*108.032°*, 18.vii.1951, C.D.Bird, 1 ♀ (CNC); idem except reared, em.: 26.vi.1946, slide prep: ovipositor, 1 ♀ (CNC); Kugluktuk [Coppermine], *67.826°* -*115.107°*, 20.vii.1951, S.D.Hicks, slide prep: ovipositor, 1 ♀ (NFRC); **YT**: Muskox L., 64.7500° -108.1667°, 17.vii.1953, J.G.Chillcott, slide prep: penis valves, 1 ♂ (NFRC); **USA**: **AK**: Umiat, *69.367°* -*152.144°*, 23.vi.1947, K.L.Knight, 1 ♀ (USNM).

Distribution. Holarctic. In the Nearctic, this species has an arctic-alpine distribution, found in the North, in the mountains of Alberta, and at high elevations in Quebec. The specimens from Mt. Albert, QC, are noteworthy in that they occur in alpine tundra noted for its southerly location; this locality is also home to the only caribou found south of the St. Laurence River (Sépaq 2022).

This species is recorded from Alaska, Yukon, Northwest Territories, Nunavut, Alberta, Manitoba, Quebec (D. R. Smith 1979, Goulet and Bennett 2021).

Genetic data. Nearctic specimens of this species belong to a single BIN: BOLD:AAG3540. Palaearctic specimens additionally belong to the BIN: BOLD:AAQ2302. Based on available genetic data (two Nearctic and two Palaearctic specimens), maximum within-species divergence is 1.2% and the nearest neighbour (*P. ruficornis*) is 1.1% different.

Hosts. *Betula* spp. (D. R. Smith 1979), recorded from *Betula pendula* Roth, *B. pubescens* Ehrh., and *B. nana* L. in the Palaearctic (Prous et al. 2017).

Comments. This species is very similar to *P. siskiyouensis*, but their respective distributions are very nearly mutually exclusive, with *P. melanocarpa* occurring in arctic-alpine habitats, and *P. siskiyouensis* occupying mainly boreo-montane habitats.

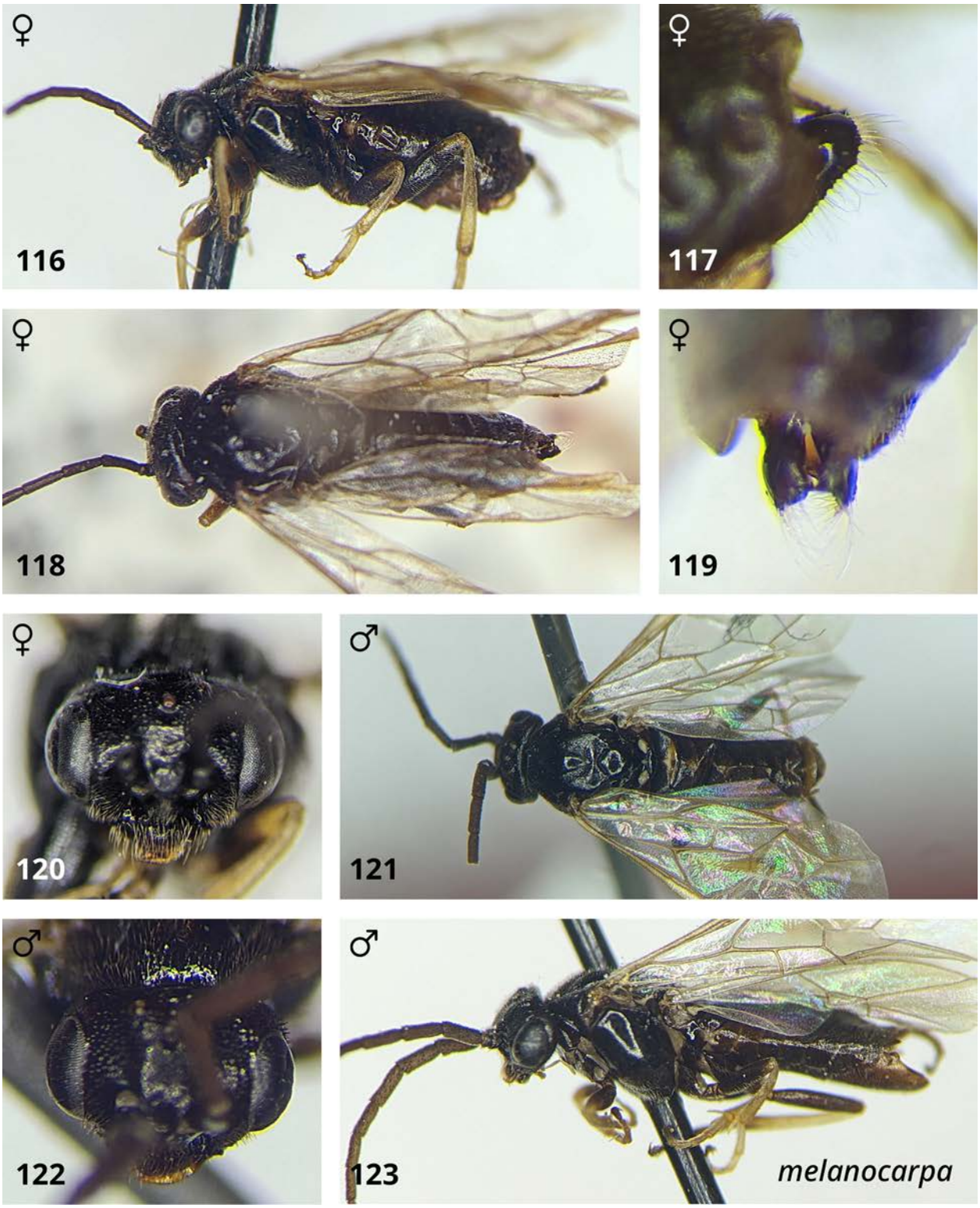

Figures 116–123. *Pristiphora melanocarpa*. **116**. Female lateral view. **117**. Sawsheath lateral view. **118**. Female dorsal view. **119**. Sawsheath dorsal view. **120**. Female head. **121**. Male dorsal view. **122**. Male head. **123**. Male lateral view.

***Pristiphora nigra* Marlatt, 1896**

(Figs. 124–131, 186, 198)

Pristiphora nigra Marlatt, 1896: 114.

Diagnosis. Individuals of both sexes of *P. nigra* can be differentiated from all other Nearctic species in the *ruficornis* group by their strong surface sculpture with mesepisternum, mesoscutum, and mesoscutellar appendage rough, coarsely imbricate (e.g. Fig. 4; one or more of these structures at most dull, imbricate, or shiny, microsculpture smooth in other species, e.g. Figs. 2–3), and parapsis dull, imbricate throughout (at most weakly imbricate and usually shiny, microsculpture smooth in all other species). The lancet is most similar to that of *P. aphanta*: both species have a rectangular tangium and very few small setae on annuli, but *P. nigra* differs by the slightly longer tangium, approximately three times as long as high (Fig. 186; approximately twice as long as high in *P. aphanta*, Fig. 178), and less sharply pointed serrulae, basal angle approximately obtuse, especially basally (serrulae with basal angle rounded-acute in *P. aphanta*). The penis valve is somewhat similar to those of *P. maura* and *P. sootryeni*, with a strongly dorsally curved valvispina and broad, at least somewhat rounded pseudoceps, but differs from in having the valvispina much larger and broader (Fig. 198; narrow, slender in *P. maura*, Fig. 196, and *P. sootryeni*, Fig. 202) and the dorsal margin of pseudoceps evenly convex, semicircular (more gently, evenly curved in *P. sootryeni*; straighter in *P. maura*).

Female. Length, 5.0–5.2 mm.

Colour: Antenna dark; head dark; mouthparts brown, mandible translucent brown except dark near base and apex; labrum dark brown. Thorax dark; tegula sometimes with apical margin translucent yellow. Legs dark, except coxae small apicoventral spot yellow-brown, trochanters

and trochantelli sometimes with narrow apical ring yellow-brown, foreleg with femur apical quarter to half dorsally, tibia, and tarsus pale, except apical two to three tarsomeres brown, midleg with femur with small apicodorsal spot, tibia, and tarsus pale, except apical two to three tarsomere brown, hindleg with femur with small apicodorsal spot pale, tibia pale except broad apical ring brown, tarsus brown except basal half of first tarsomere ventrally pale. Abdomen dark or dark brown, cerci brown or yellow-brown.

Head: Antenna length 2.5–2.6x head width; F1 0.9x length of eye; F1 longer than F2 (F1:F2 = 1.05–1.1x), longer than F3 (F1:F3 = 1.1x), proceeding flagellomeres progressively shorter (F7:F1 = 0.75–0.85x). Clypeus truncate. Malar space 1.0–1.1x OD. LOD 1.5x height of eye in frontal view. IOC:OOL = 1.3–1.4x. Head dull, imbricate.

Thorax: Pronotum rough, coarsely imbricate. Prepectus distinct & punctate, setose. Mesepisternum rough, coarsely imbricate to scabrous-coriaceous, epicnemium shiny, microsculpture smooth with few weak oblique/horizontal lineations. Mesepimeron anepimeron dull, imbricate-rugulose; katepimeron anterior half shiny smooth or weakly imbricate, posterior half rough costulate. Mesonotum rough, coarsely imbricate to scabrous-coriaceous; mesoscutellum shiny or somewhat dull, microsculpture smooth to imbricate; mesoscutellar appendage dull, coarsely imbricate & pitted. Parapsis dull, imbricate throughout. Mesopostnotum rough, coarsely imbricate. Metabasitarsus shorter than metatarsomeres 2–4 combined. Subapical tooth of tarsal claw minute, sometimes apparently or actually absent.

Abdomen: Terga somewhat dull, imbricate. Sawsheath in dorsal view emarginate or truncate depending on angle, with distinct median carina, longest setae about as long as apical width of sawsheath, visible length of sawsheath about the same length as cerci. Sawsheath in lateral view with lower margin weakly rounded and dorsal margin somewhat produced, the two meeting at a

subacute apex. Valvula 3 lateral posterior lobe produced & continuing medially along posterodorsal margin as a carinate ridge. In apical view, width of sawsheath 0.6-0.7x height setose area. Tangium of lancet rectangular and somewhat small, about three times as long as high with basoventral angle gently rounded; tangial process indistinct or small, present only for dorsal half of tangium. Lancet with first suture approximately straight, proceeding sutures weakly to distinctly sigmoid; annuli lacking setae; serrulae not especially protruding, basoventral angle rounded-obtuse to rounded-right; small spiny pectines absent from sclerora.

Male. Length, 4.2–5.0 mm.

Colour as in female except as follows. Antenna dark brown, with stout black setae. Legs somewhat darker than in female, except, foreleg with femur with only apical quarter pale, hindleg with tibia with apical third dark, tarsus dark. Structure and sculpture similar to female, except: antenna 2.9–2.9x head width; F1 0.85–1x length of eye, F1 subequal to or slightly longer than F2 (F1:F2 = 1.0–1.05x), subequal to or slightly longer than F3 (F1:F3 = 1.05–1.1x), proceeding flagellomeres progressively shorter (F7:F1 = 0.8–0.9x); LOD 1.4x height of eye in frontal view; IOC:OOL = 1.2x; IOC:OD 2.9–3.1x, frontal area may be somewhat shiny, weakly imbricate medially. T8 apical margin weakly produced and convex medially. Penis valve with valvispina large, very broad, strongly bent, approximately semicircular; pseudoceps with dorsal margin convex, broadly rounded, meeting ventral margin at approximately right angles apically; valvura with ergot absent or indistinct.

Material studied. **CANADA**: **AB**: Banff Natl. Pk., Moraine Lake, *51.328° -116.180°*, 1433m, 20.vii.1955, J.R.McGillis, slide prep: penis valves, 1 ♂ (CNC); Banff, Sunshine Lodge, *51.078° -115.784°*, 2286m, 24-27.vii.1962, Mason, Malaise trap, slide prep: penis valves, 1 ♂ (CNC); **BC**: Bear Lake, *54.495° -122.680°*, 20-29.vii.1903, R.P.Currie, slide prep: penis valves, 1 ♂

(USNM); Lisadele L., 58.6833° -133.0667°, 1219m, 7.vii.1960, W.W.Moss, slide prep: penis valves, 1 ♂ (CNC); **QC**: James Bay Hwy Km 313, Pontax II R, *51.774° -77.423°*, 9.vi.1985, H.Goulet, D.R.Smith, sweeping, 1 ♀ (CNC); **USA**: **CO**: Mt. Evans, Echo L., *39.660° -105.604°*, 3231m, 7.vii.1961, S.M.Clark, slide prep: penis valves, 1 ♂ (CNC); **NY**: Tompkins Co., Ithaca, Buttermilk Falls St. Pk., *42.406° -76.512°*, 30.iv.1972, G. & K.Eickwort, slide prep: ovipositor, 1 ♀ (NFRC); **WA**: Paradise Val., Mt. Rainier, *46.783° -121.728°*, 25.vii.1920, E.C.VanDyke, hellebore, slide prep: ovipositor, 2 ♀ (CASC); **WY**: The Thumb, Yellowstone Natl. Park, *44.417 ° -110.574°*, 19.vi.1930, E.C.VanDyke, slide prep: ovipositor, 1 ♀ (CASC).

Distribution. This species occurs in the Western Cordillera at moderate latitudes, from British Columbia and Alberta southeast to Colorado, and in the East from boreal Quebec south to New York. It is recorded from British Columbia, Alberta, Washington, Colorado, Wyoming, Quebec, and New York.

Genetic data. Based on available genetic data (two specimens), within-species divergence is 0.8% and the nearest neighbour (*P. hucksena*) is 1.0% different.

Hosts. Unknown. One specimen is labeled with “Hellebore”, but there is no indication that the specimen was observed feeding on that plant.

Comments. Males of this species were labeled by Wong with the epithets ‘bregma’ (western specimens) and ‘sculpa’ (eastern specimens), but they do not show any consistent morphological differences between one another, nor from this species, and are therefore considered to be conspecific. (Note: females labeled by Wong as ‘sculpa’ actually belong to the *micronematica* group.)

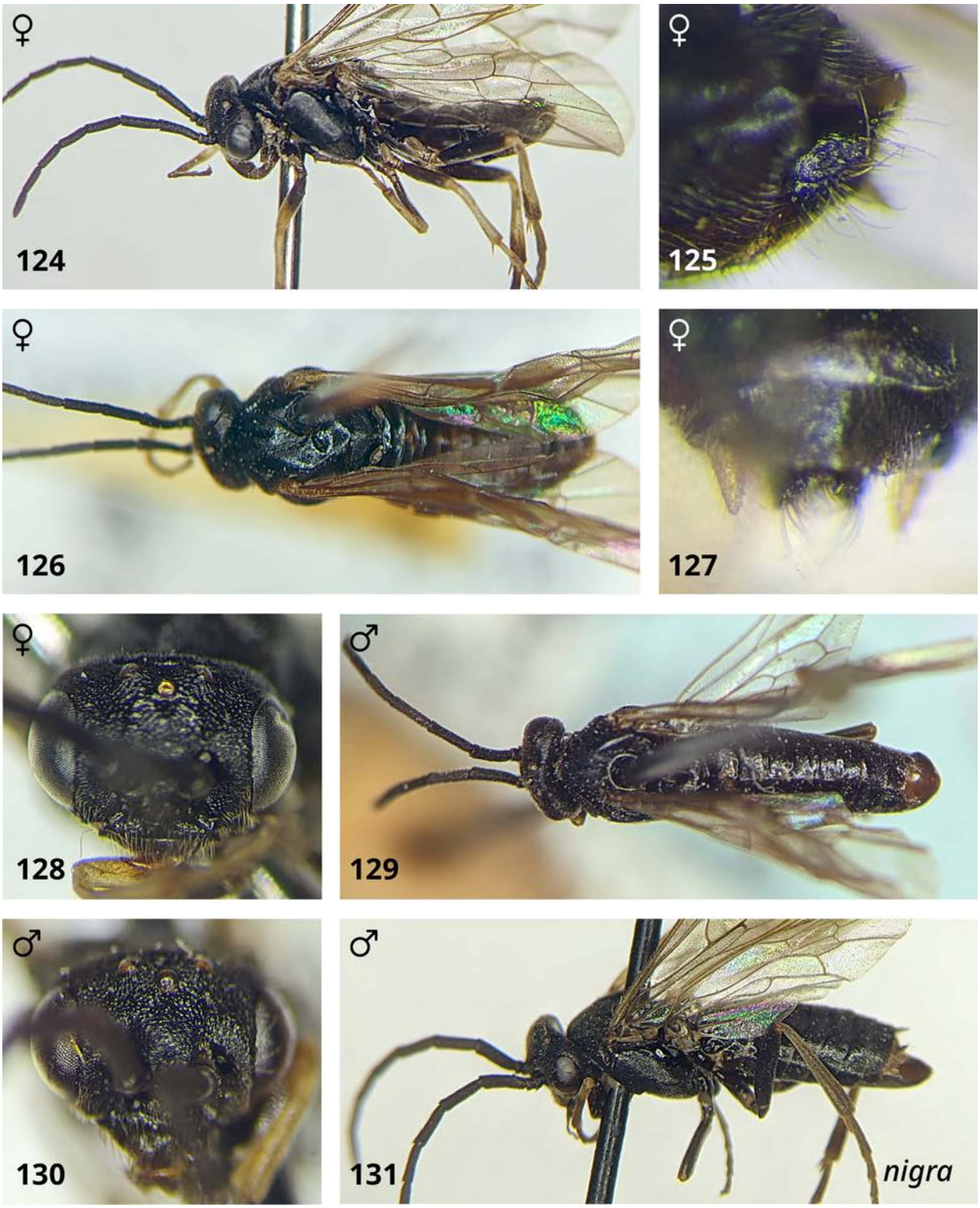

Figures 124–131. *Pristiphora nigra*. **124**. Female lateral view. **125**. Sawsheath lateral view. **126**. Female dorsal view. **127**. Sawsheath dorsal view. **128**. Female head. **129**. Male dorsal view. **130**. Male head. **131**. Male lateral view.

***Pristiphora pusilla* Malaise, 1921**

(Figs. 8, 122–139, 187, 199–200)

Pristiphora pusilla Malaise, 1921: 11-12.

Pristiphora amaura Lindqvist, 1955: 43-45.

Nematus amaurus (Lindqvist, 1955) – Zhelochovtsev and Zinovjev, 1988: 158.

Nematus pusillus (Malaise, 1921) – Zhelochovtsev and Zinovjev, 1988: 158.

Diagnosis. This species has few distinguishing characters that are visible externally. Individuals of both sexes can be differentiated from most species by the mesepisternum rough, coarsely imbricate, mesoscutum dull, imbricate (e.g. Figs. 3–4; same parts less strongly sculptured or shiny, microsculpture smooth in other species, e.g. Figs. 2–3), and subapical tooth of tarsal claw small, less than half as long as apical tooth (e.g. Fig. 172). This combination of characters should serve to separate *P. pusilla* from all but *P. kangirsummiut*, *P. nigra*, *P. staudingeri*, and *P. sycophanta*. From these species, *P. pusilla* may be differentiated by the narrow prepectus, which is less than half as wide as the adjacent portion of the epicnemium (Fig. 8; at least half as wide, often as wide as adjacent portion of epicnemium in the other four species, Fig. 7). If in doubt, lancets and penis valves should be examined. The lancet has a broad, rectangular tangium most similar to those of *P. aphanta* and *P. nigra* (two to three times as long as broad in all three species, Figs. 187, 178, 186, respectively), but differs from these two species by the more strongly sclerotized tangial process with small membranous fold (Fig. 187; lighter, not folded in *P. aphanta*, Fig. 178; and *P. nigra*, Fig. 186). Females are further differentiated from *P. nigra* by the basoventral corner of tangium more-or-less angulate (rounded in *P. nigra*) and from *P. aphanta* by the rough, coarsely imbricate mesepisternum (shiny, microsculpture smooth in *P.*

aphanta). The penis valve is most similar to those of *P. staudingeri* and *P. nigra*, with large, robust, dorsally bent valvispina and apicoventral corner of pseudoceps produced apically, but differs from *P. nigra* by the straighter, more rectangular pseudoceps (Fig. 199–200; rounded, somewhat circular in *P. nigra*; Fig. 198) and less strongly bent valvispina (strongly bent, semicircular in *P. nigra*), and from *P. staudingeri* by the much broader valvispina, greatest width at least one-third as wide as apical width of pseudoceps (narrower, greatest width clearly less than one-third as wide as apical width of pseudoceps in *P. staudingeri*, Fig. 203). Males additionally have an abrupt transition in surface sculpture on the mesepisternum, from rough, scabrous-coriaceuous in dorsal half to shine, microsculpture smooth in ventral half (mesipersternum either uniformly sculpture or transition more gradual in other species).

Female. Length, 4.6–5.0 mm.

Colour: Antenna dark, sometimes slightly paler ventrally; head dark; mouthparts brown, mandible translucent brown except dark near base and apex; labrum dark brown. Thorax dark; tegula apical margin translucent yellow. Legs dark, except coxae sometimes with apicoventral spot yellow-brown, trochanters and trochantelli sometimes with narrow apical ring pale on fore and middle leg and pale-infuscate on hind leg, foreleg with femur apical one-third to half, tibia, and tarsus pale, except apical two to three tarsomeres brown, midleg with femur broad apical ring, tibia, and tarsus pale, except apical one to two tarsomeres brown, hindleg with femur narrow apical ring, tibia, and tarsus pale, except narrow apical ring of tibia and tarsomeres brown. Abdomen dark or dark brown, T9 with broad apical margin brown, valvifer 2 brown, cerci pale or yellow-brown.

Head: Antenna length 2.4x head width; F1 0.85–1x length of eye; F1 longer than F2 (F1:F2 = 1.05–1.15x), longer than F3 (F1:F3 = 1.1–1.2x), proceeding flagellomeres progressively

shorter (F7:F1 = 0.7x). Clypeus truncate. Malar space 1.1–1.3x OD. LOD 1.4–1.5x height of eye in frontal view. IOC:OOL = 1.2x. Head shiny, weakly imbricate, gena somewhat dull, imbricate, vertexal area dull and more strongly imbricate laterally.

Thorax: Pronotum dull, imbricate. Prepectus narrow, pitted, setose. Mesepisternum rough, scabrous-coriaceous in dorsal half, shiny, microscultpure smooth in ventral half, epicnemium shiny, microsculpture smooth with few weak oblique/horizontal lineations. Mesepimeron variable, from anepimeron and katepimeron mostly shiny, microsculpture smooth, to mostly dull, imbricate and smooth only along anterior margin broadly. Mesonotum dull, imbricate; mesoscutellum shiny to somewhat dull, microsculpture smooth to imbricate; mesoscutellar appendage dull, pitted & rugulose. Parapsis shiny, weakly costulate/puncticulate. Mesopostnotum rough, coarsely textured. Metabasitarsus shorter than metatarsomeres 2–4 combined. Subapical tooth of tarsal claw small, less than half as long as apical tooth.

Abdomen: Terga somewhat dull, imbricate. Sawsheath in dorsal view emarginate or truncate depending on angle, with distinct median carina, longest setae about two-thirds as long as apical width of sawsheath, visible length of sawsheath less than cerci. Sawsheath in lateral view with lower margin evenly rounded and dorsal margin somewhat produced, the two meeting at a subacute apex, with the posterior lobes sufficiently produced to provide a squarish profile. Valvula 3 lateral posterior lobe produced & continuing medially along posterodorsal margin as a carinate ridge. In apical view, width of sawsheath about 0.6x height of setose area. Tangium of lancet rectangular, two to three times as long as high, with basoventral angle approximately right; tangial process rising only slightly above tangium, with distinct membranous fold. Lance with basal one or two sutures approximately straight, proceeding sutures more-or-less sigmoid; annuli with setae moderate in number to numerous, one-quarter to one-third width of

corresponding annulus; serrulae somewhat protruding, basoventral angle rounded-right to rounded-acute; small spiny pectines absent from sclerora.

Male. Length, 5 mm.

Colour as in female except as follows. Antenna dark, may be slightly paler ventrally, without stout black setae (some setae appear slightly thicker, darker, but these are very difficult to discern). Pronotum posterior corner with margins narrowly pale; hindleg with tibia broad apical ring and tarsus dark brown. Structure and sculpture similar to female, except: LOD 1.6x height of eye in frontal view; IOC:OOL = 0.9x; IOC:OD 3.0x; head dull, imbricate. T8 apical margin weakly produced and convex medially. Penis valve with valvispina large, very broad, moderately bent at a rounded obtuse angle, apex minutely, irregularly serrate; penis valves asymmetrical, left penis valve with dorsal margin of pseudoceps more strongly concave and valvispina more strongly bent; pseudoceps approximately rectangular and weakly produced apically; valvura with largely, either weakly or strongly produced.

Material studied. *Lectotype* ♂ (images)—**SWEDEN**: Torne Lappmark, Torne Träsk, Malaise (NHRS). *Holotype* ♀ of *amaura* (images)—**FINLAND**: South Häme, Kangasala, 30.vi.1943, Grönblom (MZH). *Additional material*—**CANADA**: **AB**: Banff, Castle Junction [Eisenhower Jct.], *51.269°* -*115.918°*, 1433m, 8.vii.1962, Mason, Malaise trap, slide prep: penis valves, 1 ♂ (CNC); **BC**: Metchosin, Camas Hill, summit, 48.3986° -123.5958°, 15-22.viii.1999, L. & C.Rosenblood, ENT017-012060, 1 ♀ (RBCM); Summit Lake, Mi392 Alaska Hwy, *58.650°* -*124.667°*, 1433m, 28.vi.1959, R.E.Leech, slide prep: penis valves, 1 ♂ (CNC); Toad River, Mi440 Alaska Hwy, *58.850°* -*125.233°*, 1372m, 19.vi.1959, R.E.Leech, 1 ♂ (CNC); Yoho National Park, 51.365° -116.528°, 25.vi-7.vii.2014, Jamie, Malaise trap, BIOUG19682-A05, 1 ♂ (BIOUG); **MB**: Churchill, *58.756°* -*94.084°*, 5.vii.1947, T.N.Freeman, slide prep: penis valves, 1

♂ (CNC); **NT**: Norman Wells, 65.2523° -126.6613°, 61m, 11-14.vi.2011, NBP field party, Malaise trap, 1 ♂ (LEMU); Reindeer Depot, Mackenzie Delta, *68.700° -134.117°*, 28.vi.1948, J.R.Vockeroth, 1 ♂ (CNC); Salmita Mines, 64.0833° -111.2500°, 1.vii.1953, J.G.Chillcott, slide prep: penis valves, 1 ♂ (CNC); idem except 4.vii.1953, 1 ♂ (CNC); idem except 2.vii.1953, slide prep: penis valves, 1 ♂ (CNC); **USA**: **AK**: 36 mi N Glennallen, 1.vii.1968, K.Goeden, 1 ♀ (USNM); Big Delta, *64.153° -145.843°*, 13.vii.1951, J.R.McGillis, slide prep: ovipositor, 1 ♀ (CNC); Big Delta, *64.153° -145.843°*, 15.vi.1951, Mason, McGillis, slide prep: penis valves, 1 ♂ (CNC); Mile 213, Richard Hwy., *63.312° -145.724°*, 12.vi.1951, W.R.M.Mason, slide prep: penis valves, 1 ♂ (CNC); Mile 24.9, Richard Hwy., *61.116° -145.737°*, 25.vi.1951, W.R.M.Mason, 1 ♂ (CNC); Naknek, *58.728° -157.014°*, 18.vii.1952, W.R.Mason, 1 ♂ (CNC); Naknek, on tundra, *58.728° -157.014°*, 8.vii.1952, W.R.Mason, 1 ♂ (CNC); **SWEDEN: LAPPLAND**: Abisko, *68.350° 18.830°*, 8.vii.1951, J.R.Vockeroth, slide prep: ovipositor, 1 ♀ (CNC); idem except 9.vii.1951, slide prep: ovipositor, 1 ♀ (CNC).

Distribution. Holarctic. In the Nearctic, this species has an arctic-alpine distribution, and is recorded from Alaska, Northwest Territories, British Columbia, Alberta, and Northern Manitoba.

Genetic data. Specimens of this species belong to a single BIN: BOLD:AAG3568. Based on available genetic data (one Nearctic and two Palaearctic specimens), maximum within-species divergence is 3.0% and the nearest neighbour (*P. bifida*) is 2.1% different.

Host. Unknown.

Comments. Genetic data suggest that the one sequenced Nearctic specimen is relatively well-differentiated from those in the Palaearctic. Specimens of this species were labeled by Wong with the epithets ‘hamata’ and ‘hysta’, but they do not exhibit any consistent morphological

differences from the description of Palaearctic specimens of this species, and moreover share the diagnostic asymmetrical penis valves of *P. pusilla* (Prous et al. 2016, 2017), the left one (Fig. 200) having the pseudoceps more strongly concave dorsally and the valvispina more strongly bent than in the right one (Fig. 199). They are therefore considered to be conspecific.

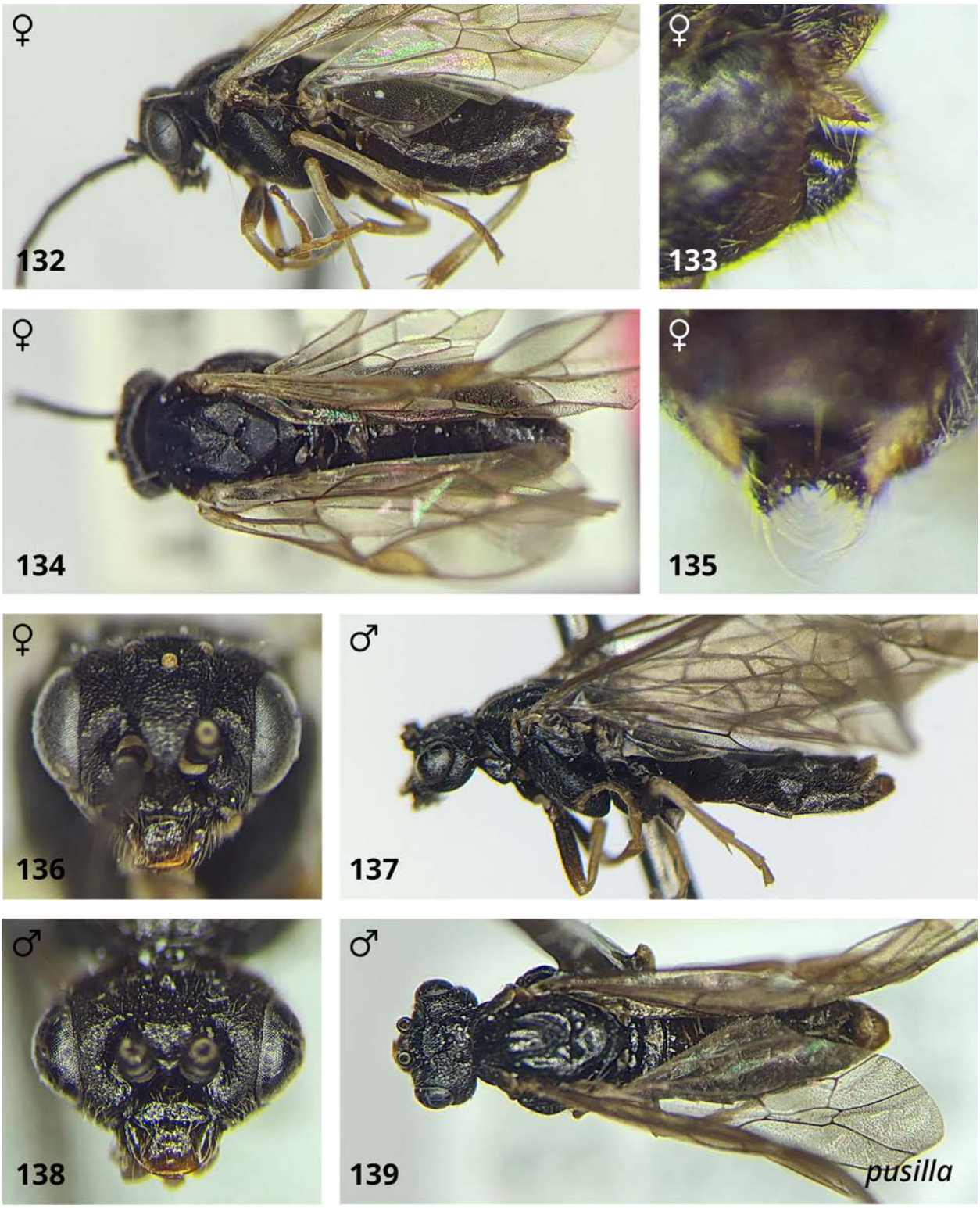

Figures 132–139. *Pristiphora pusilla*. **132**. Female lateral view. **133**. Sawsheath lateral view. **134**. Female dorsal view. **135**. Sawsheath dorsal view. **136**. Female head. **137**. Male dorsal view. **138**. Male head. **139**. Male lateral view.

***Pristiphora siskiyouensis* Marlatt, 1896**

(Figs. 64, 140–147, 188, 201)

Pristiphora siskiyouensis Marlatt, 1896: 116-117.

Pristiphora betulavora Rohwer, 1920: 219.

Diagnosis. Individuals of both sexes of *P. siskiyouensis* can be differentiated from most other Nearctic species in the *ruficornis* group by the shiny mesepisternum, microsculpture smooth (e.g. Fig. 2; at least somewhat dull, imbricate in other species, e.g. Figs. 3–4) and small subapical tooth of tarsal claw, less than half as long as apical tooth (e.g. Fig. 172; more than half as long as apical tooth or absent in other species, e.g. Figs. 173–174). This combination of characters separates females from all but *P. hucksena* and *P. melanocarpa*, and males from all but *P. maura* and *P. melanocarpa*. Females of *P. siskiyouensis* have intermediate leg colouration between that of *P. hucksena* and *P. melanocarpa*, fore coxa with narrow apical ring, middle and hind coxa apical one-quarter to one-third pale (in *P. hucksena* all coxae almost entirely pale; in *P. melanocarpa* fore and middle coxae usually entirely dark, hind coxa at most with narrow apical ring pale) and hind femur with narrow basal and apical ring pale (in *P. hucksena* entirely pale; in *P. melanocarpa* at most a small apicodorsal spot pale). The lancet closely resembles that of *P. melanocarpa*, but *P. siskiyouensis* usually differs by having the tangium at most convexly produced ventrally and evenly rounded (Fig. 188; in *P. melanocarpa* usually ventrally produced into a distinct lobe, or if weakly produced, then with distal edge of basoventral corner approximately flat, Fig. 185); additionally, the serrulae are less strongly slanted and blunter (more strongly slanted, more sharply pointed in *P. melanocarpa*, especially apically). Males can be differentiated from *P. maura* (Fig. 196) by the penis valve with membranous fold on the pseudoceps near the tip of the valvispina, a character which it shares with *P. melanocarpa* (Figs.

201, 197, respectively); from the latter, *P. siskiyouensis* can be differentiated by the broader, less strongly bent valvispina (slenderer, more strongly bent in *P. melanocarpa*) and dorsal margin of pseudoceps distinctly produced to an obtuse angle near base (evenly rounded in *P. melanocarpa*).

Female. Length, 4.8–6.3 mm.

Colour: Antenna dark, slightly paler ventrally, at least on apical four flagellomeres; head dark; mouthparts brown, mandible translucent brown except dark near base and apex; labrum apical margin usually translucent yellow-brown. Thorax dark; pronotum posterior corner sometimes with margins narrowly pale; tegula dark brown, pale, or dark basally with apical margin yellow-brown or pale. Legs dark, except coxae narrow apical ring (fore coxa) to as much as apical third (middle and hind coxa) pale, trochanters and trochantelli entirely pale, sometimes basal third brown, foreleg with femur apical third and sometimes entire dorsal surface, tibia and tarsus pale, except apical tarsomere brown, midleg with femur narrow apical ring, tibia, and tarsus pale, except apical one to two tarsomeres brown, hindleg with femur narrow basal and apical ring, tibia except broad apical band to one-quarter, and first tarsomere at least ventrally pale. Abdomen dark or dark brown, T9 sometimes with broad apical margin brown, valvifer 2 margins narrowly brown, cerci brown or dark brown.

Head: Antenna length 2.1–2.3x head width; F1 0.9–1.0x length of eye; F1 subequal to or slightly longer than F2 (F1:F2 = 1–1.1x), longer than F3 (F1:F3 = 1.1–1.2x), proceeding flagellomeres progressively shorter (F7:F1 = 0.65–0.7x). Clypeus truncate. Malar space 1.1–1.2x OD. LOD 1.4–1.5x height of eye in frontal view. IOC:OOL = 1.4–1.5x. Head shiny, microsculpture smooth.

Thorax: Pronotum somewhat dull, weakly imbricate. Prepectus distinct & pitted, setose, narrow (may be narrow/mostly hidden). Mesepisternum shiny, microsculpture smooth, epicnemium shiny, microsculpture smooth with few weak oblique/horizontal lineations. Mesepimeron anepimeron anterior half shiny, microsculpture smooth or weakly imbricate, posterior half shiny somewhat dull imbricate; katepimeron shiny, microsculpture smooth, with weak, irregular horizontal lineations in posterior half. Mesonotum shiny, weakly imbricate; lateral lobes somewhat dull, imbricate laterally; mesoscutellum shiny, microsculpture smooth or weakly imbricate; mesoscutellar appendage shiny, weakly imbricate, but deeply pitted, appearing somewhat dull with coarse sculpture. Parapsis shiny, somewhat dull, weakly imbricate/puncticulate ventrally, more weakly so dorsally. Mesopostnotum dull, coarsely imbricate. Metabasitarsus approximately same length as or longer than metatarsomeres 2–4 combined. Subapical tooth of tarsal claw small, less than half as long as apical tooth.

Abdomen: Terga variable, from shiny, weakly imbricate to somewhat dull, imbricate. Sawsheath in dorsal view emarginate or truncate depending on angle, with distinct median carina, longest setae about 0.8x as long as apical width of sawsheath, visible length of sawsheath less than cerci. Sawsheath in lateral view with lower margin evenly rounded, meeting dorsal margin at a sub-quadrate apex. Valvula 3 lateral posterior lobe produced & continuing medially along posterodorsal margin as a carinate ridge, which is shorter submedially. In apical view, width of sawsheath 0.6-0.7x height of setose area. Tangium of lancet large, broad, uconvesly produced ventrally and evenly rounded; tangial process extending slightly higher than tangium, with distinct membranous fold. Lancet with basal one or two sutures approximately straight, proceeding sutures weakly to distinctly sigmoid; annuli with few very short setae, may appear

absent; serrulae sharply pointed, basoventral angle rounded-acute; small spiny pectines absent from sclerora.

Male. Length, 4.2–5.0 mm.

Colour as in female except as follows. Antenna dark, paler ventrally, with stout black setae. Legs darker than in female, except coxae dark, trochanters and trochantelli entirely pale, sometimes entirely dark on fore and midleg, foreleg with at most apical third of femur pale, hindleg with tibia dark in apical third. Abdomen. Structure and sculpture similar to female, except: F1 0.8–0.85x length of eye, F1 subequal to or slightly longer than F2 (F1:F2 = 1–1.05x), subequal to or slightly longer than F3 (F1:F3 = 1.05x), proceeding flagellomeres progressively shorter (F7:F1 = 0.9x); malar space 0.7–0.9x OD; LOD 1.3–1.4x height of eye in frontal view ; terga dull, imbricate. T8 apical margin weakly produced and convex medially. Penis valve with valvispina long, somewhat slender, strongly bent, apical portion approximately perpendicular to basal portion; pseudoceps with distinct fold of membrane surrounding apex of valvispina, dorsal margin distinctly produced to obtuse angle near base; valvura without ergot.

Material studied. **CANADA**: **AB**: Whitecourt, *54.138*° *-116.675*°, 25.vii.1949, coll. unknown, s. alder, slide prep: ovipositor, A292F, 1 ♀ (NFRC); **BC**: Kaslo, *49.911*° *-116.905*°, date unknown, R.P.Currie, 1 ♀ (USNM); Yoho NP, Kicking Horse Campground, Amphitheatre flowered meadow, 51.424° -116.429°, 1317m, 21-24.vii.2010, BIObus 2010, Malaise trap, 10BBCHY-2669, 1 ♂ (BIOUG); **CANADA**: **MB**: Spruce Woods, *49.709*° *-99.097*°, date unknown, coll. unknown, birch, W 115 C, 1 ♀ (NFRC); **NB**: Fundy National Park, Devil`s Halfacre Road, 45.5894° -64.9556°, 61m, 30.vii-6.viii.2013, Courtney King, Malaise trap, BIOUG10976-E10, 1 ♂ (BIOUG); **NL**: Gros Morne NP, Berry Hill Pond, Hiking Trail, 49.625° -57.923°, 107m, 13.vii.2009, BIObus 2009, 09BBEHY-1116, 1 ♂ (BIOUG); **ON**: Charlton, 47.81667° -80°, date

unknown, H.S.Parish, Insect Collection 180812, 1 ♀ (INHS); Kearney, *45.556° -79.225°*, 2-9.vii.1909, M.C.VanDuzee, 3 ♀ (CASC); Swansea, 43.64385° -79.47773°, date unknown, coll. unknown, Insect Collection 180811, 1 ♀ (INHS); Pukaskwa National Park, Heron Bay, near Park Office, 48.601° -86.2893°, 631m, 6-12.viii.2013, Cavan Harpur, Malaise trap, BIOUG11566-F07, 1 ♂ (BIOUG); **USA**: **ME**: Franklin Co., Dreyden, 7.viii.1971, H.K.Townes, Malaise trap, 2 ♀ (FSCA 00091449, FSCA 00091450) (FSCA); idem except 8.viii.1971, 1 ♀ (FSCA 00091448) 1 M (FSCA 00091447) (FSCA); Mt. Desert Is., *44.334° -68.240°*, 19.v.1932, coll. unknown, slide prep: penis valves, 1 ♂ (INHS); Mt. Desert Is., *44.334° -68.240°*, 4.viii.1932, coll. unknown, slide prep: ovipositor, 1 ♀ (INHS); **NY**: Colden, *42.644° -78.685°*, 2.viii.1914, M.C.VanDuzee, 1 ♀ (CASC); Lewiston, *43.173° -79.036°*, 30.vii.1919, M.C.VanDuzee, 1 ♀ (CASC); **WA**: Paradise Val., Mt. Rainier, *46.783° -121.728°*, 25.vii.1920, E.C.VanDyke, 1 ♂ (CASC).

Distribution. This species has a boreo-temperate distribution from across North America, from British Columbia and Washington, east to Newfoundland, Labrador, and Virginia. It is recorded from British Columbia, Alberta, Washington, Saskatchewan, Manitoba, Ontario, New Brunswick, Nova Scotia, Newfoundland and Labrador, Wisconsin, New York, Maine, and Virginia (D. R. Smith 1979, Goulet and Bennett 2021). Records from Alaska, Yukon, Northwest Territories, and Nunavut (e.g. as reported in Goulet and Bennett 2021) should be considered doubtful due to probable confusion with the arctic-alpine species *P. melanocarpa*.

Genetic data. Based on available genetic data (two Nearctic specimens), within-species divergence is 2.9% and the nearest neighbour (*P. melanocarpa*) is 2.0% different.

Hosts. *Betula* spp., *Alnus* spp. (D. R. Smith 1979, D. R. Smith and Strazanac 2016).

Comments. Genetic data suggests little divergence between *P. siskiyouensis* and *P. melanocarpa*, a similar result to that observed by Prous et al. (2017) for *P. melanocarpa* and *P. ruficornis*. They are maintained as separate species due to consistent differences in morphology and geographic distribution.

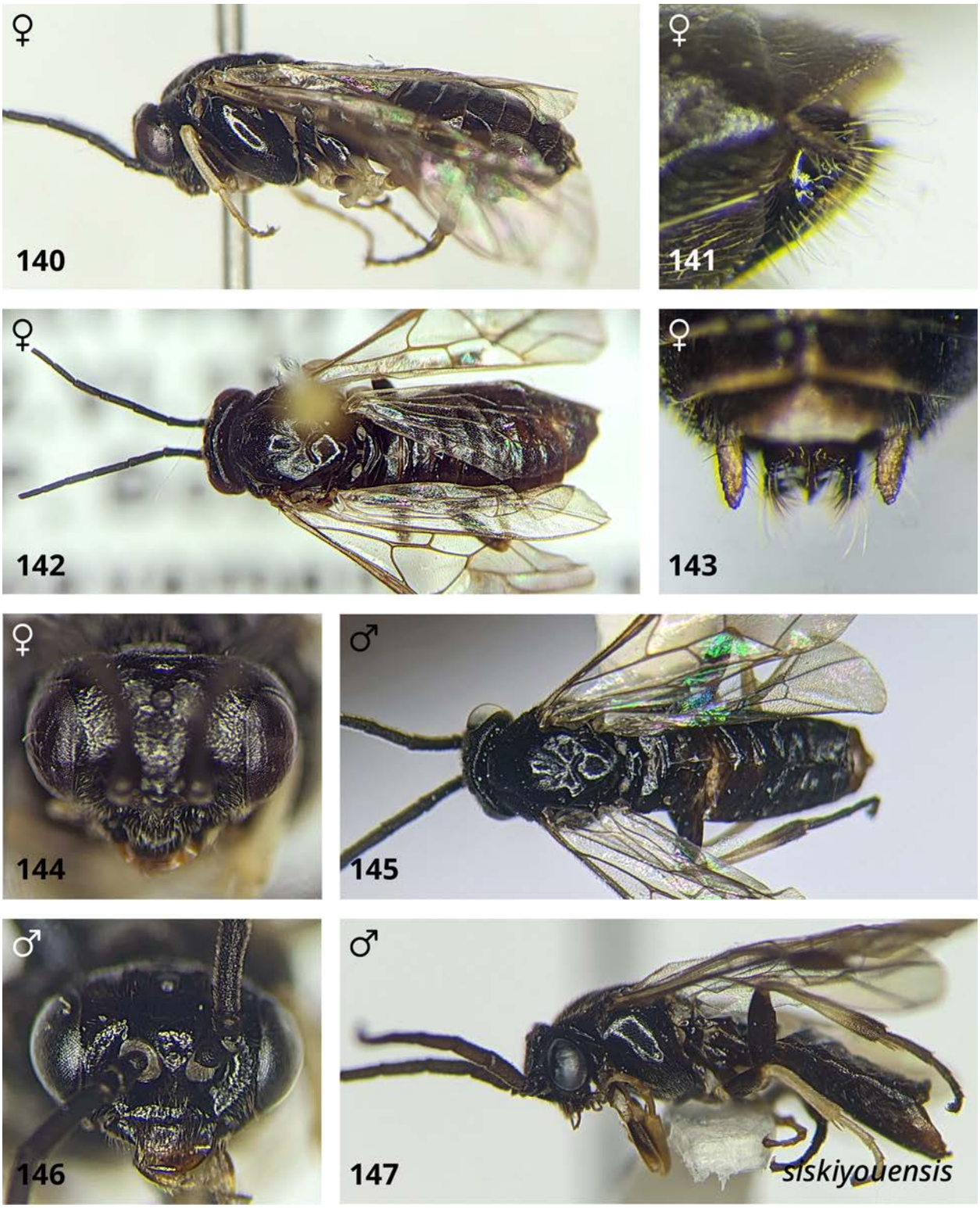

Figures 140–147. *Pristiphora siskiyouensis*. **140**. Female lateral view. **141**. Sawsheath lateral view. **142**. Female dorsal view. **143**. Sawsheath dorsal view. **144**. Female head. **145**. Male dorsal view. **146**. Male head. **147**. Male lateral view.

***Pristiphora sootryeni* Lindqvist, 1955**

(Figs. 3, 6, 148–155, 189, 202)

Pristiphora sootryeni Lindqvist, 1955: 46.

Pristiphora listoni Lacourt, 1998: 129-130.

Diagnosis. Individuals of both sexes of *P. sootryeni* can be differentiated from all other Nearctic species in the *ruficornis* group by the mesepisternum dull, imbricate (e.g. Fig. 3; shiny, microsculpture smooth, e.g. Fig. 2, or rough, scabrous-coriaceous, e.g. Fig. 4, in other species) and tarsal claw with medium to large subapical tooth, at least half as long as apical tooth and longer on hindleg (e.g. Fig. 173–174; smaller, less than half as long as apical tooth in other species, e.g. Fig. 172). The lancet is most similar to *P. maura*: both species have small spiny pectines that reach the sclerora (Figs. 184, 189; absent from sclerora in all other species) with a similarly shaped tangium. *P. sootryeni* can be differentiated by the well-developed tangial process, about one-and-a-half times the height of the tangium (Fig. 189; smaller, present only for dorsal half of tangium in *P. maura*, Fig. 184), basoventral margin of the tangium at least weakly concave, providing a slightly produced basoventral angle (evenly rounded in *P. maura*), and by the dull, coarsely imbricate mesepisternum (shiny, microsculpture smooth in *P. maura*). The penis valve (Fig. 202) has a distinctive shape that differs from all but *P. maura* (Fig. 196): both species have a very strongly dorsally curved valvispina tapering to a sharp point, apicodorsal corner of pseudoceps darkly sclerotized, and a large ergot. Differences between males of these two species are minute: *P. sootryeni* has a more strongly imbricate mesepisternum, appearing dull (more weakly sculptured, shiny or only somewhat dull in *P. maura*), valvispina broader, tapering more abruptly near apex (slenderer, tapering evenly to point in *P. maura*), and

pseudoceps with more evenly rounded shape (more rectangular in shape, apical and dorsal margins flatter in *P. maura*).

Female. Length, 4.3–6.5 mm.

Colour: Antenna dark; head dark; mouthparts dark brown, mandible translucent brown except dark near base and apex. Thorax dark; pronotum dark; tegula dark brown, apical margin broadly pale. Legs dark, except, trochanters and trochantelli sometimes with narrow apical ring yellow-brown, foreleg with femur apical one-quarter to half, tibia, and tarsus pale, midleg with femur narrow apical ring dark brown, tibia, and tarsus pale, except apical one to three tarsomeres dark, hindleg with femur narrow apical ring dark brown, tibia except apical quarter pale. Abdomen dark or dark brown, T9 and T10 brown, valvifer 2 brown, cerci dark.

Head: Antenna length 2.4–2.7x head width; F1 0.9x length of eye; F1 longer than F2 (F1:F2 = 1.1x), longer than F3 (F1:F3 = 1.1–1.2x), proceeding flagellomeres progressively shorter (F7:F1 = 0.8x). Clypeus truncate. Malar space 1.3–1.4x OD. LOD 1.5x height of eye in frontal view. IOC:OOL = 1.2–1.4x. Head dull, imbricate.

Thorax: Pronotum dull, imbricate. Prepectus narrow, pitted, setose. Mesepisternum dull, coarsely imbricate, epicnemium shiny, smooth to very weakly imbricate, with few weak oblique lineations. Mesepimeron anepimeron dull, imbricate, except anteroventral corner with margins narrowly shiny, microsculpture smooth; katepimeron shiny, microsculpture smooth to dull, imbricate in posterior half. Mesonotum dull, imbricate; mesoscutellum somewhat shiny, weakly imbricate medially. Parapsis shiny, weakly costulate/puncticulate ventrally, mostly smooth dorsally. Mesopostnotum dull, imbricate. Metabasitarsus shorter than metatarsomeres 2–4

combined. Subapical tooth of tarsal claw medium, about half as long as apical tooth, longer on hindleg, about two-thirds as long as apical tooth.

Abdomen: Terga dull, imbricate. Sawsheath in dorsal view emarginate, with distinct median carina, longest setae less than two-thirds as long as apical width of sawsheath, visible length of sawsheath about the same length as cerci. Sawsheath in lateral view with lower margin evenly rounded, meeting dorsal margin at a sub-quadrate apex. Valvula 3 lateral posterior lobe produced & continuing medially along posterodorsal margin as a carinate ridge, which is shorter submedially. In apical view, width of sawsheath about 0.9x height of setose area. Tangium of lancet approximately rectangular, at least four times longer than high, ventral margin near base at least weakly concave, providing a slightly produced basoventral angle; tangial process well-developed and about 1.5x height of tangium. Lancet slender, with first suture weakly recurved, proceeding sutures approximately straight to weakly sigmoid; annuli with setae moderate in number, about one-third width of corresponding annulus; serrulae somewhat flat, not protruding, basoventral angle rounded-right; small spiny pectines present at level of sclerora.

Male. Length, 6.5 mm.

Colour as in female except as follows. Antenna dark, with stout black setae.; tegula dark. Structure and sculpture similar to female, except: F1 0.9x length of eye, F1 subequal to F2 (F1:F2 = 1.0x), subequal to or slightly longer than F3 (F1:F3 = 1.05x), proceeding flagellomeres progressively shorter (F7:F1 = 0.9x); malar space 1.2x OD; LOD 1.4x height of eye in frontal view; IOC:OD 2.8x. T8 apical margin weakly produced and convex medially. Penis valve with valvispina long, boad, strongly bent, approximately semicircular; pseudoceps somewhat rectangular, weakly produced ventroapically; valvura with large ergot.

Material studied. *Holotype* ♂ (images)—**FRANCE**: Provence-Alpes-Côte d'Azur, St Véran, 2400m, 13.vii.1985, J.Lacourt (CTN). *Additional material*—**CANADA**: **AB**: Highwood Pass, *50.599*° *-114.985*°, 2408m, 29.vi.1962, W.R.M.Mason, slide prep: penis valves, 1 ♂ (CNC); Jasper N.P., Bald Hills, 52.7167° -117.6833°, 2316m, 20.vii-7.viii.1971, reared, em.: 26.vii.1949, P.Kuchar, 1 ♀ (CNC); **MB**: Churchill, 58.74° -93.82°, 15m, 7.vii.2010, J Wang, hand collection, BIOUG00998-F06, 1 ♀ (BIOUG); Churchill, 20.vi.1930, O.Bryant, 1 ♀ (CASC); **USA**: **AK**: Atkasuk on Meade River, about 70 miles south of Barrow, *70.469*° *-157.399*°, 13.vi.1977, T.S.Jensen, S.F.MacLean, slide prep: ovipositor, 1 ♀ (NFRC); **CO**: Pingree Park, Larimen Co., *40.561*° *-105.598*°, 17-22.viii.1925, F.C.Hottes, slide prep: penis valves, 1 ♂ (USNM).

Distribution. Holarctic. In the Nearctic, this species has a restricted arctic-alpine distribution, known only from high elevations or latitudes at a handful of localities in Alaska, Alberta, Northern Manitoba, and Colorado.

Genetic data. Specimens of this species belong to a single BIN: BOLD:AAL8292. Based on available genetic data (one Nearctic specimen) the nearest neighbour (*P. astragali*) is 3.3% different.

Hosts. Unknown in the Nearctic. In the Palaearctic, this species is recorded from *Oxytropis campestris* (Prous et al. 2017).

Comments. Studied specimens are at minimum distinct from *P. maura* and are attributed to *P. sootryeni* based on their shared barcode BIN. The possibility that they represent a distinct Nearctic species cannot be ruled out, and this should be evaluated with additional molecular evidence from nuclear loci for Palaearctic representatives *P. sootryeni* (data not available).

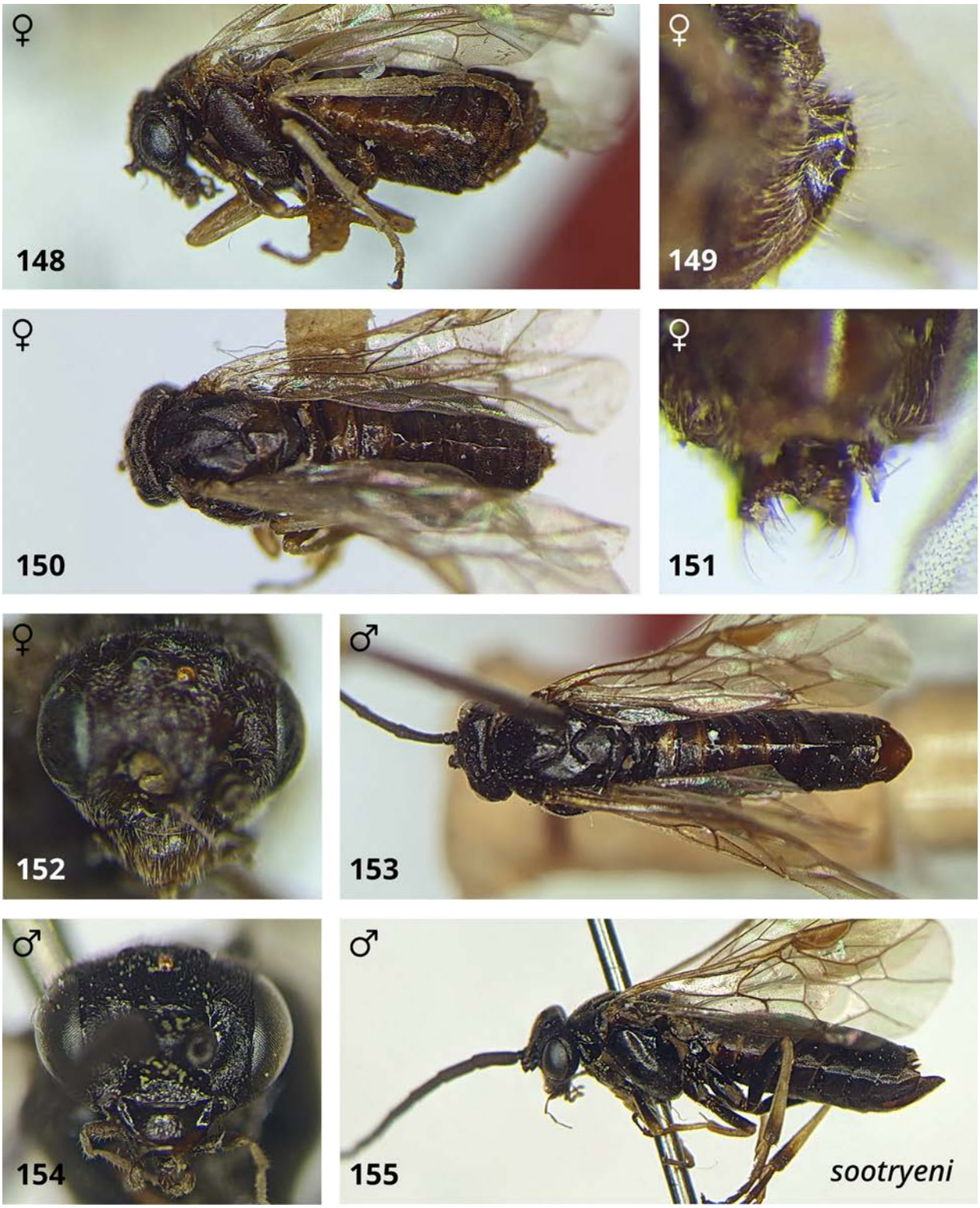

Figures 148–155. *Pristiphora sootryeni*. **148**. Female lateral view. **149**. Sawsheath lateral view. **150**. Female dorsal view. **151**. Sawsheath dorsal view. **152**. Female head. **153**. Male dorsal view. **154**. Male head. **155**. Male lateral view.

***Pristiphora staudingeri* (Ruthe, 1859)**

(Figs. 156–163, 176, 190, 203)

Nematus Staudingeri [sic] Ruthe, 1859: 306-307.

Pristiphora circularis Kincaid, 1900: 350.

Pristiphora hyperborean Malaise, 1921: 11.

Pristiphora asperlatus Benson, 1935: 35-38.

Diagnosis. Females are most similar to *P. kangirsummiut*, with which they share: head rough, coarsely imbricate, mesepisternum rough, coriaceous (e.g. Fig. 4; head and mesepisternum dull, imbricate, e.g. Fig. 3, or shiny, microsculpture smooth, e.g. Fig. 2, in most other species), tangium of lancet large, about twice as long as high (Fig. 190; longer and shorter in most other species), and tangial process extending only slightly higher than tangium (*P. elaphita* has a similarly-shaped tangium, but its tangial process extends twice as high as tangium, Fig. 180). Compared to *P. kangirsummiut*, the lancet of *P. staudingeri* has longer setae on annuli, one-third to half as long as annulus (Fig. 190; one-third width of annulus or less in *P. kangirsummiut*, Fig. 183), and the first suture is approximately straight (distinctly recurved dorsally in *P. kangirsummiut*). As well, compared to *P. kangirsummiut*, the lancet of *P. staudingeri* has more sharply pointed serrulae, with cypsellae present between apical-most serrulae (absent in *P. kangirsummiut*), and the sawsheath appears more broadly rounded in lateral view, with the lower margin evenly rounded (lower margin straighter in *P. kangirsummiut*, giving sawsheath a more slender appearance in lateral view). Males can be separated from all but *P. nigra*, *P. sootryeni*, and *P. kangirsummiut* by the rough sculpturing of the head and mesepisternum as in female; *P. kangirsummiut* and *P. staudingeri* can be separated from *P. nigra* and *P. sootryeni* by the harpes

of the genital capsule, which are relatively long and rectangular, overlapping medially at rest (Fig. 175, 176; at most meeting medially in other species, e.g. Fig. 177) and by the penis valve, with valvispina less strongly curved (e.g. Figs. 195, 203; semicircular in *P. nigra*, Fig. 198; more abruptly curved in *P. sootryeni*, Fig. 202), and pseudoceps more rectangular in shape with dorsal margin weakly rounded (in *P. nigra* and *P. sootryeni* rounder with dorsal margin broadly rounded). The valvispina of *P. staudingeri* is often widened where it bends dorsally (Fig. 203), but lacks the distinct, bulbous, enlarged section of *P. kangirsummiut* (Fig. 195). The penis valve of *P. sycophanta* is most similar to these two species, but they differ by the valvispina less strongly curved (tangents of apex and base making an obtuse angle, Figs. 195, 203; compared to approximately right in *P. sycophanta*, Fig. 204) and pseudoceps not bent dorsally, with the pseudoceps approximately in line with valvura (longitudinal axes of pseudoceps and valvura forming oblique angle in *P. sycophanta*).

Female. Length, 4.2–5.4 mm.

Colour: Antenna dark; head dark; mouthparts dark brown, mandible apical half translucent brown except dark apex; labrum sometimes apically dark brown. Thorax dark; tegula apical margin narrowly yellow-brown. Legs dark, except coxae sometimes with apicoventral spot pale, trochanters and trochantelli narrow apical ring yellow-brown, sometimes hind trochanter and trochantellus entirely pale, foreleg with femur apical quarter to half, tibia, and tarsus pale, except apical two to three tarsomeres brown, midleg with femur narrow apical ring to apical one-third, tibia, and tarsus pale, except apical two to three tarsomeres brown, hindleg with femur narrow apical ring to apical one-third, tibia except broad apical ring, and basal half of first tarsomere pale. Abdomen dark or dark brown, cerci dark or dark brown.

Head: Antenna length 2.2–2.6x head width; F1 0.75–0.9x length of eye; F1 subequal to or slightly longer than F2 (F1:F2 = 1.05x), longer than F3 (F1:F3 = 1.1x), proceeding flagellomeres progressively shorter (F7:F1 = 0.6–0.7x). Clypeus truncate, may be somewhat irregular, but not appreciably emarginate. Malar space 1.2–1.4x OD. LOD 1.5x height of eye in frontal view. IOC:OOL = 1.2–1.4x. Head rough, coarsely imbricate, gena somewhat dull weakly imbricate ventrally, rough coarsely imbricate dorsally.

Thorax: Pronotum rough, coriaceous. Prepectus distinct & pitted, setose. Mesepisternum rough, coriaceous, epicnemium shiny, with weak oblique/horizontal lineations. Mesepimeron anepimeron rough, rugulose, except anteroventral corner (to half) somewhat shiny, weakly imbricate; katepimeron anterior half (to entirely) shiny, weakly imbricate, otherwise somewhat dull, costulate. Mesonotum rough, coarsely imbricate; mesoscutellum may be somewhat shiny and weakly imbricate along anterior and lateral margins. Parapsis shiny, shallowly costulate ventrally, more-or-less smooth dorsally. Mesopostnotum rough, coarsely imbricate. Metabasitarsus approximately same length as or slightly shorter than metatarsomeres 2–4 combined. Subapical tooth of tarsal claw small, less than half as long as apical tooth.

Abdomen: Terga dull, imbricate, sometimes shiny, weakly imbricate. Sawsheath in dorsal view emarginate or truncate depending on angle, with distinct median carina, longest setae about two-thirds as long as apical width of sawsheath, visible length of sawsheath about the same length as cerci. Sawsheath in lateral view with lower margin evenly rounded, meeting dorsal margin at a sub-quadrate apex. Valvula 3 lateral posterior lobe produced & continuing medially along posterodorsal margin as a carinate ridge, which is shorter submedially. In apical view, width of sawsheath 0.7-0.8x height of setose area. Tangium of lancet large, about twice as long as high; tangial process extending only slightly higher than tangium and usually distinctly

sclerotized for a short distance. Lancet with basalmost sutures one or two sutures approximately straight, proceeding sutures distinctly sigmoid; annuli with numerous setae, one-third to one-half width of corresponding annulus; small spiny pectines absent from sclerora.

Male. Length, 3.6–4.6 mm.

Colour as in female except as follows. Antenna dark, with stout black setae, but may be somewhat difficult to discern. Legs darker than in female, except coxae entirely dark, trochanters and trochantelli entirely dark, foreleg with femur at most apical third pale, midleg with femur at most narrow apical ring pale, hindleg with femur at most narrow apical ring pale, tibia apical quarter and tarsus dark. Structure and sculpture similar to female, except: F1 0.9–0.95x length of eye, F1 subequal to or slightly shorter than F2 (F1:F2 = 0.95x), subequal to or slightly shorter than F3 (F1:F3 = 0.95x), proceeding flagellomeres progressively shorter (F7:F1 = 0.9x); malar space 1.1–1.2x OD; LOD 1.4–1.5x height of eye in frontal view , parapsis shiny to somewhat dull, or entirely dull - surfacy bumpy and weakly imbricate, sometimes weakly so and shiny dorsally; metabasitarsus shorter than metatarsomeres 2–4 combined; subapical tooth of tarsal claw smaller than in female, apical tooth moderately bent. T8 apical margin weakly produced and convex medially. Harpes of genital capsule long and rectangular, overlapping medially at rest. Penis valve with valvispina large, broad, moderately bent at a rounded obtuse angle, widest at middle of bend; pseudoceps approximately rectangular and weakly produced apically; valvura with large ergot.

Material studied. **CANADA**: **AB**: 15mi. East, Morley, *51.183° -114.542°*, 23.vi.1962, K.C.Herrmann, 1 ♀ (CNC); Kananaskis For. Exp. Stn. Seebe, *51.024° -115.029°*, 29.vi.1962, W.R.M.Mason, 1 ♂ (NFRC); Banff National Park, Corral Creek old road, 51.407° -116.154°, 1539m, 17.vi.2012, BIOBus 2012, sweep net, BIOUG03981-G05, 1 ♂ (BIOUG); **BC**: Lisadele

L., 58.6833° -133.0667°, 1219m, 6.viii.1960, W.W.Moss, 1 ♀ (CNC); **MB**: Churchill, *58.756*° -*94.084*°, 19.vi.1952, J.G.Chillcott, slide prep: ovipositor, 1 ♀ (CNC); Churchill, *58.756*° -*94.084*°, 29.vi.1936, H.E.McClure, 1 ♂ (CNC); Farnworth L. nr. Churchill, *58.705*° -*94.051*°, 26.vi.1952, J.G.Chillcott, 1 ♀ (CNC); **NT**: Muskox L., 64.7500° -108.1667°, 11.vii.1953, J.G.Chillcott, 1 ♀ (CNC); Norman Wells, *65.282*° -*126.833*°, 10.vii.1949, W.R.M.Mason, 1 ♀ (CNC); idem except 12.vi.1949, 1 ♂ (CNC); idem except 12.vii.1949, 1 ♀ (CNC); idem except 23.vii.1949, slide prep: ovipositor, 1 ♀ (CNC); idem except 4.vii.1949, 1 ♂ (CNC); Salmita Mines, 64.0833° -111.2500°, 4.vii.1953, J.G.Chillcott, 1 ♀ (CNC); **NU**: Bathurst Inlet, *66.839*° -*108.032*°, 22.vi.1951, C.D.Bird, slide prep: ovipositor, 1 ♀ (NFRC); Chesterfield, *63.335*° -*90.711*°, 15.vii.1950, J.R.Vockeroth, 1 ♀ (CNC); Kugluktuk [Coppermine], *67.826*° -*115.107*°, 20.vii.1951, S.D.Hicks, slide prep: ovipositor, 1 ♀ (CNC); Kugluktuk [Coppermine], Bloody Falls, *67.750*° -*115.333*°, 17.vii.1951, S.D.Hicks, slide prep: ovipositor, 1 ♀ (CNC); Padlei [Padley], *61.933*° -*96.650*°, 21.vii.1949, W.R.M.Mason, 1 ♂ (CNC); Quoich River, 65.0000° -94.5000°, 22.vii.1950, J.G.Chillcott, slide prep: ovipositor, 1 ♀ (CNC); Taloyoak [Spence Bay], *69.533*° -*93.536*°, 28.vi.1951, A.E.R.Downe, slide prep: ovipositor, 1 ♀ (CNC); Ukkusiksalik Bay [Wager Bay], 65.2500° -88.0000°, 22.vii.1950, J.G.Chillcott, slide prep: ovipositor, 5 ♀ 1 ♂ (CNC); **ON**: Moosonee, *51.267*° -*80.651*°, 14.vii.1934, G.S.Walley, slide prep: ovipositor, 1 ♀ (CNC); **USA**: **AK**: Big Delta, *64.153*° -*145.843*°, 30.vi.1951, W.R.M.Mason, slide prep: ovipositor, 1 ♀ (CNC); Fairbanks, *64.838*° -*147.716*°, 2.vii.1921, J.M.Aldrich, 1 ♀ (USNM); Nome, *64.512*° -*165.419*°, 15.vi.1951, D.P.Whillans, slide prep: ovipositor, 1 ♀ (CNC); idem except 9.vii.1951, slide prep: penis valves, 1 ♂ (CNC); **CO**: Nederland, Science Lodge, *40.032*° -*105.536*°, 2896m, 3.vii.1961, B.H.Poole, 1 ♀ (CNC); Summit L. Mt. Evans, *35.598*° -*105.642*°,

3901m, 10.vii.1961, W.R.M.Mason, 1 ♀ 1 ♂ (CNC); **SWEDEN**: **LAPPLAND**: Abisko, *68.350° 18.830°*, 1.vii.1951, J.R.Vockeroth, 1 ♀ 1 ♂ (CNC).

Distribution. Holarctic. In the Nearctic, this species has an arctic-alpine distribution, and is recorded from Alaska, Yukon, Northwest Territories, Nunavut, British Columbia, Alberta, Colorado, Manitoba, Ontario, Quebec, and Labrador (D. R. Smith 1979, Goulet and Bennett 2021).

Genetic data. Specimens of this species belong to a single BIN, which is shared with *P. sycophanta*: BOLD:AAG3568. Based on available genetic data (two Nearctic and five Palaearctic specimens), maximum within-species divergence is 2.7% and the nearest neighbour (*P. bifida*) is 1.7% different.

Hosts. *Salix* spp. (D. R. Smith 1979).

Comments. Among the specimens examined by Wong, a number of specimens of this species from Nunavut were labeled ‘chillcotti’ (apparently in recognition of their collector, J.G. Chillcott). Other specimens from Nunavut and the Northwest Territories were identified by Wong as *P. staudingeri*, so he presumably had good reason for setting these ones apart, but if so, it was not clearly indicated in any of the available material relating to his work. There appear to be no consistent differences between these specimens and those attributable to *P. staudingeri*, except perhaps the presence of fewer setae on sutures of the lancet in females labeled ‘chillcotti’. Lacking sufficient evidence that they lie outside the normal range of intraspecific variation for *P. staudingeri*, they are considered conspecific.

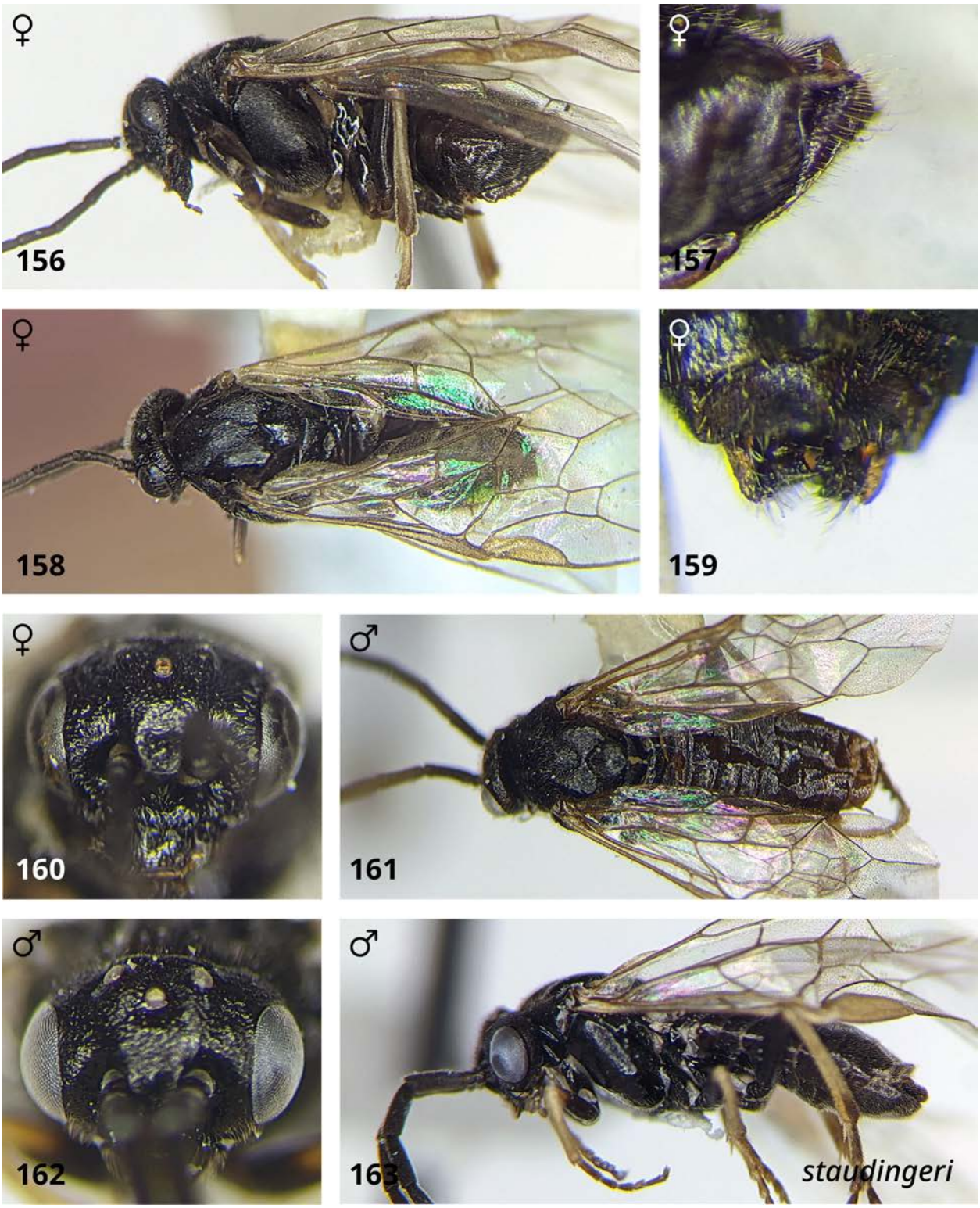

Figures 156–163. *Pristiphora staudingeri*. **156**. Female lateral view. **157**. Sawsheath lateral view. **158**. Female dorsal view. **159**. Sawsheath dorsal view. **160**. Female head. **161**. Male dorsal view. **162**. Male head. **163**. Male lateral view.

***Pristiphora sycophanta* Walsh, 1866**

(Figs. 164–171, 177, 191, 204)

Pristiphora sycophanta Walsh, 1866: 263-264.

Neotomostethus hyalinus MacGillivray, 1908: 290. **n. syn.**

Pristiphora valvangula Wong and Ross, 1960: 194. **n. syn.**

Diagnosis. This species is somewhat variable in colouration and surface sculpture, but the combination of lower face shiny, microsculpture smooth (e.g. Fig. 2) and mesepisternum at least somewhat dull, imbricate (e.g. Fig. 3) should separate females from all Nearctic species of the group except *P. pusilla*. From that species, and from all others with a rectangular tangium (three or more times as long as tall, Fig. 191), *P. sycophanta* can be separated by the broad lancet, which is almost one-third as high as the length of the lamnium (slightly more than one-quarter in other species), with dorsally very strongly apically curved sutures, especially sutures 3 to 6 (less strongly curved in other species). Males are only readily differentiated by examining the penis valve, which has a slender, dorsally bent valvispina and pseudoceps with approximately rectangular apex, similar to those of *P. kangirsummiut* and *P. staudingeri*. From those two species, *P. sycophanta* is separated by the more strongly curved valvispina (tangents of apex and base making an approximately right angle, Fig. 204; compared to obtuse in *P. kangirsummiut* and *P. staudingeri*, Figs. 195, 203) and pseudoceps strongly bent dorsally, with longitudinal axes of pseudoceps and valvura forming an oblique angle (pseudoceps and valvura approximately in line in *P. kangirsummiut* and *P. staudingeri*). The penis valves can often be seen externally, making it possible to identify this species without dissection.

Female. Length, 4.3–7.0 mm.

Colour: Antenna dark; head dark; mouthparts pale brownish, mandible translucent brown except dark near base and apex; labrum dark brown. Thorax dark; pronotum posterior corner sometimes with margins narrowly pale; tegula sometimes translucent yellow. Legs dark, except coxae narrow apical ring to as much as apical quarter pale, trochanters and trochantelli pale, foreleg with femur apical quarter to half, tibia, and tarsus pale, except apical two tarsomeres brown, midleg with femur narrow basal and apical ring or sometimes up to apical half, tibia, and tarsus pale, except apical one to three tarsomeres brown, hindleg with femur narrow basal and apical ring or sometimes up to apical half, tibia except broad apical ring, and basal half of first tarsomere pale. Abdomen dark or dark brown, T9 sometimes with broad apical margin brown, valvifer 2 sometimes yellow-brown basally, margins brown, cerci pale or yellow-brown.

Head: Antenna length 2.2–2.6x head width; F1 0.8–1.0x length of eye; F1 longer than F2 (F1:F2 = 1.05–1.1x), longer than F3 (F1:F3 = 1.1–1.2x), proceeding flagellomeres progressively shorter (F7:F1 = 0.75x). Clypeus truncate. Malar space 1.1–1.3x OD. LOD 1.4–1.5x height of eye in frontal view. IOC:OOL = 1.3x. Head shiny, microsculpture smooth, lower face dull imbricate adjacent to antennal sockets, gena somewhat dull and imbricate dorsally, vertexal area somewhat dull, weakly imbricate.

Thorax: Pronotum dull, imbricate. Prepectus distinct & pitted, setose, narrow. Mesepisternum usually rough, coriaceous, but may be somewhat shiny, imbricate; epicnemium shiny, microsculpture smooth with weak horizontal lineations. Mesepimeron anepimeron shiny microsculpture smooth, to dull imbricate at least in posterior half; katepimeron shiny, microsculpture smooth or very weakly imbricate in anterior half, somewhat dull and imbricate in posterior half. Mesonotum variable: entirely dull imbricate TO median lobe medially shiny microsculpture smooth laterally dull imbricate; lateral lobe somewhat dull, weakly imbricate;

mesoscutellum shiny to somewhat dull, microsculpture smooth to imbricate; mesoscutellar appendage dull, pitted & rugulose. Parapsis shiny, weakly costulate/puncticulate ventrally, microsculpture very weak or smooth dorsally. Mesopostnotum rough, coarsely imbricate. Metabasitarsus approximately same length as or shorter than metatarsomeres 2–4 combined. Subapical tooth of tarsal claw small, less than half as long as apical tooth.

Abdomen: Terga somewhat dull, imbricate. Sawsheath in dorsal view emarginate or truncate depending on angle, with distinct median carina, longest setae about as long as apical width of sawsheath, visible length of sawsheath about the same length as cerci. Sawsheath in lateral view with lower margin weakly rounded and dorsal margin somewhat produced, the two meeting at a subacute apex, with the posterior lobes sufficiently produced that the sawsheath appears concave below its apex. Valvula 3 lateral posterior lobe produced & continuing medially along posterodorsal margin as a carinate ridge, which is shorter submedially. In apical view, width of sawsheath 0.6-0.7x height of setose area. Tangium of lancet long and slender, approximately rectangular or slightly tapering apically, at least four times longer than high; tangial process small extending only slightly above tangium. Lancet with basal one or two sutures approximately straight or weakly sigmoid, proceeding sutures strongly sigmoid and abruptly apically curved dorsally; annuli with numerous setae, one-third to one-half width of correspondign annulus; somewhat protruding, basoventral angle rounded-right to rounded-acute; small spiny pectines absent from sclerora.

Male. Length, 4.0–5.2 mm.

Colour as in female except as follows. Antenna dark, slightly paler ventrally, with stout black setae, but may be somewhat difficult to discern. Legs darker than in female, except coxae entirely dark, trochanters and trochantelli dark, narrow apical ring pale, sometimes entirely pale

on hindleg, hindleg with tibia with apical one-quarter dark, tarsus dark except basal half of first tarsomere pale ventrally. Abdomen. Structure and sculpture similar to female, except: F1 0.85–0.9x length of eye, F1 subequal to or slightly longer than F2 (F1:F2 = 1.0–1.1x), subequal to or slightly longer than F3 (F1:F3 = 1–1.1x), proceeding flagellomeres progressively shorter (F7:F1 = 0.75–0.9x); malar space 1.0–1.1x OD; LOD 1.3–1.4x height of eye in frontal view; IOC:OOL = 1.3–1.4x; IOC:OD 2.8–3.1x; head variable somewhat dull, weakly imbricate to dull, imbricate; mesepisternum variable from rough coriaceous to shiny smooth, mesepimeron anepimerion shiny, microsculpture smooth in anterior half to dull, imbricate in posterior half; katepimerion shiny, microsculpture smooth or weakly imbricate in anterior half to dull, imbricate in posterior half; mesonotum variable somewhat dull, weakly imbricate to dull, imbricate. T8 apical margin weakly produced and convex medially. Penis valve with valvispina long, broad, strongly bent, apex nearly perpendicular to longitudinal axis of valvura; pseudoceps approximately rectangular, broader apically, bent dorsally relative to longitudinal axis of penis valve; valvura with ergot absent or indistinct.

Material studied. (Status of type specimen of *sycophanta* unknown, possibly destroyed in fire; Zinovjev and Smith 2000). *Holotype* (♀) of *hyalinus*—USA: NY: McLean, slide prep: ovipositor (INHS). *Holotype* (♂) of *valvangula*—USA: NY: Ithaca (probable locality), vii.1918, H.Yuasa, slide prep: penis valves (INHS). *Additional material*—**CANADA**: **AB**: McLeod River, *53.450*° -*116.617*°, date unknown, coll. unknown, willow, slide prep: ovipositor, 46 W-1080, 1 ♀ (CNC); Elk Island National Park, Astotin Lake, The Point, near administration/warden office, 53.685° -112.86°, 719m, 22-29.vi.2012, Stephanie Church, Malaise trap, BIOUG03052-F12, 1 ♂ (BIOUG); idem except 25.v-1.vi.2012, BIOUG03397-C06, 1 ♂ (BIOUG); idem except 6-13.vii.2012, BIOUG03742-D10, 2 ♂ (BIOUG); idem except 8-15.vi.2012, BIOUG03397-E09, 2

♂ (BIOUG); **CANADA**: **BC**: Lorna, *49.750*° *-119.417*°, 11.vii.1925, H.Richmond, Abies lasiocarpa, slide prep: ovipositor, 1 ♀ (CNC); Victoria, *48.433*° *-123.367*°, 7.ix.1899, Rev.S.W.Taylor, slide prep: ovipositor, 1 ♀ (CNC); Yoho National Park, Bunkhouse, 51.365° -116.528°, 16-30.vii.2014, Jamie, Malaise trap, BIOUG19787-F10, 1 ♂ (BIOUG); **CANADA**: **MB**: Churchill, 11 km S Churchill, Goose Creek, 58.649° -94.193°, 17.vii.2008, A.Thielman, Malaise trap, 1 ♂ (BIOUG); idem except 7.vii.2010, J Wang, hand collection, BIOUG00998-F08, 1 ♀ (BIOUG); Churchill, 23 km SE Churchill, Twin Lakes Road fen, 58.661° -93.832°, 20m, 17.vii.2008, A.Thielman, Malaise trap, PROBE-TW0444, 1 ♂ (BIOUG); Churchill, 4 km SE Churchill, Dene Village, 58.734° -94.112°, 5m, 14.vii.2008, A.Thielman, Malaise trap, PROBE-TW0462, 1 ♂ (BIOUG); Wapusk National Park, 58.723° -93.458°, 22-29.vi.2014, D.Iles, Malaise trap, BIOUG17609-E02, 1 ♂ (BIOUG); Churchill, *58.756*° *-94.084*°, 29.vi.1937, W.J.Brown, 1 ♀ (CNC); Ft. Churchill, *58.756*° *-94.084*°, 28.vi.1952, J.G.Chillcott, 1 ♀ (CNC); **NL**: Hebron, Labrador, *58.199*° *-62.626*°, 9.vii.1954, J.F.MacAlpine, Salix, slide prep: ovipositor, 1 ♀ (CNC); **NS**: Richmond Co., Isla Madame, Crichton Is., 20-22.vii.1977, G.B.Fairchild, insect flight trap, FSCA 00091438, 1 ♀ (FSCA); Victoria Co. 16 mi G. Baddick Highland Road, 29.vii-3.viii.1977, G.B.Fairchild, flight trap, FSCA 00091444, 1 ♂ (FSCA); Victoria Co., Beinn Bhreagh Baddeck, 3.vii.1977, G.B.Fairchild, flight trap, FSCA 00091436, 1 ♀ (FSCA); Victoria Co., Highland Road, Mile 16 East Road, 29.vii-3.vii.1977, G.B.Fairchild, insect flight trap, FSCA 00091439, 1 ♂ (FSCA); **NT**: Muskox L., 64.7500° -108.1667°, 11.vii.1953, J.G.Chillcott, slide prep: penis valves, 1 ♂ (CNC); idem except 25.vii.1953, slide prep: penis valves, 1 ♂ (CNC); Norman Wells, *65.282*° *-126.833*°, 3.viii.1949, W.R.M.Mason, 1 ♀ (CNC); **ON**: Ft. Erie, *42.900*° *-78.933*°, 4.vii.1910, M.C.VanDuzee, 1 ♂ (CASC); **QC**: Gt. Whale R., *55.267*° *-77.783*°, 12.vii.1949, J.R.Vockeroth, 1 ♀ (CNC); **YT**: Ivvavik National Park,

69.162° -140.155°, 365m, 17-23.vi.2014, Pinette,Pete,Sejal, Malaise trap, BIOUG16879-H01, 1 ♂ (BIOUG); Whitehorse, Mount McIntyre, 60.6344° -135.162°, 1360m, 21.vi-5.vii.2014, C.S.Guppy, Malaise trap, BIOUG26656-D01, 1 ♂ (BIOUG); **USA**: **AK**: King Salmon, Naknek R., *58.688° -156.662°*, 9.vii.1952, W.R.Mason, 1 ♀ (CNC); **AR**: Washington Co., 5 mi N. Winslow on US 71, 6.vi.1976, H.N.Greenbaum, swept, willow, FSCA 00091441, 1 ♀ (FSCA); idem except 8.vi.1976, Salix, FSCA 00091442, 1 ♀ (FSCA); Washington Co., 50 mi N. Winslow on US 71, 11.vi.1976, H.N.Greenbaum, Salix nigra, FSCA 00091440, 1 ♀ (FSCA); **CA**: Modoc Co., Cedar Pass, 41.5605° -120.2889°, 1828m, 29.vi.1955, J.C.Wells, 1 ♀ (DAV); Mono Lake State Park, boardwalk, 38.016° -119.15°, 1955m, 5.viii.2011, Biobus 2011, Malaise trap, BIOUG02645-G07, 1 ♂ (BIOUG); Plumas Co., Buck's Lake, 39.8797° -121.1486°, 1643m, 23.vi.1949, H.A.Hunt, 1 ♀ (DAV); Tuolumne Co., Stan. Natl For. Eagle Meadw, Riparian Strip, 38.2872° -120.0014°, 2289m, 12.vii.2006, S.Fullerton, E.Zoll, S.Kelly, P.Russell, UCFC 0 361 344, 1 ♂ (DAV); **GA**: Clarke Co., Athens-Whitehall, 2-5.vi.1978, H.Greenbaum, R.Turnbow, insect flight trap, FSCA 00091445, 1 ♂ (FSCA); idem except 27.v.1978, Betula nigra, FSCA 00091446, 1 ♀ (FSCA); **IL**: Algonquin, *42.166° -88.294°*, 27.vii.1911, reared, em.: 14.ii.1947, Nason, slide prep: ovipositor, 1 ♀ (NFRC); Apple River Cañ. State Park, *42.447° -90.053°*, 22.viii.1935, reared, , DeLong, Ross, Salix longifolia, 1 ♀ (NFRC); **MO**: Columbia, 27.ix.1966, S.Poe, FSCA 00091435, 1 ♀ (FSCA); **MT**: Ravalli Co., Crooked Creek, Skalkaho Divide, 4-7.vii.1966, coll. unknown, Malaise trap, FSCA 00091434, 1 ♀ (FSCA); **NJ**: Haddon Hts, 39.8773° -75.0646°, 21m, 26.v.1934, L.J.Bottimer, 1 ♀ (DAV); **NY**: Albany Co., nr. Renesselearville Huvck Preserve, 15.vii.1977, R. & J.Matthews, Malaise trap, FSCA 00091427, 1 ♂ (FSCA); idem except 16.vii.1977, FSCA 00091429, 1 ♀ (FSCA); idem except 30.vii.1977,FSCA 00091430, 1 ♀ (FSCA); idem except 31.vii.1977, FSCA 00091426, 1 ♂

(FSCA); idem except 4.vii.1977, FSCA 00091428, 1 ♀ (FSCA); Warren Co. N.Y., 2.v.1960, R.A.Morse, Salix sp., FSCA 00091433, 1 ♀ (FSCA); Westchester Co., Armonk, Calder Center, 12-18.vii.1974, C.Calmbacher, Malaise trap, 1 ♀ (FSCA 00091443) 1 ♂ (FSCA 00091437) (FSCA); **UT**: Cache Co., Logan Cyn., 41.7309° -111.79°, 1559m, 18.vi.1960, G.E.Knowlton, 1 ♀ (DAV).

Distribution. This species is common and widespread across the Nearctic, having perhaps the broadest distribution of the entire genus. It is found in subarctic, boreal, temperate, and warm temperate parts of North America, and is recorded from Alaska, Yukon, Northwest Territories, Nunavut, British Columbia, Alberta, Saskatchewan, Manitoba, Ontario, Quebec, Labrador, Oregon, Montana, Utah, Colorado, California, Illinois, Connecticut, New Jersey, Missouri, Virginia, Arkansas, and Georgia (D. R. Smith 1979, Goulet and Bennett 2021).

Genetic data. Specimens of this species belong to a single BIN, which is shared with *P. staudingeri*: BOLD:AAG3568. Based on available genetic data (one specimen) the nearest neighbour (*P. bifida*) is 1.2% different.

Hosts. *Salix* spp. (D. R. Smith 1979).

Comments. Besides the male holotype, only one other specimen identified as *P. valvangula* was encountered (a male, identified by Wong), and both are indistinguishable from *P. sycophanta*. The only character noted to differentiate the two is the shape of the valvispina, which Wong described as more slender and curved in. *P. valvangula* (Wong and Ross 1960), but which appears to be within the range of intraspecific variation for *P. sycophanta*. The only specimens encountered under the name *P. hyalina* (identified by H.N. Greenbaum) were attributable to *P. geniculata*, while the female holotype of *hyalina* fits the above diagnosis for *P. sycophanta*. Both

types were collected from near Ithaca, NY, which is within *P. sycophanta*'s range. Therefore, based on the available evidence the two are treated as junior synonyms of *P. sycophanta*.

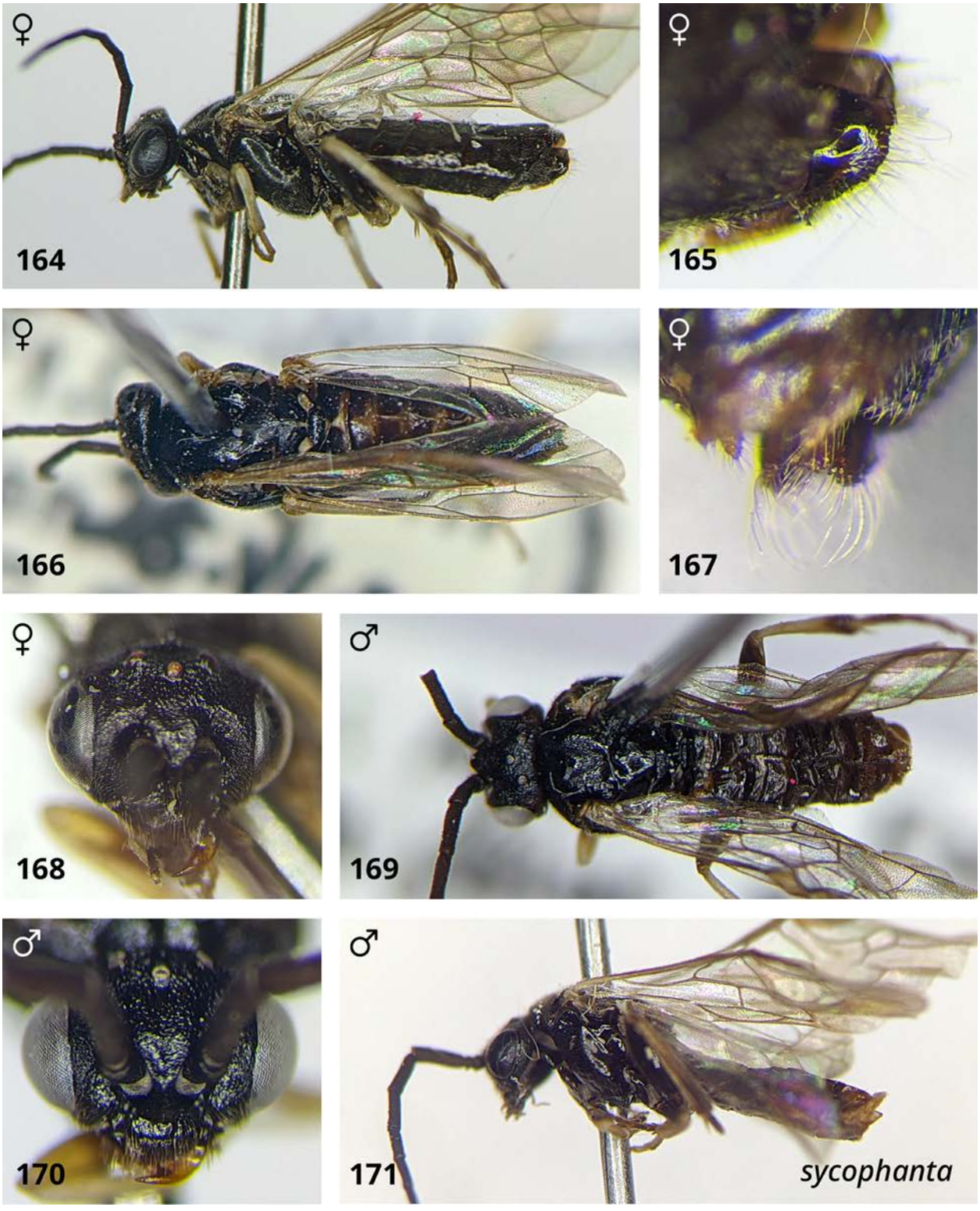

Figures 164–171. *Pristiphora sycophanta*. **164**. Female lateral view. **165**. Sawsheath lateral view. **166**. Female dorsal view. **167**. Sawsheath dorsal view. **168**. Female head. **169**. Male dorsal view. **170**. Male head. **171**. Male lateral view.

Figures 172–174. Subapical tooth of tarsal claw. **172**. Small, less than half length of apical tooth (*P. melanocarpa*). **173**. Medium, approximately half length of apical tooth (*P. aphanta*). **174**. Large, at least two–thirds length of apical tooth (*P. frigida*).

Figures 175–177. Harpes of genital capsule. **175–176**. Overlapping at rest (*P. kangirsummiut*, *P. staudingeri*). **177**. At most touching at rest (*P. sycophanta*).

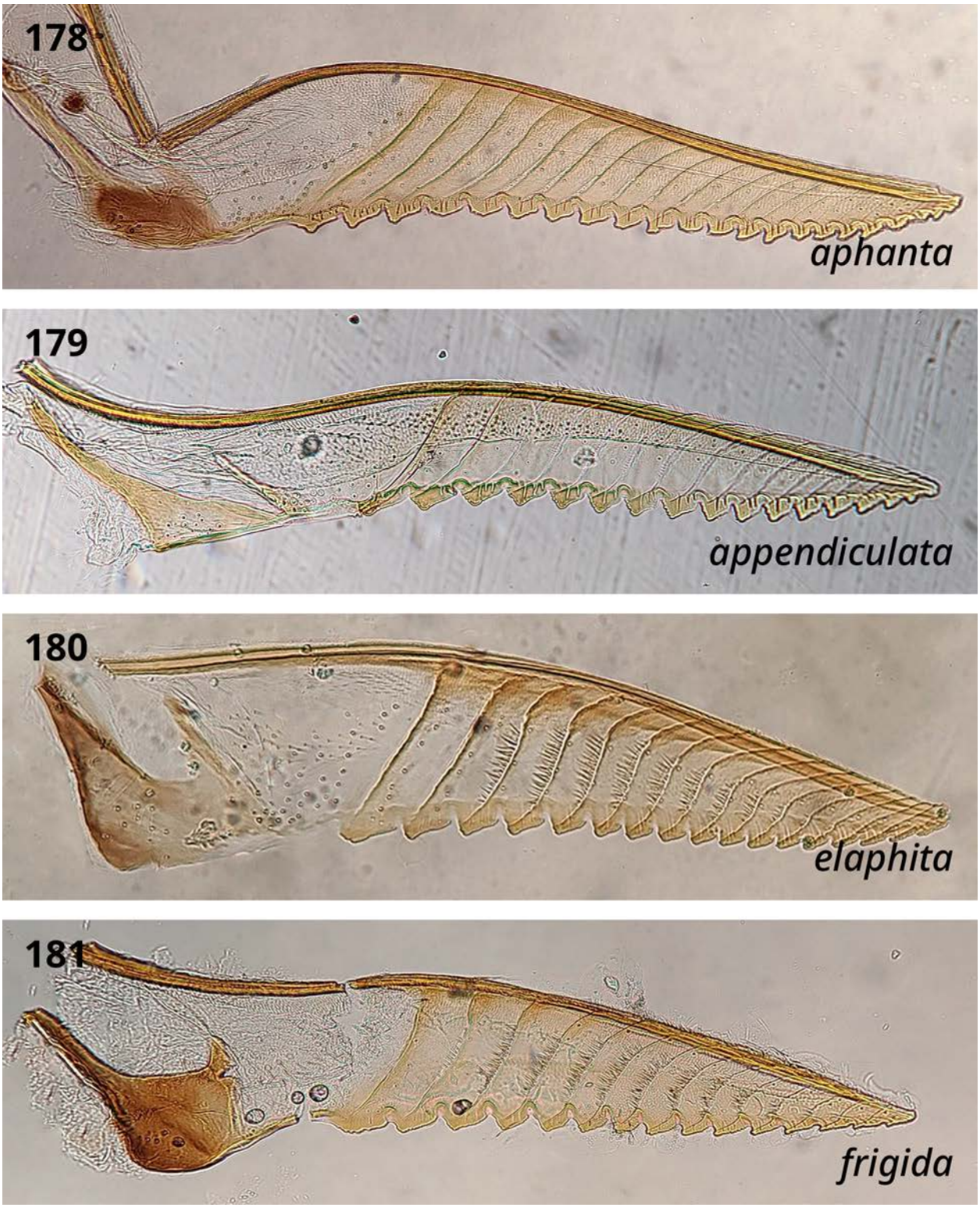

Figures 178–181. Lancets of *Pristiphora ruficornis* group (lateral view). **178**. *P. aphanta*. **179**. *P. appendiculata*. **180**. *P. elaphita*. **181**. *P. frigida*.

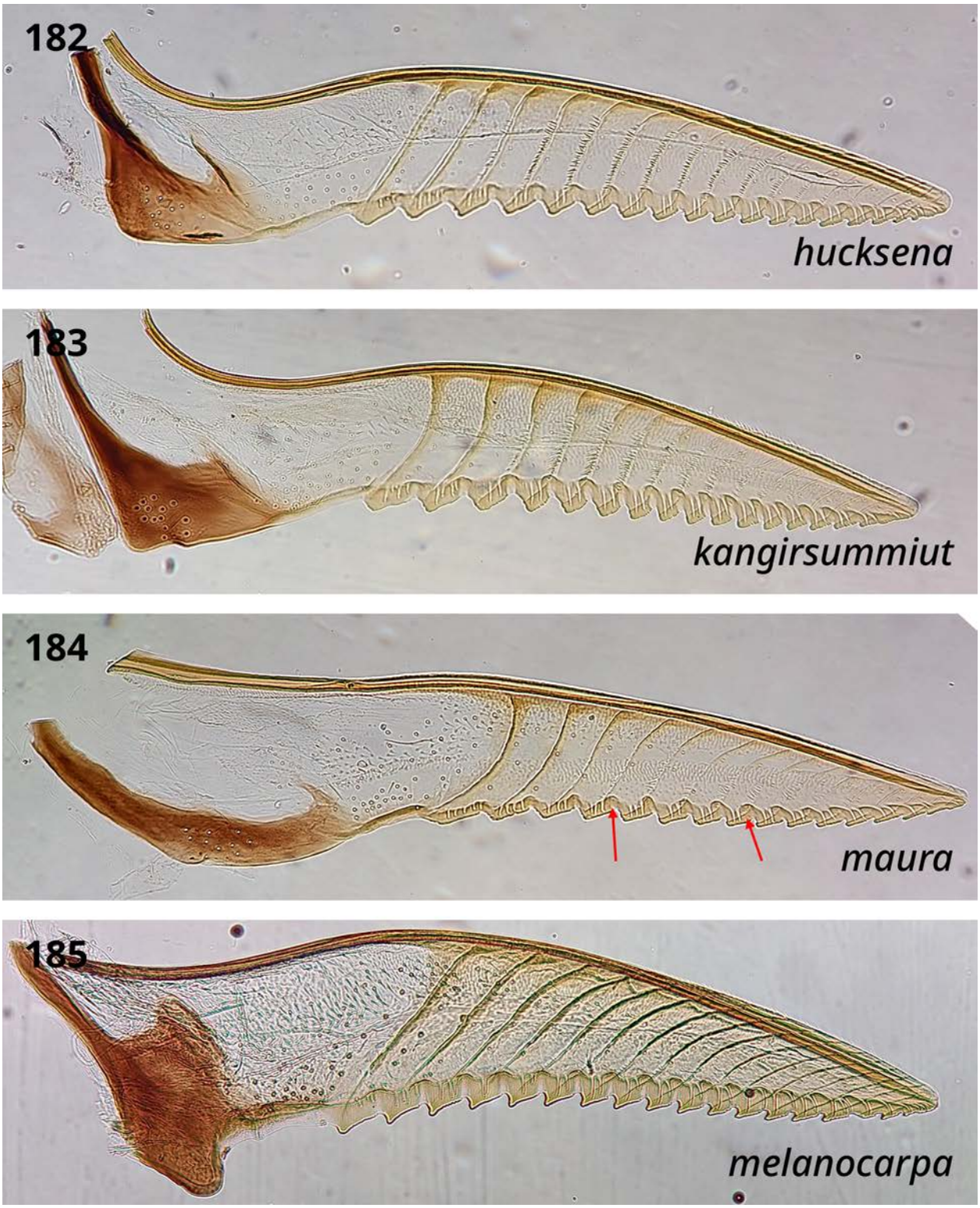

Figures 182–185. Lancets of *Pristiphora ruficornis* group (lateral view). **182**. *P. hucksena*. **183**. *P. kangirsummiut*. **184**. *P. maura*, red arrows show small spiny pectines present at level of sclerora. **185**. *P. melanocarpa*.

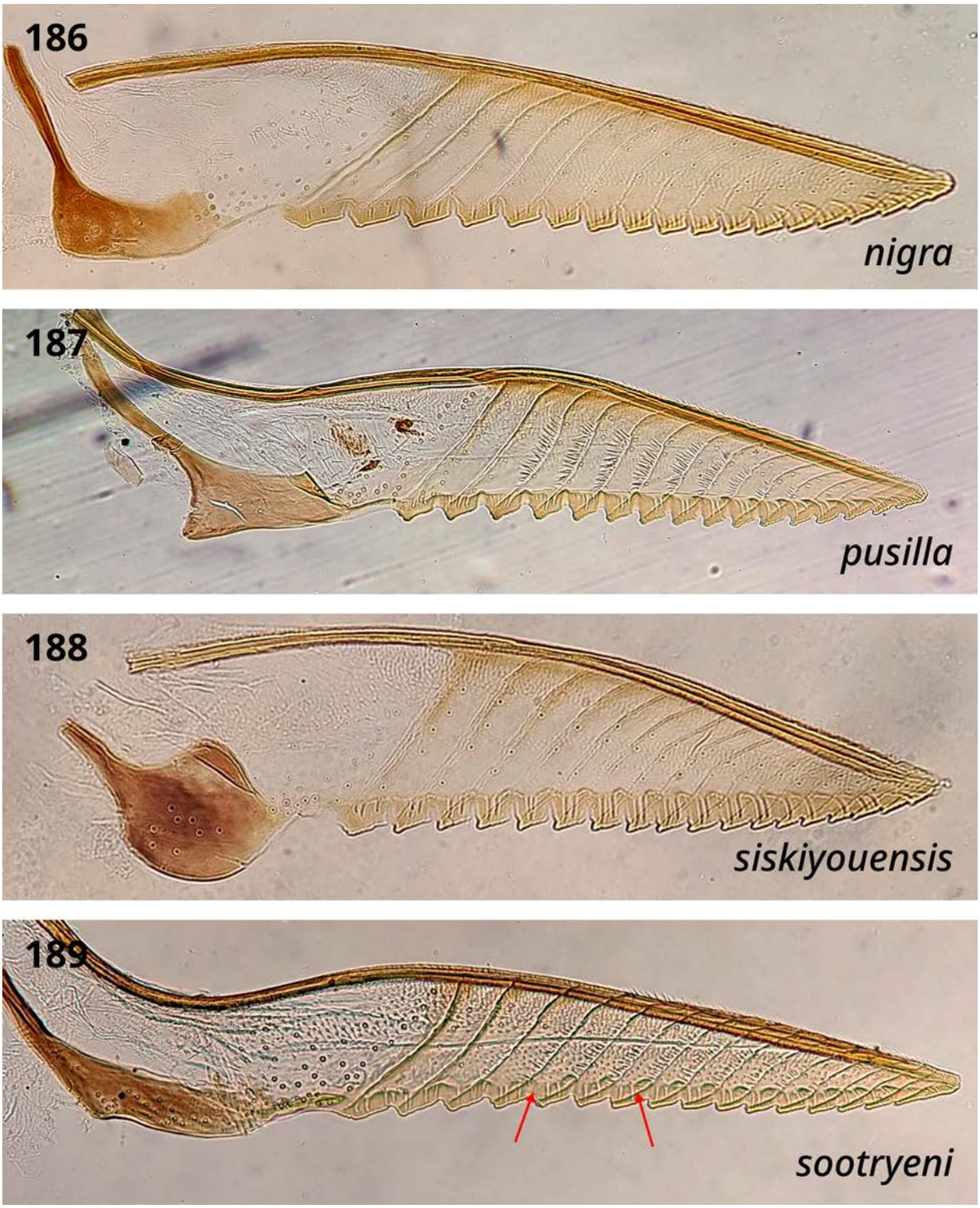

Figures 186–189. Lancets of *Pristiphora ruficornis* group (lateral view). **186**. *P. nigra*. **187**. *P. pusilla*. **188**. *P. siskiyouensis*. **189**. *P. sootryeni*, red arrows show small spiny pectines present at level of sclerora.

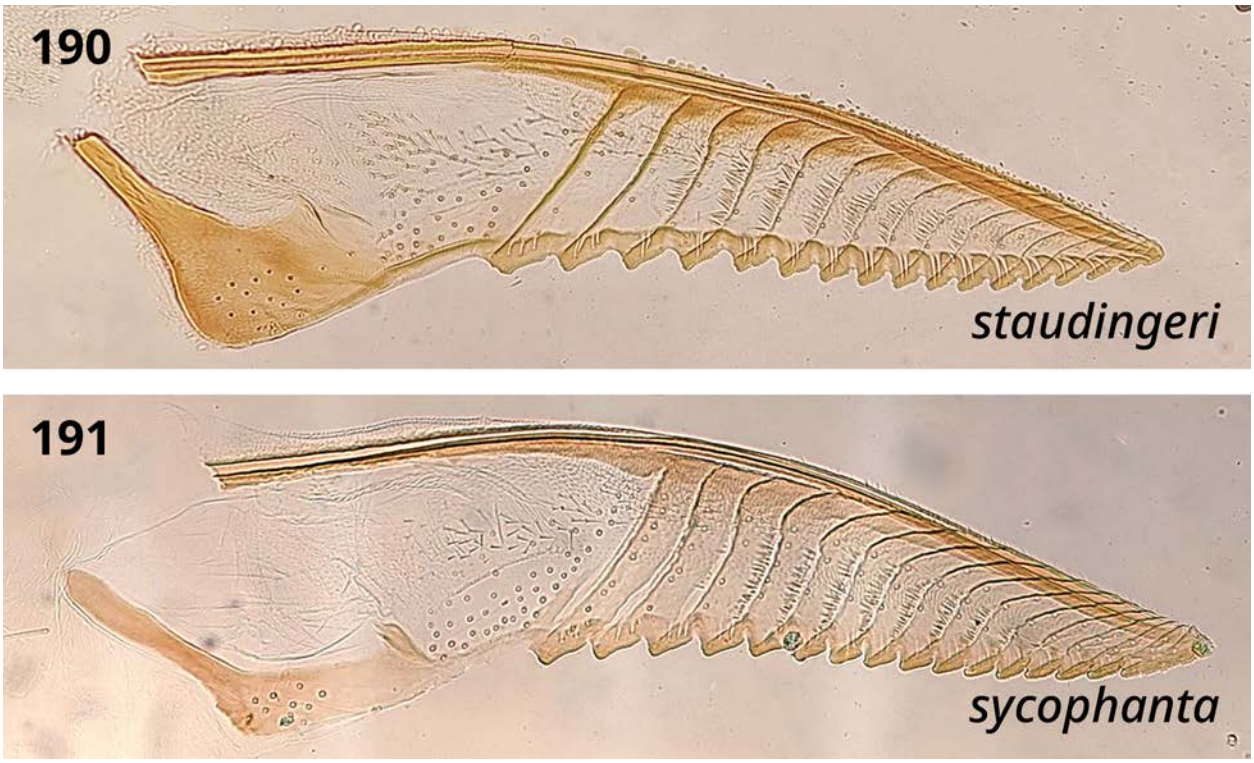

Figures 190–191. Lancets of *Pristiphora ruficornis* group (lateral view). **190**. *P. staudingeri*. **191**. *P. sycophanta*.

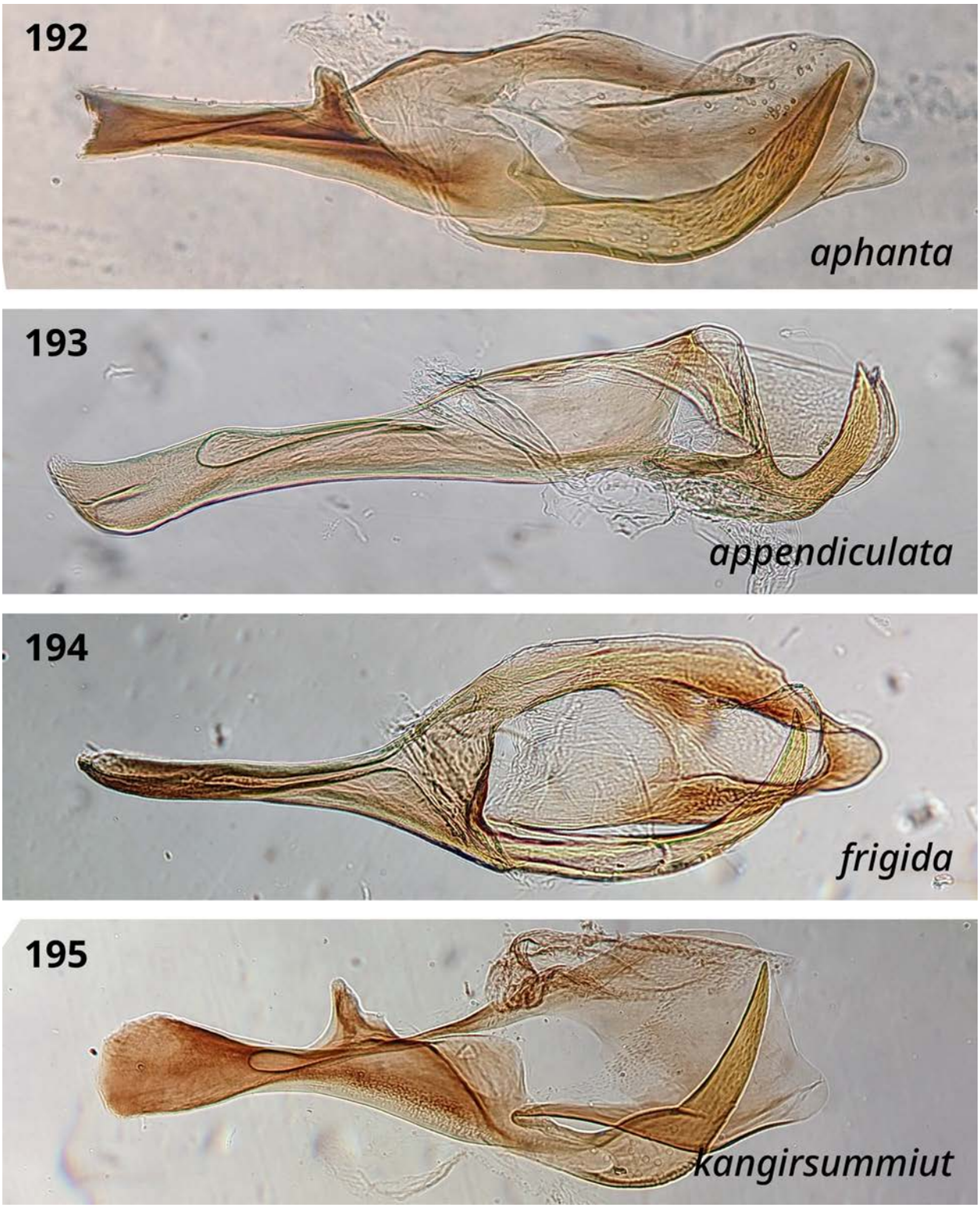

Figures 192–195. Penis valves of *Pristiphora ruficornis* group (lateral view). **192**. *P. aphanta*. **193**. *P. appendiculata*. **194**. *P. frigida*. **195**. *P. kangirsummiut*.

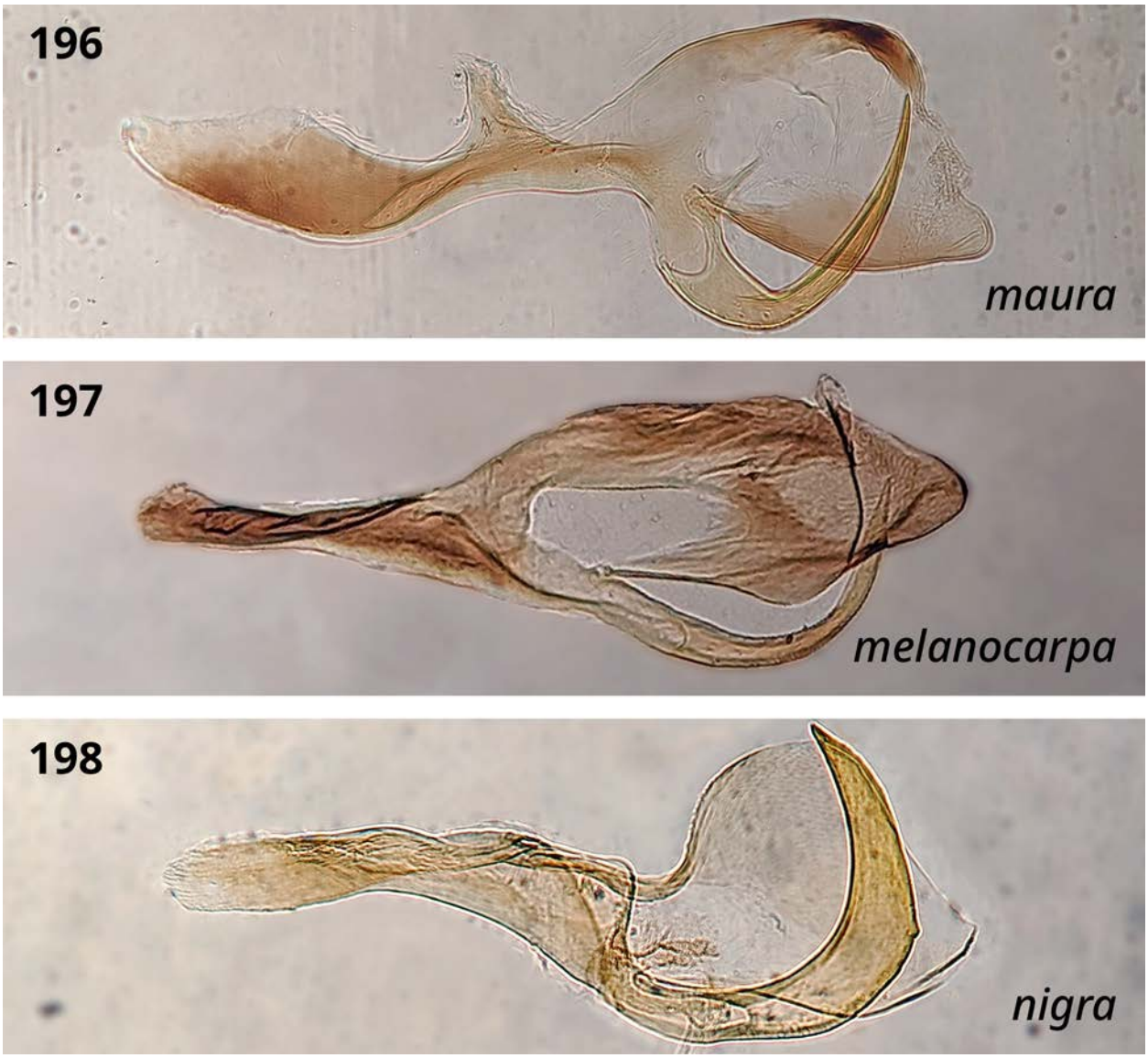

Figures 196–198. Penis valves of *Pristiphora ruficornis* group (lateral view). **196**. *P. maura*. **197**. *P. melanocarpa*. **198**. *P. nigra*.

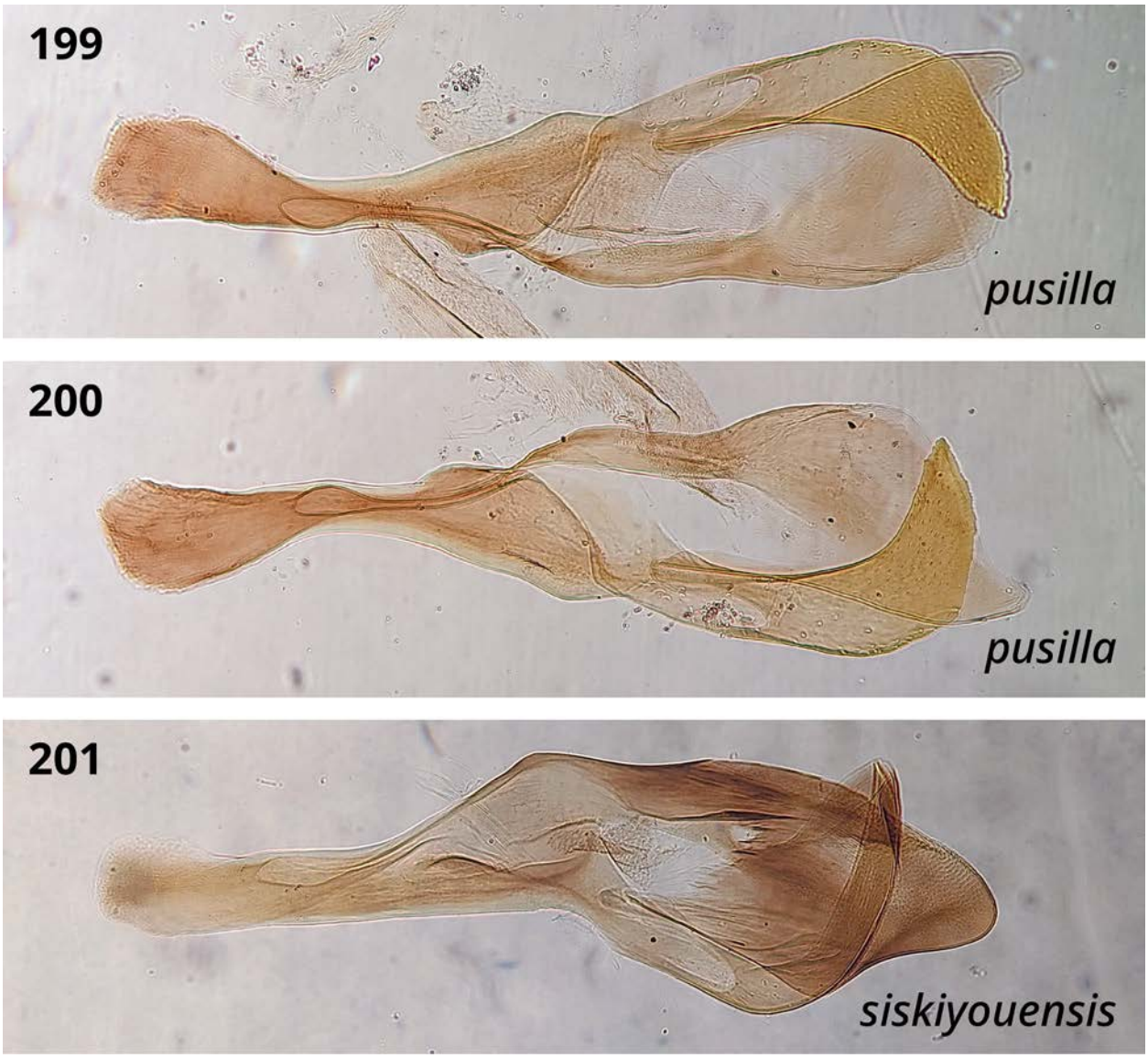

Figures 199–201. Penis valves of *Pristiphora ruficornis* group (lateral view). **199**. *P. pusilla*, right penis valve. **200**. *P. pusilla*, left penis valve. **201**. *P. siskiyouensis*.

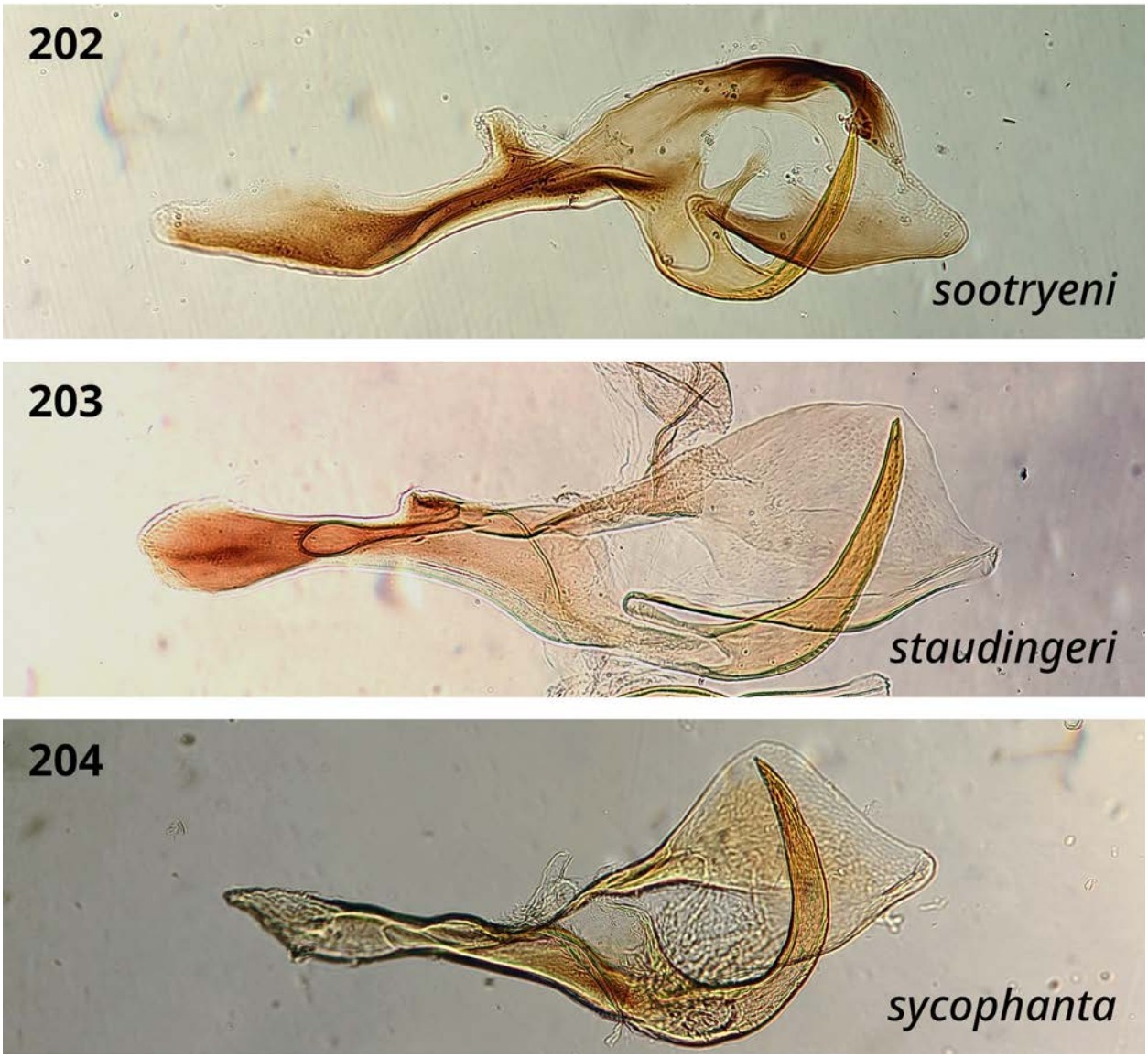

Figures 202–204. Penis valves of *Pristiphora ruficornis* group (lateral view). **202**. *P. sootryeni*. **203**. *P. staudingeri*. **204**. *P. sycophanta*.

***Pristiphora rufipes* group**

The definition of the rufipes group is here expanded to include *P. cincta* and its Nearctic relatives - *P. paloma* and *P. serrula* – as well as *P. bivittata*. Although this last species is relatively distantly related, and the structure of the lancet differs markedly (presence of setae on

annuli and curved downward apically), the penis valve is very similar to others in the *rufipes* group, and the monophyly of the entire clade is strongly supported (see Chapter 3). Penis valves in the *rufipes* group have a somewhat rectangular paravalva with a distinct valvar strut from base to apex, a small, narrow valvispina arising closer to the ventral side of the paravalva, and an unmodified, somewhat rectangular or oval-shaped pseudoceps.

Diagnosis. Externally, this group can generally be recognized by their colouration, with the labrum, apical margin of clypeus, posterior corner of pronotum usually broadly, and legs mostly pale, head and thorax otherwise dark, and abdomen either dark or with extensive yellow-orange colouration. The body is usually shiny, microsculpture smooth or weakly imbricate (although the mesepisternum of *P. cincta* is variable from shiny, microsculpture smooth to rough, coriaceous). Females have the lateral posterior lobe of valvula 3 distinctly produced, with sawsheath appearing emarginate in dorsal view. Species in this group can usually be differentiated from the *ruficornis* group by the longer postocellar space, which in dorsal view is less than twice as wide as long (IOC:OOCL ≤ 1.9x in *rufipes* group; ≥ 2.0x in *ruficornis* group) except in *P. cincta* (*rufipes* group, 1.8–2.0x) and *P. appendiculata* (*ruficornis* group, 1.6–1.8x). As well, in the *rufipes* group, the medial surface of the head between the antennal sockets is only weakly raised, appearing weakly concave in dorsal view; in the *ruficornis* group, it is usually raised as a distinct ridge, appearing at least weakly convex in dorsal view. Known host plants include *Aquilegia* L., *Crataegus* Tourn ex. L., *Spiraea* L., *Betula*, *Salix*, and *Vaccinium* L.

Key to species of the *P. rufipes* group

Females

1. Abdomen pale in whole or in part, minimally either S1–S7 entirely pale or T3–T5 and S3–S5 mostly pale (Figs. 207, 215, 239)..... 2

1'. Abdomen entirely dark (Figs. 223, 231) 4

2. At least T3–T5 with pale lateral spots but dark medially (Fig. 207), S3–S5 pale; mesepisternum mostly pale (Fig. 205) or dark; femora entirely pale except ventrally with narrow longitudinal line brown..... *P. bivittata* (paler individuals)

2'. At least T3–T5 and S3–S5 pale (Figs. 215, 239), including medially; mesepisternum dark (Figs. 213, 237); one or more femora more extensively darkened, at least a broad basal ring to entirely dark..... 3

3. Hindfemur usually mostly dark, basal and apical rings pale (but sometimes entirely brown); subapical tooth of tarsal claw small, about half as long as apical tooth or smaller (e.g. Fig. 172); lateral posterior lobe of valvula 3 projecting about as far as median carina (Fig. 216); lamnium of lance at least twice as long as radix when measured along the ventral margin, lance only weakly curved downward apically (Fig. 247)..... *P. cincta* (paler individuals)

3'. Hindfemur mostly pale except broad dark ring apically; subapical tooth of tarsal claw large, about two-thirds as long as apical tooth (e.g. Fig. 174); lateral posterior lobe of valvula 3 projecting further than median carina (Fig. 240); lamnium of lance at most 1.9x as long as radix, lance distinctly curved downward apically (Fig. 253)..... *P. serrula*

4. Femora entirely pale except ventrally with narrow longitudinal line brown, coxae pale in apical one-third to half; lancet with setae on annuli and curving downward apically (Fig. 245).....

..... *P. bivittata* (darker individuals, formerly *P. venatta*)

4'. One or more femora more extensively darkened, at least one femur with a broad basal ring dark, and coxae at least partly pale OR if femora pale as above then coxae entirely dark; lancet without setae on annuli, ventral margin approximately straight (Figs. 248, 250, 252)..... 5

5. Tarsal claw without subapical tooth; lateral posterior lobe of valvula 3 projecting much further than median carina (Fig. 232); coxae entirely dark; lancet with blunt serrulae, basoventral angle approximately obtuse (Fig. 252)..... *P. rufipes*

5'. Tarsal claw with distinct subapical tooth (e.g. Figs. 172–174); lateral posterior lobe of valvula 3 projecting only about as far as median carina (Figs. 216, 224); coxae with at least apical one-

third pale; lancet with sharper serrulae, basoventral angle rounded-right or rounded-acute (Figs. 248, 250) 6

6. Eye large, in lateral view at least 3.2x wider than gena, in frontal view LOD usually about 1.2x length of eye (at most 1.3x); subapical tooth of tarsal claw medium, about half as long as apical tooth (e.g. Fig 173); radix of lance squarish, broadly rounded dorsally, as wide as basal five annuli or wider (Fig. 249) .....*P. paloma*

6'. Eye smaller, in lateral view at most 3.2x as wide as gena, in frontal view LOD at least 1.3x length of eye; subapical tooth of tarsal claw smaller, less than half as long as apical tooth (e.g. Fig. 172); radix of lance tapering dorsally and narrower, as wide as basal four annuli or less (Fig. 247)..... *P. cincta* (darker individuals, including former *P. banksi*)

Males

1. Abdomen with T3–T5 pale at least laterally, S1-S9 entirely pale (Figs. 242, 244); penis valve (Fig. 258) with ventral margin of paravalva convexly produced basally and straight near base of valvispina .....*P. serrula*

1'. Abdomen usually entirely dark (Figs. 210, 218, 226, 234), at most S3–S5 pale; penis valve with ventral margin of paravalva either evenly rounded basally (Figs. 256, 257) or with distinct obtuse angle near base of valvispina (Figs. 255, 258) 2

2. On penis valve, ventral margin of paravalva with distinct obtuse angle near base of valvispina (Figs. 255, 258) 3

2'. On penis valve, ventral margin of paravalva straight near base of valvispina (Figs. 256, 257) 4

3. Tarsal claw with small or minute subapical tooth, much less than half as long as apical tooth (e.g. Fig. 172); coxae entirely dark; penis valve (Fig. 258) with apex of pseudoceps more-or-less evenly rounded; paravalva approximately rectangular, dorsal margin with distinct convex hump and apicodorsal margin nearly perpendicular to longitudinal axis of paravalva; valvar strut meeting ventral margin of paravalva at attachment point to valviceps.....*P. rufipes*

3'. Tarsal claw with medium subapical tooth, about half as long as apical tooth (e.g. Fig. 173); coxae pale in apical one-third to half; penis valve (Fig. 255) with apex of pseudoceps

approximately rectangular; paravalva somewhat less rectangular, apicodorsal margin sloping gradually away from valvispina; valvar strut meeting ventral margin of paravalva apically of attachment to valviceps ..... *P. bivittata*

4. Eye large, in lateral view at least 3.2x wider than gena, in frontal view LOD usually about 1.2x length of eye (at most 1.3x); penis valve (Fig. 257) relatively narrow, paravalva about 2.5x longer than wide; valvispina about one-third as long as greatest width of paravalva and more than half as long as width of pseudoceps across base of valvispina; abdomen always entirely dark.....*P. paloma*

4'. Eye smaller, in lateral view at most 3.2x as wide as gena, in frontal view LOD at least 1.3x length of eye; penis valve (Fig. 256) wider, paravalva about 3x longer than wide; valvispina shorter, about one-quarter as long as greatest width of paravalva and less than half as long as width of pseudoceps across base of valvispina; abdomen usually entirely dark, sometimes S3–S5 pale .....*P. cincta*

***Pristiphora bivittata* (Norton, 1861)**

(Figs. 201–208, 241–242, 251)

Nematus bivittatus Norton, 1861: 158.

Nematus luteolus Norton, 1867b: 200.

Pristiphora dyari Marlatt, 1896: 118.

Pristiphora koebelei Marlatt, 1896: 119-120.

Pachynematus occidentalis Marlatt, 1896: 109.

Pristiphora occidentalis Marlatt, 1896: 121-122.

Periclista patchi MacGillivray, 1923: 29-30.

Pristiphora venatta Wong & Ross, 1960: 196-198. **n. syn.**

Diagnosis. Females are variable in colour, but can usually by differentiated by the two longitudinal pale stripes on the abdomen, with T2 to T8 pale, dark medially, and corresponding sterna at least partly pale (Fig. 203; in other species: abdomen dark as in *P. paloma* and *P. rufipe*s, Figs. 218, 227; orange-banded, usually with T3 to T5 entirely pale as in *P. cincta*, Fig. 211, and sometimes *P. serrula*; or entirely pale as in most individuals of *P. serrula*, Fig. 235). Lighter individuals often have a pale or mostly pale mesepisternum, which readily distinguishes *P. bivittata* from all other Nearctic species in the *rufipes* group (Fig. 201; entirely dark in other species, Figs. 211, 219, 227, 235). Darker individuals may only have pale lateral spots on T3 to T5, differing from *P. cincta* and *P. serrula* by the terga dark medially (pale terga always pale medially in *P. cincta* and *P. serrula*), or rarely an entirely dark brown abdomen, in which case they can be separated from *P. serrula* by the dark abdomen (abdomen always at least partly pale in *P. serrula*), from *P. cincta* and *P. paloma* by the femora entirely pale except narrow longitudinal line brown ventrally (one or more femora more extensively darkened in *P. cincta* and *P. paloma*), and from *P. rufipes* by the lateral posterior lobe of valvula 3 projecting only about as far as median carina (projecting distinctly further than median carina in *P. rufipes*). The lancet is easily differentiated from others by the presence of setae on annuli (Fig. 242; absent in other species, Figs. 244, 246, 248, 250) and the shape, curving downwards toward apex, ventral margin concave (ventral margin approximately straight in other species). Males are not easily differentiated without examining the penis valve, which differs from all others in the group except *P. rufipes* by the distinct obtuse angle on ventral margin of paravalva near base of valvispina (Fig. 251; straight in other species). In *P. bivittata* the pseudoceps is approximately rectangular apically (Fig. 251; more evenly rounded in *P. rufipes*, Fig. 254), the dorsal margin of

the paravalva slopes gradually away from the valvispina (dorsal margin with distinct convex hump and paravalva more strongly rectangular in *P. rufipes*), and the valvar strut meets the ventral margin of the paravalva apically of attachment to valviceps (valvar strut meeting ventral margin at attachment point to valviceps in *P. rufipes*).

Female. Length, 6.0–6.8 mm.

Colour: Antenna dark; head dark; mouthparts pale, mandible darkening in apical third to dark brown at apex; labrum pale; clypeus apical margin pale. Thorax variable, mostly dark to extensively pale; pronotum variable, with at least posterior corner broadly pale, to entirely pale except ventral corner with margins dark; tegula pale; mesonotum variable, either entirely dark, or extensively yellow-orange lateral lobes medially, mesoscutellum medially, and mesoscutellar appendage dark; mesepisternum variable, either entirely dark, or mostly pale with pectus and posterodorsal margin broadly dark; mesepimeron either dark, or pale except posterior margin narrowly dark; metapleuron either dark, or pale except dorsal and posterior margins narrowly dark. Legs pale, except coxae dark basally, with apical one-third to half pale, trochanters and trochantelli trochantellus with basoventral spot brown, foreleg with femur sometimes partly or mostly brown, tarsus with apical two to three tarsomeres brown, sometimes entirely brown, midleg with as on foreleg, hindleg with femur sometimes brown ventrally and pale-infuscate dorsally, tibia broad apical ring and tarsus brown. Abdomen usually mostly pale, except T1 usually dark, T2 to T8 usually dark medially, T9 and T10 either pale or dark, corresponding sterna at least partly pale; abdomen occasionally much darker, with only paired brown spots on T3 to T5, valvifer 2 pale, cerci dark or yellow-brown.

Head: Antenna length 2.4–2.7x head width; F1 0.85–0.95x length of eye; F1 subequal to or slightly shorter than F2 (F1:F2 = 0.95x), subequal to F3 (F1:F3 = 1.0–1.05x), proceeding

flagellomeres progressively shorter (F7:F1 = 0.7–0.8x). Clypeus truncate/shallowly widely emarginate. Malar space 0.8x OD. LOD 1.3–1.5x height of eye in frontal view. IOC:OOL = 1.0–1.1x. Head dull, imbricate, vertexal area somewhat shiny submedially, microsculpture smooth or weakly imbricate.

Thorax: Pronotum dull, imbricate. Prepectus distinct & pitted, setose. Mesepisternum shiny, microsculpture smooth, epicnemium shiny or somewhat dull, VERY finely pitted, sometimes with week horizontal lines. Mesepimeron shiny, microsculpture smooth. Mesonotum shiny, weakly imbricate, may be somewhat dull along lateral margins of mesoscutum; mesoscutellar appendage dull, imbricate. Parapsis shiny, weakly costulate, puncticulate. Mesopostnotum rough, coarsely sculptured. Metabasitarsus shorter than metatarsomeres 2–4 combined. Subapical tooth of tarsal claw medium, about half as long as apical tooth.

Abdomen: Terga somewhat dull, imbricate. Sawsheath in dorsal view very weakly emarginate, with distinct median carina, longest setae about three-quarters as long as apical width of sawsheath, visible length of sawsheath less than cerci. Sawsheath in lateral view with lower margin evenly rounded, meeting dorsal margin at a sub-quadrate to broadly rounded apex. Valvula 3 lateral posterior lobe produced and wide, about equally as produced as median carina. In apical view, width of sawsheath 0.6-0.7x height of setose area. Lance curved downward apically, ventral margin concave; lamnium about twice as long as radix when measured along the ventral margin; radix squarish, broadly rounded dorsally, at least as wide as basal seven annuli of lamnium. Tangium of lancet approximately rectangular or slightly tapering apically; tangial process extending as high as 1.5x height of tangium. Lancet with basal one or two suture slightly recurved dorsally, proceeding sutures approximately straight and doprsally apically directed; serrulae flat and blunt, basoventral angle distinctly rounded.

Male. Length, 5.3–5.8 mm.

Colour as in female except as follows. Antenna dark, with few stout black setae; head dark; mouthparts pale, mandible translucent brown except dark near base and apex; clypeus sometimes apical margin broadly pale. Thorax dark, never with the pale colouration of some females. Abdomen dark or dark brown. Structure and sculpture similar to female, except: antenna 2.4–2.5x head width , mesoscutellum sometimes somewhat dull, weakly imbricate, mesoscutellar appendage rough, coarsely imbricate. Penis valve with paravalva approximately rectangular, ventral margin with obtuse angle near base of valvispina, margins gradually tapering apically towards base of valvispina, valvar strut extending from ventral margin beyond origin on valviceps to dorsal margin subapically; valvispina small, narrow; pseudoceps approximately rectangular apically; valvura with ergot small and difficult to discern.

Material studied. *Syntypes* (4 ♀) of *koebelei*—**USA**: **WA**: Washington (USNM). *Holotype* (♀) of *venatta*—**USA**: **ID**: Lewis Co., Vollmer, 46.24278° -116.46528°, v.1930, slide prep: ovipositor (INHS). *Additional material*—**CANADA**: **BC**: Aspen Grove, *49.931° -120.630°*, 20.v.1934, Hugh B.Leech, 1 ♂ (CNC); Cranbrook, *49.500° -115.769°*, 10.v.1922, C.B.D.Garrett, slide prep: penis valves, 1 ♂ (NFRC); Fernie, *49.505° -115.063°*, 15.vi.1934, Hugh B.Leech, 1 ♀ (CNC); Robson, *49.334° -117.695°*, 15.vi.1950, H.R.Foxlee, slide prep: penis valves, 1 ♂ (CNC); idem except 17.iv.19 (CNC); idem except 18.iv.19 (CNC); idem except 24.iv.19 (CNC); idem except 25.iv.19 (CNC); idem except 3.v.19 (CNC); Steelhead, *49.220° -122.316°*, 10.viii.1933, H.B.Leech, 1 ♀ (CNC); **BC**: Clearwater, Clearwater Secondary School, 51.65° -120.037°, 461m, 20.iv-8.v.2015, Michael Lau, Malaise trap, BIOUG22064-F02, 1 ♂ (BIOUG); **MB**: Birtle, *50.422° -101.046°*, 25.v.1928, R.D.Bird, , 1 ♂ (NFRC); **NB**: Fundy NP, Laverty Falls, 45.657° -65.015°, 404m, 11.viii.2009, BIObus 2009, , 09BBEHY-0856, 1 ♂ (BIOUG);

ON: Kearney, *45.556*° *-79.225*°, 2-9.vii.1909, M.C.VanDuzee, , 1 ♂ (CASC); Georgian Bay Islands National Park, Beausoleil Island, Cedar Spring Campground, 44.8515° -79.8744°, 177m, 30.vii-6.viii.2013, Jeff Howard, Malaise trap, BIOUG09852-E02, 1 ♂ (BIOUG); **USA**: **AK**: Kukak Bay, *58.319*° *-154.266*°, 4.vii.1899, T.Kincaid, 1 ♀ (NFRC); **CA**: Modoc Nat. For., *41.565*° *-120.892*°, 11.vi.1933, K.A.Salman, slide prep: penis valves, 1 ♂ (NFRC); Plumas Co., Buck's Lake, 39.8797° -121.1486°, 1643m, 23.vi.1949, W.F.Ehrhardt, 1 ♀ (DAV); Trinity Co., Coffee Creek , 41.0888° -122.709°, 768m, 17.v.1934, coll. unknown, 1 ♀ (DAV); **ID**: Moscow, Viola Grade, *46.810*° *-117.024*°, 914m, 24.iv.1935, W.E.Shull, 1 ♂ (NFRC); Mts. Moscow, *46.804*° *-116.853*°, 25.vi.1920, R.C.Shannon, 1 ♂ (NFRC); Sandpoint, *48.277*° *-116.553*°, 3.vii.1917, H.G.Dyer, 1 ♂ (USNM); Troy, *46.737*° *-116.769*°, 31.v.1908, coll. unknown, slide prep: ovipositor, 1 ♀ (NFRC); Vollmer, *46.243*° *-116.466*°, 30.v (year unknown), coll. unknown, 1 ♀ (USNM); **IL**: Urbana, *40.111*° *-88.207*°, 23.v.1936, B.D.Burke, 1 ♀ (NFRC); **KS**: Mission, 2.ix.1962, H.Willis, FSCA 00091356, 1 ♂ (FSCA); **MA**: Wellesley, *42.296*° *-71.293*°, 18.vii.1904, coll. unknown, slide prep: penis valves, 1 ♂ (NFRC); **ME**: Franklin Co., Dreyden, 7.viii.1971, H.K.Townes, Malaise trap, FSCA 00091354, 1 ♂ (FSCA); idem except 8.viii.1971, 2 ♀ (FSCA 00091358, FSCA 00091364) 3 M (FSCA 00091361, FSCA 00091362, FSCA 00091363) (FSCA); **MO**: Columbia, 15.v.1968, coll. unknown, FSCA 00091357, 1 ♀ (FSCA); **NH**: Pike, *44.031*° *-72.008*°, 17.vi.1908, Hayhurst, Larix, slide prep: ovipositor, 1 ♀ (USNM); **NY**: Oswego, *43.455*° *-76.510*°, 29.vii.1897, coll. unknown, 1 ♂ (USNM); Saratoga Co., 2.v.1960, R.A.Morse, Salix sp., FSCA 00091352, 1 ♀ (FSCA); Westchester Co., Armonk, Calder Center, 23-31.viii.1974, C.Calmbacher, Malaise trap, FSCA 00091359, 1 ♂ (FSCA); idem except 30.v-5.vi.1974, 1 ♀ (FSCA 00091355) 1 M (FSCA 00091353) (FSCA); idem except 5-12.vii.1974, FSCA 00091360, 1 ♀ (FSCA); **OH**: Columbus, *39.961*° *-82.999*°, v.192?, coll.

unknown, 1 ♂ (NFRC); **OR**: Corvallis, *44.565°* -*123.262°*, 11.vi.1925, E.C.VanDyke, 1 ♂ (CASC); **PA**: Huntingdon, 27.v.1935, coll. unknown, FSCA 00091365, 1 ♀ (FSCA); **WA**: Blewett, *47.425°* -*120.659°*, 4.v.1938, J.Wilcox, slide prep: penis valves, 1 ♂ (CNC); Pierce Co., Fort Lewis, 47.1087° -122.555°, 86m, 17.iv.1946, P.H.Arnaud, 1 ♀ (DAV).

Distribution. This species has a widespread, primarily temperate distribution. It is recorded from Alaska, British Columbia, Saskatchewan, Manitoba, Ontario, New Brunswick, Prince Edward Island, Nova Scotia, Washington, Oregon, Idaho, California, Maine, New Hampshire, Massachusetts, New York, Illinois, Ohio, Pennsylvania, Kansas, Missouri, and North Carolina (D. R. Smith 1979, Goulet and Bennett 2021).

Genetic data. Specimens of this species are divided among two BINs: BOLD:AAG3579 and BOLD:ACN4022. Based on available genetic data (one Nearctic specimen) the nearest neighbour (*P. werzhutskii*) is 7.1% different.

Hosts. *Spiraea* spp. (D. R. Smith and Strazanac 2016). Two specimens listed above are labeled *Larix* and *Salix*, but it is not clear if these are likely to be host plants.

Comments. The type specimen of *venatta* appears to represent a rare dark form of *P. bivittata*, which is observed to exhibit variation in the extent of pale colouration. The lancet of *venatta* is identical to that of *P. bivittata*, and the type specimen otherwise falls within the range of intraspecific variation of *P. bivittata*. Besides the female holotype, only one other specimen identified as *P. venatta* was encountered (a male, identified by Wong), which appears indistinguishable from males of *P. bivittata*. Given the available evidence, *P. venatta* is therefore treated as a junior synonym of *P. bivittata*.

Figures 205–212. *Pristiphora bivittata*. **205**. Female lateral view. **206**. Sawsheath lateral view. **207**. Female dorsal view. **208**. Sawsheath dorsal view. **209**. Female head. **210**. Male dorsal view. **211**. Male head. **212**. Male lateral view.

***Pristiphora cincta* Newman, 1837**

(Figs. 209–216, 243–244, 252)

Pristiphora cincta Newman, 1837: 259.

Nematus (*Nematus*) *Friesi* [sic] Dahlbom, 1835: 10.

Nematus quercus Hartig, 1837: 188–189.

Tenthredo borealis Zetterstedt, 1838: 353.

Pristiphora identidem Norton, 1867c: 77.

Pristiphora idiota Norton, 1867c: 77.

Pristiphora banksi Marlatt, 1896: 117-118. **n. syn.**

Pristiphora coloradensis Marlatt, 1896: 121–122.

Pristiphora hoodi Marlatt, 1896: 119.

Pristiphora seorsa Konow, 1897: 180.

Pristiphora idiotiformis Rohwer, 1910: 199–200.

Pristiphora cincta ab. nigriventris Hellén, 1943: 71.

Pristiphora cincta ab. maukeniensis Hellén, 1943: 71.

Nematus cinctus (Newman, 1837) - Zhelochovtsev & Zinovjev, 1988: 152.

Pristiphora nigrogroenblomi Haris, 2002: 74–75

Diagnosis. Females are variable in colour, either with or without an orange abdominal band spanning T3 to T5 or wider. Orange-banded individuals (e.g. Fig. 211) are easily distinguished

from *P. paloma* and *P. rufipes* (abdomen entirely dark in both species, Figs. 219, 227), and can be differentiated from *P. bivitatta* by the pale-coloured terga always pale at least medially (pale laterally, dark medially in *P. bivittata*, Fig. 203). From females of *P. serrula* with an orange abdomen, *P. cincta* can be differentiated by the sawsheath lateral posterior lobe projecting about as far as median carina (projecting further than median carina in *P. serrula*), subapical tooth of tarsal claw small, about half as long as apical tooth or smaller (e.g. Fig. 172; large, about two-thirds as long as apical tooth in *P. serrula*, e.g. Fig. 174), and hind femur usually mostly dark, basal and apical rings pale (usually mostly pale except broad dark band apically in *P. serrula*). Ideally, where the two species co-occur, lances should be compared: in *P. cincta* lamnium of lance at least twice as long as radix when measured along the ventral margin (Fig. 243; lamnium at most 1.9x as long as radix in *P. serrula*; Fig. 249), lance only weakly curved downward apically (more strongly curved in *P. serrula*). Darker females of *P. cincta* can be distinguished as follows: from *P. bivittata* by the femora mostly dark, at most broad basal and apical rings pale (hindfemur sometimes entirely brown; in *P. bivittata* femora entirely pale except ventrally with narrow longitudinal line brown); from *P. rufipes* by the less strongly produced lateral posterior lobe of valvula 3, projecting about as far as median carina (projecting further than median carina in *P. rufipes*), and tarsal claw with subapical tooth present (absent in *P. rufipes*); from *P. paloma* by the smaller eye, width in lateral view at most 3.2x width of gena (greater than 3.2x in *P. paloma*), LOD at least 1.3x as much as length of eye in frontal view (at most 1.3x, usually about 1.2x length of eye in *P. paloma*), and by shape of lance, radix tapering dorsally and narrower, about as wide as basal four annuli or less (radix squarish, broadly rounded dorsally, as wide as basal five annuli or wider in *P. paloma*, Fig. 245). Males are only easily differentiated from *P. serrula* by the darker abdomen, at most two or three sterna pale (at least S1 to S9 entirely and T3

to T5 laterally pale in *P. serrula*); otherwise one must examine the penis valve, which differs from *P. rufipes* and *P. bivittata* by the simple ventral margin (Fig. 252; ventral margin with distinct obtuse angle near base of valvispina in *P. rufipes* and *P. bivittata*, Fig. 254, 251) and rounded oval shape of pseudoceps (more rectangular in *P. rufipes* and *P. bivittata*); from *P. serrula* by the narrower paravalva with ventral margin evenly rounded towards base (wider, with ventral margin convexly produced near base in *P. serrula*, Fig. 255); from *P. paloma* by the wider penis valve, paravalva about 3x longer than wide (about 2.5x in *P. paloma*, Fig. 253), shorter valvispina, about one-quarter as long as greatest width of paravalva and less than half as long as width of pseudoceps across base of valvispina (longer, about one-third as long as width of paravalva and more than half as long as width of pseudoceps in *P. paloma*), and smaller eye, width in lateral view at most 3.2x width of gena (greater than 3.2x in *P. paloma*).

Female. Length, 4.9–6.4 mm.

Colour: Antenna dark; head dark; mouthparts pale, mandible darkening in apical third to dark brown at apex; labrum pale; clypeus variable, at least apical margin pale to apical half pale. Thorax dark; pronotum posterior corners with margins narrowly to broadly pale; tegula apical margin broadly pale or entirely pale. Legs pale, except coxae dark basally, with apical one-third to half pale, foreleg with femur broad basal ring and sometimes apical two to three tarsomeres brown, midleg with femur sometimes with ventral surface and a broad apical ring brown, or else entirely dark, tibia broad apical ring and tarsus brown, except basal half of first tarsomere pale, hindleg with femur variable, from broad basal and apical ring only to entirely brown, tibia apical one-third to half, and tarsus dark brown. Abdomen either entirely dark or with a transverse yellow-brown band: as much as T2 to T6 entirely and T7 laterally pale, with corresponding sterna pale, cerci dark brown.

Head: Antenna length 2.3–2.5x head width; F1 0.8–0.9x length of eye; F1 longer than F2 (F1:F2 = 1.1x), longer than F3 (F1:F3 = 1.2x), proceeding flagellomeres progressively shorter (F7:F1 = 0.65–0.75x). Clypeus truncate. Malar space 1.0–1.3x OD. LOD 1.3–1.5x height of eye in frontal view. IOC:OOL = 1.0–1.25x. Head variable from shiny, microscrulpture smooth to somewhat dull, imbricate, gena somewhat shiny, weakly imbricate.

Thorax: Pronotum dull, imbricate. Prepectus distinct & pitted, setose. Mesepisternum variable from shiny, microsculpture smooth to rough, coriaceous, epicnemium shiny, microsculpture smooth, sometimes with weak horizontal lines. Mesepimeron variable from shiny, microsculpture smooth to somewhat dull, weakly imbricate. Mesonotum dull, imbricate. Parapsis dull, imbricate, somewhat shiny posteriorly. Mesopostnotum rough, coarsely imbricate. Metabasitarsus shorter than metatarsomeres 2–4 combined. Subapical tooth of tarsal claw small, half as long as apical tooth or smaller.

Abdomen: Terga dull, imbricate. Sawsheath in dorsal view deeply emarginate, with distinct median carina, longest setae about 0.8-0.9x as long as apical width of sawsheath, visible length of sawsheath less than cerci. Sawsheath in lateral view with lower margin evenly rounded, meeting dorsal margin at a sub-quadrate apex. Valvula 3 lateral posterior lobe produced and narrow, about equally as produced as median carina. In apical view, width of sawsheath 0.7-0.8x height of setose area. Lance with ventral margin approximately straight; lamnium at least twice as long as radix when measured along the ventral margin; radix tapering dorsally, at most as wide as basal four annuli of lamnium. Tangium of lancet gradually tapering apically; tangial process absent or indistinct. Lancet with first suture approximately straight, proceeding sutures approximately straight to dorsally apically curved; annuli without setae; serrulae neither especially sharp nor blunt, basoventral angle rounded-right to rounded-acute.

Male. Length, 4.7–6.0 mm.

Colour as in female except as follows. Antenna dark, with numerous stout black setae. Legs usually more extensively pale than in female, except coxae apical half pale, trochanters and trochantelli pale, foreleg with femur entirely pale, midleg with femur entirely pale or with ventral surface brown in basal half, hindleg with femur pale except basal half on ventral surface and a broad dorsoapical spot brown. Abdomen dark, sometimes with a few middle sterna pale. Structure and sculpture similar to female, except: antenna 2.8–3.2x head width; F1 0.95–1.0x length of eye, F1 subequal to F2 (F1:F2 = 0.95–1.05x), subequal to or slightly longer than F3 (F1:F3 = 1.0–1.1x), proceeding flagellomeres progressively shorter (F7:F1 = 0.8–0.9x); malar space 0.8–1.0x OD; LOD 1.2–1.4x height of eye in frontal view , mesopostnoum dull, imbricate laterally, shiny, microsculpture smooth medially; metabasitarsus approximately same length as or slightly shorter than metatarsomeres 2–4 combined. Penis valve with paravalva rounded-rectangular, about three times longer than wide, gradually tapering apically towards base of valvispina, valvar strut extending from ventral margin at origin on valviceps to dorsal margin subapically; valvispina, small, narrow, about one-quarter as long as greatest width of paravalva and less than half as long as width of pseudoceps across base of valvispina; pseudoceps oval-shaped apically; valvura with ergot small, visible as an elongate sclerotized patch.

Material studied. *Syntypes* (1 ♀ 1 ♂) of *idiotiformis*—**CANADA**: **NL**: Labrador, Great Caribou Island, 27.vii.1906 (USNM). *Syntype*s (1 ♀ 1 ♂) of *banksi*—**USA**: **NY**: Long Island, Sea Cliff, N.Banks, 1 ♂ (USNM); Ithaca, 1 ♀ (USNM). *Syntype* (♀) of *quercus* (images)—**GERMANY**: Berlin (ZSM). *Syntype* (♀) of *seorsa* (images)—**RUSSIA**: Irkutsk (SDEI). *Holotype* (♂) of *nigrogroenblomi* (images)—**MONGOLIA**: Central aimak, Tosgoni ovoo, 10 km N of Ulan-Baatar, 1700-1900m, 23-24.vii.1967, Z.Kaszab (HNHM). *Additional material*—**CANADA**: **AB**:

Snow Cr. Pass, *51.608*° *-115.813*°, 2256m, 20.vii.1962, Edith Mason, slide prep: ovipositor, 1 ♀ (CNC); **CANADA**: **BC**: Lakelse L. bog nr Terrace, *54.367*° *-128.550*°, 4.viii.1960, C.H.Mann, 1 ♂ (CNC); Stanley, *53.040*° *-121.719*°, 11.vii.1931, W.G.Mathers, Abies lasiocarpa, slide prep: ovipositor, 1 ♀ (CNC); Summit Lake, Mi392 Alaska Hwy, *58.650*° *-124.667*°, 1372m, 2-4.vii.1959, E.E.MacDougall, 2 ♂ (CNC); idem except 29-30.vi.1959, 1 ♂ (CNC); idem except 28.vi.1959, R.E.Leech, 1 ♂ (CNC); Burnt Cabin Bog Ecological Reserve, near Banner Mountainlodge, 54.761° -126.931°, 795m, 6.vii.2014, BIObus 2014, sweep net, BIOUG25128-D09, 1 ♂ (BIOUG); Kootenay National Park, Kootenay Crossing, 50.885° -116.052°, 1160m, 21-29.vii.2014, P.Langan, Malaise trap, BIOUG18478-A05, 1 ♂ (BIOUG); **MB**: Churchill, 11 km S Churchill, Goose Creek, 58.662° -94.165°, 7.vii.2010, J Wang, hand collection, BIOUG00998-F09, 1 ♂ (BIOUG); Churchill, 11 km S Churchill, Goose Creek, First Bridge, grasses along creek, 58.666° -94.16°, 23.vii.2010, Brandon Laforest, sweep net, 10PROBE-29430, 1 ♂ (BIOUG); Churchill, 12 km ESE Churchill, Launch Road, 58.754° -93.998°, 19.vii.2010, Brandon Laforest, sweeping, 2 ♂ (10PROBE-29224, 10PROBE-29225) (BIOUG); Churchill, 12 km ESE Churchill, Launch Road, 58.754° -93.997°, 10m, 5.vii.2010, J Wang, Malaise trap, BIOUG00998-G02, 1 ♂ (BIOUG); Churchill, 4 km SE Churchill, Dene Village, 58.734° -94.112°, 5m, 14.vii.2008, A.Thielman, Malaise trap, PROBE-TW0463, 1 ♂ (BIOUG); Clearwater Lake, *53.990*° *-100.968*°, date unknown, coll. unknown, dogwood, slide prep: ovipositor, W52-3640, 1 ♀ (NFRC); Rennie, Life Table Plot, *49.852*° *-95.554*°, 27.viii.1963, coll. unknown, 1 ♀ (NFRC); **NB**: Fundy National Park, Caribou Plain Trail, 45.625° -65.06°, 336m, 22-30.v.2013, BIObus 2013, Malaise trap, BIOUG13656-D07, 1 ♂ (BIOUG); **NL**: Battle Harbor, *52.272*° *-55.584*°, 30.vii-4.viii, coll. unknown, slide prep: ovipositor, 1 ♀ (USNM); Cartwright, *53.706*° *-57.020*°, 11.vii.1955, E.E.Sterns, 1 ♂ (CNC); Cartwright, *53.706*° *-57.020*°,

17.vii.1955, E.E.Sterns, slide prep: penis valves, 1 ♂ (CNC); Cartwright, *53.706° -57.020°*, 19.vii.1935, W.J.Brown, 1 ♀ (CNC); **NS**: Halifax, Point Pleasant Park, 44.623° -63.569°, 30m, 14-22.vi.2013, Tyler Zemlak, Malaise trap, BIOUG07372-A02, 1 ♂ (BIOUG); Grand R, *45.645° -60.662°*, 3.viii.1931, reared, em.: 16.ii.1953, C.C.Smith, slide prep: penis valves, 1 ♂ (NFRC); Halifax, *44.649° -63.575°*, 15.vi.1915, J.Perrin, 1 ♀ (CNC); **ON**: Lk. Temagami, *46.989° -80.070°*, 12.viii.1909, W.J.Palmer, slide prep: ovipositor, 3 ♀ (CASC); Kawartha Lakes, Balsam Lake Provincial Park, 44.6286° -78.8614°, 274m, 2-16.vi.2014, CBG Collections Staff, Malaise trap, BIOUG32838-A09, 1 ♂ (BIOUG); idem except 6-12.viii.2013, 4 ♂ (BIOUG11566-F11, BIOUG11566-F10, BIOUG11566-G03, BIOUG11574-A10) (BIOUG); Pukaskwa National Park, Heron Bay, near Park Office, 48.601° -86.2893°, 631m, 6-12.viii.2013, Cavan Harpur, Malaise trap, 4 ♂ (BIOUG11566-F11, BIOUG11566-F10, BIOUG11566-G03, BIOUG11574-A10) (BIOUG); **QC**: Mingan Archipelago National Park Reserve, Quarry Island, 50.2135° -63.7979°, 16-24.vii.2013, Park Staff, Malaise trap, BIOUG12454-D04, 1 ♂ (BIOUG); idem except 30.vii-6.viii.2013, BIOUG12487-A08, 1 ♂ (BIOUG); **USA**: **AK**: McKinley Park, *63.733° -148.914°*, date unknown, reared, em.: 4.vii.1947, F.Morand, slide prep: ovipositor, 1 ♀ (USNM); Mile 148, Steese Hwy, *65.712° -144.301°*, 29.vii.1959, R.A.Cook, beating, Picea glauca, 1 ♀ (USNM); **CA**: Mono Co., 1 mi. S Saddlebag L., 37.9552° -119.2659°, 2982m, 15.vii.1961, J.S.Buckett, 2 ♀ (DAV); **GA**: Brasstown Bald, *34.874° -83.811°*, 19.viii.1957, J.G.Chillcott, 1 ♀ (CNC); **IL**: Castle Rock, Grand Detour, *41.968° -89.379°*, 2.vii.1932, Dozier and Mohr, slide prep: ovipositor, 1 ♀ (INHS); **MA**: East Wareham, *41.758° -70.674°*, vi.1947, coll. unknown, cranberry, slide prep: ovipositor, 2 ♀ (NFRC); idem except reared, em.: 7-11.vii.1947, slide prep: penis valves, 2 ♂ (NFRC); idem except em.: 4.vii.1947, slide prep: penis valves & ovipositors, 3 ♀ 2 ♂ (NFRC); idem except em.: 6.vii.1947, slide prep: penis valves, 2

♂ (NFRC); Mt. Everett, *42.102*° *-73.433*°, 792m, 21.viii.1904, coll. unknown, slide prep: penis valves, 1 ♂ (NFRC); Wakefield, *42.506*° *-71.073*°, 16.v.1932, coll. unknown, Vaccinium, slide prep: ovipositor, 1 ♀ (NFRC); Woods Hole, *41.524*° *-70.669*°, vii.1900, A.L.Melander, slide prep: penis valves, 1 ♂ (NFRC); **MD**: Nr. Cumberland, *39.653*° *-78.762*°, 27.vi.1953, L.Walkley, 1 ♀ (NFRC); Powder Mill Bog., Beltsville, *39.031*° *-76.952*°, 21.vi.1936, A.Stone, 1 ♀ (NFRC); **ME**: Augusta, *44.311*° *-69.779*°, 18.vi.1928, K.A.Salman, slide prep: ovipositor, 1 ♀ (NFRC); Portland, *43.661*° *-70.255*°, 9.vii.1909, E.P.VanDuzee, slide prep: penis valves, 1 ♂ (CASC); **MI**: Bay City, *43.595*° *-83.889*°, 20.v.1936, Frison, Ross, slide prep: ovipositor, 2 ♀ (NFRC); Curtisville, *44.560*° *-83.867*°, 21.v.1936, Frison, Ross, Salix, slide prep: ovipositor, 1 ♀ (NFRC); **NC**: Raleigh, *35.772*° *-78.639*°, 12.vii.1935, C.S.Brimley, slide prep: ovipositor, 1 ♀ (NFRC); **NH**: Durham, *43.134*° *-70.926*°, date unknown, W. & F., 1 ♀ (NFRC); Mt. Washington, *44.270*° *-71.304*°, 1524m, 13.viii.1951, G.S.Walley, slide prep: ovipositor, 2 ♀ (CNC); Mt. Wash'n, *44.270*° *-71.304*°, date unknown, coll. unknown, slide prep: penis valves, 1 ♂ (NFRC); White Mts., *44.270*° *-71.304*°, date unknown, Fiske, slide prep: ovipositor, 1 ♀ (NFRC); **NJ**: Burlington Co., Atsion, 39.7426° -74.726°, 15m, 26.vii.1974, A.S.Menke, 1 ♀ (DAV); **NY**: Canton, *44.596*° *-75.169*°, 14.viii.1916, T.H.Frison, slide prep: penis valves, 1 ♂ (NFRC); Grand Isd., *43.033*° *-78.963*°, 29.viii.1909, M.C.VanDuzee, slide prep: ovipositor, 1 ♀ (CASC); McLean, *42.552*° *-76.291*°, 2-3.vii.1904, coll. unknown, slide prep: ovipositor, 1 ♀ (NFRC); Orient, L.I., *42.139*° *-72.303*°, 24.vii.1947, Roy Latham, 1 ♂ (CNC); idem except 20.vii.1947, slide prep: penis valves, 1 ♂ (NFRC); idem except 29.vii.1947, slide prep: ovipositor, 1 ♀ (NFRC); idem except 9.v.1953, slide prep: ovipositor, 1 ♀ (NFRC); idem except 11.viii.1923,slide prep: ovipositor, 1 ♀ (USNM); Ringwood Ithaca, *42.451*° *-76.364*°, 6.vii.1918, coll. unknown, slide prep: penis valves, 1 ♂ (NFRC); Ringwood, Ithaca, *42.451*° *-76.364*°,

11.viii.1923, coll. unknown, slide prep: ovipositor, 1 ♀ (NFRC); Riverhead, L.I., *40.917°* -*72.662°*, 11.x.1947, Roy Latham, slide prep: ovipositor, 1 ♀ (NFRC); **SC**: Mountain Rest, Oconee Co., *34.869°* -*83.153°*, 457m, 26.vii.1957, J.G.Chillcott, slide prep: penis valves, 1 ♂ (CNC); **UT**: Logan Canyon, *41.740°* -*111.794°*, 9.vi.1932, G.F.Knowiton, slide prep: ovipositor, 1 ♀ (NFRC); **VT**: Mt. Mansfield, *44.543°* -*72.815°*, 1349m, 21.vii.1891, coll. unknown, slide prep: penis valves, 2 ♂ (USNM); **WA**: Paradise Val., Mt. Rainier, *46.783°* -*121.728°*, 25.vii.1920, E.C.VanDyke, 1 ♂ (CASC); **WV**: Cheat Mt., *38.733°* -*79.958°*, 610m, vi (year unknown), coll. unknown, slide prep: ovipositor, 1 ♀ (NFRC); Hardy Co., Lost River State Park, 38.9229° -78.8895°, 882m, 19.vii.1974, A.S.Menke, 2 ♂ (DAV).

Distribution. Holarctic. In the Nearctic, this species has a widespread boreo-temperate distribution, found across most of the continent of North America. It is recorded from Alaska, Yukon, Northwest Territories, Nunavut, British Columbia, Alberta, Manitoba, Ontario, Quebec, New Brunswick, Nova Scota, Newfoundland and Labrador, Washington, California, Utah, Colorado, Minnesota, Illinois, Michigan, Maine, Vermont, New Hampshire, Massachusetts, New York, New Jersey, Maryland, West Virginia, Tennessee, North Carolina, South Carolina, Alabama, and Georgia (D. R. Smith 1979, Goulet and Bennett 2021).

Genetic data. Specimens of this species belong to a single BIN, which is shared with *P. paloma*: BOLD:AAG3565. Based on available genetic data (one Nearctic and one Palaearctic specimen), within-species divergence is 3.1% and the nearest neighbour (*P. thalictri*) is 3.0% different.

Hosts. *Betula* spp., *Salix* spp., *Vaccinium* spp. (D. R. Smith 1979, D. R. Smith and Strazanac 2016).

Comments. Individuals identified as *P. banksi* appear to represent a dark form of *P. cincta*, with females having an entirely dark abdomen. In unpublished correspondence with D. R. Smith (pers. obs.) Wong noted that *P. cincta* includes dark females, differentiating *P. banksi* based on a shorter, stouter, more blunt-tipped lancet, with steeper serrulae and a distinct crepidium. However, upon seeing males associated with *P. banksi*, Wong remarked that, "[they] and other specimens I have seen strongly suggest that *P. banksi* is synonymous with *P. cincta*". Indeed, orange-banded individuals of *P. cincta* can be found to exhibit any combination of the above characters, not one of which appears to differ consistently between dark and orange-banded females – nor do any external characters besides colouration. Therefore, lacking any morphological evidence to maintain it as a separate species, *P. banksi* is hereby considered a junior synonym of *P. cincta*.

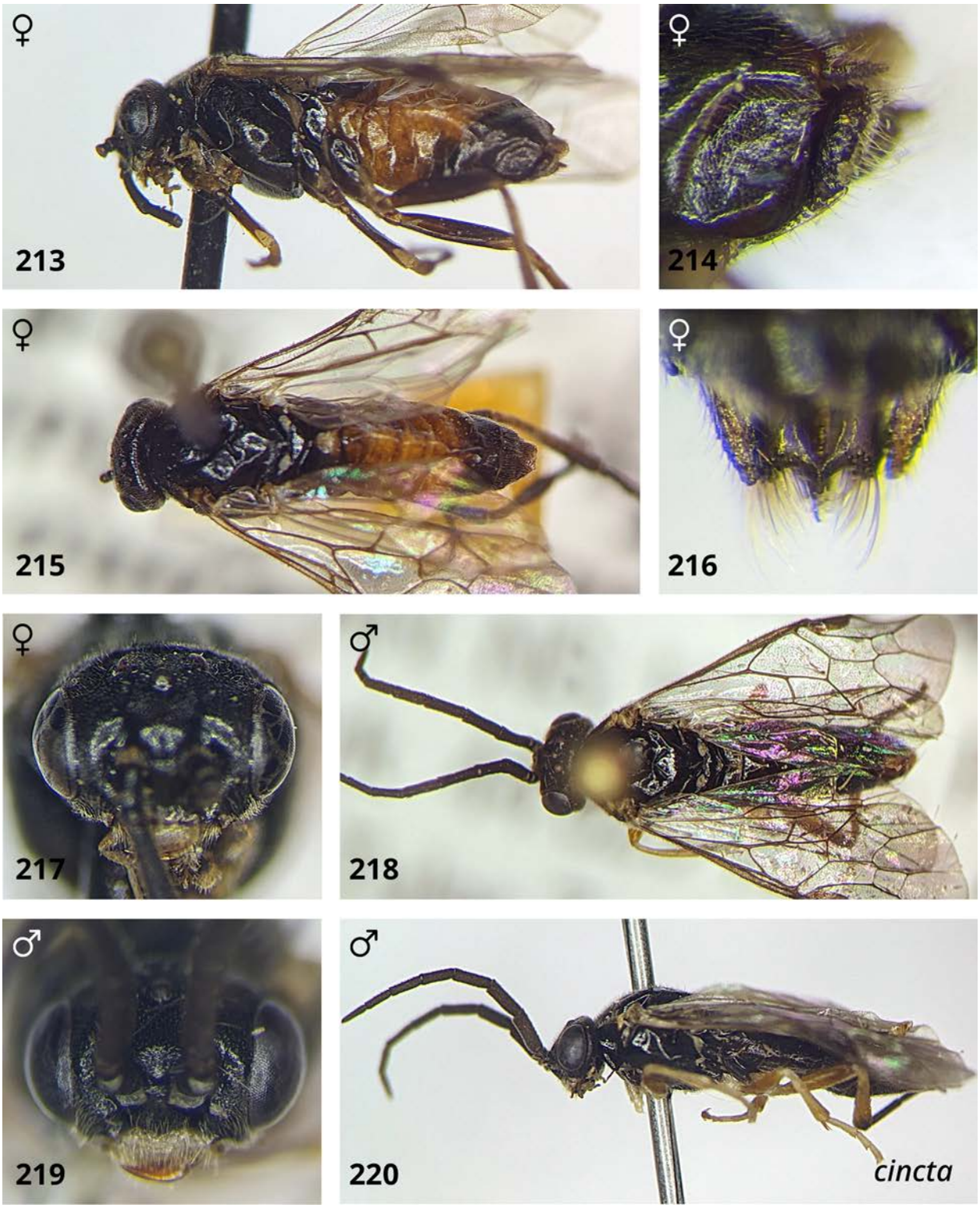

Figures 213–220. *Pristiphora cincta*. **213**. Female lateral view. **214**. Sawsheath lateral view. **215**. Female dorsal view. **216**. Sawsheath dorsal view. **217**. Female head. **218**. Male dorsal view. **219**. Male head. **220**. Male lateral view.

***Pristiphora paloma* Wong & Ross, 1960**

(Figs. 217–224, 245–246, 253)

Pristiphora paloma Wong & Ross, 1960: 196.

Diagnosis. Individuals of both sexes of *P. paloma* can be recognized by their large eye relative to size of head, width in lateral view at least 3.2x width of gena (less than 3.2x in other species), LOD at most 1.3x, usually about 1.2x length of eye in frontal view (at least 1.3x in females and usually males of other species). The entirely dark abdomen separates both sexes from *P. serrula* (Figs. 219, 222; females at least T3 to T5 pale, males at least sterna and T3 to T5 partly pale in *P. serrula*, Figs. 235, 240), and females from individuals of *P. bivittata* and *P. cincta* that have a partly pale abdomen (females at least T3 to T5 partly pale in *P. bivittata* and *P. cincta*, Figs. 203, 211). From *P. bivittata*, both sexes can be separated by the darker femora, profemur at least ventrally, midfemur narrow basal and apical ring, and hindfemur at least wide basal ring dark (in *P. bivittata* femora entirely pale except ventrally with narrow longitudinal line brown). From *P. rufipes*, both sexes can be separated by the tarsal claw with subapical tooth present (e.g. Figs. 172-174; absent in *P. rufipes*), and females by the less strongly produced lateral posterior lobe of valvula 3, projecting about as far as median carina (projecting further than median carina in *P. rufipes*). From *P. cincta*, both sexes can be separated by the larger eye (see above), females by shape of lance with radix squarish, broadly rounded dorsally, as wide as basal five annuli or wider (Fig. 245; tapering dorsally and narrower, as wide as basal four annuli or less in *P. cincta*; Fig. 243), males by the narrower penis valve, paravalva about 2.5x longer than wide (Fig. 253; about 3x in *P. cincta*, Fig. 252), longer valvispina, about one-third as long as greatest width of paravalva and more than half as long as width of pseudoceps across base of valvispina (shorter,

about one-quarter as long as width of paravalva and less than half as long as width of pseudoceps in *P. cincta*).

Female. Length, 4.9–7.4 mm.

Colour: Antenna dark; head dark; mouthparts pale, mandible pale in basal third, apical two thirds translucent brown, narrowly dark near base and apex; labrum pale; clypeus sometimes with apical margin broadly pale. Thorax dark; pronotum posterior corner with margins narrowly pale; tegula pale. Legs dark, except coxae variable, dark basally with apical one-third to half pale, sometimes fore and middle coxa almost entirely pale only narrow dark basally, trochanters and trochantelli pale, foreleg with femur apical third and sometimes entire dorsal surface, tibia and tarsus pale, except apical one to two tarsomeres dark brown, midleg with femur narrow basal and apical ring, tibia except small apicodorsal spot, and tarsus pale, except apical one to two tarsomere dark brown, hindleg with femur wide basal ring to basal half, tibia basal half to two-thirds pale. Abdomen dark or dark brown, cerci dark.

Head: Antenna length 2.6–2.8x head width; F1 0.9–0.95x length of eye; F1 longer than F2 (F1:F2 = 1.1–1.2x), longer than F3 (F1:F3 = 1.1–1.2x), proceeding flagellomeres progressively shorter (F7:F1 = 0.65–0.7x). Clypeus truncate. Malar space 0.7–0.8x OD. LOD 1.2–1.3x height of eye in frontal view. IOC:OOL = 1.3–1.4x. Head somewhat dull, weakly imbricate, gena dull, imbricate, vertexal area dull imbricate laterally.

Thorax: Pronotum dull, imbricate. Prepectus distinct & punctate, setose, broad. Mesepisternum shiny, microsculpture smooth, epicnemium shiny, microsculpture smooth, sometimes with weak horizontal lines. Mesepimeron shiny, microsculpture smooth. Mesonotum shiny microsculpture smooth, except mesoscutum frequently dull imbricate in anterior half.

Parapsis shiny, microsculpture smooth. Mesopostnotum dull, imbricate laterally, shiny, microsculpture smooth medially. Metabasitarsus longer than metatarsomeres 2–4 combined. Subapical tooth of tarsal claw medium, half as long as apical tooth.

Abdomen: Terga dull, imbricate. Sawsheath in dorsal view deeply emarginate, with distinct median carina, longest setae about three-quarters as long as apical width of sawsheath, visible length of sawsheath less than cerci. Sawsheath in lateral view with lower margin evenly rounded, meeting dorsal margin at a broadly rounded apex. Valvula 3 lateral posterior lobe produced and narrow, about equally as produced as median carina. In apical view, width of sawsheath 0.7-0.8x height of setose area. Lance with ventral margin approximately straight; lamnium at least twice as long as radix when measured along the ventral margin; radix squarish, broadly rounded dorsally, at least as wide as basal five annuli of lamnium. Tangium of lancet gradually tapering apically; tangial process absent or indistinct. Lancet with sutures dorsally apically curved; annuli without setae; serrulae distinctly pointed, basoventral angle rounded-acute.

Male. Length, 4.2–5.7 mm.

Colour as in female except as follows. Antenna dark, with stout black setae; clypeus entirely pale; supraclypeal area dark or pale.; pronotum often more extensively pale than in female, with entire lateral portion pale., midleg with sometimes femur entirely pale-infuscate and darker on posterior surface. Structure and sculpture similar to female, except: antenna 2.8–3.0x head width, F1 subequal to or slightly longer than F2 (F1:F2 = 1.05x), longer than F3 (F1:F3 = 1.1x), proceeding flagellomeres progressively shorter (F7:F1 = 0.75–0.8x); malar space 0.7x OD; LOD 1.25x height of eye in frontal view; IOC:OOL = 1.3–1.5x; IOC:OD 2.5–2.8x; head variable from shiny, microscrulpture smooth to somewhat dull, weakly imbricate ; subapical tooth of tarsal claw smaller than in female, less than half as long as apical tooth. Penis valve with paravalva

rounded-rectangular, about 2.5x longer than wide, gradually tapering apically towards base of valvispina, valvar strut extending from ventral margin at origin on valviceps to dorsal margin subapically; valvispina, small, narrow, arising more-or-less in line with ventral margin of paravalva, about one-third as long as greatest width of paravalva and more than half as long as width of pseudoceps across base of valvispina; pseudoceps oval-shaped apically; valvura with ergot small, visible as an elongate sclerotized patch.

Material studied. *Holotype* ♂—**USA**: **IL**, Lake Co., Antioch, Channel Lake, 42.477° -88.096°, 24.viii.1935, D.M.DeLong, H.H.Ross (INHS). *Allotype* ♀—Same data as holotype, slide prep: ovipositor (INHS). *Additional material*—**USA**: **AR**: Washington Co., Fayetteville, 17-19.vi.1975, H.N.Greenbaum, Malaise trap, FSCA 00091416, 1 ♂ (FSCA); **FL**: Alachua Co. Gainesville Pierce's Homestead S9-T1OS-R18E, 12-22.xi.1975, W.H.Pierce, Malaise trap, FSCA 00091396, 1 ♂ (FSCA); Alachua Co., 2 mi. N. Gainesville Cypress Dome Project, 27.x-2.xi.74, H.Davis, W.Jetter, ramp trap, FSCA 00091400, 1 ♀ (FSCA); Alachua Co., 9 Mi. N.W. Gainesville UF Hort. Unit – SR 232, 1.iv.1975, H.N.Greenbaum, Malaise trap, FSCA 00091412, 1 ♀ (FSCA); idem except 11-14.iv.1975, 2 M (FSCA 00091415, FSCA 00091417) (FSCA); idem except 12-18.iv.1977, FSCA 00091420, 1 ♂ (FSCA); idem except 13-16.iv.1977, FSCA 00091421, 1 ♂ (FSCA); idem except 2.iv.1975, 1 ♀ (FSCA 00091410) 1 M (FSCA 00091411) (FSCA); idem except 25-29.iii.1977, FSCA 00091414, 1 ♂ (FSCA); idem except 26.vii-2.viii.1977, FSCA 00091419, 1 ♂ (FSCA); idem except 8-13.iv.1977, 1 ♀ (FSCA 00091422) 1 M (FSCA 00091423) (FSCA); idem except 9.iv.1975, FSCA 00091418, 1 ♀ (FSCA); Alachua Co., E. Gainesville, 27.iii.1975, H.N.Greenbaum, Malaise trap, FSCA 00091413, 1 ♂ (FSCA); Columbia & Baker Co. line, Osceola Nat. Forest nr Jct US90, 8-20.x.1976, J.R.Wiley, Malaise trap, FSCA 00091398, 1 ♀ (FSCA); Gainesville, Doyle Conner Building, 17.ix.1973,

H.V.Weems Jr., Malaise trap, FSCA 00091402, 1 ♀ (FSCA); idem except 25-27.viii.1973, FSCA 00091403, 1 ♀ (FSCA); Liberty Co., Torreya State Park, v.1968, H.V.Weems Jr., Malaise trap, FSCA 00091394, 1 ♂ (FSCA); Orange Park, 18.iv.1970, C.F.Zeiger, FSCA 00091409, 1 ♀ (FSCA); Torreya State Park Liberty Co., v.1968, H.V.Weems Jr., Malaise trap, 2 ♀ (FSCA 00091397, FSCA 00091408) 2 M (FSCA 00091404, FSCA 00091408) (FSCA); Wahullah Co., Ochlochonee River St. Park Appalachicola Nat. Forest, 9-10.iv.1977, G.B.Fairchild, insect flight trap, FSCA 00091424, 1 ♂ (FSCA); **LA**: Evangeline Co., Bayou Chicot, 11-18.iii.1971, D.Shaneck, Malaise trap, FSCA 00091401, 1 ♀ (FSCA); idem except 22-29.ix.1971, FSCA 00091399, 1 ♂ (FSCA); idem except 25.viii-1.ix.1971, FSCA 00091406, 1 ♀ (FSCA); idem except 6-13.x.1971, FSCA 00091405, 1 ♂ (FSCA); **MS**: Yalobusha Co. Water Valley, 25.ix-9.x.1971, M.Horan, Malaise trap, FSCA 00091407, 1 ♀ (FSCA); **NY**: Westchester Co., Armonk, Calder Center, 23-31.viii.1974, coll. unknown, FSCA 00091395, 1 ♀ (FSCA).

Distribution. This species is mainly found in the Southeastern and Coastal Plains of the United States. It is recorded from Illinois, New York, Arkansas, Louisiana, Mississippi, and Florida.

Genetic data. Specimens of this species belong to a single BIN, which is shared with *P. cincta*: BOLD:AAG3565. Based on available genetic data (one Nearctic specimen) the nearest neighbour (*P. serrula*) is 3.0% different.

Host. Unknown.

Comments. This species appears to mostly replace *P. cincta* in the southeastern United States as the most commonly encountered species in the genus for that region.

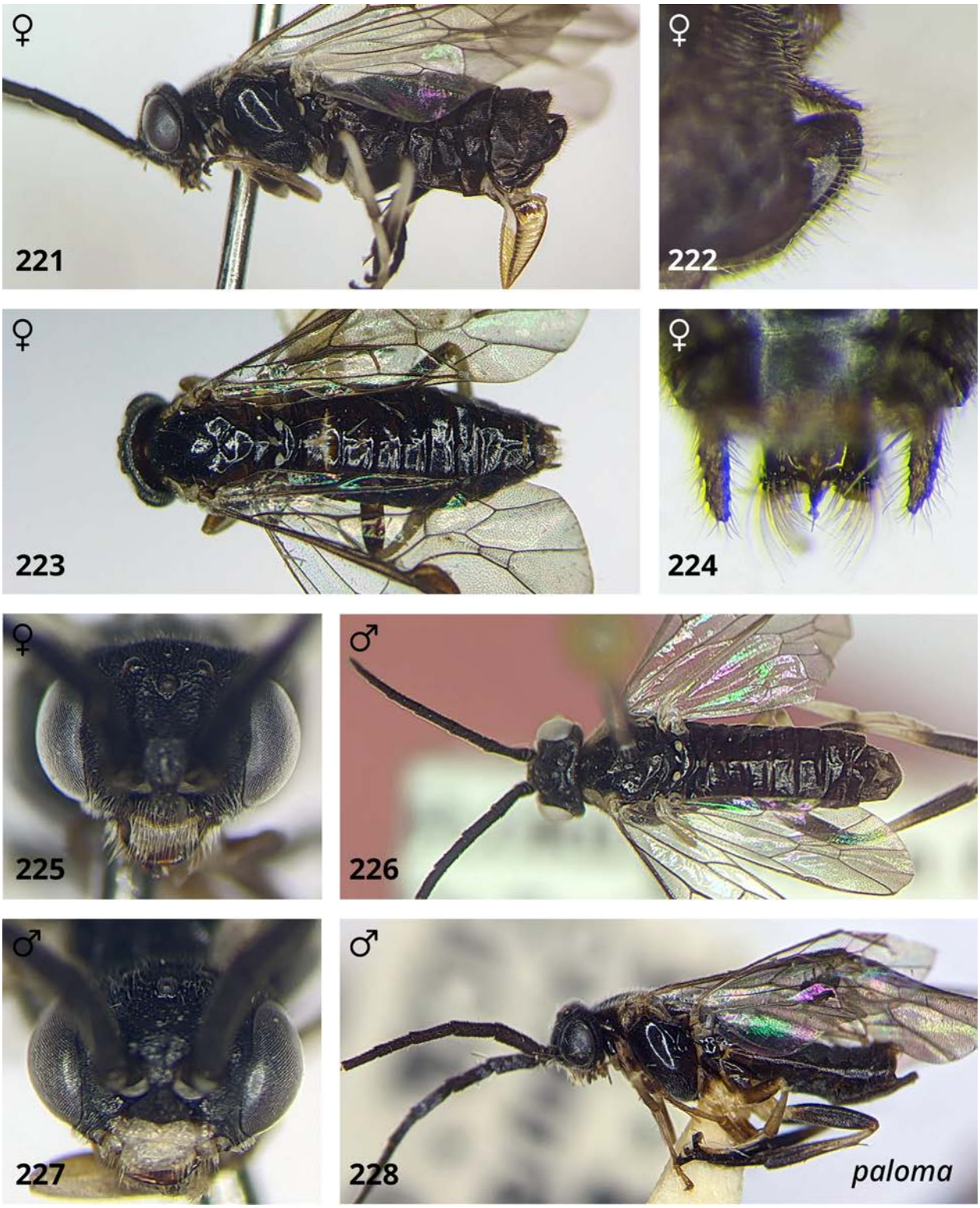

Figures 221–228. *Pristiphora paloma*. **221**. Female lateral view. **222**. Sawsheath lateral view. **223**. Female dorsal view. **224**. Sawsheath dorsal view. **225**. Female head. **226**. Male dorsal view. **227**. Male head. **228**. Male lateral view.

***Pristiphora rufipes* Serville, 1823**

(Figs. 224–232, 247–248, 254)

Pristiphora rufipes Serville, 1823: 75.

Pristiphora fusca Serville, 1823: 75–76.

Nematus suessionensis Serville, 1823: 68.

Pristiphora rufipes Lepeletier, 1823: 60.

Pristiphora fusca Lepeletier, 1823: 60.

Nematus Suessionensis [sic] Lepeletier, 1823: 66.

Nematus selandrioides Costa, 1859: 21–22.

Nematus aquilegiae Snellen van Vollenhoven, 1866: 202–205.

Diagnosis. Females of *P. rufipes* can be separated from all other Nearctic species in the *rufipes* group by the absence of subapical tooth of tarsal claw (present in other species, e.g. Figs. 172-174), from *P. serrula* and most individuals of *P. bivitatta* by the entirely dark abdomen (Fig, 227; at least T3 to T5 partly pale in *P. serrula* and most individuals of *P. bivitatta*, Figs. 203, 235), from all but *P. serrula* by the strongly produced lateral posterior lobe, projecting much further than median carina (projecting about as far as median carina in *P. bivittata*, *P.cincta*, and *P. paloma*). Males have a small or minute subapical tooth of the tarsal claw, much less than half as long as apical tooth, which only reliably differentiates them from *P. bivittata* (e.g. Fig. 172; subapical tooth about half as long as apical tooth or only slightly less in other species, e.g. Fig. 173), and both sexes can be further differentiated by the dark coxae (at least apical one-third pale in other species). The lancet is very similar to others in the *rufipes* group that lack setae (i.e. all

but *P. bivittata*, from which it can be further differentiated on this basis), but usually has less sharply pointed serrulae, basoventral angle of serrulae approximately obtuse (Fig. 246; serrulae with basoventral angle rounded-right or rounded-acute in *P. cincta*, *P. paloma*, and *P. serrula*; Figs. 244, 246, 250). The penis valve differs from all others in the group except *P. bivittata* by the distinct obtuse angle on ventral margin of paravalva near base of valvispina (Figs. 251, 254; straight in other species, Figs. 252–253). In *P. rufipes* the pseudoceps is more evenly rounded apically (approximately rectangular in *P. bivittata*, Fig. 251), the paravalva is more strongly rectangular, dorsal margin with distinct convex hump (dorsal margin slopes gradually away from the valvispina in *P. bivittata*), and the valvar strut meets the ventral margin of the paravalva at attachment point to valviceps (valvar strut meeting ventral margin apically of attachment to valviceps in *P. bivittata*).

Female. Length, 6.1–6.5 mm.

Colour: Antenna dark; head dark; mouthparts pale, mandible darkening in apical third to dark brown at apex; labrum pale; clypeus sometimes with apical margin pale. Thorax dark; pronotum posterior corner with margins very narrowly pale; tegula pale. Legs variable, mostly pale to mostly dark, except coxae dark, trochanters and trochantelli variable, entirely pale or dark basally, apically yellow-brown or pale, foreleg with variable, femur with large anteroventral spot at midlength, narrow apical ring of tarsomeres, and apical tarsomere brown, to femur dark with only broad basal and apical rings pale, midleg with as on foreleg, hindleg with variable, femur sometimes with large anteroventral spot at midlength brown, tibia with broad dorsoapical spot dark, tarsus brown except apical half of apical tarsomere pale, to femur dark with only broad basal and narrow apical ring pale. Abdomen dark or dark brown, T9 marginally and sometimes T10 entirely yellow-brown, valvifer 2 dark, sometimes with basoventral margin brown, cerci.

Head: Antenna length 2.4–2.5x head width; F1 0.9x length of eye; F1 subequal to or slightly longer than F2 (F1:F2 = 1.0–1.1x), longer than F3 (F1:F3 = 1.1–1.2x), proceeding flagellomeres progressively shorter (F7:F1 = 0.7–0.8x). Clypeus subtruncate to shallowly emarginate. Malar space 0.8–1.1x OD. LOD 1.3–1.5x height of eye in frontal view. IOC:OOL = 1.05–1.1x. Head variable, from shiny, microsculpture smooth to somewhat dull, imbricate.

Thorax: Pronotum variable, from shiny, weakly imbricate to dull, imbricate. Prepectus distinct & punctate, setose. Mesepisternum shiny, microsculpture smooth, epicnemium shiny, microsculpture smooth (weakly delineated). Mesepimeron shiny, microsculpture smooth. Mesonotum shiny, microsculpture smooth. Parapsis shiny, weakly imbricate. Mesopostnotum shiny medially and weakly imbricate, somewhat dull and more strongly imbricate laterally. Metabasitarsus shorter than metatarsomeres 2–4 combined. Tarsal claw simple, without subapical tooth.

Abdomen: Terga somewhat dull, imbricate. Sawsheath in dorsal view deeply emarginate, with distinct median carina, longest setae about two-thirds as long as apical width of sawsheath, visible length of sawsheath about the same length as cerci. Sawsheath in lateral view with lower margin evenly rounded, meeting dorsal margin at a rounded apex, longest point below dorsal margin. Valvula 3 lateral posterior lobe produced and narrow, extending beyond height of median carina. In apical view, width of sawsheath 0.8-0.9x height of setose area. Lance with ventral margin approximately straight; lamnium at least twice as long as radix when measured along the ventral margin; lamnium at least 2.5x as long as radix when measured along the ventral margin; radix squarish, broadly rounded dorsally, about as wide as basal four annuli of lamnium. Tangium of lancet gradually tapering apically; tangial process absent or indistinct. Lancet with

sutures dorsally apically curved; annuli without setae; serrulae blunt, basoventral angle rounded-obtuse.

Male. Length, 4.9–5.5 mm.

Colour as in female except as follows. Antenna dark, with few stout black setae.; pronotum posterior corner variable from dark or broadly pale. Structure and sculpture similar to female, except: antenna 2.6–2.7x head width; F1 0.75–0.85x length of eye, F1 subequal to or slightly shorter than F2 (F1:F2 = 0.9–1.0x), subequal to or slightly shorter than F3 (F1:F3 = 0.9–1.0x), proceeding flagellomeres progressively shorter (F7:F1 = 0.8–0.9x); malar space 0.8–0.9x OD; LOD 1.4x height of eye in frontal view; IOC:OOL = 1.0–1.1x; IOC:OD 2.4–2.8x ; metabasitarsus approximately same length as or slightly shorter than metatarsomeres 2–4 combined; tarsal claw present, but small or minute, much less than half as long as apical tooth. Penis valve with paravalva approximately rectangular, dorsal margin with broad convex hump subapically, ventral margin with obtuse angle near base of valvispina, margins gradually tapering apically towards base of valvispina, valvar strut extending from ventral margin at origin on valviceps to dorsal margin subapically; valvispina small, narrow; pseudoceps approximately rounded-rectangular apically; valvura with ergot small, visible as a narrow sclerotized patch.

Material studied. **CANADA**: **ON**: Ancaster, *43.226° -79.977°*, 24.vi.1955, reared, em.: 12.vii, O.Peck, slide prep: penis valves, 1 ♂ (CNC); Ottawa, *45.421° -75.689°*, 3.vii.1963, reared, em.: 15.vii, G.MacNay, columbine, slide prep: penis valves, 1 ♂ (CNC); idem except em.: 14.vii, slide prep: penis valves, 1 ♂ (CNC); Ottawa, *45.421° -75.689°*, 4.vii.1963, reared, em.: 17.vii, H.E.Milliron, columbine, slide prep: ovipositor, 1 ♀ (CNC); idem except em.: 13.vii, slide prep: penis valves, 1 ♂ (CNC); Ottawa, *45.421° -75.689°*, 4.vii.1963, H.E.Milliron, columbine, slide prep: ovipositor, 1 ♀ (CNC); Brockville, St. Francis Catholic School, 44.589° -75.689°, 85m,

22.ix-3.x.2014, Dawn Morva, Malaise trap, BIOUG16039-C09, 1 ♂ (BIOUG); **QC**: Lac Bernard, *50.867° -63.367°*, 13.v.1962, S.M.Clark, slide prep: penis valves, 1 ♂ (CNC); **USA**: **NY**: Westchester Co., Armonk, Calder Center, 30.v-5.vi.1974, C.Calmbacher, Malaise trap, FSCA 00091425, 1 ♀ (FSCA).

Distribution. Palaearctic, but introduced in the Nearctic region (Prous et al. 2017). It appears to be established in most populated areas of temperate North America, and is recorded from British Columbia, Alberta, Washington, Idaho, Montana, Utah, Colorado, Ontario, Quebec, Newfoundland, New York, and Illinois (D. R. Smith 1979, Goulet and Bennett 2021).

Genetic data. Specimens of this species belong to a single BIN: BOLD:AAI2590. Based on available genetic data (two Palaearctic specimens), within-species divergence is 0.4% and the nearest neighbour (*P. brevis*) is 1.0% different.

Hosts. *Aquilegia* spp. (D. R. Smith 1979, Prous et al. 2017). In the Nearctic, this species is more commonly encountered on cultivated columbine than on wild columbine (pers. obs.).

Comments. Prior to clarification by Blank and Taeger (1995) and Lacourt (1999), this name was normally applied to what is correctly called *P. appendiculata*; in fact, three names were routinely applied to these two species by researchers in North America: *P. rufipes* and *P. pallipes* for *P. appendiculata*, and *P. aquilegiae* for *P. rufipes*. As a consequence, any North American specimens identified as *P. rufipes* before 1999 should have their identifications validated.

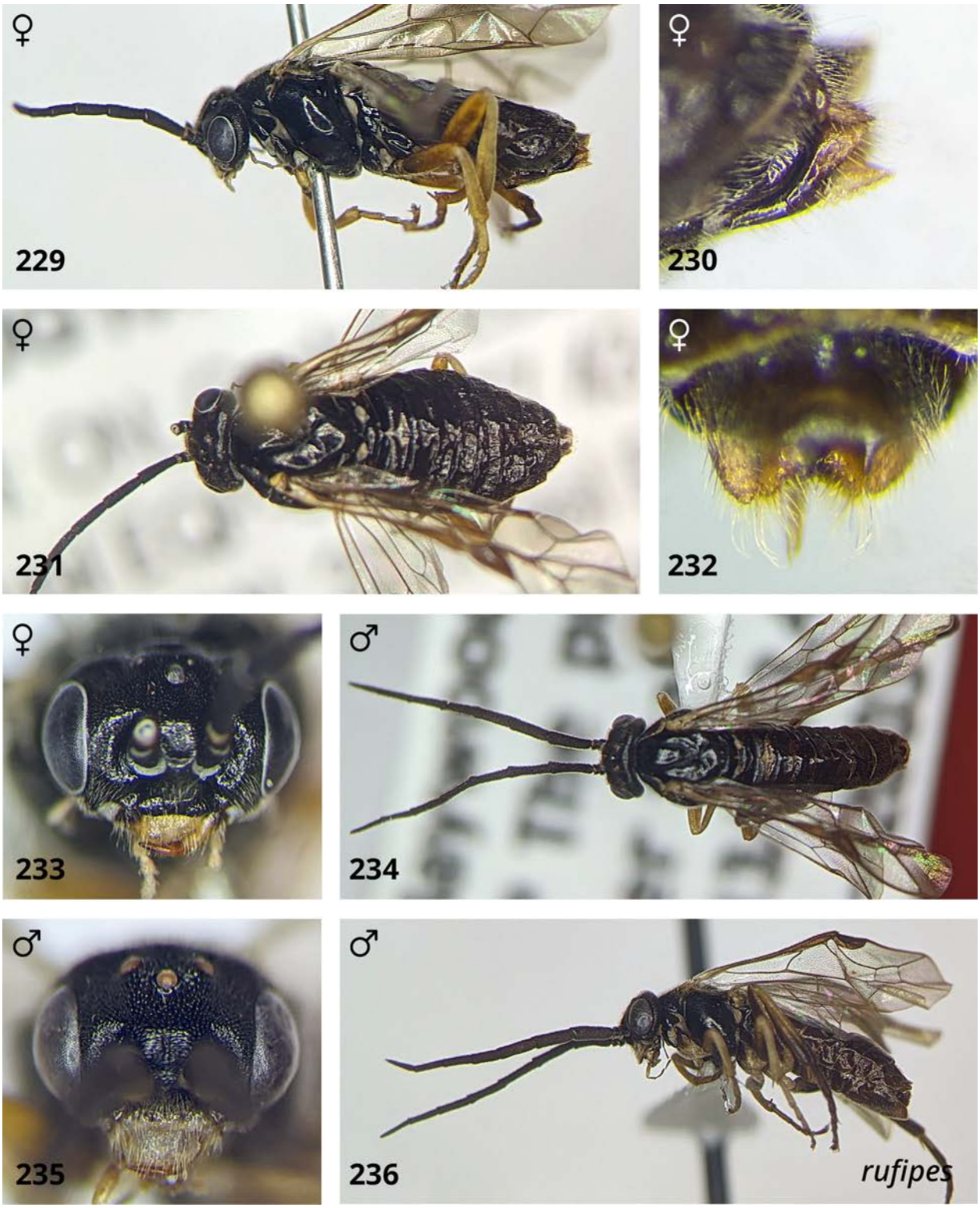

Figures 229–236. *Pristiphora rufipes*. **229**. Female lateral view. **230**. Sawsheath lateral view. **231**. Female dorsal view. **232**. Sawsheath dorsal view. **233**. Female head. **234**. Male dorsal view. **235**. Male head. **236**. Male lateral view.

***Pristiphora serrula* Wong & Ross, 1960**

(Figs. 233–240, 249–250, 255)

Pristiphora serrula Wong & Ross, 1960: 196.

Diagnosis. Individuals of both sexes of *P. serrula* can be differentiated from all but the females of *P. bivittata* and *P. cincta* by the abdomen partly to entirely pale, in females at least T3 to T5 pale (Fig. 235), in males at least sterna and T3 to T5 partly pale (Fig. 238; abdomen entirely dark in *P. paloma*, Figs. 219, 222; *P. rufipes*, Figs. 227, 230; males of *P. bivittata*, Fig. 206; and dark females of *P. cincta*; at most two or three sterna pale in males of *P. cincta*). Females can be differentiated from *P. bivittata* by the pale terga pale medially (pale terga always dark medially in *P. bivittata*), and from orange-banded *P. cincta* by the sawsheath lateral posterior lobe projecting further than median carina (about as far as median carina in *P. cincta*), subapical tooth of tarsal claw large, about two-thirds as long as apical tooth (e.g. Fig. 174; small, about half as long as apical tooth or smaller in *P. cincta*, e.g. Figs. 172–173), and hind femur usually mostly pale, broad dark band apically (usually mostly dark, basal and apical rings pale in *P. cincta*). Ideally, where *P. serrula* and *P. cincta* co-occur, lances should be compared: in *P. serrula* lamnium of lance at most 1.9x as long as radix when measured along the ventral margin (Fig. 249; lamnium at least twice as long as radix in *P. cincta*, Fig. 243), lance distinctly downwardly curved apically (less strongly curved in *P. cincta*). The penis valve differs from those of *P. bivittata* and *P. rufipes* by the straight ventral margin of paravalva near base of valvispina (Fig. 255; ventral margin with distinct obtuse angle in *P. bivittata* and *P. rufipes*, Figs. 251, 254) and from those of *P. cincta* and *P. paloma* by the wider paravalva with ventral margin convexly produced near base (narrower, ventral margin evenly rounded towards base *P. cincta* and *P. paloma*, Figs. 252–253).

Female. Length, 5.0–6.8 mm.

Colour: Antenna dark; head dark; mouthparts pale, mandible darkening in apical third to dark brown at apex; labrum pale; clypeus variable, either entirely brown, with apical margin pale, or sometimes entirely pale. Thorax dark; pronotum variable, at least posterior corner with margins browdly pale, to mostly pale except ventral corner, anterovental margin, and collar dark; tegula pale translucent; metapleuron metepimeron dark, brown in lower half except margins dark; metepisternum variable from brown except narrowly dark on margins to entirely dark. Legs pale, except coxae at least basolateral corner with margins narrowly, and as much as basal half dark, trochanters and trochantelli pale, foreleg with apical two to three tarsomeres brown, rarely basal half of femur dark brown, midleg with femur often with brown apicodorsal spot and sometimes dark along ventral margin, apical two to three tarsomeres brown, hindleg with femur broad apical ring to apical one-fifth, tibia apical one-quarter to half, and tarsus dark. Abdomen yellowish orange, usually with at least T1 dark brown, T8 apical margin, T9, and T10 brown, but variable from entirely pale to as much as T1 entirely, T2 basal two-thirds, T6 except laterally and narrowly along basal margin, S1, and S7 dark brown; valvula 3 variable, entirely dark to mostly pale with only margins dark; valvifer 2 brown or pale; cerci dark brown or yellow-brown.

Head: Antenna length 2.5x head width; F1 0.75–0.85x length of eye; F1 subequal to F2 (F1:F2 = 1.0x), subequal to or slightly longer than F3 (F1:F3 = 1.05–1.1x), proceeding flagellomeres progressively shorter (F7:F1 = 0.75–0.85x). Clypeus truncate. Malar space 0.9–1.2x OD. LOD 1.3–1.5x height of eye in frontal view. IOC:OOL = 1.2–1.4x. Head shiny, weakly imbricate to somewhat dull, imbricate, lower face more strongly imbricate adjacent to eye.

Thorax: Pronotum dull, imbricate. Prepectus distinct & pitted, setose. Mesepisternum shiny, smooth or very weakly imbricate, epicnemium shiny, microsculpture smooth. Mesepimeron

shiny, microsculpture smooth. Mesonotum shiny, weakly imbricate, may be somewhat dull along lateral margins of mesoscutum; mesoscutellum shiny, microsculpture smooth; mesoscutellar appendage dull, pitted & rugulose. Parapsis shiny, weakly/shallowly puncticulate. Mesopostnotum dull, imbricate. Metabasitarsus shorter than metatarsomeres 2–4 combined. Tarsal claw large at least two-thirds as long as apical tooth.

Abdomen: Terga shiny, distinctly but very shallowly imbricate. Sawsheath in dorsal view emarginate, with distinct median carina, longest setae about as long as apical width of sawsheath, visible length of sawsheath less than cerci. Sawsheath in lateral view with lower margin evenly rounded, meeting dorsal margin at a broadly rounded apex. Valvula 3 lateral posterior lobe produced and narrow, extending beyond height of median carina. In apical view, width of sawsheath 0.6-0.7x height of setose area. Lance curved downward apically, ventral margin slightly concave; lamnium less than twice as long as radix (≤1.9x) when measured along the ventral margin; radix tapering somewhat dorsally, approximately as wide as basal five annuli of lamnium. Tangium of lancet gradually tapering apically; tangial process indistinct, weakly sclerotized, not extending above tangium. Lancet with first suture approximately straight, proceeding sutures dorsally apically curved; annuli without setae; serrulae somewhat sharply pointed, basoventral angle rounded-acute.

Male. Length, 5.2–5.8 mm.

Colour as in female except as follows. Antenna brown or dark dorsally, brown ventrally, with few stout black setae. Abdomen dark or dark brown, at least S1 to S9 entirely and T3 to T5 laterally pale, often T3 and T4 entirely pale. Structure and sculpture similar to female, except: antenna 2.4–2.5x head width; malar space 0.x8 OD; LOD 1.2–1.4x height of eye in frontal view ; tarsal claw smaller than in female, about half as long as apical tooth, sometimes less; terga dull,

imbricate. Penis valve with paravalva approximately rectangular, dorsal margin with broad convex hump subapically, ventral margin convexly produced near base, margins gradually tapering apically towards base of valvispina, valvar strut extending from ventral margin at origin on valviceps to dorsal margin subapically; pseudoceps oval-shaped apically; valvura with ergot small, visible as a sclerotized bump.

Material studied. *Holotype* ♀—**USA**: **CA**: Trinity Co., Carsville, 2400-2500', 1.vi.1934, E.C.VanDyke, slide prep: ovipositor (CASC). *Additional material*—**CANADA**: **AB**: Banff, Castle Junction [Eisenhower Jct.], *51.269°* -*115.918°*, 1433m, 8.vii.1962, Mason, Malaise trap, 1 ♀ (CNC); Castle Lookout, Banff N.P. [Eisenhr. Lookout, Banff], *51.294°* -*115.675°*, 1402m, 7.vii.1962, K.C.Herrmann, 1 ♀ (CNC); Wabamun, *53.560°* -*114.468°*, 24.vii.1939, E.H.Strickland, slide prep: ovipositor, 1 ♀ (CNC); **BC**: Burton, *49.987°* -*117.880°*, 11.vii.1962, coll. unknown, Crataegus sp., slide prep: ovipositor, 62-5941-01, 2 ♀ (CNC); Keremeos, *49.208°* -*119.825°*, 11.vii.1923, C.B.Garrett, slide prep: ovipositor, 1 ♀ (CNC); Keremeos, *49.208°* -*119.825°*, 30.vi.1923, C.B.Garrett, slide prep: ovipositor, 1 ♀ (CNC); Langford, *48.450°* -*123.505°*, 14.v.1956, coll. unknown, hawthorne, slide prep: penis valves, 55-1568-01, 1 ♂ (CNC); Langford, *48.450°* -*123.505°*, 4.v.1956, coll. unknown, hawthorne, slide prep: ovipositor, 55-1568-01, 1 ♀ 1 ♂ (CNC); Likely, *52.617°* -*121.550°*, 7.vii.1938, G.S.Walley, slide prep: ovipositor, 1 ♀ (CNC); Summit Lake, Mi392 Alaska Hwy, *58.650°* -*124.667°*, 1433m, 15.vii.1959, R.E.Leech, slide prep: ovipositor, 1 ♀ (CNC); idem except 19-21.vii.1959, slide prep: ovipositor, 1 ♀ (CNC); Pacific Rim NP, Willowbrae Trail, 48.977° -125.596°, 53m, 3-8.vii.2010, BIObus 2010, Malaise trap, 10BBCHY-2459, 1 ♂ (BIOUG); Yoho National Park, Bunkhouse, 51.365° -116.528°, 16-30.vii.2014, Jamie, Malaise trap, BIOUG19787-F09, 1 ♂ (BIOUG); **NS**: Sable Island National Park Reserve, Environment Canada Weather Station,

43.933° -60.008°, 7.5m, 25.viii-8.ix.2014, B.McLean, Malaise trap, BIOUG19562-C04, 1 ♀ (BIOUG); **ON**: Lindsay, Pine Springs, 30.vii.1956, coll. unknown, slide prep: ovipositor, S 56-3027-01, 1 ♀ (CNC); Simcoe, 14.vi.1939, G.E.Shewell, slide prep: ovipositor, 1 ♀ (CNC); **SK**: Prince Albert, *53.201° -105.749°*, 3.vi.1952, coll. unknown, W-435, 1 ♀ (NFRC); **USA**: **AK**: Birch L. near Fairbanks, *64.314° -146.645°*, 10.vii.1951, W.R.M.Mason, 1 ♀ (CNC); **CA**: Siskiyou Co., *41.733° -122.638°*, 2.vi.1911, F.W.Nunenmacher, 1 ♀ (NFRC); **OR**: Corvallis, *44.565° -123.262°*, 11.vi.1925, E.C.VanDyke, slide prep: ovipositor, 1 ♀ (CASC); High Cascade Mountains, Linn Co., *44.425° -121.846°*, 20.vii.1909, J.C.Bridwell, 1 ♀ (USNM); **WA**: Paradise Val., Mt. Rainier, *46.783° -121.728°*, 7.viii.1919, C.L.Fox, slide prep: ovipositor, 1 ♀ (EMEC).

Distribution. This species has a primarily boreo-alpine distribution, and is most commonly encountered in the West, although it also occurs in the East. It is recorded from Alaska, British Columbia, Alberta, Washington, Oregon, California, Ontario, and Nova Scotia, Maine New Hampshire (D. R. Smith 1979).

Genetic data. Specimens of this species belong to a single BIN: BOLD:AAU8834. Based on available genetic data (one Nearctic specimen) the nearest neighbour (*P. paloma*) is 3.0% different.

Hosts. *Crataegus* sp., newly reported from specimen data recorded above. The three specimens associated with *Crataegus* (hawthorne) were collected as part of the Forest Insect Survey (FIS), for which careful host plant observations were made (Lonsdale and Huber 2011). They are therefore considered credible host records.

Comments. An unidentified larva potentially attributable to this species has been documented feeding on *Crataegus* sp., *Prunus serotina* Ehrh., and *Prunus virginiana* L. (Fig. 260). This is discussed in more detail in the results section regarding new records.

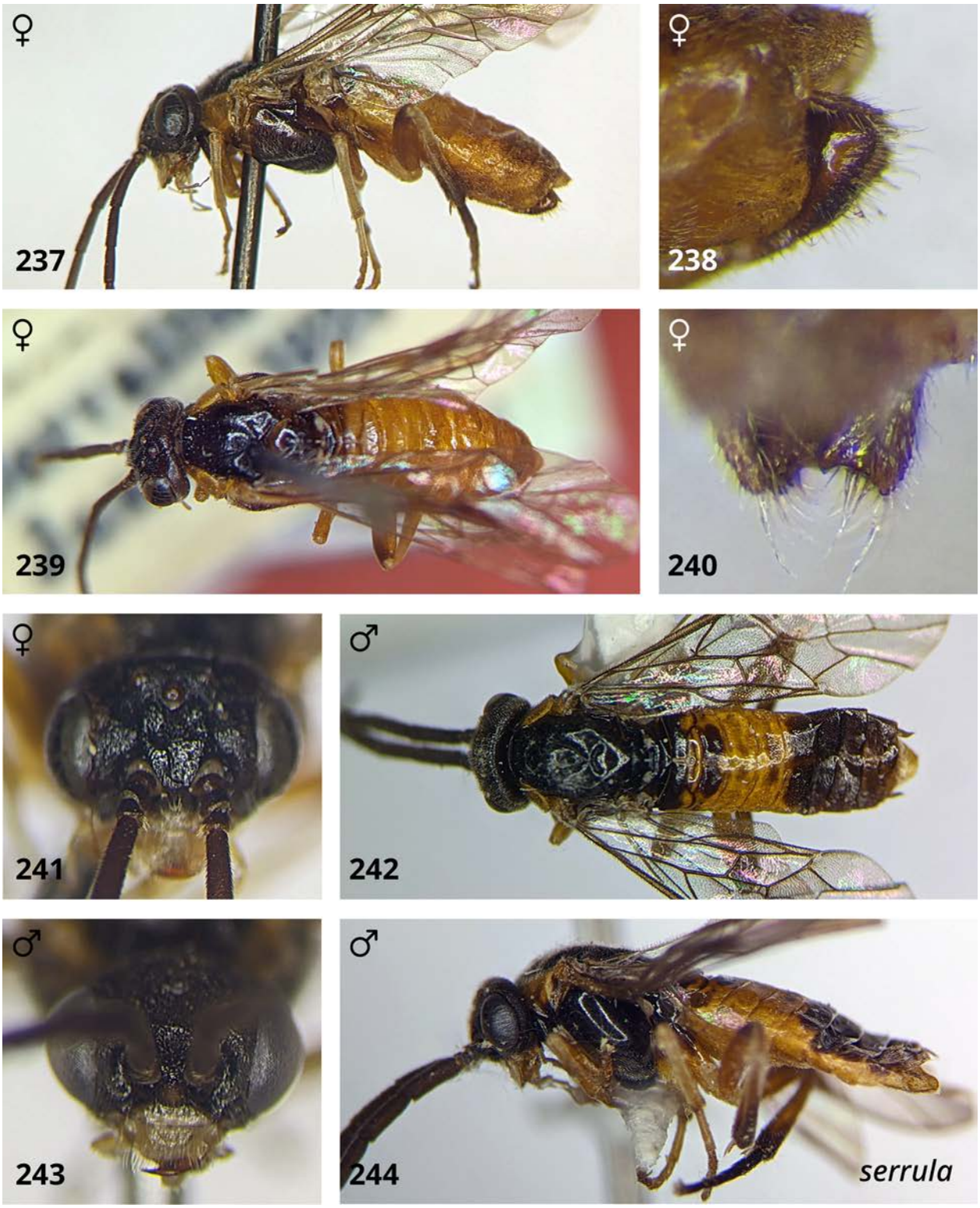

Figures 237–244. *Pristiphora serrula*. **237**. Female lateral view. **238**. Sawsheath lateral view. **239**. Female dorsal view. **240**. Sawsheath dorsal view. **241**. Female head. **242**. Male dorsal view. **243**. Male head. **244**. Male lateral view.

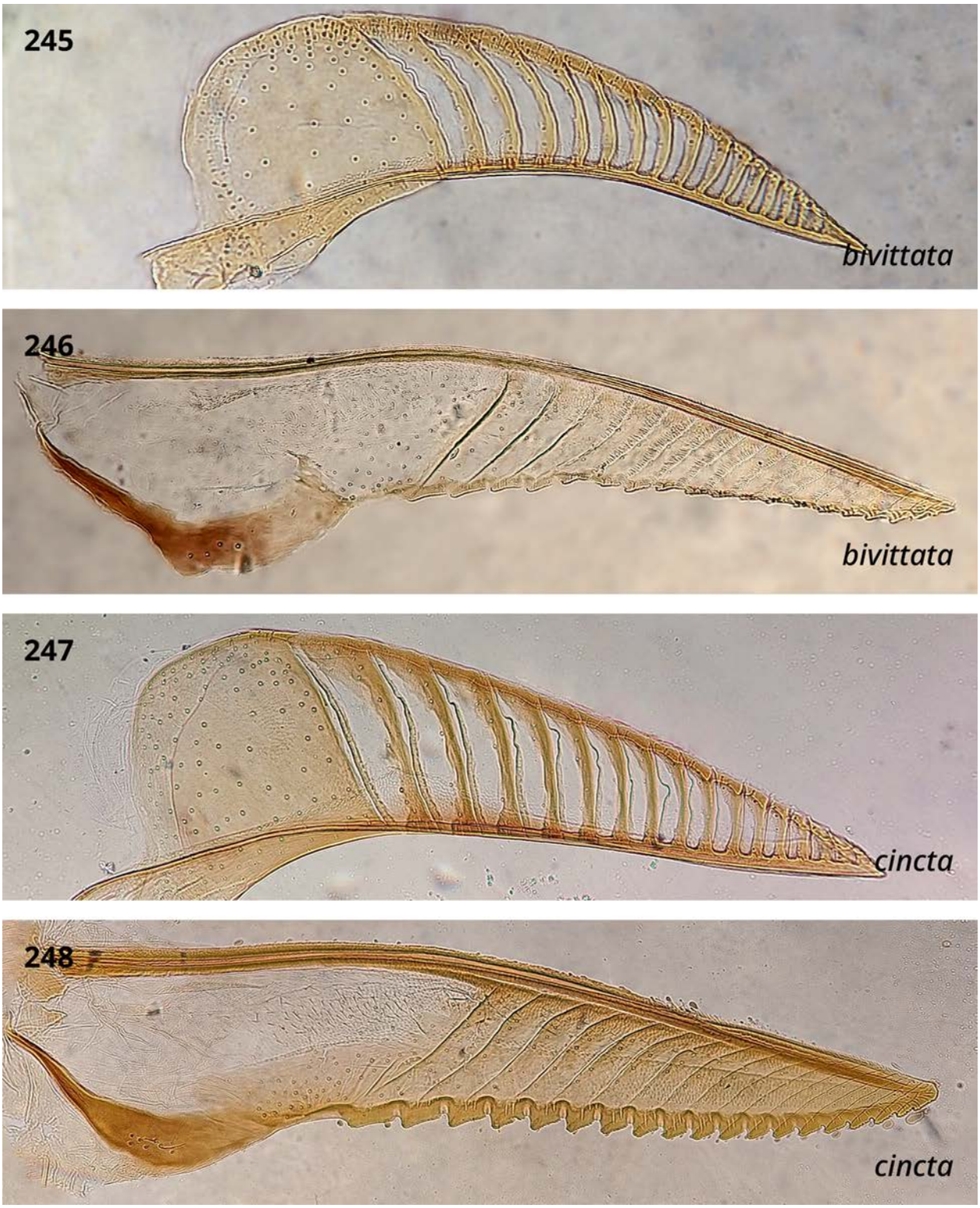

Figures 245–248. Ovipositors of *Pristiphora rufipes* group (lateral view). **245**. *P. bivittata*, lance. **246**. *P. bivittata*, lancet. **247**. *P. cincta*, lance. **248**. *P. cincta*, lancet.

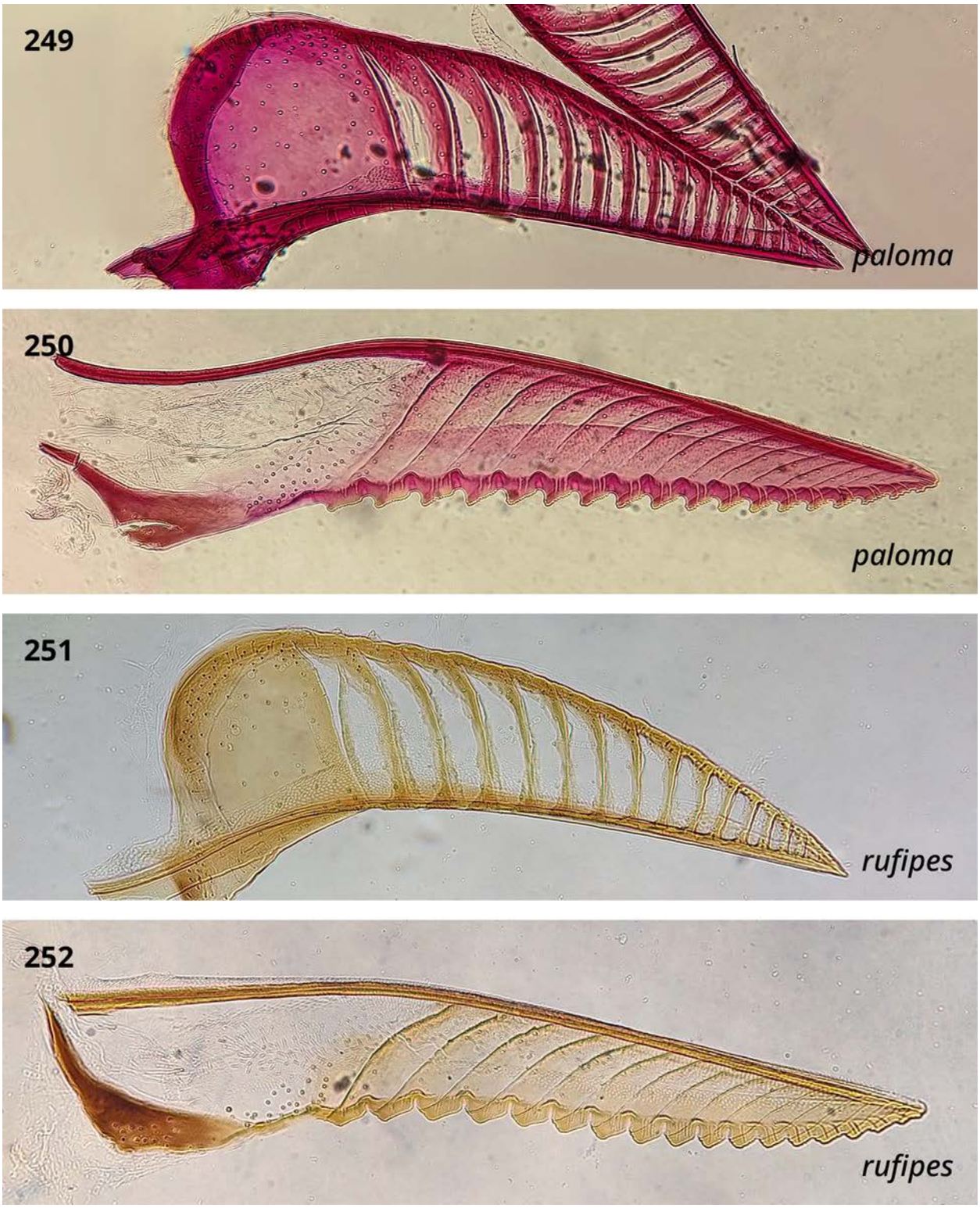

Figures 249–252. Ovipositors of *Pristiphora rufipes* group (lateral view). **249**. *P. paloma*, lance (holotype, paired right lance also visible). **250**. *P. paloma*, lancet (holotype). **251**. *P. rufipes*, lance. **252**. *P. rufipes*, lancet.

Figures 253–254. Ovipositors of *Pristiphora rufipes* group (lateral view). **253**. *P. serrula*, lance (holotype). **254**. *P. serrula*, lancet (holotype).

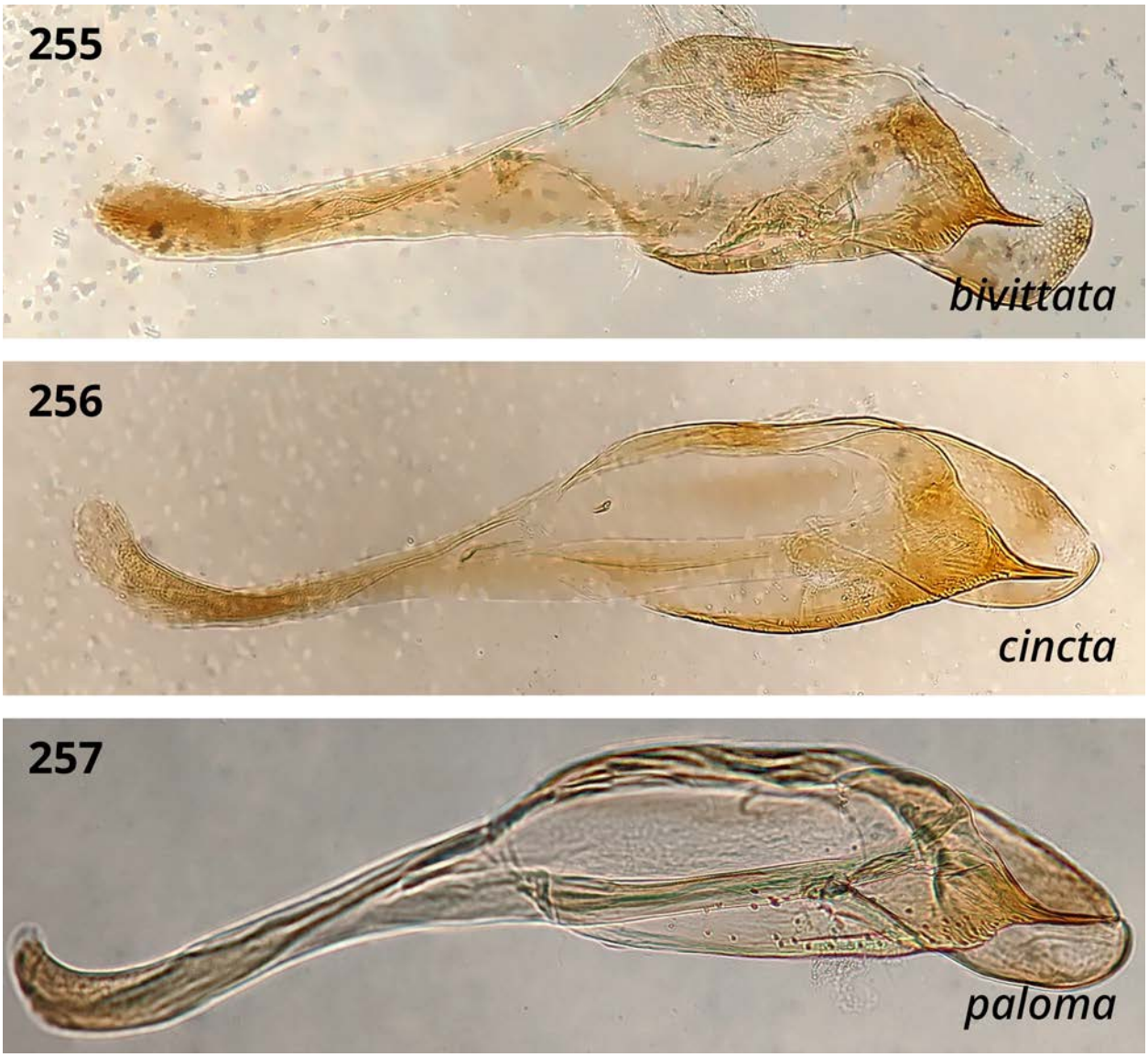

Figures 255–257. Penis valves of *Pristiphora rufipes* group (lateral view). **255**. *P. bivittata*. **256**. *P. cincta*. **257**. *P. paloma*.

Figures 258–259. Penis valves of *Pristiphora rufipes* group (lateral view). **258**. *P. rufipes*. **259**. *P. serrula*.

Comments on undescribed diversity

Based on examination of Wong's material, specimens borrowed from across North America, and barcode sequences available in BOLD, a conservative estimate is that there are eleven undescribed *Pristiphora* species present in the Nearctic. The numbers of expected undescribed species by group are: *P. abietina* group, 1 sp.; *P. alpestris* group, 2 spp.; *P. carinata* group, 2 spp.; *P. micronematica* group, 3 spp.; *P. pallidiventris* group, 1 sp.; *P. pseudocoactula* group, 1 sp.; not assigned to a group, but closely related to *P. chlorea*, 1 sp. Among Wong's material, 38 new epithets were noted. Seven of those were associated with specimens from the *P. ruficornis* group, and in most cases these turned out either to apply to existing Palaearctic species (newly recorded for the Nearctic), or to represent the alternate sex of an existing Nearctic species – although one is described as a new species below (*P. kangirsummiut*). In one case, a single

epithet (‘sculpa’) was used to mistakenly label male specimens from the *P. ruficornis* group (attributable to *P. nigra*) as the alternate sex of a series of females from the *P. micronematica* group (an undetermined species).

Comments on morphological characters

The most reliable characters for identification are associated with the female ovipositor and male penis valves. The lancet of the ovipositor continues to yield characters of taxonomic value: in addition to characters used extensively by previous authors (e.g. shape and length of serrulae, number and length of setae on annuli, presence/absence of tangial process; Ross 1937, Benson 1958, Wong and Ross 1960, Prous et al. 2017), characters related to the shape and dimensions of the tangium and the shape and orientation of the basal sutures should be considered. The lance has rarely been used for the identification of species, but differences in the shape, dimensions, and relative lengths of the radix and lamnium are sometimes useful for this purpose (e.g. as in the *P. rufipes* group), including the presence/absence and size of the radical process. Penis valves usually show distinct differences among closely related species, and probably offer the easiest way to differentiate species. In cases where males have particularly large and/or distinctively shaped valvispinae and/or pseudoceps, species identifications can be made without dissection if these structures are visible externally; this is frequently possible for *P. aphanta*, *P. appendiculata*, *P. pusilla*, and *P. sycophanta*. The margins of the paravalva and pseudoceps often feature folds, undulations, and angulations that are stable within species, and these structures should be examined carefully for such characters. For example, several species in the *P. carinata* group have a sharp “tooth” on the ventral margin of the paravalva below the valvispina, which has not previously been noted. In some species, the pseudoceps includes a membranous extension in the lateral dimension (e.g. *P. melanocarpa*, *P. siskiyouensis*, and *P. punctifrons*

(Thomson)), which may not be evident when penis valves are examined as wet mounts in lateral view; its presence/absence and shape should be considered when comparing against similar species. The ergot of the penis valve is usually either indistinct, distinct and short/tapered, or distinct and elongate. The genital capsule apparently does not vary much among species, but in some cases the size and shape of the harpes is useful for identification (e.g. *P. staudingeri* and *P. kangirsummiut*).

Frequently used external characters include the surface sculpture of various sclerites on the thorax, body colouration (especially the legs and, when not entirely black, the mesepisternum), presence/absence and size of subapical tooth of tarsal claw, and characters associated with valvula 3. Colouration is often variable within species, and there can be considerable overlap between closely related species, but it is often still useful for identification when consistent differences are noted. The microsculpture of the mesepisternum is stable in most species, but can sometimes vary from completely smooth to quite roughly sculptured (e.g. *P. cincta*, *P. sycophanta*), therefore it is important to examine a broad sample of specimens of both sexes when assessing this character for descriptions. Often, one can use the combination of microsculpture on the head, mesepisternum, and mesonotum to narrow down the list of similar species, making it easier to differentiate among them using other characters. The presence of stout black setae on the male antenna (particularly F1) was suggested by Goulet (1992) as a diagnostic character for the genus; in fact, these setae may be absent, indistinct, or variable in number among species, making this character useful in some cases for distinguishing similar species.

Two characters have been observed to vary among representatives of the early diverging lineages of *Pristiphora*, including *P. abbreviata* (Hartig), *P. chlorea*, *P. mollis* (Hartig), *P. punctifrons*,

and the *P. laricis*, *P. macnabi*, and *P. litura* groups (see phylogenetic results in Chapter 3). In these groups, the prepectus is apparently absent or severely reduced, and the velum of the protibial spur is lacking (except in the *litura* group, in which the velum is usually absent in females and present in males). Both structures are otherwise present in the remaining majority of *Pristiphora*, although the width of the prepectus is sometimes variable, which can be useful for identification particularly when its width is given relative to that of the adjacent portion of the epicnemium.

New records for the Nearctic region

In this study, *P. pusilla* Malaise and *P. sootryeni* Lindqvist are newly recorded as present in the Nearctic. Their identification is based upon comparison to images of the primary types of both species, which are available on ECatSym (Taeger et al. 2018). In neither case could any morphological differences be found that reliably differentiate Nearctic specimens from Palaearctic ones. One Nearctic specimen of *P. sootryeni* additionally belongs to one of the same BINs as *P. astragali* and *P. sootryeni* (BOLD:AAL8292; Prous et al. 2017), which is distinct from the BIN associated with its closest Nearctic relative, *P. maura* Rohwer (BOLD:ADA5136).

Two previously overlooked specimens collected in Guelph, ON, in 1992 were identified as the introduced species *P. subbifida*: CANADA, ON, Fergus, back yard, 26.v.1992, S.A. Marshall, 2 ♀♀ (DEBU). This species was first noted in North America from specimens collected in Virginia in 2000 (D. R. Smith 2016), and later, the “first report” of *P. subbifida* in Canada was made from specimens collected in Guelph in 2009-2011 (M. A. Smith et al. 2018). The two specimens reported above – collected by researchers at the same institution, seventeen years earlier, and deposited in a collection approximately 100 metres to the east – therefore represent the earliest known occurrence of *P. subbifida* in Canada. In their note, M. A. Smith et al. (2018)

recognize the usefulness of DNA barcode data for making the identification possible, however it should be stated that this species is very easily identified by its distinctive colouration, which is unique among all species of *Pristiphora* found in the Nearctic (D. R. Smith 2016). In this case, allocating the same resources to traditional "low-tech" curation and morphological identification would have provided a more accurate picture of this species' introduction to North America – and much earlier.

As a result of reviewing observations of sawflies on online community science and social media platforms during this study (iNaturalist, BugGuide, Twitter), the presence of an unknown larva of *Pristiphora* feeding on *Prunus* spp. and *Crataegus* sp. was noted. A total of seven examples of this unidentified larva have been found (listed at: https://inaturalist.ca/journal/skmonckton/44033-larval-nematinae) and are assumed to represent a single species based on consistent colouration and pattern of raised bumps on the abdominal segments. It is recorded from British Columbia, Oregon, Missouri, Ontario, and Pennsylvania. The larva bears a strong resemblance to *P. cincta* (Fig. 260), but that species is recorded only from *Betula*, *Salix*, and *Vaccinium*, and differs by the distinctly divided yellow blotches, with two large blotches subdorsally on each abdominal segment, compared to a single larger blotch above a diffuse cluster of smaller yellow spots on the unidentified larva. While *Crataegus* is a known host for *P. serrula* Wong & Ross, these are the first records of any North American nematine feeding on *Prunus* (Baine et al. 2022) – although several Palaearctic species (Lacourt 1999, Prous et al. 2017) and one Neotropical species (D. R. Smith 2003b) have been documented on it. Based on this larva's similarity to *P. cincta*, its distribution, and its association with *Crataegus*, it appears likely attributable to *P. serrula*.

Figure 260. Comparison of two larvae. **256a**. Larva of *Pristiphora cincta*, observed in the United Kingdom feeding on *Betula* sp. (image courtesy of Ian Andrews). **256b**. Unidentified larva from Pennsylvania (image courtesy of John Rosenfeld), resembling *P. cincta* but differing in the arrangement of yellow blotches (see text); similar larvae are documented on *Prunus* and *Crataegus* in the Nearctic.

Discussion

In the present work, three high-priority species groups in the Nearctic are revised, providing detailed differential diagnoses and descriptions for 23 of the 57 species of the genus now known

for the Nearctic. Based on available material, there does not appear to be any need to revise the species of the *P. macnabi* group (*P. clarki* Wong, *P. macnabi* Ross, *P. ferruginosa* Wong, *P. fructicola* Smith & Dolan, *P. resinicolor* (Marlatt)), and the combination of two existing references remains sufficient to identify its species (Wong 1968a, D. R. Smith and Dolan 2016). Therefore, with the addition of the revisionary work presented here, approximately half of the known species of *Pristiphora* in the Nearctic (28 of 57) are now thoroughly documented.

Taxonomic decisions in the course of this work were made in the interest of taxonomic stability, with the goal of simplifying the identification of the diverse North American Nematinae. Therefore, if any specimens not attributable to Nearctic species could instead be reliably attributed to Palaearctic species, they were, but no Nearctic species are here considered synonymous with any Palaearctic ones (even if a good argument may exist for doing so, for example as for *P. hucksena* with *P. luteipes*). As well, newly proposed synonymies have been made only in cases of species that were described as singleton individuals, with the notable except of *P. banksi*. In that instance, large numbers of specimens in several collections are stored under the name *P. banksi*, such that this synonymy is likely to be the only one to have a meaningful impact on collections, biodiversity databases, and identifications.

One important outcome of examining such a broad sample of *Pristiphora* – especially representatives of the *P. litura* and *P. macnabi* groups – is that there appears to be good morphological evidence in support of adjusting generic boundaries. Specifically, representatives of most early-diverging lineages (i.e. *P. laricis* group and *P. mollis*; *P. litura* group; *P. macnabi* group; *P. malaisei* group and *P. punctifrons*; *P. abbreviata*; see Fig. 1, Chapter 3) have a reduced or absent prepectus and have lost the velum of the protibial spur, whereas these characters are seemingly universally present in the alternate state in the clade that comprises most of the

remaining *Pristiphora* (i.e. the group labeled Clade D in Chapter 3, Figs. 1–5). Interestingly, both the reduction/loss of the prepectus and loss of the velum apparently represent derived states (present and distinct in the other Nematini), and both structures are secondarily reacquired for the remaining *Pristiphora*. There appears therefore to be both morphological and molecular support for the re-definition of *Pristiphora* as a more restrictive taxon, with the re-acquired prepectus and velum serving as synapomorphies for the genus. Each of the previously-diverging lineages – most of which appear to receive strong support from molecular evidence – would then need to be promoted to the genus level. This would involve resurrecting *Neopareophora* (= *Nepionema*) and *Pristola* (= *Melastola*), elevating the clade formed by *P. mollis* and the *P. laricis* group to the genus level, giving it the name *Oligonematus* Zhelochovtsev (type species *P. laricis*), and potentially establishing a new genus for the clade comprising the *P. malaisei* group and *P. punctifrons*, and for the clade that includes *P. abbreviata*, *P. biscalis* (Förster), *P. monogyniae* (Hartig), and *P. dedeara* Liston & Prous. *Neopareophora* (i.e. *litura* group) and *Pristola* (i.e. *macnabi* group) each have clear diagnoses, which are given in the results above, while *Oligonematus*, in this sense, could be diagnosed thus: prepectus absent; lancet with numerous long, stiff setae on annuli; paravalva narrow, approximately half as wide as pseudoceps or less; pseudoceps with longitudinal membranous fold on dorsal margin. It is unclear whether any good morphological support exists for the remaining two potential genera, or whether indeed the prepectus and velum exhibit consistent characters states within and among lineages nearer to the root of a more strictly-defined *Pristiphora*. Any such changes should be accompanied by a thorough morphological and molecular analysis of the Palaearctic representatives of those lineages, especially the *P. malaisei* group, *P. depressa* group, and the relatives of *P. abbreviata*, which were not examined as part of this study.

Further work on the Nearctic fauna should prioritize the *P. micronematica* group, *P. carinata* group, and *P. alpestris* group, in order of most to least urgent. The *P. micronematica* group deserves the highest priority not only because it includes the greatest number of undescribed species, but also because its members are also found primarily in boreal and arctic/subarctic habitats, which continue to exhibit ever-greater impacts from climate change (Høye and Forchhammer 2008, Høye and Sikes 2013, Kankaanpää et al. 2020, Myers-Smith et al. 2020). Moreover, identification of species in the *P. micronematica* group (and similarly for the *P. carinata* group) is complicated by the unclear species boundaries according to both morphological and molecular evidence, and especially by the very similar females (Prous et al. 2016, 2017). The greatest difficulties facing such work are the relatively small numbers of available specimens, the lack of recently collected material to provide molecular data, and the sometimes-maddening variation in individual penis valves and lancets. Although Wong's material represents a formidable resource (especially now, having been sorted and databased), it is clear in retrospect that the morphological monotony of the genus was an enormous obstacle to his research – leading him for example to erroneously associate males and females of unrelated species, or to assign numerous new epithets to series of specimens apparently based more upon locality and collecting event than on good morphological differences. Revisions of these groups should therefore ideally be supported by extensive fieldwork across the North and/or using high-throughput sequencing techniques to obtain molecular data from older museum specimens, such as targeted capture (e.g. Wood et al. 2018, Zhang et al. 2019, Ma et al. 2020) or shotgun phylogenomics (Allio et al. 2020). On the other hand, it is possible instead that considerable progress can be made by relying on COI barcode BINs, especially with the recent launch of the Arctic BIOSCAN project of the International Barcode of Life Consortium (ARCBIO;

https://arcticbioscan.ca/), which will generate large volumes of data from arthropods sampled across the North.

The current work presents meaningful progress towards clarifying the taxonomy of Nearctic *Pristiphora*, including a regional revision of its most diverse species group, the description of two new species, thoroughly detailed re-descriptions of 21 existing species, first records of two formerly Palaearctic species (now Holarctic), first descriptions of the males of six species and the female of one, four new synonymies, and notes on morphological characters, generic boundaries, and future directions.

References

Allio R, Scornavacca C, Nabholz B, Clamens AL, Sperling FAH, Condamine FL (2020) Whole genome shotgun phylogenomics resolves the pattern and timing of swallowtail butterfly evolution. Systematic Biology 69: 38–60. doi: 10.1093/sysbio/syz030

André E (1880a) Species des Hyménoptères d'Europe & d'Algérie. 1: 97–160.

André E (1880b) Species des Hyménoptères d'Europe & d'Algérie. 1: CXLIX–CXCVI, 49–96.

Baine Q, Looney C, Monckton SK, Smith DR, Schiff NM, Goulet H, Redford AJ (2022) USDA APHIS PPQ Identification Technology Program (ITP) and Washington State Department of Agriculture Sawfly GenUS. April 2022. Fort Collins, CO Available from: https://idtools.org/id/sawfly/ (July 11, 2022).

Benson RB (1935) The high mountain sawflies of Britain (Hymenoptera Symphyta). Transactions of the Royal Entomological Society of London 83: 23–39. doi: 10.1111/j.1365-2311.1935.tb00412.x

Benson RB (1958) Hymenoptera (Symphyta): Subfamily Nematinae. In: Handbooks for the Identification of British Insects. Royal Entomological Society of London, London, 139–252. Available from: http://www.royensoc.co.uk.

Benson RB (1960) Some more high-alpine sawflies (Hymenoptera Tenthredinidae). Journal of the Swiss Entomological Society 33: 173–182.

Blank SM, Taeger A (1995) Comments on the taxonomy of Symphyta (Hymenoptera) (Preliminary studies for a catalogue of Symphyta, part 4). In: Taeger A., Blank SM (Eds), Pflanzenwespen Deutschlands (Hymenoptera, Symphyta): Kommentierte Bestandsaufnahme. Goecke & Evers, Keltern, 141–174.

Boheman CH (1865) Spetsbergens Insekt-Fauna. Öfversigt af Kongliga Vetenskaps-Akademiens förhandlingar 22: 563–575.

Brischke CGA (1884) Beobachtungen über die Arten der Blatt- und Holzwespen von C. G. A. Brischke, Hauptlehrer a. D. in Langfuhr und Dr. Gustav Zaddach, Professor in Königsberg, mitgetheilt von Brischke aus Zaddach's Manuscripten. Schriften der physi- kalisch-ökonomischen Gesellschaft zu Königsberg 24.

Costa A (1859) Fauna del Regno di Napoli. Imenotteri. Parte III. - Trivellanti Sessiliventri. [Tentredinidei]. Antonio Cons, Napoli [1859-1860]: 1–116, 1–5.

Costa A (1894) Prospetto degli Imenotteri Italiani. III, Tenthredinidei e Siricidei. Atti della Reale Accademia delle Scienze Fisiche e Matematiche, Napoli 3: 1–290.

Dahlbom G (1835) Clavis Novi Hymenopterorum Systematis adjecta Synopsi Larvarum ejusdem ordinis Scandinavicarum Eruciformium. C. F. Berling, Lundae, i–v, 1–40; 1 pl. pp.

Dalla Torre KW v. (1894) Catalogus Hymenopterorum hucusque descriptorum systematicus et synonymicus. Vol. 1: Tenthredinidae incl. Uroceridae (Phyllophaga & Xylophaga). Sumptibus Guilelmi Engelmann, Lipsiae, I–VIII; 1–459 pp.

Ferrari RR (2019) A revision of *Colletes* Latreille (Hymenoptera: Colletidae: Colletinae) from Brazil, Paraguay and Uruguay. Zootaxa 4606: 1–91. doi: 10.11646/zootaxa.4606.1.1

Ferri E, Barbuto M, Bain O, Galimberti A, Uni S, Guerrero R, Ferté H, Bandi C, Martin C, Casiraghi M (2009) Integrated taxonomy: traditional approach and DNA barcoding for the identification of filarioid worms and related parasites (Nematoda). Frontiers in Zoology 6: 1. doi: 10.1186/1742-9994-6-1

Förster A (1854) Neue Blattwespen. Verhandlungen des naturhistorischen Vereines der preussischen Rheinlande und Westfalens 1: 265–350.

Gibbs J (2009) Integrative taxonomy identifies new (and old) species in the *Lasioglossum* (*Dialictus*) *tegulare* (Robertson) species group (Hymenoptera, Halictidae). Zootaxa 38: 1–38.

Goulet H (1992) The Insects and Arachnids of Canada, Part 20 The Genera and Subgenera of Sawflies of Canada and Alaska: Hymenoptera: Symphyta. 1–235 pp. Available from: http://esc-sec.ca/aafcmonographs/insects_and_arachnids_part_20.pdf.

Goulet H, Bennett AMR (2021) Checklist of the sawflies (Hymenoptera) of Canada, Alaska and Greenland. Journal of Hymenoptera Research 82: 21–67. doi: 10.3897/JHR.82.60057

Haris A (2002) Symphyta from Mongolia. IV. Folia Entomologica Hungarica 63: 62–65.

Haris A (2006) Study on the Palaearctic *Pristiphora* species (Hymenoptera: Tenthredinidae).

Natura Somogyiensis 9: 201–277. Available from: http://www.smmi.hu/termtud/ns/ns9/haris2 kicsi.pdf.

Harris TW (1835) VIII. Insects. In: Part IV. Catalogues of animals and plants. In: Hitchcock E (Ed), Report on the geology, mineralogy, botany, and zoology of Massachusetts. Press of J. S. and C. Adams, Amherst, 553–602.

Hartig T (1837) 1 Die Aderflügler Deutschlands mit besonderer Berücksichtigung ihres Larvenzustandes und ihres Wirkens in Wäldern und Gärten für Entomologen, Wald- und Gartenbesitzer. Die Familien der Blattwespen und Holzwespen nebst einer allgemeinen Einleitung zur Naturg. Haude und Spener, Berlin, i–xiv, 1–416; Tab. I-VIII pp.

Hartig T (1840) Hymenopterologische Mittheilungen vom Forstrathe Dr. Th. Hartwig. Entomologische Zeitung 1: 19–28.

Hellén W (1943) Mitteilungen über einige Tenthredinoiden Finnlands II. Notulae Entomologicae, Helsingfors 23: 63–72.

Herrich-Schäffer GAW (1840) europäischen Insecten; F. Pustet, Regensburg, VIII+1-40+1-244 pp.

Høye TT, Forchhammer MC (2008) Phenology of High-Arctic Arthropods: Effects of Climate on Spatial, Seasonal, and Inter-Annual Variation. Advances in Ecological Research 40: 299–324. doi: 10.1016/S0065-2504(07)00013-X

Høye TT, Sikes DS (2013) Arctic entomology in the 21st century. The Canadian Entomologist 145: 125–130. doi: 10.4039/tce.2013.14

Kankaanpää T, Vesterinen E, Hardwick B, Schmidt NM, Andersson T, Aspholm PE, Barrio IC,

Beckers N, Bêty J, Birkemoe T, DeSiervo M, Drotos KHI, Ehrich D, Gilg O, Gilg V, Hein N, Høye TT, Jakobsen KM, Jodouin C, Jorna J, Kozlov M V., Kresse J, Leandri-Breton D, Lecomte N, Loonen M, Marr P, Monckton SK, Olsen M, Otis J, Pyle M, Roos RE, Raundrup K, Rozhkova D, Sabard B, Sokolov A, Sokolova N, Solecki AM, Urbanowicz C, Villeneuve C, Vyguzova E, Zverev V, Roslin T (2020) Parasitoids indicate major climate-induced shifts in arctic communities. Global Change Biology 26: 6276–6295. doi: 10.1111/gcb.15297

Kincaid T (1900) Papers from the Harriman Alaska Expedition. VII. Entomological results (1): the Tenthredinoidea. Proceedings of the Washington Academy of Sciences 2: 341–365. doi: 10.1126/science.11.265.158

Klug F (1816) Die Blattwespen nach ihren Gattungen und Arten zusammengestellt. Der Gesellschaft Naturforschender Freunde zu Berlin Magazin für die neuesten Entdeckungen in der gesamten Naturkunde, Berlin 8: 42–84.

Konow FW (1890) Catalogus Tenthredinidarum Europae (Hymenopterorum XVI familiae). Deutsche Entomologische Zeitschrift 34: 241–255.

Konow FW (1897) Neue palaearctische Tenthrediniden. Wiener entomologische Zeitung 16: 173–187.

Konow FW (1902) Die Nematiden-Gattung Pristiphora Latr. (Hymenoptera, Tenthedinidae) soweit dieselbe bisher aus der palaearctischen Zone bekannt ist. Ezhegodnik Zoologitscheskago Muzeja 7.

Konow FW (1905) Hymenoptera. Fam. Tenthredinidae. Genera Insectorum 29: 1–176.

Lacourt J (1998) Pristiphora listoni, nouvelle espèce des Alpes françaises (Hymenoptera, Tenthredinidae). Nouvelle Revue d'Entomologie 15: 129–130.

Lacourt J (1999) Répertoire des Tenthredinidae ouest-paléarctiques (Hymenoptera: Symphyta). Mémoires de la Société Entomologique de France 3: 1–432.

Lepeletier de Saint-Fargeau A (1823) Monographia Tenthredinetarum, synonymia extricata. Societatis Parisiensis Historiae Naturalis Membro, Paris, 1–176 pp.

Lindqvist E (1955) Über einige Pristiphora-Arten aus Fennoskandien (Hym., Tenthredinidae). Notulae Entomologicae, Helsingfors 35: 35–50.

Lonsdale O, Huber JT (2011) Insect Collections of Canada Series: Canadian National Collection of Insects, Arachnids & Nematodes, Ottawa. Newsletter of the Biological Survey of Canada 30: 15–40.

Ma L, Zhang Y, Lohman DJ, Wahlberg N, Ma F, Nylin S, Janz N, Yago M, Aduse-Poku K, Peggie D, Wang M, Zhang P, Wang H (2020) A phylogenomic tree inferred with an inexpensive PCR-generated probe kit resolves higher-level relationships among Neptis butterflies (Nymphalidae: Limenitidinae). Systematic Entomology 45: 924–934. doi: 10.1111/syen.12435

MacGillivray AD (1908) Blennocampinæ—descriptions of new genera and species—synonymical notes. The Canadian Entomologist 40: 289–297.

MacGillivray AD (1923) A Century of Tenthredinoidea. University of Illinois Bulletin 20: 1–38.

Malaise R (1921) Beiträge zur Kenntnis schwedischer Blattwespen. Entomologisk Tidskrift 41: 1–20.

Marlatt CL (1896) Revision of the Nematinae of North America. Bulletin of the United States Department of Agriculture, Division of Entomology, Technical Series 3: 1–135. Available from: http://www.biodiversitylibrary.org/item/106469.

Masters BC, Fan V, Ross HA (2011) Species Delimitation – a Geneious plugin for the exploration of species boundaries. Molecular Ecology Resources 11: 154–157. doi: 10.1111/j.1755-0998.2010.02896.x

Monckton SK (2016) A revision of *Chilicola* (*Heteroediscelis*), a subgenus of xeromelissine bees (Hymenoptera, Colletidae) endemic to Chile: taxonomy, phylogeny, and biogeography, with descriptions of eight new species. ZooKeys 591: 1–144. doi: 10.3897/zookeys.591.7731

Myers-Smith IH, Kerby JT, Phoenix GK, Bjerke JW, Epstein HE, Assmann JJ, John C, Andreu-Hayles L, Angers-Blondin S, Beck PSA, Berner LT, Bhatt US, Bjorkman AD, Blok D, Bryn A, Christiansen CT, Cornelissen JHC, Cunliffe AM, Elmendorf SC, Forbes BC, Goetz SJ, Hollister RD, de Jong R, Loranty MM, Macias-Fauria M, Maseyk K, Normand S, Olofsson J, Parker TC, Parmentier FJW, Post E, Schaepman-Strub G, Stordal F, Sullivan PF, Thomas HJD, Tømmervik H, Treharne R, Tweedie CE, Walker DA, Wilmking M, Wipf S (2020) Complexity revealed in the greening of the Arctic. Nature Climate Change 10: 106–117. doi: 10.1038/s41558-019-0688-1

Newman E (1837) Notes on Tenthredinina. The Entomological Magazine, London 4: 258–263.

Norton E (1861) Catalogue of several genera of the Tenthredinidae in the United States. Proceedings of the Boston Society of Natural History 8: 150–161.

Norton E (1867a) Catalogue of the described Tenthredinidae and Uroceridae of North America.

Transactions of the American Entomological Society, Philadelphia 1: 225–280.

Norton E (1867b) Catalogue of the described Tenthredinidae and Uroceridae of North America. Transactions of the American Entomological Society, Philadelphia 1: 193–224.

Norton E (1867c) Catalogue of the described Tenthredinidae and Uroceridae of North America. Transactions of the American Entomological Society, Philadelphia 1: 31–84.

Onuferko TM (2018) A revision of the cleptoparasitic bee genus *Epeolus* Latreille for nearctic species, north of Mexico (Hymenoptera, Apidae). ZooKeys 2018: 1–185. doi: 10.3897/zookeys.755.23939

Pires AC, Marinoni L (2010) DNA barcoding and traditional taxonomy unified through Integrative Taxonomy: a view that challenges the debate questioning both methodologies. Biota Neotropica 10: 339–346. doi: 10.1590/S1676-06032010000200035

Pirurvik Centre (2022) Where are you from? Inuktut Tusaalanga. Available from: https://tusaalanga.ca/index.php/node/4714 (July 7, 2022).

Prous M, Blank SM, Goulet H, Heibo E, Liston A, Malm T, Nyman T, Schmidt S, Smith DR, Vårdal H, Viitasaari M, Vikberg V, Taeger A (2014) The genera of Nematinae (Hymenoptera, Tenthredinidae). Journal of Hymenoptera Research 40: 1–69. doi: 10.3897/JHR.40.7442

Prous M, Kramp K, Vikberg V, Liston A (2017) North-Western Palaearctic species of *Pristiphora* (Hymenoptera, Tenthredinidae). Journal of Hymenoptera Research 59: 1–190. doi: 10.3897/jhr.59.12656

Prous M, Kramp K, Vikberg V, Liston A (2018) Corrigenda: North-Western Palaearctic species

of *Pristiphora* (Hymenoptera, Tenthredinidae). Journal of Hymenoptera Research 59: 1–190. https://doi.org/10.3897/jhr.59.12656. Journal of Hymenoptera Research 63: 125–126. doi: 10.3897/jhr.63.23888

Prous M, Lee KM, Mutanen M (2020) Cross-contamination and strong mitonuclear discordance in Empria sawflies (Hymenoptera, Tenthredinidae) in the light of phylogenomic data. Molecular Phylogenetics and Evolution 143: 106670. doi: 10.1016/j.ympev.2019.106670

Prous M, Liston A, Kramp K, Savina H, Vårdal H, Taeger A (2019) The West Palaearctic genera of Nematinae (Hymenoptera, Tenthredinidae). ZooKeys 875: 63–127. doi: 10.3897/zookeys.875.35748

Prous M, Liston A, Mutanen M (2021) Revision of the West Palaearctic *Euura bergmanni* and *oligospila* groups (Hymenoptera, Tenthredinidae). Journal of Hymenoptera Research 84: 187–269. doi: 10.3897/JHR.84.68637

Prous M, Vikberg V, Liston A, Kramp K (2016) North-Western Palaearctic species of the *Pristiphora ruficornis* group (Hymenoptera, Tenthredinidae). Journal of Hymenoptera Research 51: 1–54. doi: 10.3897/jhr.51.9162

Ratnasingham S, Hebert PDN (2007) BOLD: The Barcode of Life Data System. Molecular Ecology Notes 7: 355–364. doi: 10.1111/j.1471-8286.2006.01678.x

Ratnasingham S, Hebert PDN (2013) A DNA-Based Registry for All Animal Species: The Barcode Index Number (BIN) System. PLoS ONE 8: e66213. doi: 10.1371/journal.pone.0066213

Rohwer SA (1908) New western Tenthredinidae. Journal of the New York Entomological

Society 16: 103–114.

Rohwer SA (1910) On a collection of Tenthredinoidea from Eastern Canada. Proceedings of the U.S. National Museum 38: 197–209.

Rohwer SA (1911) New sawflies in the collections of the United States National Museum. Proceedings of the United States National Museum 41: 377–411. doi: 10.5479/si.00963801.41-1866.377

Rohwer SA (1920) Descriptions of twenty-five new species of North American Hymenoptera. Proceedings of the United States National Museum 57: 209–231.

Ross HH (1935) The Nearactic [sic!] sawflies of the *Dineura* complex (Hymen.: Tenthredinidae). The Canadian Entomologist 67: 201–205. doi: 10.1017/CBO9781107415324.004

Ross HH (1937) A generic classification of the Nearctic sawflies (Hymenoptera, Symphyta). Illinois Biological Monographs 15: 1–173. Available from: https://www.ideals.illinois.edu/browse?value=Ross,+Herbert+Holdsworth,+1908-&type=author.

Ross HH (1945) A new tribe and genus of Nematine sawfly (Hymenoptera, Tenthredinidae). The Pan-Pacific entomologist. 21: 153–156.

Ross HH (1955) The taxonomy and evolution of the sawfly genus *Neodiprion*. Forest Science 1: 196–209.

Ruthe JF (1859) Verzeichniss der von Dr. Staudinger im Jahre 1856 auf Island gesammelten Hymenopteren. Entomologische Zeitung 20: 305–322.

Sépaq (2022) Parc national de la Gaspésie. Available from: https://www.sepaq.com/pq/gas/index.dot?language_id=1 (July 12, 2022).

Serville AJG (1823) Hyménoptères. In: Vieillot P, Desmarest AG, de Blainville HMD, Prévost C, Serville A, Lepelletier Saint-Fargeau A (Eds), Faune Française, ou histoire naturelle, générale et particuliére, des animaux qui se trouvent en France. Paris, 1–96.

Sheth BP, Thaker VS (2017) DNA barcoding and traditional taxonomy: an integrated approach for biodiversity conservation Adamowicz S (Ed). Genome 60: 618–628. doi: 10.1139/gen-2015-0167

Smith DR (1979) Symphyta. In: Krombein K V., Hurd PDJ, Smith DR, Burks BD (Eds), Catalog of Hymenoptera in America North of Mexico. Volume 1. Smithsonian Institution Press, Washington D.C., 1–137.

Smith DR (1988) A synopsis of the sawflies (Hymenoptera: Symphyta) of America south of the United States: introduction, Xyelidae, Pamphiliidae, Cimbicidae, Diprionidae, Xiphydriidae, Siricidae, Orussidae, Cephidae. Transactions of the American Entomological Society 13: 205–261.

Smith DR (1992) A synopsis of the sawflies (Hymenoptera: Symphyta) of America south of the United States: Argidae. Memoirs of the American Entomological Society 39: 1–201. doi: 10.1080/00305316.2003.10417360

Smith DR (1994) *Nepionema*, a nematine sawfly genus new to North America, and an unusual new species of *Nematus* (Hymenoptera: Tenthredinidae). Proceedings of The Entomological Society of Washington 96: 133–138.

Smith DR (2003a) A Synopsis of the Sawflies (Hymenoptera: Symphyta) of America South of the United States: Tenthredinidae (Allantinae). Journal of Hymenoptera Research 12: 148–192.

Smith DR (2003b) A Synopsis of the Sawflies (Hymenoptera: Symphyta) of America South of the United States: Tenthredinidae (Nematinae, Heterarthrinae, Tenthredininae). Transactions of the American Entomological Society 129: 1–45.

Smith DR (2016) Pristiphora subbifida (Thomson) (Hymenoptera: Tenthredinidae), a Palearctic Sawfly New to North America. Proceedings of the Entomological Society of Washington 118: 297–299. doi: 10.4289/0013-8797.118.2.297

Smith DR, Dolan AC (2016) A new species of huckleberry sawfly of the former tribe Pristolini (Hymenoptera: Tenthredinidae) from Montana. Proceedings of the Entomological Society of Washington 118: 594–601. doi: 10.4289/0013-8797.118.4.594

Smith DR, Strazanac JS (2016) Annotated list of West Virginia sawflies (Hymenoptera: Symphyta). Proceedings of the Entomological Society of Washington 118: 602–616. doi: 10.4289/0013-8797.118.4.602

Smith MA, Smith DR, R J (2018) First report of the Palearctic sawfly Pristiphora subbifida (Thomson 1871) (Hymenoptera : Tenthredinidae) in Canada. 149: 15–19.

Stein R von (1885) Neue Afterraupen. Wiener entomologische Zeitung, Wien 4: 302–306.

Taeger Andreas, Liston AD, Prous M, Groll EK, Gehroldt T, Blank SM (2018) ECatSym – Electronic World Catalog of Symphyta (Insecta, Hymenoptera). Available from: https://sdei.de/ecatsym/.

Tang P, Zhu J, Zheng B, Wei S, Sharkey M, Chen X, Vogler AP (2019) Mitochondrial phylogenomics of the Hymenoptera. Molecular Phylogenetics and Evolution 131: 8–18. doi: 10.1016/j.ympev.2018.10.040

Viitasaari M (2002) Sawflies (Hymenoptera, Symphyta) I. A review of the suborder, the Western Palaearctic taxa of Xyeloidea and Pamphilioidea. Tremex Press Ltd., Helsinki, 1–516 pp.

Vollenhoven SSC van (1866) De inlandsche bladwespen in hare gedaantewisseling en levenswijze beschreven. Tijdschrift voor Entomologie 9: 189–208.

Walsh BD (1866) On the Insects, coleopterous, hymenopterous and dipterous, inhabiting the Galls of certain species of Willow. -Part 2d and last. Proceedings of The Entomological Society of Philadelphia 6: 223–288.

Wong HR (1968a) A revision of the tribe Pristolini (Hymenoptera: Tenthredinidae). The Canadian Entomologist 100: 1049–1057.

Wong HR (1968b) *Pristiphora gelida*, a new species from Alaska (Hymenoptera: Tenthredinidae). Journal of Natural History 2: 185–186. doi: 10.1080/00222936800770801

Wong HR (1969) *Pristiphora acidovalva*, a new sawfly on willow (Hymenoptera: Tenthredinidae). The Canadian Entomologist 101: 970–972.

Wong HR (1975) The *abietina* group of *Pristiphora* (Hymenoptera: Tenthredinidae). Canadian Entomologist 107: 451–463. Available from: http://journals.cambridge.org.ezproxy.library.yorku.ca/download.php?file=/TCE/TCE107_04/S0008347X00033009a.pdf&code=aaf912807fecd8f43395fd739ff44a29.

Wong HR (1976) American Species of *Pristiphora* South of the United States. Annals of the

Entomological Society of America 69: 525–526.

Wong HR, Ross HH (1960) New Nearctic Species of the Genus Pristiphora Latreille (Hymenoptera: Tenthredinidae). The Canadian Entomologist 92: 193–198. doi: 10.4039/Ent92193-3

Wood HM, González VL, Lloyd M, Coddington J, Scharff N (2018) Next-generation museum genomics: Phylogenetic relationships among palpimanoid spiders using sequence capture techniques (Araneae: Palpimanoidea). Molecular Phylogenetics and Evolution 127: 907–918. doi: 10.1016/j.ympev.2018.06.038

Yoder MJ, Mikó I, Seltmann KC, Bertone MA, Deans AR (2010) A Gross Anatomy Ontology for Hymenoptera Moreau CS (Ed). PLoS ONE 5: e15991. doi: 10.1371/journal.pone.0015991

Zetterstedt JW (1838) Ordo IV. Hymenoptera. In: Zetterstedt JW (Ed), Insecta Lapponica descripta. Sectio Secunda. Hymenoptera. Lipsiae, L. Voss, 326–358.

Zhang Y, Deng S, Liang D, Zhang P (2019) Sequence capture across large phylogenetic scales by using pooled PCR-generated baits: A case study of Lepidoptera. Molecular Ecology Resources 19: 1037–1051. doi: 10.1111/1755-0998.13026

Zhelochovtsev AN, Zinovjev AG (1988) Keys to the Insects of the European Part of the USSR. Volume III Hymenoptera. Part VI Symphyta. i–xviii; 1–432 pp.

Zinovjev AG, Smith DR (2000) Sawflies (Hymenoptera: Tenthredinidae) described by Benjamin D. Walsh, with notes on their hosts and biology. Proceedings of the Entomological Society of Washington 102: 974–990.

CHAPTER 3: Phylogenetic analysis and biogeography of *Pristiphora* Latreille (Hymenoptera: Tenthredinidae)

Introduction

As currently defined, *Pristiphora* Latreille is the second largest genus in the subfamily Nematinae (Tenthredinidae), with over 220 species found almost exclusively in the Northern Hemisphere (Taeger et al. 2018). Along with the rest of the Nematinae, they are remarkable for their diversity and abundance at higher latitudes, being a common fixture in cool-temperate, boreo-montane, and arctic-alpine habitats (Ross 1937, Nyman et al. 2010). This has earned them the distinction of being one of only a few taxa whose diversity declines towards the tropics (Kouki et al. 1994, Kouki 1999), such that their latitudinal diversity gradient opposes that of most other living taxa (Wallace 1878, Hillebrand 2004). Nematine sawflies therefore present interesting opportunities to study speciation in cool-adapted groups across the Northern Hemisphere.

Previous work in this area has attempted to test the hypothesis that ecological speciation is responsible for the diversity of the Nematinae (Nyman et al. 2010) – i.e. in this case, speciation as a result of switching host plants. Although nematine sawflies do tend to prefer one or a few host plant species (Marlatt 1896, Nyman et al. 2000, Nyman Farrell et al. 2006), Nyman et al. (2010) found that ecological speciation occurred in only about 20% of cases, and was most common in gall-forming species (*Pristiphora* are mostly external feeders; gallers represent over one-third of the subfamily's more than 1250 species; Roininen et al. 2005, Nyman et al. 2010, Taeger et al. 2018). Instead, those authors suggested an alternative hypothesis in the form of the high latitude speciation machine (HLSM). This hypothesis proposes that past periods of climatic

oscillation led to repeated cycles of range contractions, expansions, and overlap for entire ecosystems, each time offering opportunities for isolation, divergence, and speciation across multiple trophic levels (Ross 1972, Esselstyn et al. 2009). During these periods of cyclical climatic change, ranges are fragmented and populations become isolated, where they may diverge through founder effects or genetic drift. As suitable habitat once again becomes available over a large continuous range, these isolated populations come into secondary contact and may continue to diverge through reinforcement (Dynesius and Jansson 2000, Clarke and Crame 2010). In principle, the hypothesis is similar to the conventional phylogeographic paradigm of diversification through the Pleistocene glaciations (Rand 1948, Hewitt 2011), with similar principles applied to larger phylogenetic and temporal scales. In contrast to similar 'species pump' hypotheses intended to explain the diversity of montane taxa (e.g. Hall 2005, Ghalambor 2006, Kozak and Wiens 2006, Schoville et al. 2012), the HLSM operates in reverse: the ranges of high-latitude species would have expanded during warmer periods and contracted during cooler ones. Putative examples of such climate-associated diversification (primarily during the Pleistocene) have been observed in birds (Avise and Walker 1998, Johnson and Cicero 2004, Arcones et al. 2021), rodents (Conroy and Cook 2000, Fletcher et al. 2019), herptiles (Ruane et al. 2014), fishes (Clarke and Crame 2010), trees (Dynesius and Jansson 2000), and invertebrates (Carisio et al. 2004, Shell and Rehan 2016, García-Vázquez et al. 2017, Sánchez-Vialas et al. 2020). For the Nematinae, Nyman et al. (2010) specifically pointed to climatic oscillations beginning in the early Oligocene ca. 34 Ma (Zachos et al. 2008), which appear to correspond well with the timing of increased diversification for the subfamily (Nyman Zinovjev et al. 2006).

Importantly, the HLSM hypothesis gives rise to a few predictions that can be tested phylogenetically. First, if diversity arises primarily due to climate-driven range shifts, then

lineages should be expected to accumulate primarily in sympatry (i.e. within either North America or Eurasia) as opposed to allopatrically (i.e. via dispersal and/or vicariance across land bridges with subsequent radiation). Second, the timing and rate of diversification should correspond to periods of regular climatic oscillations, like those that occurred during the Oligocene on a 405-kyr period (Pälike et al. 2006).

A test of the HLSM hypothesis requires a densely-sampled phylogeny. Of the three most diverse genera of Nematinae (*Euura* Newman, *Nematus* Panzer, *Pristiphora*; Prous et al. 2014), *Pristiphora* is perhaps taxonomically best-known, having been the subject of recent, detailed taxonomic study (Prous et al. 2017; and see Chapter 2), making it possible to achieve dense taxon sampling and test the HLSM hypothesis. Besides this, there are other practical reasons to infer an updated phylogeny for *Pristiphora*. For one, previous phylogenetic analyses have primarily sampled Palaearctic taxa (Nyman Zinovjev et al. 2006, Nyman et al. 2010, Prous et al. 2014, 2017), and resulted in several primarily Nearctic former genera (*Neopareophora* MacGillivray, *Nepionema* Benson, *Melastola* Wong, and *Pristola* Ross) being synonymized under *Pristiphora* (Prous et al. 2014). Meanwhile, morphological evidence supports the expansion of some informal species groups (Prous et al. 2017) to include additional Nearctic and Holarctic species; a molecular phylogeny should provide an independent test of these hypothesized expansions. If a better understanding of diversity and taxonomy of this clade is to be had, a greater sampling of Nearctic species is desirable.

A second reason is that the current best estimates for the age of the Nematinae are based upon minimum age constraints on the families Tenthredinidae and Cimbicidae (Nyman Zinovjev et al. 2006). However, the presence of fossil Nematinae from the early Eocene of the Okanagan Highlands (Archibald et al. 2018) dated to 52.10 ± 0.26 Ma (Rubino et al. 2021), contradicts that

study's lower estimate of 50 Ma for the age of the subfamily. Previously, the oldest known fossil Nematinae were from Florissant, Colorado (Cockerell 1906, 1915, 1927, Brues 1908, Rohwer 1908c, 1908b, Zhelochovtzev and Rasnitsyn 1972). Thus, the Okanagan fossils not only increase the minimum age of the subfamily, but also offers a second, independent calibration point from within the subfamily for a dated analysis.

Finally, a dated phylogeny offers the opportunity for an historical biogeographic analysis of the genus. Such an analysis would not only provide insight into the geographic origins of the genus (expected to be Nearctic; Wong 1960, Nyman Zinovjev et al. 2006), but would also offer a better-informed test of the HLSM hypothesis by shedding light on the role of biogeography in the group's diversification. Earlier studies have quite clearly shown that there is a complex relationship between the Palaearctic and Nearctic species in this genus (Wong 1960, Prous et al. 2017) owing to the fact that most of the apparently monophyletic species groups are found in both regions (Prous et al. 2017). This suggests that there have been numerous dispersals between the two landmasses, presumably mainly across the Bering Land Bridge (Hultén 1937, Harington 2005, DeChaine 2008). Dispersal across the North Atlantic Land Bridge may have also occurred until at least 50 Mya, and perhaps as recently as 34 Mya (Sanmartín et al. 2001, Brikiatis 2014). Wong (1960) suggested a minimum of nineteen dispersals between Eurasia and North America, an estimate that was reached based on an incomplete knowledge of the Holarctic fauna. The actual number might well be much higher, and given that land bridges can be drivers of diversification (Sanmartín et al. 2001, Meseguer et al. 2015), this presents an additional hypothesis to explain the diversity in this group.

Resolving relationships among *Pristiphora* – particularly between Palaearctic and Nearctic lineages – is important for understanding the role that biogeography has played in the

diversification of the genus, and in turn for understanding the origins of their unusual reverse latitudinal diversity gradient. The objectives of this chapter are therefore to produce a robust, time-calibrated phylogenetic hypothesis for the genus, to evaluate its classification, and to test biogeographic hypotheses about its diversification.

Methods

Taxon sampling and specimens

For this phylogenetic analysis, sequences from 207 specimens were used, representing 136 species from the Holarctic region: 1 specimen from each of 34 species were sampled as outgroups, with the remaining 173 specimens representing an ingroup of 102 species of *Pristiphora*. Of these, 51 specimens representing 34 species are newly sampled from the Nearctic, such that a total of 42 of the 57 species presently known from the Nearctic region are sampled here. Outgroups were chosen to represent the full diversity of the Nematinae. The so-called 'Higher Nematinae', which includes *Pristiphora*, are represented by *Euura* Newman (22 spp.), *Nematus* Panzer (5 spp.), *Fagineura* Vikberg & Zinovjev (1 sp.), *Mesoneura* Hartig (1 sp.), and *Megadineura* Malaise (1 sp.), while the 'basal' grade of the subfamily is represented by *Cladius* Illiger, *Dineura* Dahlbom, *Hemichroa* Stephens, and *Hoplocampa* Hartig (1 sp. ea.; Prous et al. 2014). Specimen data are provided in Table A1 (Appendix A).

Sequences from outgroup and Palaearctic specimens were provided by Marko Prous (University of Tartu, Estonia). The associated material is deposited at: the Collection of Mikk Heidemaa, Tartu, Estonia (CMH), the Swedish Museum of Natural History, Stockholm, Sweden (NHRS), the Collection of Ole Lonnve, Oslo, Norway (OLCO), the Senckenberg German Entomological

Institute, Müncheberg, Germany (SDEI), the University of Tartu Natural History Museum, Tartu, Estonia (TUZ), and the University of Oulu Zoological Museum, Oulu, Finland (ZMUO). Sequences for the four early-diverging species of Nematinae were obtained from GenBank (as they were deposited by sawfly systematists, their identification is considered likely correct). For newly obtained sequences of Nearctic specimens of *Pristiphora*, material was either borrowed from museum collections or collected during field trips to Yukon (2016, 2018), Churchill, MB (2016), and Ontario (2019). Although fieldwork was planned for 2020 to obtain additional specimens for DNA sampling, it was unable to proceed due to the global COVID-19 pandemic. Museum specimens are from the Biodiversity Institute of Ontario, University of Guelph, Guelph, ON (BIOUG), the Department of Biological Sciences, University of Calgary, Calgary, AB (DBUC), the Lyman Entomological Museum, McGill University, Ste. Anne-de-Bellevue, QC (LEMU), the Royal British Columbia Museum, Victoria, B.C. (RBCM), and the U.S. National Museum of Natural History, Smithsonian Institution, Washington, DC (USNM). Newly collected specimens are deposited in the Packer Collection at York University, Toronto, ON (PCYU).

Loci, DNA extraction, amplification, and sequencing

Specimens were sampled for one mitochondrial and three nuclear regions, with the choice of loci designed to leverage existing datasets for the Nematinae, and for *Pristiphora* in particular (Prous et al. 2014, 2017, 2019). The sampled mitochondrial region is a large fragment (1087 bp) of cytochrome *c* oxidase subunit I (COI), which includes the 658-bp standard barcode region for animals (Hebert et al. 2003). The sampled nuclear regions are sodium/potassium-transporting ATPase subunit alpha (NaK), DNA dependent RNA polymerase II subunit RPB1 (POL2), and triose-phosphate isomerase gene (TPI). The sampled fragment of NaK is an almost-complete 1654-bp sequence of its longest exon. The TPI fragment is a 676-bp sequence spanning nearly

the complete gene. The POL2 fragment is 2474-2709 bp in length depending on the primer set used.

For newly sampled Nearctic specimens, total DNA was extracted using one of two approaches. For a minority of specimens, DNA was extracted from thoracic muscle tissue using a Mag-Bind Blood & Tissue DNA HDQ 96 Kit (Omega Bio-tek, Inc., Norcross, GA) and a KingFisher Flex Purification System (Thermo Scientific). For the rest, non-destructive extractions were performed by submerging specimens in digestion buffer overnight in a shaking incubator (12-16 hours at 55°C) and proceeding with the manufacturer's protocol for the Zymo Quick-DNA Miniprep Plus Kit (Zymo Research, Irvine, CA). PCR reactions were performed in a total volume of 50 µL containing 1–5 µL of extracted DNA, 2.5 µL (25 pmol) of each primer and 25 µL of Hot Start *Taq* 2X Master Mix (New England Biolabs, Whitby, ON). The PCR protocol consisted of an initial DNA polymerase activation step at 95 °C for 5 min, followed by 40 cycles of 30 s at 95 °C, 90–120 s at 49–60 °C (depending on primer set), and 60–150 s at 72 °C (depending on amplicon size); and a final 30 min extension step at 68 °C. Amplification success was assessed by gel electrophoresis and concentrations were quantified using a Qubit 4 Fluorometer (Thermo Fisher Scientific, Waltham, MA). Good-quality PCR products were sent to Bio Basic Inc. (Toronto, ON) for purification and Sanger sequencing. Primers used for PCR and sequencing are listed in Table A2 (Appendix A). When amplifications of the full fragments of TPI and NaK failed, alternate primer pairs for smaller fragments were used (TPI_111Fb + TPI_275Ri; NaK_1250Fv2 + NaK_1918R). POL2 was amplified in one to three fragments.

Newly obtained sequences were trimmed, assembled, and aligned using Geneious Prime 2022.1.1. Trimming was performed with an error probability limit of 3%, and sequences were discarded if they contained fewer than 30% of nucleotides with quality scores above 30. Multiple

sequence alignment was performed using the MUSCLE algorithm with default settings in Geneious Prime, and resulting alignments were inspected by eye. Each locus was aligned separately.

For two of the sampled specimens (both *P. ferruginosa* Wong) COI could not be amplified, and alternate sequences were obtained from BOLD (Barcode of Life Data System Database; Ratnasingham and Hebert 2007) to be used in analyses. Identifications of the two BOLD specimens were verified using available photographs and their conspecificity is considered unambiguous.

Phylogenetic analyses

Single-locus trees were estimated by maximum likelihood (ML) analysis using IQ-TREE v2.0.7 (Minh Schmidt et al. 2020). Partitions were assigned for each codon position of each locus, with best-fit partitioning scheme and associated substitution models determined using ModelFinder (Chernomor et al. 2016, Kalyaanamoorthy et al. 2017). Branch support was assessed by computing ultrafast bootstrap support values from 1000 bootstrap replicates (Hoang et al. 2018), which correspond roughly to the probability that the clade is true (Minh et al. 2013). This analysis was repeated to infer a multi-locus tree and assess concordance with each single-locus tree (Minh Hahn et al. 2020).

A dated multi-locus phylogeny was inferred via Bayesian analysis in BEAST v2.6.3 (Bouckaert et al. 2019) using a fossilized birth-death (FBD) model, which treats observed fossils as part of the prior on node times (Stadler 2010, Heath et al. 2014). The FBD model explicitly incorporates fossil observations as a part of the diversification process that gave rise to the tree. Each locus was assigned a single partition for which the substitution model was estimated using bModelTest, which jointly estimate the tree and substitution models using model averaging

(Bouckaert and Drummond 2017). Two fossil sawflies were included in the analysis: *Hoplocampa ilicis* Cockerell, 1927 and an undescribed fossil from the McAbee formation in the Okanagan Highlands (Archibald et al. 2018). Constraints of monophyly were added to the clades in which these fossils are believed to belong: *H. ilicis* is assigned to its genus based on the forewing vein 2m-cu meeting cell 2Rs near its midpoint (apomorphic for *Hoplocampa* and *Susana* Rohwer & Middleton), combined with the presence of a small basal anal cell in the forewing (vein 2A+3A fused to vein 1A) and presence of forewing vein 2r-rs (Cockerell 1927); the undescribed McAbee fossil is assigned to the Dineurini based on the presence of a large basal anal cell in the forewing (vein 2A+3A fused to vein 1A for a short distance, apparently apomorphic and shared with the fossil *Eohemichroa eophila* Cockerell; Zhelochovtzev and Rasnitsyn 1972), combined with forewing vein 2m-cu meeting cell 1Rs (pers. obs. of images provided by S.B. Archibald). Fossils were assigned uniform priors for their estimated age: 34.07 ± 0.10 Ma for *H. ilicis* (Evanoff et al. 2001) and 52.10 ± 0.26 Ma for the McAbee fossil (Rubino et al. 2021). BEAST analysis was run for 250 million generations. Maximum clade credibility trees were computed using TreeAnnotator after removing 20% of the trees as burn-in (Bouckaert et al. 2019). Both multi-locus trees were plotted and annotated using the R package GGTREE v3.5.0.900 (G. Yu et al. 2017), with the geological time scale supplied by deeptime v0.2.2 (Gearty 2022). Reading and writing of trees of varying file formats was facilitated by the R packages ape v5.6-2 (Paradis and Schliep 2019) and treeio v.1.19.2 (Wang et al. 2019).

Diversification through time

To investigate potential changes in diversification rates through time, a lineage-through-time (LTT) plot was constructed from the dated tree using the R package phytools v1.0-3 (Revell 2012). This tool also calculates the gamma statistic (γ) of Pybus and Harvey (2000) which, under

a pure-birth speciation model, is expected to have a normal distribution centered on zero. The function ‘gammatest’ computes a p-value used to assess whether a calculated γ-statistic differs significantly from that of a pure-birth process. Shifts in diversification were further investigated using MEDUSA (Alfaro et al. 2009) with the R package geiger v2.0.10 (Pennell et al. 2014). This method detects rate shifts using a stepwise AIC approach, fitting increasingly complex diversification models to a tree and stopping at an automatically computed threshold in model fit. Both the LTT and MEDUSA analyses were performed on a portion of the dated tree, representing only the ingroup of *Pristiphora*.

Biogeographic analysis

Ancestral range reconstruction on the dated phylogeny was performed using RASP v4.3’s (Y. Yu et al. 2020) implementation of BioGeoBEARS (Matzke 2013). Specifically, a likelihood-based dispersal-extinction-cladogenesis approach (DEC; Ree and Smith 2008) was used to estimate ranges based on two biogeographic areas: the Nearctic (A) and the Palaearctic (B). Ranges were assigned to species based on information from the World Catalogue of Symphyta (Taeger et al. 2018), recent revisions of western Palaearctic *Pristiphora* (Prous et al. 2016, 2017), and the latest checklist of the sawflies of Canada (Goulet and Bennett 2021). Holarctic species were assigned a range of AB. The J parameter, which allows for long-distance “jump dispersal” was not used, partly due to problems associated with that model (Ree and Sanmartín 2018), and partly because sawflies are not strong flyers and are unlikely to achieve long distance dispersals without assistance (Marlatt 1896, Wong 1960, Goulet 1992).

Results

Maximum likelihood analysis

The results of the multi-locus ML analysis are shown in Figs. 1–3. Overall support for the tree was moderately good, with 71.6% of recovered clades having ultrafast bootstrap support values of 95% or higher. The proportion of nodes in the multi-locus tree that were recovered in two or more of the single-locus trees was 51.5% (recovered by only one locus: 27.5%; recovered only in the multi-locus tree: 21%).

Previously recognized species groups were mostly recovered with high support, along with many of the same relationships between larger clades as seen in previous analyses (Prous et al. 2017). Notable deviations include the placement of *P. insularis* Rohwer in a clade with *P. pallidiventris* (Fallén) with strong support, placement of *P. bivittata* (Norton) as sister to the clade comprising *P. cincta* Newman, *P. banksi* Marlatt, *P. paloma* Wong & Ross, and the *rufipes* group (here collectively called Clade D; note *P. banksi* is a new synonym of *P. cincta* as presented in Chapter 2), and the recovery of the *macnabi* group (former *Pristola* and *Melastola*) and *litura* group (former *Neopareophora* and *Nepionema*) as successive sister groups to a larger clade of *Pristiphora* here labeled Clade A (Prous et al. (2017) recovered these two clades as a monophyletic sister pair). Clades with a poorly defined prepectus and lacking a velum on the protibial spur (as discussed in Chapter 2) are recovered as successive sister groups to a poorly-supported clade comprising the majority of *Pristiphora*, labeled Clade B. There was maximum support for the clade comprising the *laricis* group, *leucopodia* group, and *P. mollis* – here labeled Clade C – which formed the sister group to a maximally supported clade of all remaining species. However, support for the monophyly of *Pristiphora* was only 86%, which is considered low.

(Text continues on p. 234.)

Figure 1. (Following page.) Cladogram of maximum likelihood tree of *Pristiphora* based on multi-locus analysis of one mitochondrial (COI) and three nuclear loci (NaK, POL2, TPI). Boxes above branches indicate topological concordance between this and individual single-locus trees. Numbers below ingroup branches indicate ultrafast bootstrap support values based on 1000 replicates. Recognized species groups are listed to the right of tip labels. Shaded, unannotated portions of the tree are shown in Figs. 2 & 3. Clades labeled 'A' to 'C' are discussed in the text.

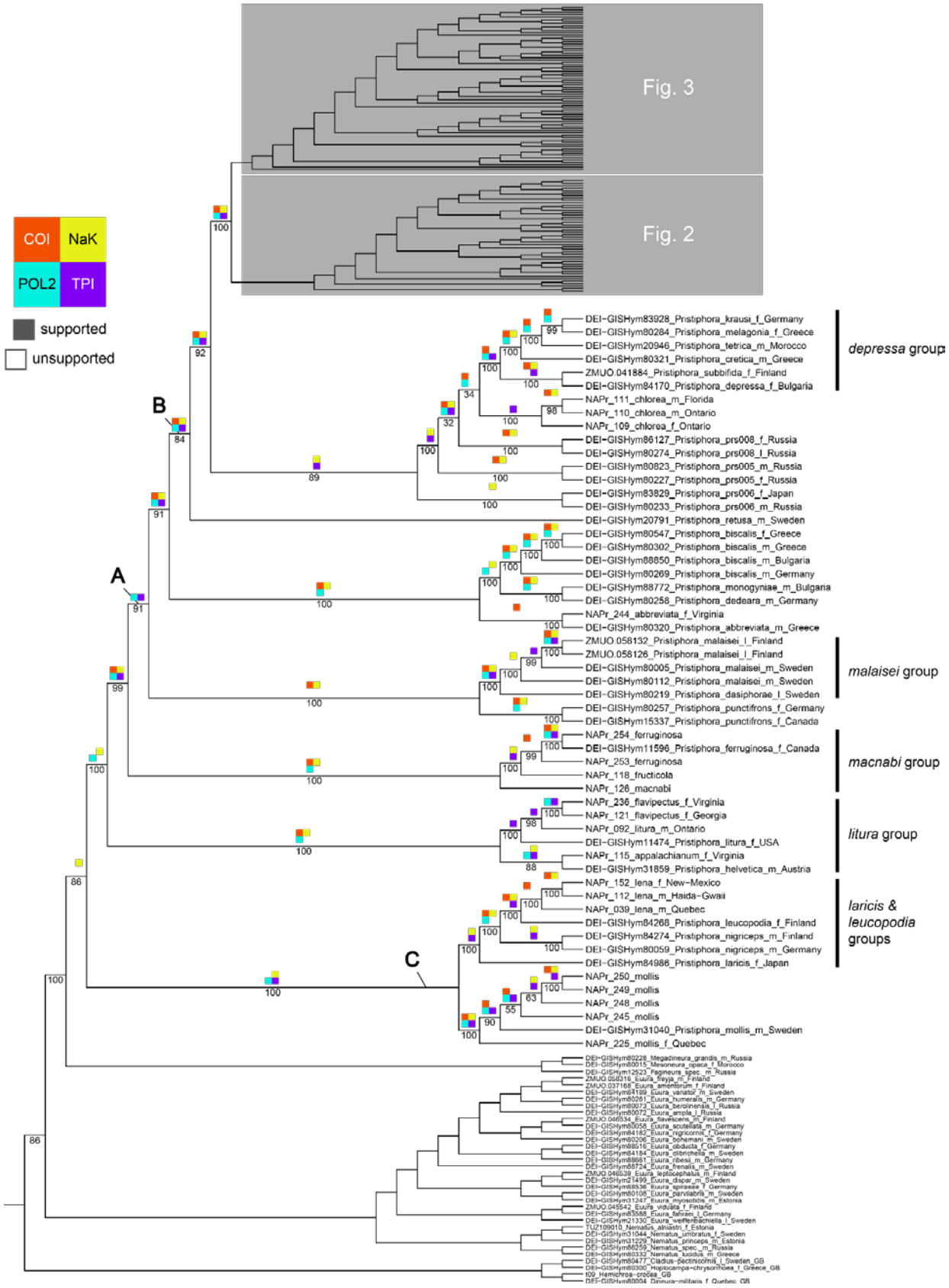
Fig. 3
Fig. 2
COI
NaK
POL2
TPI
supported
unsupported
A
B
C
depressa group
malaisei group
macnabi group
litura group
laricis & leucopodia groups
DEI-GISHym83928_Pristiphora_krausi_f_Germany
DEI-GISHym80284_Pristiphora_melagonia_f_Greece
DEI-GISHym20946_Pristiphora_tetrica_m_Morocco
DEI-GISHym80321_Pristiphora_cretica_m_Greece
ZMUO.041884_Pristiphora_subbifida_f_Finland
DEI-GISHym84170_Pristiphora_depressa_f_Bulgaria
NAPr_111_chlorea_m_Florida
NAPr_110_chlorea_m_Ontario
NAPr_109_chlorea_f_Ontario
DEI-GISHym86127_Pristiphora_prs008_f_Russia
DEI-GISHym80274_Pristiphora_prs008_l_Russia
DEI-GISHym80823_Pristiphora_prs005_m_Russia
DEI-GISHym80227_Pristiphora_prs005_f_Russia
DEI-GISHym83829_Pristiphora_prs006_f_Japan
DEI-GISHym80233_Pristiphora_prs006_m_Russia
DEI-GISHym20791_Pristiphora_retusa_m_Sweden
DEI-GISHym80547_Pristiphora_biscalis_f_Greece
DEI-GISHym80302_Pristiphora_biscalis_m_Greece
DEI-GISHym88850_Pristiphora_biscalis_m_Bulgaria
DEI-GISHym80269_Pristiphora_biscalis_m_Germany
DEI-GISHym88772_Pristiphora_monogyniae_m_Bulgaria
DEI-GISHym80258_Pristiphora_dedeara_m_Germany
NAPr_244_abbreviata_f_Virginia
DEI-GISHym80320_Pristiphora_abbreviata_m_Greece
ZMUO.058132_Pristiphora_malaisei_l_Finland
ZMUO.058126_Pristiphora_malaisei_l_Finland
DEI-GISHym80005_Pristiphora_malaisei_m_Sweden
DEI-GISHym80112_Pristiphora_malaisei_m_Sweden
DEI-GISHym80219_Pristiphora_dasiphorae_l_Sweden
DEI-GISHym80257_Pristiphora_punctifrons_f_Germany
DEI-GISHym15337_Pristiphora_punctifrons_f_Canada
NAPr_254_ferruginosa
DEI-GISHym11596_Pristiphora_ferruginosa_f_Canada
NAPr_253_ferruginosa
NAPr_118_fructicola
NAPr_126_macnabi
NAPr_236_flavipectus_f_Virginia
NAPr_121_flavipectus_f_Georgia
NAPr_092_litura_m_Ontario
DEI-GISHym11474_Pristiphora_litura_f_USA
NAPr_115_appalachianum_f_Virginia
DEI-GISHym31859_Pristiphora_helvetica_m_Austria
NAPr_152_lena_f_New-Mexico
NAPr_112_lena_m_Haida-Gwaii
NAPr_039_lena_m_Quebec
DEI-GISHym84268_Pristiphora_leucopodia_f_Finland
DEI-GISHym84274_Pristiphora_nigriceps_m_Finland
DEI-GISHym80059_Pristiphora_nigriceps_m_Germany
DEI-GISHym84986_Pristiphora_laricis_f_Japan
NAPr_250_mollis
NAPr_249_mollis
NAPr_248_mollis
NAPr_245_mollis
DEI-GISHym31040_Pristiphora_mollis_m_Sweden
NAPr_225_mollis_f_Quebec

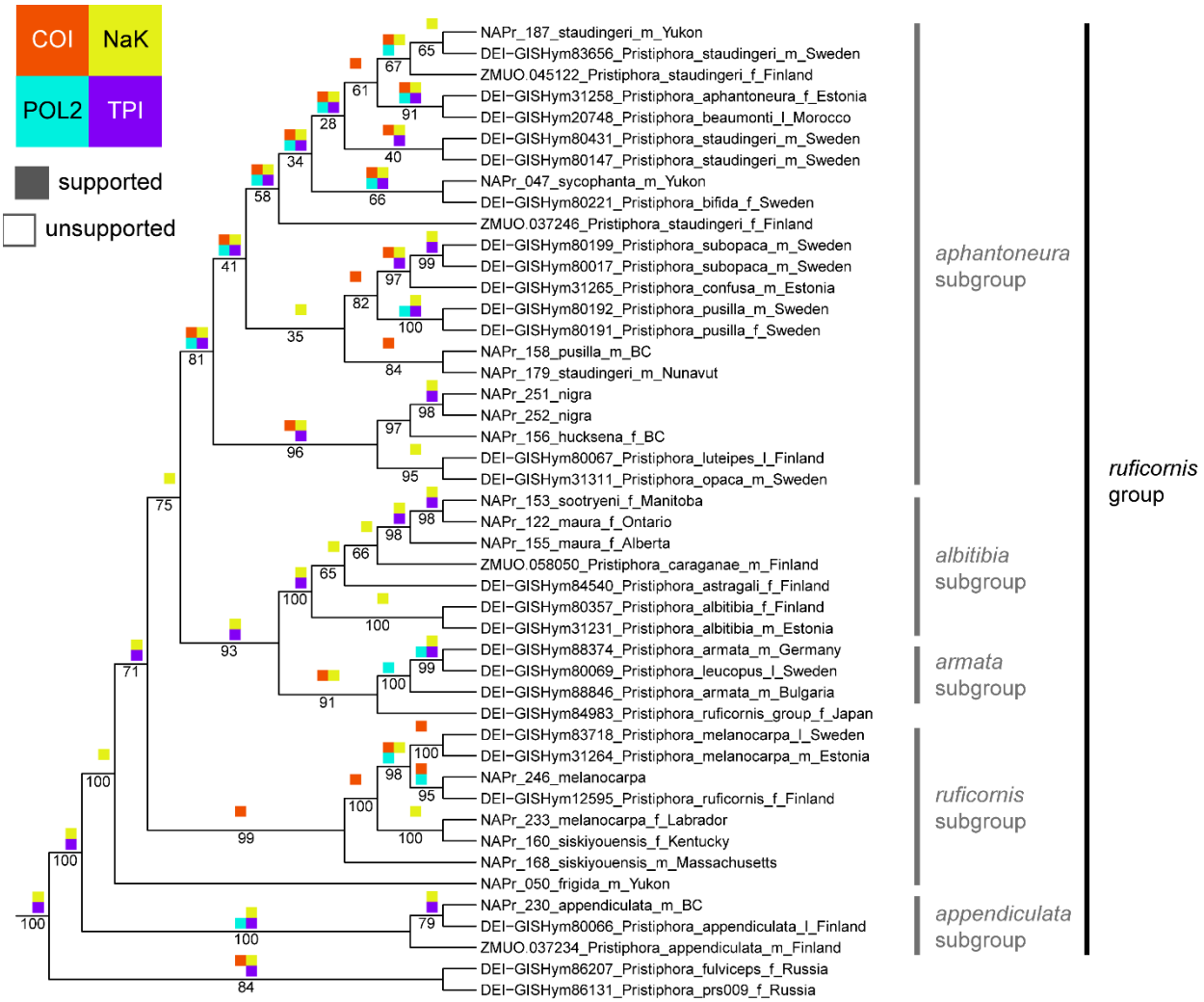

Figure 2. Part of the maximum likelihood tree shown in Fig. 1. Boxes above branches indicate topological concordance between the multi-locus and single-locus trees. Numbers below ingroup branches indicate ultrafast bootstrap support values based on 1000 replicates. Recognized species groups are listed to the right of tip labels.

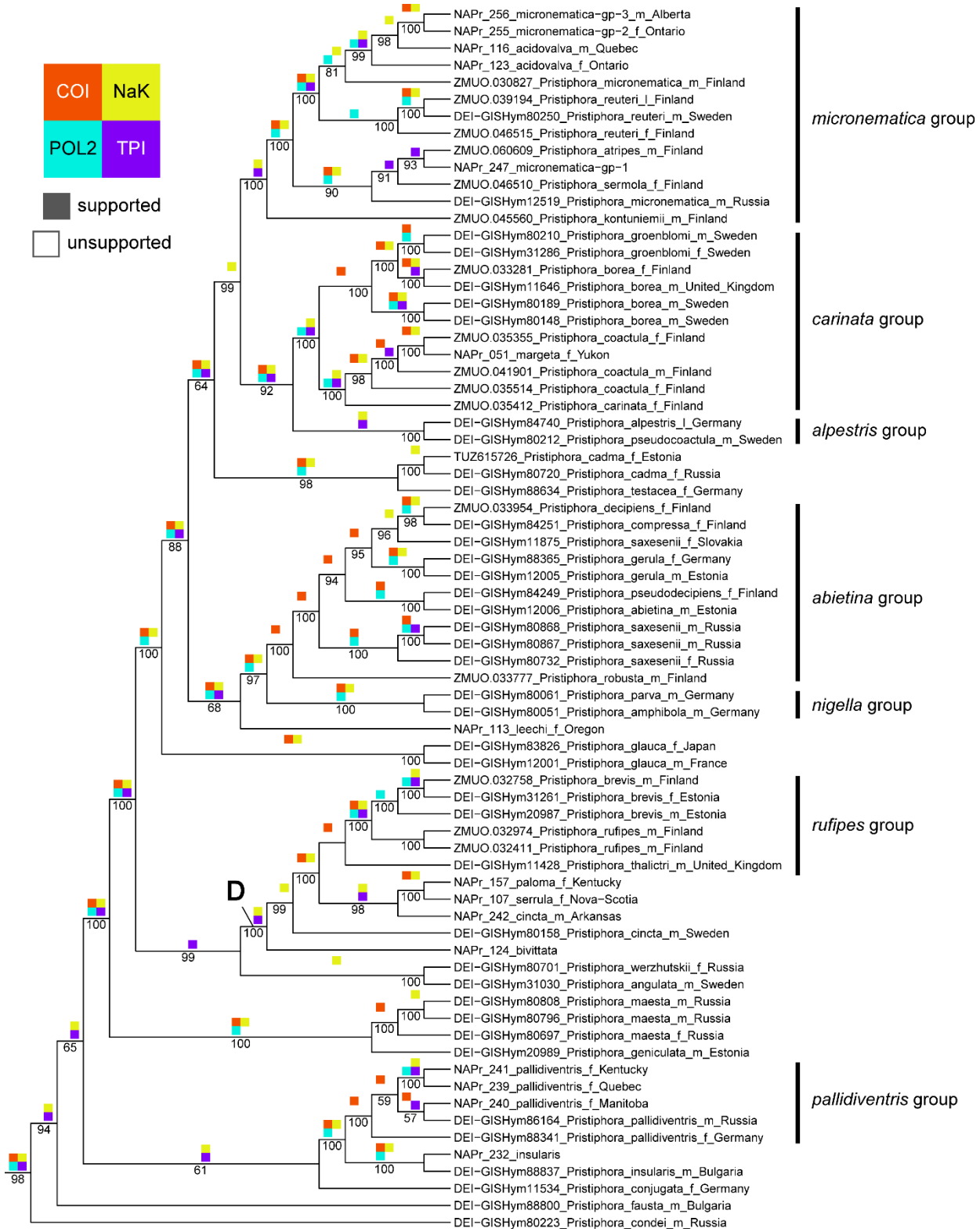

Figure 3. Part of the maximum likelihood tree shown in Fig. 1. Boxes above branches indicate topological concordance between the multi-locus and single-locus trees. Numbers below ingroup branches indicate

ultrafast bootstrap support values based on 1000 replicates. Recognized species groups are listed to the right of tip labels. Clade 'D' is discussed in the text.

Dated phylogeny and biogeographic analysis

The results of the Bayesian analysis are in Figs. 4 & 5. The ML and Bayesian trees are broadly in agreement. The Bayesian tree had more strongly supported branches overall, with the least-supported branches receiving low support in both analyses. The Bayesian analysis found much higher support for the monophyly of *Pristiphora* (PP = 0.98), along with a few other differences from the ML tree: the *P. litura* group was recovered as sister to Clade C, replicating the same relationship between these taxa as observed by Prous et al. (2014), albeit with moderately low support; two of the unnamed Russian species swapped places with *P. chlorea* (Norton) in their clade within the *P. depressa* group; there were several rearrangements within the subgroups of the *P. ruficornis* group (mainly involving branches that were poorly supported in both analyses), but the subgroups themselves and their relationships to one another were strongly supported in both cases; finally, the placement of *P. glauca* Benson relative to nearby clades differed between the two trees, although its placement is poorly supported in the Bayesian tree.

According to the dated analysis, the most recent common ancestor (MRCA) of *Pristiphora* arose in the Early Cretaceous (110.2 Ma, 95% highest probability density [HPD] 31.3–222.2 Ma), while the MRCA of Clade A (i.e. the largest clade that excludes the former genera *Pristola*, *Melastola*, *Neopareophora*, and *Nepionema*) arose in the Late Cretaceous (94.8 Ma, 95% HPD 33.5–189.8 Ma). The MRCA of Clade C arose in the Paleocene (64.4 Ma, 95% HPD 18.6–136.2 Ma), while those of the *P. litura* and *P. macnabi* groups arose in the Middle Eocene (respectively: 43.1 Ma, 95% HPD 11.1–93.8 Ma; 41.8 Ma, 95% HPD 7.7–92.2 Ma). All of the major clades of *Pristiphora* were extant by the Late Eocene to very early Oligocene (ca. 33–40 Ma): the MRCA of the *ruficornis* group was dated to 50.3 Ma (95% HPD 16.1–102.4 Ma), the

carinata group to 33.3 Ma (95% HPD 11.3–65.0 Ma), the *micronematica* group to 33.0 Ma (95% HPD 11.6–65.3 Ma), and Clade D to 36.5 Ma (95% HPD 11.6–74.5 Ma).

From the results of the DEC analysis, early nodes show a consistent pattern for ancestral range reconstructions, with a 50-60% probability of a Palaearctic range, and 20-25% each for Nearctic and Holarctic ranges. The tendency for ancestral ranges to skew towards the Palaearctic may reflect the better-sampled Palaearctic fauna rather than actual biogeographic history. Given the mainly Nearctic range of the *litura* and *macnabi* groups, and the Holarctic range of *P. mollis* and the *laricis* group – together representing the three earliest-diverging lineages of *Pristiphora* – it seems likely that the ancestral range of the genus was either Nearctic or Holarctic.

Early diverging branches of the tree tended to produce clades with more homogenous distributions; for example the entirely Palaearctic *depressa* and *malaisei* groups are separated from their closest Holarctic and Nearctic relatives by at least 55 Ma. On the other hand, clades that arose more recently – i.e. in the Oligocene or Miocene, such as the *ruficornis, alpestris, carinata,* and *micronematica* groups – tended to have more heterogeneous distributions, with Holarctic, Palaearctic, and Nearctic species intermingled with one another. The DEC analysis estimated 97 dispersal events, mostly associated with Holarctic lineages. All dispersals were inferred to have occurred in the same direction, from the Palaearctic to the Nearctic. The age of these dispersals ranges from the Middle Cretaceous (ca. 100 Ma) to the end of the Pliocene (ca. 2.6 Ma).

Figure 4. (Following page.) Maximum clade credibility tree resulting from Bayesian analysis of the multi-locus dataset with BEAST. The tree has been pruned to show only the ingroup. Numbers above branches are posterior probabilities for the corresponding clades (not shown if PP = 1). Pie charts indicate ancestral geographic ranges inferred under the DEC model in BioGeoBEARS using RASP. Present-day distributions are indicated at the tips. Red branches indicate rate accelerations inferred by MEDUSA analysis. The shaded, unannotated portion of the tree is shown in Fig. 5. Clades labeled ‘A’ to ‘C’ are discussed in the text. Pal = Paleocene; Eo = Eocene; Ol = Oligocene; Mio = Miocene; Pli = Pliocene; Ple = Pleistocene.

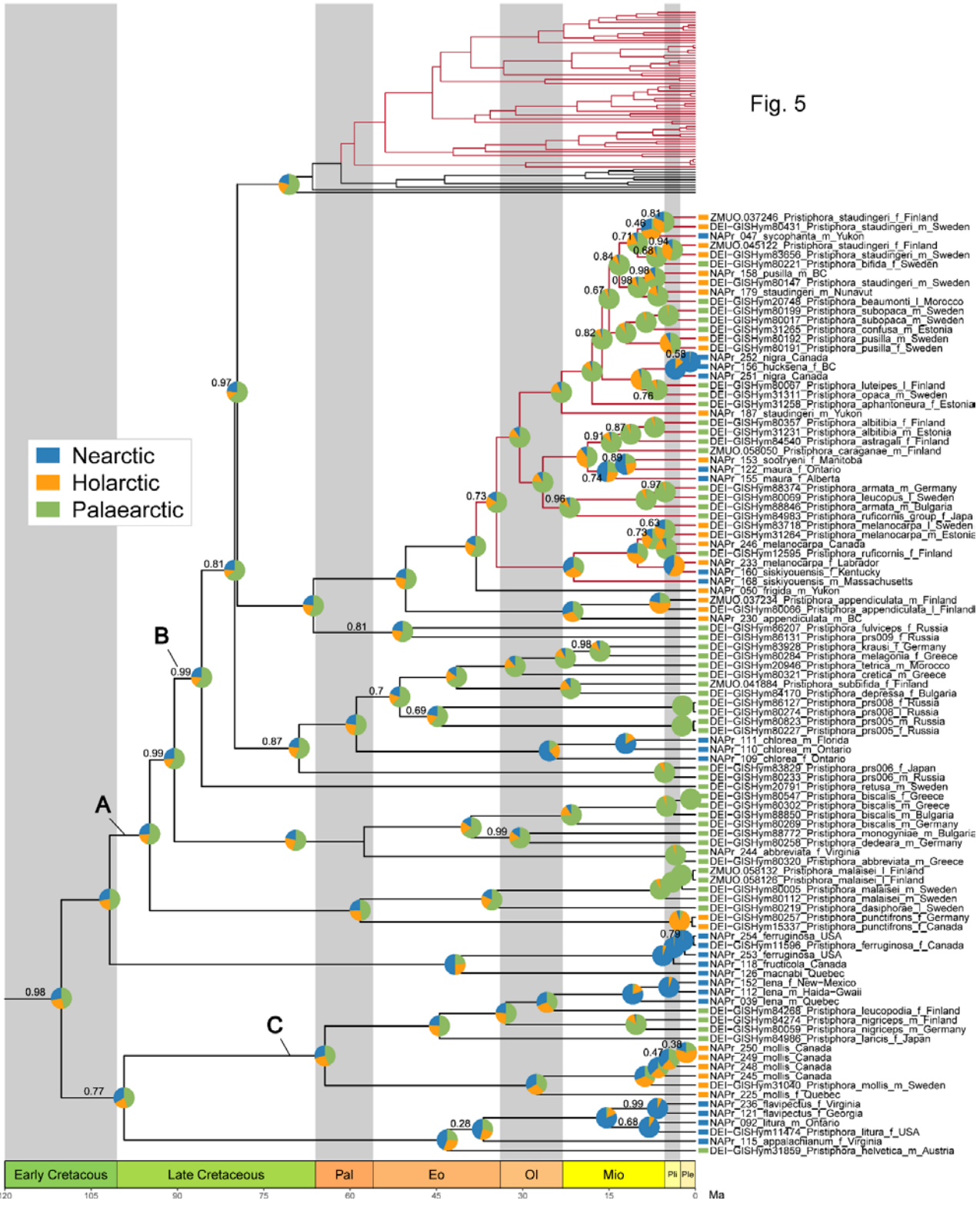
Fig. 5
Nearctic
Holarctic
Palaearctic
A
B
C
Early Cretaceous
Late Cretaceous
Pal
Eo
Ol
Mio
Pli
Ple
120
105
90
75
60
45
30
15
0
Ma

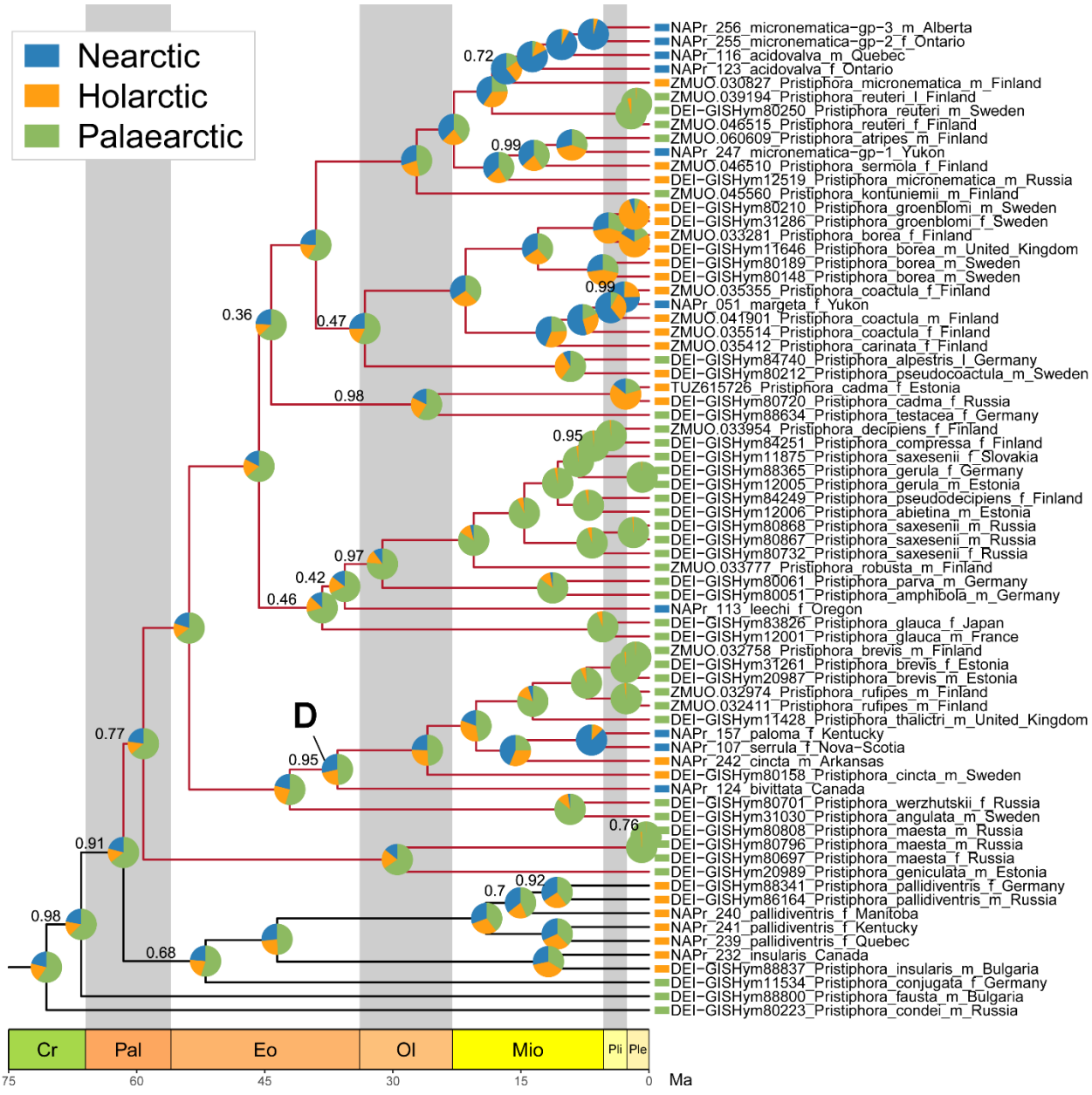

Figure 5. Part of the maximum clade credibility tree shown in Fig. 4. Numbers above branches are posterior probabilities for the corresponding clades (not shown if PP = 1). Pie charts indicate ancestral geographic ranges inferred under the DEC model in BioGeoBEARS using RASP. Present-day distributions are indicated at the tips. Red branches indicate rate accelerations inferred by MEDUSA analysis. Present-day distributions are indicated at the tips. Clade 'D' is discussed in the text. Pal = Paleocene; Eo = Eocene; Ol = Oligocene; Mio = Miocene; Pli = Pliocene; Ple = Pleistocene.

Diversification through time

The lineage-through-time plot for the dated *Pristiphora* subtree shows a modest increase in diversification rates beginning at approximately 16 Ma (Fig. 6), with a significant gamma value ($\gamma = 1.99$, $p = 0.047$). The LTT curve indicates a reduction in lineage accumulation from ca. 30 to 17 Ma (Late Oligocene through Early Miocene), followed by the observed acceleration in the Middle Miocene onwards. Analysis with MEDUSA identified two significant increases in diversification rate, which are highlighted on the trees in Figs. 4–6. The corresponding nodes have estimated ages in the End Eocene (34.5 Ma, 95% HPD 12.5–68.9 Ma; a clade comprising most of the *ruficornis* group) and 59.2 Ma, 95% HPD 22.99–117.6 Ma; a large clade containing the *rufipes*, *carinata*, *alpestris*, *micronematica* groups and related species). Note that MEDUSA assumes high turnover rates, and thus places shifts at stem nodes (Alfaro et al. 2009); this can be interpreted either as a rate acceleration at the stem node with extinction having eliminated some tips, or as a radiation near the tips.

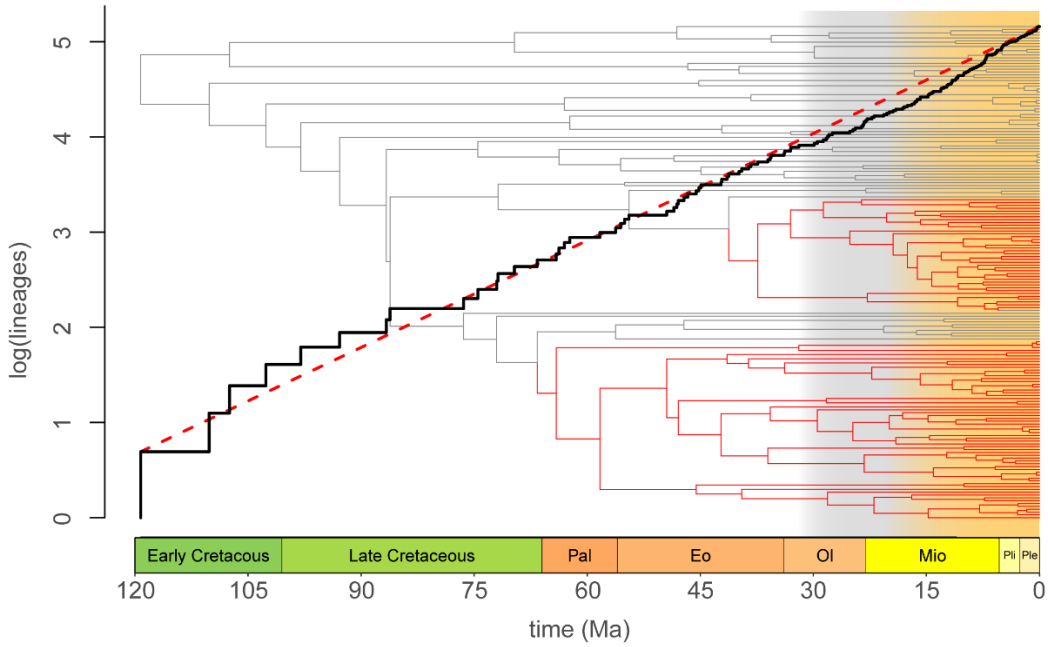

Figure 6. Semilogarithmic lineage-through-time (LTT) plot of maximum clade credibility tree inferred through Bayesian analysis with BEAST (outgroup pruned), which is shown in the background. The dashed red line represents diversification under a pure-birth model. The plotted curve has a significant gamma value (γ = 1.99, p = 0.047) indicating an increase in diversification rate, which can be seen from ca. 17 Ma to present (orange-shaded area), preceded by a slight decrease ca. 30 to 17 Ma (grey shaded area). Red branches on the background tree indicate rate accelerations inferred by MEDUSA analysis. Pal = Paleocene; Eo = Eocene; Ol = Oligocene; Mio = Miocene; Pli = Pliocene; Ple = Pleistocene.

Discussion

Phylogeny and classification

The results presented here include the most comprehensive phylogeny of *Pristiphora* yet inferred, in terms of the number of species sampled and their geographic coverage. The results indicate general agreement across analyses in terms of recovered clades and provide additional support for previously proposed species groups. In addition, there appears to be justification for expanding the boundaries of certain species groups: the *malaisei* group forms a clade with *P. punctifrons* (Thomson) (sister to the former), the *pallidiventris* group forms a clade with *P. insularis* (sister to the former), and the *rufipes* group is nested within Clade D. Another species

group might reasonably be raised for the clade that includes *P. abbreviata* (Hartig), *P. biscalis* (Förster), *P. dedeara* (Liston & Prous), and *P. monogyniae* (Hartig), as it received strong support and represents an early-diverging branch off the *Pristiphora* tree, although this should be done with support from morphological evidence (these Palaearctic species were not examined in the course of this study). Relatively low support for the monophyly of *Pristiphora* in the ML analysis might indicate that the genus' boundaries should be revisited, ideally with evidence from a more extensive data set. The monophyly and placement of the *litura* and *macnabi* groups is interesting in that it is consistent with their former status as small genera closely related to *Pristiphora* (they are also morphologically quite distinct; Wong 1968, Smith 1994, Prous et al. 2014). These groups were synonymized under *Pristiphora* partly due to their ambiguous relationship to what is here called Clade C (Prous et al. 2014), but in this and the last study by Prous et al. (2017), all three clades were unambiguously monophyletic – although whether or not the *litura* group and Clade C are sister taxa remains unclear. A more desirable arrangement might be to promote Clade C to the genus level – resurrecting the genus group name *Oligonematus* Zhelochovtsev, 1988 – and to resurrect *Neopareophora* (= *Nepionema*) and *Pristola* (= *Melastola*) as genera (see Chapter 2), in which case the evidence should weighed for redefining *Pristiphora* as synonymous with either Clade A or Clade B (the latter requiring the erection of perhaps four more genera). Neither clade received strong support in the ML analysis, but Clade B is apparently supported by morphological evidence in the form of a (re-acquired) well-defined prepectus and velum on the protibial spur (see Chapter 2).

Historical biogeography

The historical biogeography of *Pristiphora* appears to defy simple explanation. Consistent with earlier studies (Wong 1960, Prous et al. 2017), the results presented here show that the

distributions of species in this genus are the product of perhaps dozens of dispersals between the Palaearctic and the Nearctic, over the course of more than 100 million years. The fact that these insects have been so geographically mobile likely has much to do with their status as cool-adapted insects (Marlatt 1896, Wong 1960, Rosner and Führer 1996, Humble 2006), allowing them to have crossed high-latitude land bridges at various points in the past, even when these routes may have been inhospitable to most other taxa (e.g. Hines 2008, Praz et al. 2008, Praz and Packer 2014, Trunz et al. 2016).

The most selective of these routes was likely the North Atlantic Land Bridge (NALB; actually two routes, the De Geer and Thulean routes; Brikiatis 2014), which maintained connections between North America and Eurasia until as recently as ca. 56 Ma (Brikiatis 2014). Ancestors of the *macnabi* group and *P. chlorea* may have used this route at some point, separating them from their closest Palaearctic relatives and giving rise to these well-differentiated lineages. The *laricis* group might have done the same thing in the opposite direction, with the Nearctic members of this group being the result of a much-later back-dispersal sometime during the late Oligocene or Miocene.

Most of the dispersals, however, are likely to have occurred via the Bering Land Bridge (BLB), which has been exposed for most of the last 50-60 million years, and intermittently before that time (Hopkins 1967, Sanmartín et al. 2001, Brikiatis 2014). Holarctic and mixed Nearctic/Palaearctic groups of *Pristiphora* probably achieved their distributions through extensive use of the BLB. In some cases these appear to have been previously Nearctic or Palaearctic groups that, during episodes of past connection, dispersed from one landmass to the other; e.g. *P. mollis* may have crossed the BLB ca. 8.7 Ma during a period of low sea level (Hopkins 1959, Sanmartín et al. 2001, Ehlers and Gibbard 2007), giving rise to a Eurasian

lineage nested among Nearctic ones (Clade B, Fig. 4). Many such dispersals seem to have taken place in the Miocene or later –especially during the Pliocene, when the BLB was at its widest – such as those seen among species in the *ruficornis*, *pallidiventris*, *carinata*, *alpestris*, and *micronematica* groups. It is difficult to say whether these dispersals have played a significant role in the diversification of the genus, particularly because so many Holarctic species seem to have remained conspecific despite their separation, based upon both morphological and molecular evidence (Prous et al. 2017). On the other hand, there may be considerable genetic diversity within many of these Holarctic species (see Chapter 4, for example), which might indicate ongoing diversification.

The present analysis does not include any of the nine neotropical species of *Pristiphora* due to a lack of sequence data, although their relation to the Nearctic fauna and timing of arrival in the neotropics is a question of interest for future research. Specifically, if *Pristiphora* is considered a cool-adapted taxon, how and when did it cross the Isthmus of Panama? At least some of the neotropical species have morphological characters in common with *P. chlorea* (pers. obs.; Smith 2003), which is found as far south as Texas and feeds on *Quercus*. In the dated phylogeny (Fig. 4), *P. chlorea* diverged from its Palaearctic relatives in the Paleocene, approximately 58.9 Ma, but would likely not have had the opportunity to disperse to South America until much more recently – i.e. ca. 3.5 Ma onward (Coates and Stallard 2013). Given that most of the neotropical species are known only from relatively moist environments at higher elevations (>1000m; Smith 2003), it is likely that they reached Central and South America during a period of cooler climate during the Pleistocene (Hines 2008, Graham 2018).

Tempo and mode of diversification

One of the predictions of the HLSM hypothesis is that lineages should accumulate primarily in sympatry (i.e. within either North America or Eurasia) resulting from expansion and contraction of ecosystems across large geographic regions. Although this was not directly tested, it does appear to have been the case for some clades of *Pristiphora* and not others; early-diverging clades, in particular, appear to have a greater tendency to have diversified within their respective regions (Figs. 4 & 5). On the other hand, dispersal between landmasses has apparently been much more important for some of the more recently diverged groups, especially the *ruficornis*, *carinata*, and *micronematica* groups. Incidentally, these are also the most diverse species groups in the genus, being found primarily at high latitudes, and including the majority of the representatives of clades for which rate shifts were inferred (Figs. 4–6). In other words, the groups exhibiting the greatest diversification seem to exhibit a contradictory biogeographic pattern to that predicted by the HLSM hypothesis.

A second prediction is that lineages should accumulate more rapidly during periods of climatic oscillations – e.g. during the Oligocene. Although *Pristiphora* did show some evidence of accelerated diversification rates, this was dated to the Miocene roughly corresponding with the cooling that followed the Middle Miocene Climatic Optimum (ca. 15 Ma onwards; Mudelsee et al. 2014). In fact, although there were oscillating cold and warm intervals in the Early Miocene (ca. 23 to 17.5 Ma; Mudelsee et al. 2014, Levy et al. 2016), *Pristiphora* actually exhibited reduced lineage accumulation during that time. Instead, it seems the genus underwent diversification primarily alongside the expansion and establishment of cool-temperate, boreal, and arctic/subarctic biotas across high latitudes in the Northern Hemisphere (Pound et al. 2012). However, this acceleration was probably modest (Fig. 6), and the accumulation of diversity in

Pristiphora is perhaps better characterized as slow and gradual. Thus, a better explanation for its unusual diversity gradient may simply be temperate conservatism (Pyron and Burbrink 2009, Corser et al. 2014). That is: through a combination of historical biogeography and phylogenetic niche conservation, *Pristiphora* (and perhaps the other Nematinae) have simply had more time to accumulate lineages at high latitudes compared to most other taxa.

Conclusions

This study outlines a complex biogeographic history for the genus *Pristiphora*, characterized by a high degree of mobility between the Nearctic and Palaearctic regions. While there is no particularly strong evidence in support of the HLSM applying to *Pristiphora*, the most diverse, high-latitude species groups have apparently increased their rate of diversification alongside the expansion and establishment of cool temperate and cold boreal biotas in the Northern Hemisphere, exhibiting slightly accelerated diversification over the last 15 Myr especially. The phylogenetic analyses additionally provide support for further changes to the classification of *Pristiphora*, including potentially resurrecting the genera *Oligonematus*, *Neopareophora*, and *Pristola* as genera, and re-defining *Pristiphora* as a more restrictive taxon.

References

Alfaro ME, Santini F, Brock C, Alamillo H, Dornburg A, Rabosky DL, Carnevale G, Harmon LJ (2009) Nine exceptional radiations plus high turnover explain species diversity in jawed vertebrates. Proceedings of the National Academy of Sciences 106: 13410–13414. doi: 10.1073/pnas.0811087106

Archibald SB, Rasnitsyn AP, Brothers DJ, Mathewes RW (2018) Modernisation of the Hymenoptera: Ants, bees, wasps, and sawflies of the early Eocene Okanagan Highlands of

western North America. Canadian Entomologist 150: 205–257. doi: 10.4039/tce.2017.59

Arcones A, Ponti R, Ferrer X, Vieites DR (2021) Pleistocene glacial cycles as drivers of allopatric differentiation in Arctic shorebirds. Journal of Biogeography 48: 747–759. doi: 10.1111/jbi.14023

Avise JC, Walker DE (1998) Pleistocene phylogeographic effects on avian populations and the speciation process. Proceedings of the Royal Society B: Biological Sciences 265: 457–463. doi: 10.1142/9789814350709_0006

Bouckaert R, Drummond AJ (2017) bModelTest: Bayesian phylogenetic site model averaging and model comparison. BMC Evolutionary Biology 17: 42. doi: 10.1186/s12862-017-0890-6

Bouckaert R, Vaughan TG, Barido-Sottani J, Duchêne S, Fourment M, Gavryushkina A, Heled J, Jones G, Kühnert D, De Maio N, Matschiner M, Mendes FK, Müller NF, Ogilvie HA, du Plessis L, Popinga A, Rambaut A, Rasmussen D, Siveroni I, Suchard MA, Wu C-H, Xie D, Zhang C, Stadler T, Drummond AJ (2019) BEAST 2.5: An advanced software platform for Bayesian evolutionary analysis Pertea M (Ed). PLOS Computational Biology 15: e1006650. doi: 10.1371/journal.pcbi.1006650

Brikiatis L (2014) The De Geer, Thulean and Beringia routes: key concepts for understanding early Cenozoic biogeography Ali J (Ed). Journal of Biogeography 41: 1036–1054. doi: 10.1111/jbi.12310

Brues CT (1908) New phytophagous Hymenoptera from the Tertiary of Florissant, Colorado. Bulletin of the Museum of Comparative Zoology 51: 259–276.

Carisio L, Cervella P, Palestrini C, DelPero M, Rolando A (2004) Biogeographical patterns of genetic differentiation in dung beetles of the genus *Trypocopris* (Coleoptera, Geotrupidae) inferred from mtDNA and AFLP analyses. Journal of Biogeography 31: 1149–1162. doi: 10.1111/j.1365-2699.2004.01074.x

Chernomor O, von Haeseler A, Minh BQ (2016) Terrace Aware Data Structure for Phylogenomic Inference from Supermatrices. Systematic Biology 65: 997–1008. doi: 10.1093/sysbio/syw037

Clarke A, Crame JA (2010) Evolutionary dynamics at high latitudes: Speciation and extinction in polar marine faunas. Philosophical Transactions of the Royal Society B: Biological Sciences 365: 3655–3666. doi: 10.1098/rstb.2010.0270

Coates AG, Stallard RF (2013) How old is the Isthmus of Panama? Bulletin of Marine Science 89: 801–813. doi: 10.5343/bms.2012.1076

Cockerell TDA (1906) Fossil Saw-flies from Florissant Colorado. Bulletin of the American Museum of Natural History 22: 499–501.

Cockerell TDA (1915) Miocene fossil insects. Proceedings of the Academy of Natural Sciences of Philadelphia 66: 634–648.

Cockerell TDA (1927) Hymenoptera and a Caddis Larva from the Miocene of Colorado. The Annals and Magazine of Natural History, including Zoology, Botany, and Geology 20: 429–435.

Conroy CJ, Cook JA (2000) Molecular systematics of a Holarctic rodent (*Microtus*: Muridae). Journal of Mammalogy 81: 344–359. doi: 10.1644/1545-

1542(2000)081<0344:MSOAHR>2.0.CO;2

Corser JD, White EL, Schlesinger MD (2014) Odonata origins, biogeography, and diversification in an Eastern North American hotspot: Multiple pathways to high temperate forest insect diversity. Insect Conservation and Diversity 7: 393–404. doi: 10.1111/icad.12065

DeChaine EG (2008) A bridge or a barrier? Beringia's influence on the distribution and diversity of tundra plants. Plant Ecology & Diversity 1: 197–207. doi: 10.1080/17550870802328660

Dynesius M, Jansson R (2000) Evolutionary consequences of changes in species' geographical distributions driven by Milankovitch climate oscillations. Proceedings of the National Academy of Sciences 97: 9115–9120. doi: 10.1073/pnas.97.16.9115

Ehlers J, Gibbard PL (2007) The extent and chronology of Cenozoic Global Glaciation. Quaternary International 164–165: 6–20. doi: 10.1016/j.quaint.2006.10.008

Esselstyn JA, Timm RM, Brown RM (2009) Do geological or climatic processes drive speciation in dynamic archipelagos? The tempo and mode of diversification in southeast asian shrews. Evolution 63: 2595–2610. doi: 10.1111/j.1558-5646.2009.00743.x

Evanoff E, McIntosh WC, Murphey PC (2001) Denver Museum of Nature & Science Stratigraphic summary and 40Ar/39Ar geochronology of the Florissant Formation, Colorado. Evanoff Emmett, Gregory-Wodzicki KM, Johnson KR (Eds). Proceedings of the Denver Museum of Nature & Science.

Fletcher NK, Acevedo P, Herman JS, Paupério J, Alves PC, Searle JB (2019) Glacial cycles drive rapid divergence of cryptic field vole species. Ecology and Evolution 9: 14101–

14113. doi: 10.1002/ece3.5846

García-Vázquez D, Bilton DT, Foster GN, Ribera I (2017) Pleistocene range shifts, refugia and the origin of widespread species in western Palaearctic water beetles. Molecular Phylogenetics and Evolution 114: 122–136. doi: 10.1016/j.ympev.2017.06.007

Gearty W (2022) deeptime: Plotting Tools for Anyone Working in Deep Time. Available from: https://cran.r-project.org/package=deeptime.

Ghalambor CK (2006) Are mountain passes higher in the tropics? janzen's hypothesis revisited. Integrative and Comparative Biology 46: 5–17. doi: 10.1093/icb/icj003

Goulet H (1992) The Insects and Arachnids of Canada, Part 20 The Genera and Subgenera of Sawflies of Canada and Alaska: Hymenoptera: Symphyta. 1–235 pp. Available from: http://esc-sec.ca/aafcmonographs/insects_and_arachnids_part_20.pdf.

Goulet H, Bennett AMR (2021) Checklist of the sawflies (Hymenoptera) of Canada, Alaska and Greenland. Journal of Hymenoptera Research 82: 21–67. doi: 10.3897/JHR.82.60057

Graham A (2018) Land Bridges: Ancient Environments, Plant Migrations, and New World Connections. University of Chicago Press, 310 pp.

Hall JPW (2005) Montane speciation patterns in *Ithomiola* butterflies (Lepidoptera: Riodinidae): Are they consistently moving up in the world? Proceedings of the Royal Society B: Biological Sciences 272: 2457–2466. doi: 10.1098/rspb.2005.3254

Harington CR (2005) The eastern limit of Beringia: Mammoth Remains from Banks and Melville Islands, Northwest Territories. Arctic 58: 361–369. doi: 10.2307/40513103

Heath TA, Huelsenbeck JP, Stadler T (2014) The fossilized birth-death process for coherent

calibration of divergence-time estimates. Proceedings of the National Academy of Sciences of the United States of America 111. doi: 10.1073/pnas.1319091111

Hebert PDN, Ratnasingham S, deWaard JR (2003) Barcoding animal life: cytochrome c oxidase subunit 1 divergences among closely related species. Proceedings. Biological sciences / The Royal Society 270 Suppl: S96–S99. doi: 10.1098/rsbl.2003.0025

Hewitt GM (2011) Quaternary phylogeography: The roots of hybrid zones. Genetica 139: 617–638. doi: 10.1007/s10709-011-9547-3

Hillebrand H (2004) On the Generality of the Latitudinal Diversity Gradient. The American Naturalist 163: 192–211. doi: 10.1086/381004

Hines HM (2008) Historical biogeography, divergence times, and diversification patterns of bumble bees (Hymenoptera: Apidae: *Bombus*). Systematic Biology 57: 58–75. doi: 10.1080/10635150801898912

Hoang DT, Chernomor O, von Haeseler A, Minh BQ, Vinh LS (2018) UFBoot2: Improving the Ultrafast Bootstrap Approximation. Molecular Biology and Evolution 35: 518–522. doi: 10.1093/molbev/msx281

Hopkins DM (1959) Cenozoic History of the Bering Land Bridge. Science 119: 1519–1528. doi: 10.1038/098448b0

Hopkins DM (1967) The Bering Land Bridge. Stanford University Press, Stanford, California, xiii, 495 pp.

Hultén E (1937) Outline of the History of Arctic and Boreal Biota during the Quaternary Period. In: Lomolino M V., Sax DF, Brown JH (Eds), Foundations of Biogeography: Classic Papers

with Commentaries. University of Chicago Press, Chicago, 464–512.

Humble LM (2006) Overwintering adaptations in Arctic sawflies (Hymenoptera: Tenthredinidae) and their parasitoids: Cold tolerance. Canadian Entomologist 138: 59–71. doi: 10.4039/N05-804

Johnson NK, Cicero C (2004) New mitochondrial DNA data affirm the importance of pleistocene speciation in North American birds. Evolution 58: 1122–1130. doi: 10.1111/j.0014-3820.2004.tb00445.x

Kalyaanamoorthy S, Minh BQ, Wong TKF, von Haeseler A, Jermiin LS (2017) ModelFinder: fast model selection for accurate phylogenetic estimates. Nature Methods 14: 587–589. doi: 10.1038/nmeth.4285

Kouki J (1999) Latitudinal Gradients in Species Richness in Northern Areas: Some Exceptional Patterns. Ecological Bulletins: 30–37. Available from: http://www.jstor.org/stable/20113224.

Kouki J, Niemela P, Viitasaari M (1994) Reversed latitudinal gradient in species richness of sawflies (Hymenoptera, Symphyta). Ann. Zool. Fennici 31: 83–88.

Kozak KH, Wiens JJ (2006) Does niche conservatism promote speciation? A case study in North American salamanders. Evolution 60: 2604–2621.

Levy R, Harwood D, Florindo F, Sangiorgi F, Tripati R, von Eynatten H, Gasson E, Kuhn G, Tripati A, DeConto R, Fielding C, Field B, Golledge N, McKay R, Naish T, Olney M, Pollard D, Schouten S, Talarico F, Warny S, Willmott V, Acton G, Panter K, Paulsen T, Taviani M (2016) Paleoceanography of the east equatorial Pacific over the past 16 Myr and

Pacific–Atlantic comparison: High resolution benthic foraminiferal δ18O and δ13C records at IODP Site U1337. Proceedings of the National Academy of Sciences 113: 3453–3458. doi: 10.1073/pnas.1516030113

Marlatt CL (1896) Revision of the Nematinae of North America. Bulletin of the United States Department of Agriculture, Division of Entomology, Technical Series 3: 1–135. Available from: http://www.biodiversitylibrary.org/item/106469.

Matzke NJ (2013) BioGeoBEARS: BioGeography with Bayesian (and likelihood) evolutionary analysis in R Scripts.

Meseguer AS, Lobo JM, Ree R, Beerling DJ, Sanmartín I (2015) Integrating fossils, phylogenies, and niche models into biogeography to reveal ancient evolutionary history: The case of Hypericum (Hypericaceae). Systematic Biology 64: 215–232. doi: 10.1093/sysbio/syu088

Minh BQ, Hahn MW, Lanfear R (2020) New Methods to Calculate Concordance Factors for Phylogenomic Datasets Rosenberg M (Ed). Molecular Biology and Evolution 37: 2727–2733. doi: 10.1093/molbev/msaa106

Minh BQ, Nguyen MAT, von Haeseler A (2013) Ultrafast Approximation for Phylogenetic Bootstrap. Molecular Biology and Evolution 30: 1188–1195. doi: 10.1093/molbev/mst024

Minh BQ, Schmidt HA, Chernomor O, Schrempf D, Woodhams MD, von Haeseler A, Lanfear R (2020) IQ-TREE 2: New Models and Efficient Methods for Phylogenetic Inference in the Genomic Era Teeling E (Ed). Molecular Biology and Evolution 37: 1530–1534. doi: 10.1093/molbev/msaa015

Mudelsee M, Bickert T, Lear CH, Lohmann G (2014) Cenozoic climate changes: A review based on time series analysis of marine benthic δ18O records. Reviews of Geophysics 52: 333–374. doi: 10.1002/2013RG000440.Received

Nyman T, Farrell BD, Zinovjev AG, Vikberg V (2006) Larval habits, host-plant associations, and speciation in nematine sawflies (Hymenoptera: Tenthredinidae). Evolution 60: 1622–1637. doi: 10.1111/j.0014-3820.2006.tb00507.x

Nyman T, Vikberg V, Smith DR, Boevé J-L (2010) How common is ecological speciation in plant-feeding insects? A “Higher” Nematinae perspective. BMC evolutionary biology 10: 266.

Nyman T, Widmer A, Roininen H (2000) Evolution of gall morphology and host-plant relationships in willow-feeding sawflies (Hymenoptera: Tenthredinidae). Evolution 54: 526–533. doi: 10.1111/j.0014-3820.2000.tb00055.x

Nyman T, Zinovjev AG, Vikberg V, Farrell BD (2006) Molecular phylogeny of the sawfly subfamily Nematinae (Hymenoptera: Tenthredinidae). Systematic Entomology 31: 569–583. doi: 10.1111/j.1365-3113.2006.00336.x

Pälike H, Norris RD, Herrle JO, Wilson PA, Coxall HK, Lear CH, Shackleton NJ, Tripati AK, Wade BS (2006) The Heartbeat of the Oligocene Climate System. Online 314: 1894–1899. doi: 10.1126/science.1133822

Paradis E, Schliep K (2019) ape 5.0: an environment for modern phylogenetics and evolutionary analyses in R Schwartz R (Ed). Bioinformatics 35: 526–528. doi: 10.1093/bioinformatics/bty633

Pennell MW, Eastman JM, Slater GJ, Brown JW, Uyeda JC, Fitzjohn RG, Alfaro ME, Harmon LJ (2014) geiger v2.0: an expanded suite of methods for fitting macroevolutionary models to phylogenetic trees. Bioinformatics 30: 2216–2218.

Pound MJ, Haywood AM, Salzmann U, Riding JB (2012) Global vegetation dynamics and latitudinal temperature gradients during the Mid to Late Miocene (15.97-5.33Ma). Earth-Science Reviews 112: 1–22. doi: 10.1016/j.earscirev.2012.02.005

Praz CJ, Müller A, Danforth BN, Griswold TL, Widmer A, Dorn S (2008) Molecular Phylogenetics and Evolution Phylogeny and biogeography of bees of the tribe Osmiini (Hymenoptera: Megachilidae). Molecular Phylogenetics and Evolution 49: 185–197. doi: 10.1016/j.ympev.2008.07.005

Praz CJ, Packer L (2014) Molecular Phylogenetics and Evolution Phylogenetic position of the bee genera *Ancyla* and *Tarsalia* (Hymenoptera: Apidae): A remarkable base compositional bias and an early Paleogene geodispersal from North America to the Old World. Molecular Phylogenetics and Evolution 81: 258–270. doi: 10.1016/j.ympev.2014.09.003

Prous M, Blank SM, Goulet H, Heibo E, Liston A, Malm T, Nyman T, Schmidt S, Smith DR, Vårdal H, Viitasaari M, Vikberg V, Taeger A (2014) The genera of Nematinae (Hymenoptera, Tenthredinidae). Journal of Hymenoptera Research 40: 1–69. doi: 10.3897/JHR.40.7442

Prous M, Kramp K, Vikberg V, Liston A (2017) North-Western Palaearctic species of *Pristiphora* (Hymenoptera, Tenthredinidae). Journal of Hymenoptera Research 59: 1–190. doi: 10.3897/jhr.59.12656

Prous M, Liston A, Kramp K, Savina H, Vårdal H, Taeger A (2019) The West Palaearctic genera

of Nematinae (Hymenoptera, Tenthredinidae). ZooKeys 875: 63–127. doi: 10.3897/zookeys.875.35748

Prous M, Vikberg V, Liston A, Kramp K (2016) North-Western Palaearctic species of the *Pristiphora ruficornis* group (Hymenoptera, Tenthredinidae). Journal of Hymenoptera Research 51: 1–54. doi: 10.3897/jhr.51.9162

Pybus OG, Harvey PH (2000) Testing macro-evolutionary models using incomplete molecular phylogenies. Proceedings of the Royal Society B: Biological Sciences 267: 2267–2272. doi: 10.1098/rspb.2000.1278

Pyron RA, Burbrink FT (2009) Can the tropical conservatism hypothesis explain temperate species richness patterns? An inverse latitudinal biodiversity gradient in the New World snake tribe Lampropeltini. Global Ecology and Biogeography 18: 406–415. doi: 10.1111/j.1466-8238.2009.00462.x

Rand AL (1948) Glaciation, an isolating factor in speciation. Evolution 2: 314–321.

Ratnasingham S, Hebert PDN (2007) BOLD: The Barcode of Life Data System. Molecular Ecology Notes 7: 355–364. doi: 10.1111/j.1471-8286.2006.01678.x

Ree RH, Sanmartín I (2018) Conceptual and statistical problems with the DEC+J model of founder-event speciation and its comparison with DEC via model selection. Journal of Biogeography 45: 741–749. doi: 10.1111/jbi.13173

Ree RH, Smith SA (2008) Maximum Likelihood Inference of Geographic Range Evolution by Dispersal, Local Extinction, and Cladogenesis Baker A (Ed). Systematic Biology 57: 4–14. doi: 10.1080/10635150701883881

Revell LJ (2012) phytools: An R package for phylogenetic comparative biology (and other things). Methods in Ecology and Evolution 3: 217–223.

Rohwer SA (1908a) On the Tenthredinoidea of the Florissant shales. Bulletin of the American Museum of Natural History 24: 521–530.

Rohwer SA (1908b) The tertiary Tenthredinoidea of the expedition of 1908 to Florissant, Colo. Bulletin of the American Museum of Natural History 24: 591–595.

Roininen H, Nyman T, Zinovjev A (2005) Biology, Ecology, and Evolution of Gall-inducing Sawflies (Hymenoptera: Tenthredinidae and Xyelidae). In: Raman A, Schaefer CW, Withers TM (Eds), Biology, Ecology, and Evolution of Gall-inducing Arthropods. Science Publishers, Inc., Enfield, NH, 467–494.

Rosner S, Führer E (1996) Zur Überwinterungsstrategie der Kleinen Fichtenblattwespe, Pristiphora abietina Christ. (Hym., Tenthredinidae). Journal of Applied Entomology 120: 225–230. doi: 10.1111/j.1439-0418.1996.tb01595.x

Ross HH (1937) A generic classification of the Nearctic sawflies (Hymenoptera, Symphyta). Illinois Biological Monographs 15: 1–173. Available from: https://www.ideals.illinois.edu/browse?value=Ross,+Herbert+Holdsworth,+1908-&type=author.

Ross HH (1972) The Origin of Species Diversity in Ecological Communities. Taxon 21: 253–259.

Ruane S, Bryson RW, Pyron RA, Burbrink FT (2014) Coalescent species delimitation in Milksnakes (Genus *Lampropeltis*) and impacts on phylogenetic comparative analyses.

Systematic Biology 63: 231–250. doi: 10.1093/sysbio/syt099

Rubino E, Leier A, Cassel EJJ, Archibald SBB, Foster-Baril Z, Barbeau DLL (2021) Detrital zircon U–Pb ages and Hf-isotopes from Eocene intermontane basin deposits of the southern Canadian Cordillera. Sedimentary Geology 422: 105969. doi: 10.1016/j.sedgeo.2021.105969

Sánchez-Vialas A, García-París M, Ruiz JL, Recuero E (2020) Patterns of morphological diversification in giant *Berberomeloe* blister beetles (Coleoptera: Meloidae) reveal an unexpected taxonomic diversity concordant with mtDNA phylogenetic structure. Zoological Journal of the Linnean Society 189: 1249–1312. doi: 10.1093/zoolinnean/zlz164

Sanmartín I, Enghoff H, Ronquist F (2001) Patterns of animal dispersal, vicariance and diversification in the Holarctic. Biological Journal of the Linnean Society 73: 345–390. doi: 10.1006/bijl.2001.0542

Schoville SD, Roderick GK, Kavanaugh DH (2012) Testing the “Pleistocene species pump” in alpine habitats: Lineage diversification of flightless ground beetles (Coleoptera: Carabidae: *Nebria*) in relation to altitudinal zonation. Biological Journal of the Linnean Society 107: 95–111. doi: 10.1111/j.1095-8312.2012.01911.x

Shell WA, Rehan SM (2016) Recent and rapid diversification of the small carpenter bees in eastern North America. Biological Journal of the Linnean Society 117: 633–645. doi: 10.1111/bij.12692

Smith DR (1994) *Nepionema*, a nematine sawfly genus new to North America, and an unusual new species of *Nematus* (Hymenoptera: Tenthredinidae). Proceedings of The Entomological Society of Washington 96: 133–138.

Smith DR (2003) A Synopsis of the Sawflies (Hymenoptera: Symphyta) of America South of the United States: Tenthredinidae (Nematinae, Heterarthrinae, Tenthredininae). Transactions of the American Entomological Society 129: 1–45.

Stadler T (2010) Sampling-through-time in birth–death trees. Journal of Theoretical Biology 267: 396–404. doi: 10.1016/j.jtbi.2010.09.010

Taeger A, Liston AD, Prous M, Groll EK, Gehroldt T, Blank SM (2018) ECatSym – Electronic World Catalog of Symphyta (Insecta, Hymenoptera). Available from: https://sdei.de/ecatsym/.

Trunz V, Packer L, Vieu J, Arrigo N, Praz CJ (2016) Comprehensive phylogeny, biogeography and new classification of the diverse bee tribe Megachilini: Can we use DNA barcodes in phylogenies of large genera? Molecular Phylogenetics and Evolution 103: 245–259. doi: 10.1016/j.ympev.2016.07.004

Wallace AR (1878) Tropical Nature, and Other Essays. MacMillan and Co., London, 356 pp. doi: 10.1016/0003-6870(73)90259-7

Wang L-G, Lam TT-Y, Xu S, Dai Z, Zhou L, Feng T, Guo P, Dunn CW, Jones BR, Bradley T, Zhu H, Guan Y, Jiang Y, Yu G (2019) Treeio: An R Package for Phylogenetic Tree Input and Output with Richly Annotated and Associated Data. Molecular Biology and Evolution 37: 599–603. doi: 10.1093/molbev/msz240

Wong HR (1960) Evolution of the sawfly genus *Pristiphora*. Interim Report. Forest Biology Laboratory, Winnipeg, Manitoba, i–v, 1–111 pp.

Wong HR (1968) A revision of the tribe Pristolini (Hymenoptera: Tenthredinidae). The

Canadian Entomologist 100: 1049–1057.

Yu G, Smith DK, Zhu H, Guan Y, Lam TTY (2017) GGTREE: an R Package for Visualization and Annotation of Phylogenetic Trees With Their Covariates and Other Associated Data. Methods in Ecology and Evolution 8: 28–36. doi: 10.1111/2041-210X.12628

Yu Y, Blair C, He X (2020) RASP 4: Ancestral State Reconstruction Tool for Multiple Genes and Characters Yoder A (Ed). Molecular Biology and Evolution 37: 604–606. doi: 10.1093/molbev/msz257

Zachos JC, Dickens GR, Zeebe RE (2008) An early Cenozoic perspective on greenhouse warming and carbon-cycle dynamics. Nature 451: 279–283. doi: 10.1038/nature06588

Zhelochovtsev AN, Zinovjev AG (1988) Keys to the Insects of the European Part of the USSR. Volume III Hymenoptera. Part VI Symphyta. i–xviii; 1–432 pp.

Zhelochovtzev AN, Rasnitsyn AP (1972) On Some Tertiary Sawflies (Hymenoptera, Symphyta) From Colorado. Psyche (New York) 79: 315–327. doi: 10.1155/1972/63630

CHAPTER 4: Collections-based genomics uncovers phylogeographic patterns in the Holarctic sawfly *Pristiphora cincta* Newman

Introduction

The Pleistocene glaciations had enormous impacts on the distribution and diversity of high-latitude taxa. This is especially true in North America, much of which was completely covered by the Laurentide and Cordilleran ice sheets during the Last Glacial Maximum (Hewitt 2004a, Hofreiter and Stewart 2009, Nogués-Bravo et al. 2018). As the ice receded, previously inaccessible regions were recolonized on a continental scale, with the result that present populations of high-latitude species reflect the legacy of these movements (Hewitt 2004a, 2011). The resulting patterns of genetic diversity provide important insights into how these populations arose, helping to understand the processes that give rise to and maintain diversity across Northern North America.

Sawflies in the subfamily Nematinae (Hymenoptera: Tenthredinidae) are a compelling group in which to investigate these patterns, being abundant and diverse throughout the northern-temperate, boreal, and arctic/subarctic parts of North America (Marlatt 1896, D. R. Smith 1979, Goulet 1992, Kouki et al. 1994, Kouki 1999, Nyman et al. 2010). As most of their present range was previously glaciated, they must have persisted in unglaciated refugia to the south of the Laurentide ice sheet, in Beringia, and perhaps in other isolated refugia such as remote unglaciated parts of the High Arctic, and unglaciated nunataks in the Western Cordillera (Shafer et al. 2010, Eidesen et al. 2013). Along what routes they repopulated the northern half of the continent, and from where, remain questions of great interest for understanding patterns of diversity for sawflies in particular and for northern insects in general.

These questions are particularly pressing given that the Arctic is warming at a rate more than double the global average (Richter-Menge et al. 2019) with the consequence that its biotic communities are changing significantly (Koltz et al. 2018, Myers-Smith et al. 2020). As herbivores, sawflies' life histories depend on those of their host plants, such that they are particularly sensitive to changing climate, and may serve as early indicators of an ecosystem's broader response to warming (Brodo 2000, Høye and Sikes 2013). For this reason, an improved understanding of their diversity has potential to better inform conservation efforts in the North, and to better anticipate the responses of northern taxa to future changes.

Pristiphora cincta Newman is a widespread Holarctic species that is abundant across its range. It occurs throughout the northern-temperate, boreal, and arctic/subarctic parts of North America and Eurasia, where it feeds on various species of *Betula* L., *Salix* L., and *Vaccinium* L. (Prous et al. 2017). Its broad host range and distribution make it an ideal candidate for phylogeographic study, not only because it is commonly encountered in samples, but also because any inferences about its population history might be reasonably generalized to many of its more than 220 congeners. These features also make it a good choice to study broader questions about nematine diversity. In particular, a high-latitude speciation machine (HLSM) – as hypothesized by Nyman et al. (2010) and discussed in more detail in Chapter 3 –powered by past periods of oscillating climatic conditions, might explain episodes of diversification during the subfamily's evolutionary past. As ranges contract and expand, populations diverge in isolation and mix upon secondary contact, generating new diversity with each cycle (Ross 1972, Esselstyn et al. 2009). Although intended to explain species diversity for the entire subfamily, the hypothesis can be generalized to lower taxonomic levels over shorter time scales. For a species such as *P. cincta*, one would expect the climatic cycles of the Quaternary period (Hofreiter and Stewart 2009) to

have caused a proliferation of genetic lineages that today occur across the species' distribution. These lineages should be more diverse near the sites of small, isolated refugia – e.g. cryptic refugia in the High Arctic, nunataks in the Cordilleran ice sheet (Hewitt 2004b, Shafer et al. 2010, Eidesen et al. 2013) – but less diverse where refugial populations enjoyed larger, continuous distributions – e.g. Beringia, areas south of the Laurentide ice sheet. As well, one might expect to see relatively high population differentiation simply because different locations may have been recolonized by different genetic lineages purely by chance.

To investigate the phylogeographic history of *P. cincta*, this study leverages a hybridization capture technique called hyRAD (Suchan et al. 2016) to sample museum specimens from across North America, with a particular interest in the North, and with additional representatives from Europe and East Asia. This method makes it possible to obtain high-throughput sequencing data from historical pinned specimens up to one hundred years old. Through a combination of genetic cluster analyses, model-based population history inference, standard population genetics approaches, and phylogenetic analysis, this chapter aims to investigate the phylogeographic history of *P. cincta* (including glacial refugia and routes of postglacial recolonization), and to evaluate whether the observed patterns are consistent with the HLSM hypothesis.

Methods

Specimens and DNA extraction

A total of 860 museum specimens of *P. cincta* were borrowed from the Canadian National Collection of Insects, Ottawa, ON (CNC), and the Smithsonian National Museum of Natural History, Washington, D.C. (USNM). Additional recently collected specimens (i.e. fresh material) – used to prepare RAD probes – were selected from among the USNM material, as well as material borrowed from the Centre for Biodiversity Genomics, Guelph, ON (BIOUG) and the

Lyman Entomological Museum, Montreal, QC (LEMU), or else collected during field trips to Yukon in 2018 and Ontario in 2019. All specimens were databased, and any lacking GPS coordinates were georeferenced using a combination of OpenStreetMap.org, Google Maps, the Canadian Geographical Names Database, and the Biological Survey of Canada's Canadian Locality Database. Specimen records were mapped using QGIS Desktop v3.22.5 (QGIS Development Team 2022). Specimens were selected with the goal of representing discrete portions of the species' full distribution in North America, plus additional representatives from Eurasia. A total of 72 historical specimens (ranging in age from 15 to 93 years old; median age 66 years) and 5 fresh specimens (2 to 10 years old, collected via Malaise trap into ≥95% EtOH and either immediately pinned or stored at -20°C) were selected for DNA extraction (Table B1, Appendix B). Identifications were verified through morphological examination and comparison to material previously studied by H.R. Wong. To avoid haploid males and minimize the risk of identification error, only female specimens with an orange abdominal band were chosen. Closely related species have either a black abdomen (*P. paloma* Wong & Ross), a pair of longitudinal bands (*P. bivittata* Norton), or are similarly coloured (*P. serrula* Wong & Ross). The latter species co-occurs with *P. cincta* in Western North America and is differentiated based on the tarsal claw with a large subapical tooth (small in *P. cincta*) and more strongly produced lateral posterior lobe of valvula 3 (only produced about as high as median carina in *P. cincta*).

Non-destructive DNA extractions were performed using the Zymo Quick-DNA Miniprep Plus Kit (Zymo Research, Irvine, CA). Extractions from historical specimens were performed using sterilized, dedicated equipment and consumables in a laminar flow hood. The equipment and workspace were exposed to UV light for 30 minutes before each laboratory session. As well, prior to DNA extractions, specimens were removed from their pins, placed in microcentrifuge

tubes, and exposed to UV light for 30 minutes to eliminate any exogenous DNA. Specimens were submerged in digestion buffer and placed in a 55°C shaking incubator overnight (12-16 hours). Elution was performed using warmed elution buffer in two rounds, for a final volume of 70 uL. DNA concentrations were quantified using a Qubit 4 Fluorometer (Thermo Fisher Scientific, Waltham, MA). Fresh specimens were subject to the same protocol minus UV sterilization, and extractions were performed after finishing library prep with museum specimens to minimize the risk of cross-contamination.

Library preparation and sequencing

Illumina sequencing libraries were prepared according to the hyRAD method (hybridization capture using RAD probes) developed by Suchan et al. (2016). In this hybridization capture approach, RAD fragments from fresh samples are used as probes to capture homologous fragments from shotgun sequencing libraries that are prepared from museum specimens. The protocol was performed as follows: (i) double-digest RAD libraries were prepared from five fresh samples from across *P. cincta*'s North American distribution (Yukon, Northwest Territories, Oregon, Ontario, and Virginia; Table B1, Appendix B). Narrow peak size selection (centered on 270 bp) was performed on a Pippin Prep system (Sage Science, Beverly, MA) at the London Regional Genomics Centre (London, ON). Size-selected fragments were amplified using indexed PCR primers, then adaptors were removed, and fragments were biotinylated to generate probes. (ii) Shotgun sequencing libraries were prepared from museum samples using the NEBNext Ultra II DNA Library Prep Kit (New England Biolabs, Whitby, ON). Preparations followed the manufacturer's protocol, with optimizations for historical specimens proposed by Sproul and Maddison (2017). Libraries from individual samples were barcoded using dual-index PCR primers (NEBNext Multiplex Oligos for Illumina, New England Biolabs, Whitby, ON) to

allow multiplexing. (iii) Shotgun libraries were pooled in equimolar ratios and captured using the biotinylated RAD probes. Reactions were washed to retain only the hybridization-enriched products. (iv) Captured libraries were reamplified using universal PCR primers and sequenced on a single lane of an Illumina NovaSeq 6000 SP flow cell for 150-bp paired-end reads at The Centre for Advanced Genomics (TCAG; Toronto, ON). Throughout the protocol, samples were quantified via Qubit and their profiles were verified on a Bioanalyzer system at TCAG. The complete protocol is available online (https://skmonckton.com/data/hyRAD-protocol-extraction-to-libraries.html).

Data processing

Because the target sequences are not flanked by restriction enzyme recognition sites, hyRAD datasets cannot be analyzed using standard RADseq bioinformatics pipelines. Instead, a custom pipeline is described here, based on the approach used by Suchan et al. (2016). Briefly: (i) reads from a small number of specimens are aligned to provide a reference assembly; (ii) reads from all specimens are mapped to the reference assembly; (iii) SNPs are called and filtered for information content and quality, then used for downstream analyses.

Reads were demultiplexed by the sequencing facility (TCAG), then cleaned with Trimmomatic (Bolger et al. 2014) using default “gentle” settings (sufficient to remove the lowest quality leading and trailing reads), and finally visually inspected with FastQC (Andrews 2019) and MultiQC (Ewels et al. 2016) to check for any problematic trends or biases in sequence content, quality, or duplication levels.

De novo reference assembly

Eight samples were selected from among those with the greatest number of trimmed reads, from across the full distribution of the species (Yukon, Alberta, Manitoba, Michigan, New Brunswick, Sweden, Korea). *De novo* assembly was performed with MaSuRCA v4.0.3 (Zimin et al. 2013). Assembled contigs were checked for contamination with Kraken v2.1.2 (D. E. Wood et al. 2019) and local BLAST search (Camacho et al. 2009). Contigs classified by Kraken as either *Homo sapiens*, bacteria, or viruses were further investigated via BLAST search within their respective taxa. All contigs were also BLASTed against NCBI's available mitochondrial sequences for Tenthredinoidea, and against all available Apoidea sequences (in case of contamination from bee specimens processed in the same lab space). BLAST hits with E-values below 10^{-100} were individually aligned to the corresponding contigs, and any contigs confirmed to be contaminants were removed from the assembly.

Mapping and SNP calling

Raw reads were mapped to the reference assembly with BWA-MEM v0.7.17 (Li 2013) and marked for PCR duplicates with Picard v2.26.3 (http://broadinstitute.github.io/picard/). Calling of SNPs was performed with GATK v4.2.4.0 (McKenna et al. 2010) using HaplotypeCaller in GVCF mode (GATK Team 2022). Resulting SNPs were filtered to retain only high-quality and informative sites using VCFtools v0.1.16 (Danecek et al. 2011). Only biallelic sites present in all samples, and having a PHRED quality score above 30, a minor allele count above 11, and a minimum read depth of six were kept. For further analyses, the filtered VCF file was converted to BED format using Plink v2.00 (Chang et al. 2015) and to PHYLIP format using PGDSpider v2.1.1.5 (Lischer and Excoffier 2012).

Genetic structure

To investigate population genetic structure, individuals were assigned to eleven groups intended to stand in for populations, defined according to geographic location (Table B1, Appendix B). Genetic structure was investigated using fastStructure v1.0 (Raj et al. 2014), which uses a Bayesian approach to estimate population structure. The analysis was performed for values of *k* from 1 to 10 clusters, and the bundled 'chooseK.py' script was used to select a value of *k* that best explains model complexity. Cluster membership bar plots were generated using the package pophelper v2.3.1 (Francis 2017) in R v4.1.3 (R Core Team 2022). Individuals were also assigned to clusters using discriminant analysis of principal components (DAPC; Jombart et al. 2010) from the R package adegenet v.2.1.5 (Jombart 2008). DAPC transforms population genetic data using principal components analysis, and then identifies genetic clusters using discriminant analysis. The supplied cross-validation function 'xvalDapc' was used to select an appropriate number of principal components, and the value of *k* was chosen as to minimize BIC (Bayesian Information Criterion, a measure of model quality). Pie charts showing DAPC cluster membership for each part of the species' range were plotted on a map using QGIS.

Genetic structure was quantified with the R package hierfstat v0.5-11 (Goudet et al. 2022), which was used to compute overall F_{ST}, pairwise F_{ST} values between locations, and observed heterozygosity for each location. Calculations of F_{ST} follow Nei (1987).

Population history

Population history was inferred using DIYABC-RF v1.2.1 (Collin et al. 2021), which combines approximate Bayesian computation (ABC; Beaumont et al. 2002) and random forest (RF) analysis to permit model choice and parameter estimation for a set of user-defined scenarios. In this approach, the posterior probabilities of models (i.e. scenarios) and their parameters are

estimated based on similarity of summary statistics calculated from observed and simulated data. DIYABC allows the comparison of scenarios with any combination of population divergence events, admixture events, or changes in population size through time (Cornuet et al. 2014, Collin et al. 2021). To lower the computational demand for these analyses, VCFtools was used to generate a random subset of SNPs from the full dataset, sampled at a rate of 3.5%. As well, some locations were combined to represent larger regions, reducing the number of modeled locations from 11 to 8 (Table B1, Appendix B). Scenarios for DIYABC were devised according to hypothesized population histories, differing in the number of refugia and geodispersals, and informed by geography and genetic cluster membership (the latter as determined with fastStructure and DAPC). Two rounds of simulation and random forest search were performed: an initial round comparing six scenarios containing only population divergences and six with a single admixture event; and a second round comparing nine scenarios consisting of minor variations on the top-performing models from the first round. All scenarios are listed in Figs. B2–B3 (Appendix B). A total of 48,000 and 36,000 datasets were simulated for the first and second round, respectively, using uniform priors with the following distributions: population sizes from 10 to 10,000 individuals, time parameters from 10 to 100,000 years, and admixture rate from 0.1 to 0.99 where applicable. Random forest searches for scenario choice were performed with 1000 trees for each round.

Phylogenetic analysis

A maximum likelihood phylogenetic analysis was performed with RAxML-NG v1.0.1 (Kozlov et al. 2019). The best-fitting substitution model was determined using ModelTest-NG v0.1.7 (Darriba et al. 2020) on the basis of the Akaike Information Criterion (AIC). The best-scoring topology was selected from 40 tree searches using 20 random and 20 parsimony-based starting

trees. Node supports were determined based on 1000 bootstrap replicates. The final unrooted tree was annotated using the R package ggtree v3.5.0.900 (G. Yu et al. 2017).

Results

Preparation of hyRAD libraries was successful for 70 of the 72 selected museum specimens (Table B1 Appendix B). Sequencing yielded a total of 312,617,212 raw reads, of which 82.7% passed quality filtering. There was no evidence of specimen age having any effect on sequencing success or number of obtained reads. *De novo* assembly of reads from the eight reference specimens yielded 291,968 contigs (N50 = 586 bp, min.–max. = 66–5819 bp, mean = 524 bp, GC = 32.6%), of which 28 were identified as either suspected contaminants (n = 6) or mitochondrial DNA (n = 22) and excluded from further analyses. Alignment and variant calling yielded a dataset of 144,163 SNPs after quality filters were applied.

Genetic structure

Analysis with fastStructure revealed that the genetic structure was best explained using seven clusters (k = 7), with considerable admixture between locations (Fig. 1). There was a tendency for certain clusters to show up in higher proportions either in the West and Eurasia (clusters 1–3) or in the East (clusters 6 & 7), although two of them (clusters 4 & 5) were found throughout the species' distribution.

Analysis with DAPC also identified seven clusters (k = 7), which were well-differentiated (Fig. B1, Appendix B). Cluster membership is summarized by location and plotted on the map in Fig. 2. Consistent with the fastStructure results, certain clusters tended to show up in higher proportions in the West and Eurasia (clusters 1–3) or in the East (clusters 6 & 7), with two (clusters 4 & 5) that were found throughout the species' distribution. In both analyses, Korea was

the only location for which all specimens were unambiguously assigned to the same cluster. (Note that cluster numbers are arbitrary and have been changed to ease comparisons between these two anlayses.)

Overall Nei's F_{ST} was determined to be 0.23, indicating moderate genetic differentiation among locations. Pairwise F_{ST} values had a mean of 0.25, ranging from 0.02 (between Eastern Ontario and Atlantic Canada) to 0.62 (between Colorado and Korea). Korea was consistently well-differentiated from all other locations, with an average value of 0.509; Northwest Territories and Nunavut was the least-differentiated location, with an average pairwise F_{ST} of 0.134. All pairwise F_{ST} values are reported in Table 1. Observed heterozygosity was generally low, with overall H_O = 0.064. The lowest value was observed for Korea (H_O = 0.027), and the highest for Eastern Ontario (H_O = 0.103). Heterozygosities for all locations are listed in Table 2.

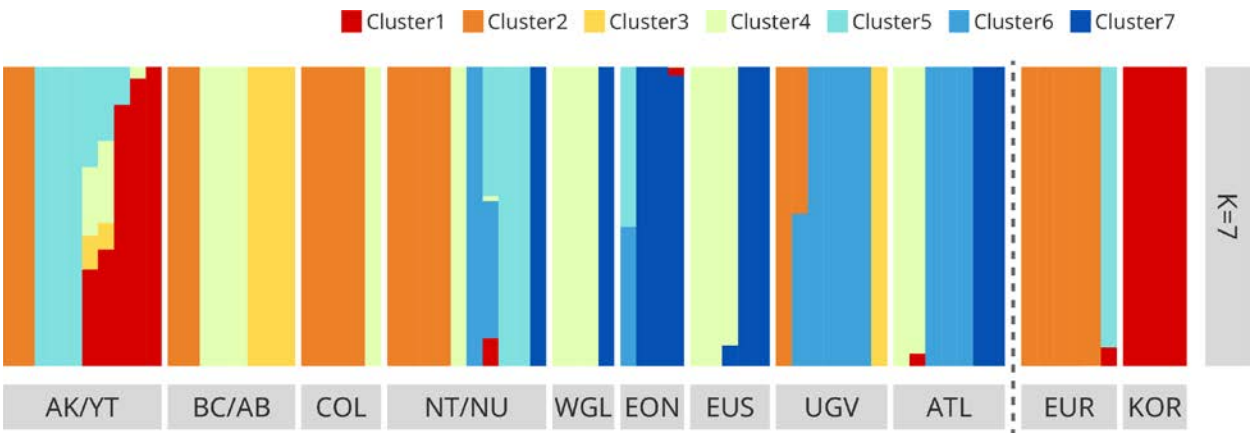

Figure 1. Bar plot of genetic cluster membership based on Bayesian analysis of 144,163 SNPs using fastStructure. The number of clusters (k = 7) was chosen as the appropriate level of model complexity that maximizes marginal likelihood. Cluster numbers are arbitrarily assigned. Locations are: AK/YT: Alaska and Yukon; BC/AB: British Columbia and Alberta; COL: Colorado; NT/NU: Northwest Territories and Nunavut; WGL: Western Great Lakes; EON: Eastern Ontario; EUS: Eastern United States; UGV: Ungava Peninsula (Northern Quebec and Labrador); ATL: Atlantic Canada; EUR: Europe (Ireland and Sweden); KOR: Korea.

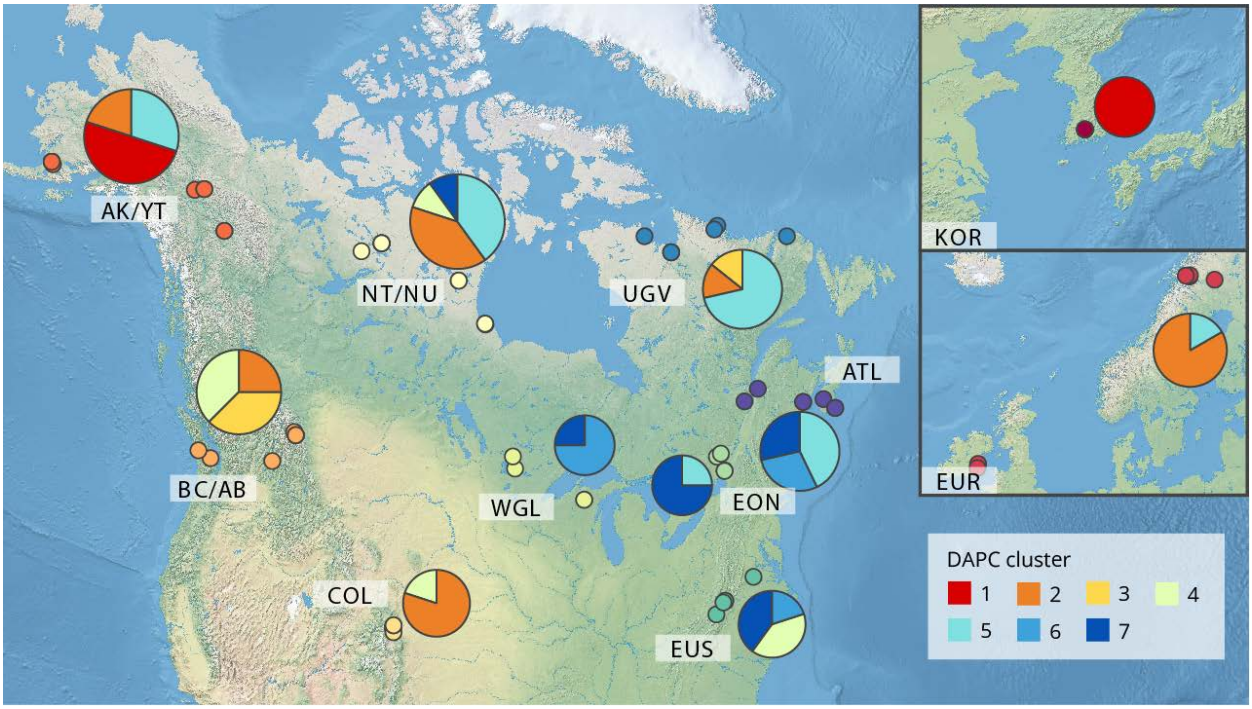

Figure 2. Geographic locations of sampled individuals (coloured dots) and corresponding DAPC-based genetic structure (pie charts), with the proportion of individuals from each location assigned to each cluster shown in different colours. DAPC clusters were assigned based on Bayesian analysis of 144,163 SNPs. Cluster numbers are arbitrarily assigned. Locations are: AK/YT: Alaska and Yukon; BC/AB: British Columbia and Alberta; COL: Colorado; NT/NU: Northwest Territories and Nunavut; WGL: Western Great Lakes; EON: Eastern Ontario; EUS: Eastern United States; UGV: Ungava Peninsula (Northern Quebec and Labrador); ATL: Atlantic Canada; EUR: Europe (Ireland and Sweden); KOR: Korea.

Table 1. Genetic differentiation between populations, as expressed by pairwise F_{ST} values. Values are shaded on a continuous colour scale from white (low) to green (high). Overall F_{ST} was 0.23.

Population	AB/BC	COL	NT/NU	WGL	EON	EUS	UGV	ATL	EUR	KOR
AK/YT	0.176	0.243	0.036	0.259	0.228	0.185	0.080	0.149	0.181	0.360
AB/BC		0.145	0.094	0.217	0.342	0.134	0.172	0.239	0.195	0.530
COL			0.075	0.370	0.434	0.279	0.251	0.349	0.158	0.617
NT/NU				0.201	0.170	0.118	0.040	0.119	0.085	0.406
WGL					0.248	0.065	0.235	0.125	0.383	0.610
EON						0.122	0.125	0.022	0.411	0.565
EUS							0.143	0.061	0.298	0.507
UGV								0.037	0.221	0.428
ATL									0.322	0.465
EUR										0.604

Table 2. Observed heterozygosity (H_O) for each population and across entire sample. Population values in bold are higher than the overall value.

Population	H_O
AK/YT	0.057
AB/BC	0.048
COL	0.057
NT/NU	**0.091**
WGL	0.042
EON	**0.103**
EUS	0.042
UGV	**0.096**
ATL	**0.068**
EUR	**0.073**
KOR	0.027
Overall	0.064

Population history

The input dataset for analysis in DIYABC-RF consisted of 5,081 randomly subsampled SNPs. The best-supported scenario of population history was scenario 5 (Fig. 3), which received 274 votes out of 1000 trees (compared to 142/1000 for scenario 1, 136/1000 for scenario 7; Fig. B3, Appendix B). The posterior probability of scenario 5 was 0.916. This scenario suggests an early split between one population that gave rise to present-day populations in Korea (KOR), Alaska and Yukon (AK/YT), and one that gave rise to those in the Northwest Territories and Nunavut (NT/NU) and Northern Quebec and Labrador (UGV). According to the chosen scenario, these ancestral populations were also involved in a single admixture event that gave rise to the populations in Europe (EUR), Western North America (WNA), Eastern North America (ENA), and Atlantic Canada (ATL). This scenario also requires a minimum of two geodispersals between Eurasia and North America. Checking simulated parameter values against observed data, however, showed highly significant differences for virtually all parameters and across all

scenarios, indicating incompatibility between simulated and observed datasets. In light of this, another 18 manually reformulated and 72 randomly generated scenarios were tested (scenarios and results not reported), but none were found to fit the observed data, and they consistently resulted in lower posterior probabilities.

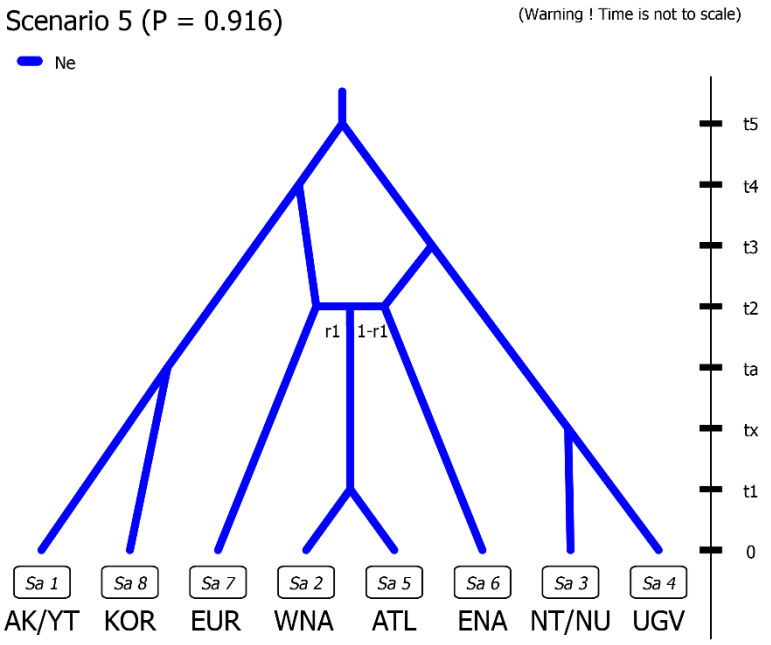

Figure 3. Best-supported scenario describing the population history of *Pristiphora cincta* according to approximate Bayesian computation (ABC) with DIYABC-RF. Analysis was performed on a reduced dataset of 5,081 SNPs. Posterior probability (PP) = 0.916. 'Ne' and 'r1' are parameters describing population size and admixture rate, respectively, both given uniform priors. Populations are: AK/YT: Alaska and Yukon; WNA: Western North America (BC/AB & COL); NT/NU: Northwest Territories and Nunavut; ENA: Eastern North America (WGL, EON & EUS); UGV: Ungava Peninsula (Northern Quebec and Labrador); ATL: Atlantic Canada; EUR: Europe (Ireland and Sweden); KOR: Korea.

Phylogenetic analysis

The best substitution model according to AIC was GTR+G4. The unrooted ML tree is shown in Fig. 4. Lacking data from a suitable outgroup and any information about the rate of sequence evolution, the tree can neither be rooted nor time-calibrated. Branch support values were

generally high, although a handful of branches had bootstrap values around 50%. Most locations have their sampled individuals scattered throughout the tree, and only the individuals from Korea (KOR) represent an apparently monophyletic group – although subsets of individuals from Alaska and Yukon (AK/YT), B.C. and Alberta (BC/AB), and Colorado (COL) appear to be monophyletic as well. Because the tree is unrooted, inferences about ancestry and descent must be tentative at best; however, assuming the labeled groups in Fig. 4 are indeed monophyletic, the relationships in clade A appear to be consistent with a stepwise west-to-east expansion of populations beginning from Beringia (i.e. individuals from more eastern populations are nested within lineages from the West), while clade B appears to show a stepwise expansion east to Nunavut, and then south along the Western Cordillera to Colorado. The phylogeny also supports a minimum of four geodispersals between Eurasia and North America. One of these, inferred from the placement of a single individual from Sweden, is apparently associated with an independent recolonization event from Beringia westward across Europe.

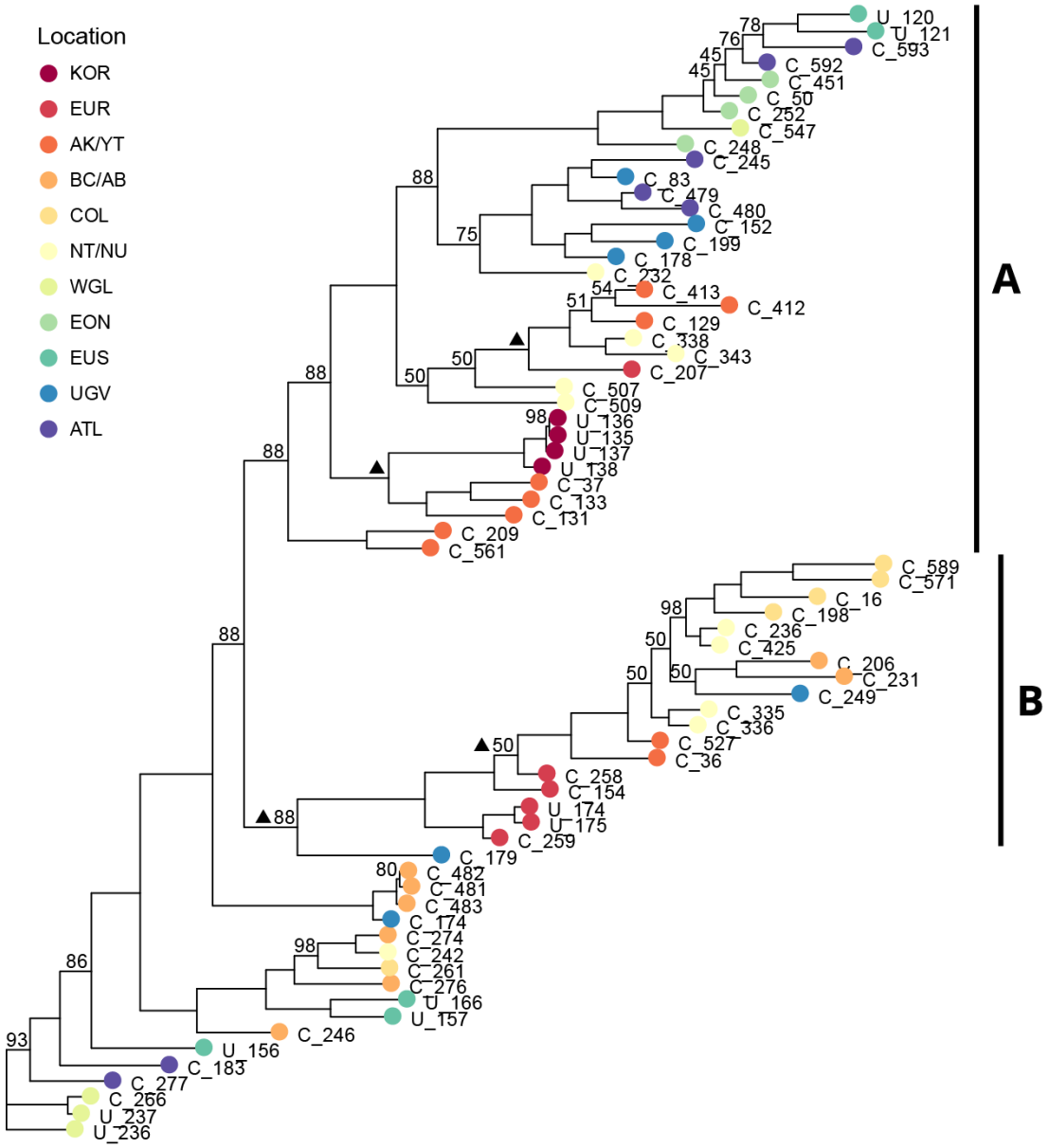

Figure 4. Unrooted maximum-likelihood phylogenetic tree inferred using RAxML-NG, based on analysis of 144,163 SNPs. Bootstrap branch support values were determined based on 1000 bootstrap replicates; only values below 100 are shown. Tips are labeled according to location of origin: AK/YT: Alaska and Yukon; BC/AB: British Columbia and Alberta; COL: Colorado; NT/NU: Northwest Territories and Nunavut; WGL: Western Great Lakes; EON: Eastern Ontario; EUS: Eastern United States; UGV: Ungava Peninsula (Northern Quebec and Labrador); ATL: Atlantic Canada; EUR: Europe (Ireland and Sweden); KOR: Korea. Labeled groups show identifiable patterns of postglacial recolonization: (A) an approximately stepwise expansion of populations from Beringia eastward; (B) traversal of the Bering Land Bridge followed by expansion east to Nunavut and south to Colorado. Branches labeled with black triangles (▲) indicate geodispersal events between Eurasia and North America.

Discussion

The purpose of this study was to gain insight into the genetic structure and phylogeography of *Pristiphora cincta* in North America, using genome-wide SNP markers obtained from historical museum specimens. With hyRAD, high-quality sequences from tens of thousands of homologous loci were successfully obtained from specimens up to 93 years old. This 'museum genomics' approach demonstrates that historical specimens can be successfully leveraged to achieve a wide geographic coverage across a species' distribution – even for non-model organisms, and even lacking a reference genome against which to align sequences. In this case, insects collected during the Northern Insect Survey (1947–1961; Renaud et al. 2012) were an invaluable source of data for populations in Northern Canada. While in this case they were mainly used for lack of more recently collected samples, specimens from the Northern Insect Survey could be similarly used to obtain historical data for the North, making it possible to measure things like changes in effective population size and genetic diversity (e.g. Schmid et al. 2018; not investigated in the present study) in response to warming over the past six to seven decades.

Genetic structure

The inferred genetic clusters were broadly consistent for both clustering methods (fastStructure and DIYABC) and suggest a high degree of admixture across locations, with most clusters present at multiple locations that are separated by thousands of kilometres (Figs. 1 & 2). In the DAPC analysis, the two most geographically restricted clusters were found across temperate parts of Eastern North America (Cluster 6), and in Alaska, Yukon, and Korea (Cluster 1). The fastStructure analysis suggested a greater degree of admixture than the DAPC results, with only one cluster being similarly restricted (Cluster 1 in Alaska, Yukon, and Korea, and present in

small proportions for single individuals elsewhere). Broadly speaking, these results are consistent with predictions of the HLSM hypothesis in that they seem to indicate that multiple distinct genetic lineages arose within isolated populations and were maintained upon secondary contact.

In general, the observed heterozygosity was low (overall value of 0.064; Table 2), while overall genetic structure was moderately high (F_{ST} = 0.23), suggesting that, despite observed admixture, genetic diversity is geographically structured, with different locations having distinct combinations of lineages present.

The Northwest Territories and Nunavut incorporate the greatest number of clusters of any location, which might indicate the presence of one or more small refugia in the High Arctic (Tremblay and Schoen 1999, Shafer et al. 2010, Klütsch et al. 2017). This location also has relatively high heterozygosity (Table 2) and relatively low genetic differentiation from other locations (Table 1), which further supports the idea of nearby refugia as a potential source of lineages recolonizing the rest of the continent.

Alaska and Yukon (i.e. Beringia) exhibit relatively low heterozygosity and high pairwise F_{ST} values with other North American locations (except the Northwest Territories, Nunavut, Northern Quebec, and Labrador). Therefore, it does not seem to have been an important source for lower latitudes, and its refugial populations were probably relatively homogeneous. The latter is consistent with a large, uninterrupted refugium in Beringia.

British Columbia, Alberta, and Colorado exhibit relatively low heterozygosity and low differentiation from the Northwest Territories and Nunavut. Therefore, it is possible that small populations survived in unglaciated nunataks above the Cordilleran ice sheet and/or along the

Pacific coast (Shafer et al. 2010) with subsequent exchange with the central North. Alternatively, these locations may have been recolonized from the Northwest Territories and Nunavut.

Eastern Ontario exhibits the highest heterozygosity, and locations in Eastern North America in general are well-differentiated from those of the West and Eurasia. This may indicate the use of refugial areas south of the Laurentide ice sheet in the East. The relatively high heterozygosity of Northern Quebec and Labrador may indicate that the Ungava Peninsula was recolonized by a mix of unrelated lineages from Eastern and Northern North America.

Population history

The best-supported scenario for population history (Fig. 3) suggests the existence of two ancestral populations that underwent a large admixture event (or events) prior to the establishment of any of the modern populations. Taken at face value, this would be consistent with two distinct refugia and admixture occurring between glaciations. However, given the results of the other analyses, this is clearly only a part of the explanation. Indeed, the poor fit of the simulated data to the observed data requires that the selected scenario be interpreted only very tentatively. The incompatibility of the simulated data is perhaps not surprising, given that the supplied models (Figs. B2–B3, Appendix B) make the implicit assumption that populations are cohesive lineages. Instead, as the studied locations seem to be comprised of mixtures of distinct lineages, it is likely that an accurate model of *P. cincta*'s population history would have to be extremely complex to generate compatible data. Furthermore, it is possible that different lineages or genetic clusters each have their own unique population histories, such that the observed data effectively represent multiple patterns layered on top of one another. At minimum, there was a general preference for scenarios that included a basal split and a large admixture event (Figs. B2–B3, Appendix B), which is interpreted here as supporting at least two major

refugia (one of these being Beringia) with population expansion and mixing during interglacial periods.

Phylogenetic analysis

The inferred phylogeny supports the notion that most locations incorporate multiple genetically distinct (phylogenetically distant) groups. It also supports the existence of multiple overlapping population histories, which is evident from the two labeled clades (Fig. 4): clade A shows an approximately stepwise expansion from Beringia to Eastern North America, while clade B suggests that a Eurasian lineage made an independent crossing of the Bering Land Bridge, its descendants ultimately settling in Western and Northern North America. The placement of the Eurasian individuals additionally supports a minimum of four independent geodispersals across the Bering Land Bridge, which have apparently contributed to this species' genetic diversity.

Conclusions

There have been very few phylogeographic studies of northern insects (Weider and Hobæk 2000, Maresova et al. 2019), with most studies of cold-adapted taxa being centered on rodents (Fedorov and Stenseth 2002, Cook et al. 2004, Galbreath and Cook 2004, Kohli et al. 2015), plants (Tremblay and Schoen 1999, Thomson et al. 2015), or aquatic invertebrates (Lindholm et al. 2016). Yet, cold-adapted insects hold great promise for studying phylogeographic events since the Pleistocene, given their widespread northern distributions and tendency to respond to climatic changes in a manner contrary to their thermophilic counterparts (Schmitt 2007). This study presents the first phylogeographic analysis of a cold-adapted hymenopteran taxon using genome-wide data from SNPs.

From the results, it is evident that *P. cincta* has had a complicated phylogeographic history, characterized by episodes of dispersal and admixture across its North American distribution. The results of the various analyses appear to be consistent with predictions of the HLSM hypothesis: locations exhibit a heterogeneous mix of genetically distinct lineages, which appear to have accumulated over time and spread across North America following deglaciation. Although this species has crossed the Bering Land Bridge at least four times, much of its genetic diversity appears to be associated not with Beringia, but instead with Northwest Territories & Nunavut and temperate Eastern North America; genetic diversity therefore appears to have accumulated in areas associated with small, isolated refugia in the High Arctic and south of the Laurentide ice sheet – promoting divergence in isolation and increasing genetic diversity upon secondary contact – rather than in the large unglaciated expanse of Beringia, where refugial populations may have more easily maintained genetic contact. Nevertheless, the Bering Land Bridge provided important opportunities for intercontinental exchange and associated divergence, which presumably provided some fuel for the high-latitude speciation machine.

The observed degree of admixture and results of the phylogenetic analysis presumably rule out the existence of any cryptic species within *P. cincta*. While the phylogeographic results are perhaps not unlike what one would expect to see for several, recently-diverged sympatric species, there is no morphological evidence to suggest that this is the case. However, there is certainly potential for future speciation from within *P. cincta*. For example, Clade B (Fig. 4) appears to be a well-differentiated group with an arctic-alpine distribution, and given the broad host range of the species (Prous et al. 2017), it is entirely possible that this clade is already at least partly reproductively isolated through host plant switching (Nyman et al. 2010). Indeed, *P. cincta*'s closest relatives are two Nearctic species, *P. serrula* and *P. paloma* (see Chapters 1-2):

the former is distributed throughout the temperate parts of *P. cincta*'s range with *Crataegus* L. as its host, while the latter is found in Eastern North America from Ontario south to Texas and Florida. The three species are recently diverged and exhibit only very small morphological differences, such that this entire clade might well represent an ongoing radiation.

Further study of cold-adapted Northern insects holds promise for investigating the rich phylogeographic history of Northern North America. If cold-adapted taxa preferentially used isolated refugia in the High Arctic during past glaciations, then the patterns seen here – namely high genetic diversity across the North – may well be the rule rather than the exception. Given the disproportionate impact of warming on Northern ecosystems (Koltz et al. 2018, Myers-Smith et al. 2020, Moon et al. 2021), there is a clear and urgent need to study these patterns if one hopes to predict the responses of Northern biotas to present warming.

References

Andrews S (2019) FastQC: A quality control tool for high throughput sequence data. Available from: https://www.bioinformatics.babraham.ac.uk/projects/fastqc/.

Beaumont MA, Zhang W, Balding DJ (2002) Approximate Bayesian computation in population genetics. Genetics 162: 2025–2035. doi: Genetics December 1, 2002 vol. 162 no. 4 2025-2035

Bolger AM, Lohse M, Usadel B (2014) Trimmomatic: A flexible trimmer for Illumina sequence data. Bioinformatics 30: 2114–2120. doi: 10.1093/bioinformatics/btu170

Camacho C, Coulouris G, Avagyan V, Ma N, Papadopoulos J, Bealer K, Madden TL (2009) BLAST+: Architecture and applications. BMC Bioinformatics 10: 1–9. doi: 10.1186/1471-2105-10-421

Chang CC, Chow CC, Tellier LCAM, Vattikuti S, Purcell SM, Lee JJ (2015) Second-generation PLINK: Rising to the challenge of larger and richer datasets. GigaScience 4: 1–16. doi: 10.1186/s13742-015-0047-8

Collin FD, Durif G, Raynal L, Lombaert E, Gautier M, Vitalis R, Marin JM, Estoup A (2021) Extending approximate Bayesian computation with supervised machine learning to infer demographic history from genetic polymorphisms using DIYABC Random Forest. Molecular Ecology Resources 21: 2598–2613. doi: 10.1111/1755-0998.13413

Cook JA, Runck AM, Conroy CJ (2004) Historical biogeography at the crossroads of the northern continents: molecular phylogenetics of red-backed voles (Rodentia: Arvicolinae). Molecular Phylogenetics and Evolution 30: 767–777. doi: 10.1016/S1055-7903(03)00248-3

Cornuet JM, Pudlo P, Veyssier J, Dehne-Garcia A, Gautier M, Leblois R, Marin JM, Estoup A (2014) DIYABC v2.0: A software to make approximate Bayesian computation inferences about population history using single nucleotide polymorphism, DNA sequence and microsatellite data. Bioinformatics 30: 1187–1189. doi: 10.1093/bioinformatics/btt763

Danecek P, Auton A, Abecasis G, Albers CA, Banks E, DePristo MA, Handsaker RE, Lunter G, Marth GT, Sherry ST, McVean G, Durbin R (2011) The variant call format and VCFtools. Bioinformatics 27: 2156–2158. doi: 10.1093/bioinformatics/btr330

Darriba D, Posada D, Kozlov AM, Stamatakis A, Morel B, Flouri T (2020) ModelTest-NG: A New and Scalable Tool for the Selection of DNA and Protein Evolutionary Models. Molecular Biology and Evolution 37: 291–294. doi: 10.1093/molbev/msz189

Eidesen PB, Ehrich D, Bakkestuen V, Alsos IG, Gilg O, Taberlet P, Brochmann C (2013) Genetic roadmap of the Arctic: Plant dispersal highways, traffic barriers and capitals of

diversity. New Phytologist 200: 898–910. doi: 10.1111/nph.12412

Esselstyn JA, Timm RM, Brown RM (2009) Do geological or climatic processes drive speciation in dynamic archipelagos? The tempo and mode of diversification in southeast asian shrews. Evolution 63: 2595–2610. doi: 10.1111/j.1558-5646.2009.00743.x

Ewels P, Magnusson M, Lundin S, Käller M (2016) MultiQC: Summarize analysis results for multiple tools and samples in a single report. Bioinformatics 32: 3047–3048. doi: 10.1093/bioinformatics/btw354

Fedorov VB, Stenseth NC (2002) Multiple glacial refugia in the North American Arctic: inference from phylogeography of the collared lemming (*Dicrostonyx groenlandicus*). Proceedings of the Royal Society London, Biology 269: 2071–2077. doi: 10.1098/rspb.2002.2126

Francis RM (2017) POPHELPER: an R package and web app to analyse and visualize population structure. Molecular Ecology Resources 17: 27–32. doi: 10.1111/1755-0998.12509

Galbreath KE, Cook JA (2004) Genetic consequences of Pleistocene glaciations for the tundra vole (*Microtus oeconomus*) in Beringia. Molecular Ecology 13: 135–148. doi: 10.1046/j.1365-294X.2003.02026.x

GATK Team (2022) Calling variants on cohorts of samples using the HaplotypeCaller in GVCF mode. Genome Analysis Toolkit. Available from: https://gatk.broadinstitute.org/hc/en-us/articles/360035890411-Calling-variants-on-cohorts-of-samples-using-the-HaplotypeCaller-in-GVCF-mode (April 8, 2022).

Goudet J, Jombart T, Kamvar ZN, Archer E, Hardy O (2022) hierfstat: Estimation and Tests of Hierarchical F-Statistics. Available from: https://github.com/jgx65/hierfstat.

Goulet H (1992) The Insects and Arachnids of Canada, Part 20 The Genera and Subgenera of Sawflies of Canada and Alaska: Hymenoptera: Symphyta. 1–235 pp. Available from: http://esc-sec.ca/aafcmonographs/insects_and_arachnids_part_20.pdf.

Hewitt GM (2004a) Genetic consequences of climatic oscillations in the Quaternary Willis KJ, Bennett KD, Walker D (Eds). Philosophical Transactions of the Royal Society of London. Series B: Biological Sciences 359: 183–195. doi: 10.1098/rstb.2003.1388

Hewitt GM (2004b) The structure of biodiversity – insights from molecular phylogeography. Frontiers in zoology 1: 1–16. doi: 10.1186/1742-9994-1-4

Hewitt GM (2011) Quaternary phylogeography: The roots of hybrid zones. Genetica 139: 617–638. doi: 10.1007/s10709-011-9547-3

Hofreiter M, Stewart J (2009) Ecological Change, Range Fluctuations and Population Dynamics during the Pleistocene. Current Biology 19: R584–R594. doi: 10.1016/j.cub.2009.06.030

Jombart T (2008) adegenet: a R package for the multivariate analysis of genetic markers. Bioinformatics 24: 1403–1405. doi: 10.1093/bioinformatics/btn129

Jombart T, Devillard S, Balloux F, Falush D, Stephens M, Pritchard J, Pritchard J, Stephens M, Donnelly P, Corander J, Waldmann P, Sillanpaa M, Tang J, Hanage W, Fraser C, Corander J, Lee C, Abdool A, Huang C, Jombart T, Jombart T, Devillard S, Dufour A, Pontier D, Jombart T, Pontier D, Dufour A, McVean G, Novembre J, Stephens M, Patterson N, Price A, Reich D, Price A, Patterson N, Plenge R, Weinblatt M, Shadick N, Reich D, Hotelling H,

Hotelling H, Pearson K, Liu N, Zhao H, Fisher R, Lachenbruch P, Goldstein M, Aitchison J, Reyment R, Beharav A, Nevo E, Fraley C, Raftery A, Cann H, Toma C de, Cazes L, Legrand M, Morel V, Piouffre L, Bodmer J, Bodmer W, Bonne-Tamir B, Cambon-Thomsen A, Ramachandran S, Deshpande O, Roseman C, Rosenberg N, Feldman M, Cavalli-Sforza L, Rosenberg N, Pritchard J, Weber J, Cann H, Kidd K, Zhivotovsky L, Feldman M, Wang S, Lewis C, Jakobsson M, Ramachandran S, Ray N, Bedoya G, Rojas W, Parra M, Molina J, Gallo C, Balloux F, Rosenberg N, Mahajan S, Ramachandran S, Zhao C, Pritchard J, Feldman M, Rambaut A, Pybus O, Nelson M, Viboud C, Taubenberger J, Holmes E, Russell C, Jones T, Barr I, Cox N, Garten R, Gregory V, Gust I, Hampson A, Hay A, Hurt A, Smith D, Lapedes A, Jong J de, Bestebroer T, Rimmelzwaan G, Osterhaus A, Fouchier R, Holmes E, Ghedin E, Miller N, Taylor J, Bao Y, George KS, Grenfell B, Salzberg S, Fraser C, Lipman D, Young J, Palese P, Benson D, Karsch-Mizrachi A, Lipman D, Ostell J, Wheeler D, Larkin M, Blackshields G, Brown N, Chenna R, McGettigan P, McWilliam H, Valentin F, Wallace I, Wilm A, Lopez R, Waterhouse A, Procter J, Martin D, Clamp M, Barton G, Paradis E, Claude J, Strimmer K, Handley LL, Manica A, Goudet J, Balloux F, Serre D, Paabo S, Corander J, Marttinen P, Siren J, Tang J, Francois O, Ancelet S, Guillot G, Hunley K, Healy M, Long J, Kittles R, Weiss K, Manica A, Prugnolle F, Balloux F, Prugnolle F, Manica A, Balloux F, Romero I, Manica A, Handley LL, Balloux F, Amos W, Hoffman J, Fraley C, Raftery A, Peres-Neto P, Jackson D, Somers K, Saporta G, Paradis E, Dray S, Dufour A, Schwarz G, Evanno G, Regnaut S, Goudet J, Jakobsson M, Rosenberg N, Chessel D, Dufour A, Thioulouse J, Dray S, Dufour A, Chessel D, Venables W, Ripley B, Nei M (2010) Discriminant analysis of principal components: a new method for the analysis of genetically structured populations. BMC Genetics 11: 1–15. doi:

10.1186/1471-2156-11-94

Klütsch CFC, Manseau M, Anderson M, Sinkins P, Wilson PJ (2017) Evolutionary reconstruction supports the presence of a Pleistocene Arctic refugium for a large mammal species. Journal of Biogeography 44: 2729–2739. doi: 10.1111/jbi.13090

Kohli BA, Fedorov VB, Waltari E, Cook JA (2015) Phylogeography of a Holarctic rodent (*Myodes rutilus*): Testing high-latitude biogeographical hypotheses and the dynamics of range shifts. Journal of Biogeography 42: 377–389. doi: 10.1111/jbi.12433

Koltz AM, Schmidt NM, Høye TT (2018) Differential arthropod responses to warming are altering the structure of Arctic communities. Royal Society Open Science 5: 171503. doi: 10.1098/rsos.171503

Kouki J (1999) Latitudinal Gradients in Species Richness in Northern Areas: Some Exceptional Patterns. Ecological Bulletins: 30–37. Available from: http://www.jstor.org/stable/20113224.

Kouki J, Niemela P, Viitasaari M (1994) Reversed latitudinal gradient in species richness of sawflies (Hymenoptera, Symphyta). Ann. Zool. Fennici 31: 83–88.

Kozlov AM, Darriba D, Flouri T, Morel B, Stamatakis A (2019) RAxML-NG: A fast, scalable and user-friendly tool for maximum likelihood phylogenetic inference. Bioinformatics 35: 4453–4455. doi: 10.1093/bioinformatics/btz305

Li H (2013) Aligning sequence reads, clone sequences and assembly contigs with BWA-MEM. arXiv 1303.3997v: 1–3. doi: 10.48550/arXiv.1303.3997v2

Lindholm M, D'Auriac MA, Thaulow J, Hobæk A (2016) Dancing around the pole: holarctic

phylogeography of the Arctic fairy shrimp *Branchinecta paludosa* (Anostraca, Branchiopoda). Hydrobiologia 772: 189–205. doi: 10.1007/s10750-016-2660-7

Lischer HEL, Excoffier L (2012) PGDSpider: An automated data conversion tool for connecting population genetics and genomics programs. Bioinformatics 28: 298–299. doi: 10.1093/bioinformatics/btr642

Maresova J, Habel JC, Neve G, Sielezniew M, Bartonova A, Kostro-Ambroziak A, Fric ZF (2019) Cross-continental phylogeography of two Holarctic Nymphalid butterflies, *Boloria eunomia* and *Boloria selene*. PLoS ONE 14: 1–22. doi: 10.1371/journal.pone.0214483

Marlatt CL (1896) Revision of the Nematinae of North America. Bulletin of the United States Department of Agriculture, Division of Entomology, Technical Series 3: 1–135. Available from: http://www.biodiversitylibrary.org/item/106469.

McKenna A, Hanna M, Banks E, Sivachenko A, Cibulskis K, Kernytsky A, Garimella K, Altshuler D, Gabriel S, Daly M, DePristo MA (2010) The Genome Analysis Toolkit: A MapReduce framework for analyzing next-generation DNA sequencing data. Genome Research 20: 1297–1303. doi: 10.1101/gr.107524.110

Moon TA, Druckenmiller ML, Thoman RL eds. (2021) Arctic Report Card 2021. doi: 10.25923/5S0F-5163

Myers-Smith IH, Kerby JT, Phoenix GK, Bjerke JW, Epstein HE, Assmann JJ, John C, Andreu-Hayles L, Angers-Blondin S, Beck PSA, Berner LT, Bhatt US, Bjorkman AD, Blok D, Bryn A, Christiansen CT, Cornelissen JHC, Cunliffe AM, Elmendorf SC, Forbes BC, Goetz SJ, Hollister RD, de Jong R, Loranty MM, Macias-Fauria M, Maseyk K, Normand S, Olofsson J, Parker TC, Parmentier FJW, Post E, Schaepman-Strub G, Stordal F, Sullivan

PF, Thomas HJD, Tømmervik H, Treharne R, Tweedie CE, Walker DA, Wilmking M, Wipf S (2020) Complexity revealed in the greening of the Arctic. Nature Climate Change 10: 106–117. doi: 10.1038/s41558-019-0688-1

Nei M (1987) Molecular Evolutionary Genetics. Columbia University Press, New York.

Nogués-Bravo D, Rodríguez-Sánchez F, Orsini L, de Boer E, Jansson R, Morlon H, Fordham DA, Jackson ST (2018) Cracking the Code of Biodiversity Responses to Past Climate Change. Trends in Ecology and Evolution 33: 765–776. doi: 10.1016/j.tree.2018.07.005

Nyman T, Vikberg V, Smith DR, Boevé J-L (2010) How common is ecological speciation in plant-feeding insects? A “Higher” Nematinae perspective. BMC evolutionary biology 10: 266.

Prous M, Kramp K, Vikberg V, Liston A (2017) North-Western Palaearctic species of *Pristiphora* (Hymenoptera, Tenthredinidae). Journal of Hymenoptera Research 59: 1–190. doi: 10.3897/jhr.59.12656

QGIS Development Team (2022) QGIS Geographic Information System. Available from: https://www.qgis.org.

R Core Team (2022) R: A language and environment for statistical computing. Available from: https://www.r-project.org/.

Raj A, Stephens M, Pritchard JK (2014) fastSTRUCTURE: Variational Inference of Population Structure in Large SNP Data Sets. Genetics 197: 573–589. doi: 10.1534/genetics.114.164350

Renaud AK, Savage J, Roughley RE (2012) Muscidae (Diptera) diversity in Churchill, Canada,

between two time periods: evidence for limited changes since the Canadian Northern Insect Survey. The Canadian Entomologist 144: 29–51. doi: 10.4039/tce.2012.6

Richter-Menge J, Druckenmiller ML, Jeffries M (2019) Arctic Report Card 2019. doi: 10.1002/2014JC010136

Ross HH (1972) The Origin of Species Diversity in Ecological Communities. Taxon 21: 253–259.

Schmid S, Neuenschwander S, Pitteloud C, Heckel G, Pajkovic M, Arlettaz R, Alvarez N (2018) Spatial and temporal genetic dynamics of the grasshopper *Oedaleus decorus* revealed by museum genomics. Ecology and Evolution 8: 1480–1495. doi: 10.1002/ece3.3699

Schmitt T (2007) Molecular biogeography of Europe: Pleistocene cycles and postglacial trends. Frontiers in Zoology 4: 1–13. doi: 10.1186/1742-9994-4-11

Shafer ABA, Cullingham CI, Côté SD, Coltman DW (2010) Of glaciers and refugia: A decade of study sheds new light on the phylogeography of northwestern North America. Molecular Ecology 19: 4589–4621. doi: 10.1111/j.1365-294X.2010.04828.x

Smith DR (1979) Symphyta. In: Krombein K V., Hurd PDJ, Smith DR, Burks BD (Eds), Catalog of Hymenoptera in America North of Mexico. Volume 1. Smithsonian Institution Press, Washington D.C., 1–137.

Sproul JS, Maddison DR (2017) Sequencing historical specimens: successful preparation of small specimens with low amounts of degraded DNA. Molecular Ecology Resources 17: 1183–1201. doi: 10.1111/1755-0998.12660

Suchan T, Pitteloud C, Gerasimova NS, Kostikova A, Schmid S, Arrigo N, Pajkovic M, Ronikier

M, Alvarez N (2016) Hybridization Capture Using RAD Probes (hyRAD), a New Tool for Performing Genomic Analyses on Collection Specimens Orlando L (Ed). PLOS ONE 11: e0151651. doi: 10.1371/journal.pone.0151651

Thomson AM, Dick CW, Dayanandan S (2015) A similar phylogeographical structure among sympatric North American birches (*Betula*) is better explained by introgression than by shared biogeographical history. Journal of Biogeography 42: 339–350. doi: 10.1111/jbi.12394

Tremblay NO, Schoen DJ (1999) Molecular phylogeography of *Dryas integrifolia*: glacial refugia and postglacial recolonization. Molecular Ecology 8: 1187–1198.

Weider LJ, Hobæk A (2000) Phylogeography and arctic biodiversity: A review. Annales Zoologici Fennici 37: 217–231.

Wood DE, Lu J, Langmead B (2019) Improved metagenomic analysis with Kraken 2. Genome Biology 20: 1–13. doi: 10.1186/s13059-019-1891-0

Yu G, Smith DK, Zhu H, Guan Y, Lam TTY (2017) GGTREE: an R Package for Visualization and Annotation of Phylogenetic Trees With Their Covariates and Other Associated Data. Methods in Ecology and Evolution 8: 28–36. doi: 10.1111/2041-210X.12628

Zimin A V., Marçais G, Puiu D, Roberts M, Salzberg SL, Yorke JA (2013) The MaSuRCA genome assembler. Bioinformatics 29: 2669–2677. doi: 10.1093/bioinformatics/btt476

CHAPTER 5: Conclusions and future directions for the study of Nearctic Nematinae

This dissertation makes meaningful progress towards understanding the evolutionary history, biogeography, and taxonomy of the genus *Pristiphora* Latreille – and thereby of sawflies and northern hemisphere biogeography more broadly. In Chapter 2, three species groups of *Pristiphora* are revised with respect to species found in the Nearctic: the *P. litura* group, the *P. ruficornis* group, and the *P. rufipes* group. Two new species are described, four new synonymies are proposed, and two formerly Palaearctic species are newly reported for the Nearctic, being thus now considered Holarctic. The *P. rufipes* group is also expanded to include four additional species (one Holarctic and three Nearctic) relative to its earlier definition. Thorough descriptions and diagnoses are provided for all species of these groups found in the Nearctic. Evidence is also presented to suggest that the genus boundaries of *Pristiphora* should be re-drawn in light of both morphological (Chapter 2) and molecular (Chapter 3) findings. Phylogenetic evidence presented in Chapter 3 suggests a relatively recent radiation among *Pristiphora* - especially within the speciose *P. ruficornis*, *P. micronematica*, and *P. carinata* species groups - corresponding to the establishment of cool-temperate, boreal, and arctic/subarctic biotas across the Holarctic beginning in the later half of the Miocene (ca. 15 Ma). Ancestral range reconstructions also indicate dozens of geodispersals between the Palaearctic and Nearctic at various times in the genus' 110-million-year-long history. In Chapter 4, a phylogeographic analysis of *Pristiphora cincta* Newman presents further evidence in support of the HLSM hypothesis at the intraspecific level, suggesting that climatic cycles during the Pleistocene led to the diversification of lineages within this species, resulting in relatively heterogeneous populations. The highest genetic

diversity is in Eastern and Northern North America, with some indication that small, isolated refugia in the High Arctic may have been used by *P. cincta* during the most recent glaciations.

In addition to the findings presented here, work conducted in the course of this research also resulted in the recognition of an invasive sawfly species newly introduced to North America – the elm zigzag sawfly, *Aproceros leucopoda* Takeuchi (Martel et al. 2022) - and the publication of a matrix-based key to the genera of Tenthredinidae of North America, with an updated list of all known host plants (Baine et al. 2022). Work is also in progress describing the introduction of a North American sawfly to Portugal (manuscript in preparation), and there is ongoing collaboration with researchers in Europe on the taxonomy of Holarctic Nematinae, in part facilitated by DNA barcode data from the Centre for Biodiversity Genomics, Guelph, ON.

Future study should prioritise revisions of the remaining species groups of *Pristiphora* for the Nearctic, especially the *P. micronematica* group due to its difficult identification, northern bias, and the existence of at least three probable undescribed species. As well, a thoroughly sampled phylogeny of the subfamily, especially the Nematini, is desirable to further clarify genus boundaries and evaluate the proposals presented in Chapters 2 and 3 to resurrect *Neopareophora* MacGillivray and *Pristola* Ross and promote *Oligonematus* Zhelochovtsev (among potentially others) as recognized genera based on a more robust analysis. For practical reasons, the extent to which COI barcodes alone can productively inform nematine taxonomy needs to be seriously considered. Although barcode BINs provide reliable identifications of *Pristiphora* only about half of the time - with many examples of multiple species being recovered in a single BIN, or else multiple BINs being applied to a single species (Prous et al. 2017) - they nevertheless provide a valuable means for a "first-pass" sort of available material. For insects like these, whose identification generally requires painstaking dissections, the value of barcodes as a

heuristic device should not be underestimated. Ideally, the underlying biological causes of these barcode-taxonomy mismatches should be investigated (e.g. in the allantine genus *Empria* Lepeletier & Serville, mitochondrial introgression is at least partly to blame; Prous et al. 2020), in hopes of better understanding why and in which taxa the problem is more or less severe. On the other hand, sawflies might present a useful study taxon in which to investigate alternative barcode markers and/or extensions of traditional barcode-based identification methods (e.g. Coissac et al. 2016, Gibbs 2017).

Regarding biogeography, it would be productive to examine a more densely sampled phylogeny with respect to Nearctic species, as the ancestral range reconstructions presented in Chapter 3 were fairly ambiguous for early nodes/ancestors - although some divergences are sufficiently early that they preceded the final breakup of Laurasia across the North Atlantic (Sanmartín et al. 2001). Holarctic species also deserve a close look, with the goal of understanding when they achieved their circumpolar distribution, and what this might mean for past instances of intercontinental dispersal. For example, do certain traits favour a Holarctic distribution? Do Holarctic species typically use Holarctic host plants (e.g. *Oxytropis campestris* (L.) for *P. sootryeni* Lindqvist), do they exhibit higher host plasticity, or is it some combination of both? Similar questions can be posed of well-separated populations of North American species. For example, *Pristiphora lena* Kincaid feeds on *Picea glauca* (Moench) Voss across much of its range in Canada, but is also known from Haida Gwaii off the Pacific Coast and from Redondo Peak in New Mexico (data not reported); *Picea glauca* does not occur in either of the latter localities, and the two also have mutually exclusive lists of Pinaceae species present (Flora of North America Editorial Committee 1993), suggesting that *P. lena* has either expanded onto at least two alternative hosts in these places, or represents multiple cryptic species.

In short, there is virtually no end to the interesting questions that can be posed for the Nematinae, but it is foremost necessary to have a stable species-level taxonomy to expand their potential for use in the study of northern arthropods. The presented research represents a useful and valuable contribution to that objective and plots a course towards a fuller understanding of sawfly diversity and evolution in the Nearctic.

References

Baine Q, Looney C, Monckton SK, Smith DR, Schiff NM, Goulet H, Redford AJ (2022) USDA APHIS PPQ Identification Technology Program (ITP) and Washington State Department of Agriculture Sawfly GenUS. April 2022. Fort Collins, CO Available from: https://idtools.org/id/sawfly/ (July 11, 2022).

Coissac E, Hollingsworth PM, Lavergne S, Taberlet P (2016) From barcodes to genomes: Extending the concept of DNA barcoding. Molecular Ecology 25: 1423–1428. doi: 10.1111/mec.13549

Flora of North America Editorial Committee ed. (1993) 1–28 Flora of North America North of Mexico. New York and Oxford.

Gibbs J (2017) DNA barcoding a nightmare taxon: assessing barcode index numbers and barcode gaps for sweat bees. Genome 31: 1–11. doi: 10.1139/gen-2017-0096

Martel V, Morin O, Monckton SK, Eiseman CS, Béliveau C, Cusson M, Blank SM (2022) Elm zigzag sawfly, Aproceros leucopoda (Hymenoptera: Argidae), recorded for the first time in North America through community science. The Canadian Entomologist 154: 1–18. doi: 10.4039/tce.2021.44

Prous M, Kramp K, Vikberg V, Liston A (2017) North-Western Palaearctic species of *Pristiphora* (Hymenoptera, Tenthredinidae). Journal of Hymenoptera Research 59: 1–190. doi: 10.3897/jhr.59.12656

Prous M, Lee KM, Mutanen M (2020) Cross-contamination and strong mitonuclear discordance in Empria sawflies (Hymenoptera, Tenthredinidae) in the light of phylogenomic data. Molecular Phylogenetics and Evolution 143: 106670. doi: 10.1016/j.ympev.2019.106670

Sanmartín I, Enghoff H, Ronquist F (2001) Patterns of animal dispersal, vicariance and diversification in the Holarctic. Biological Journal of the Linnean Society 73: 345–390. doi: 10.1006/bijl.2001.0542

Appendix A: Supplementary data (Chapter 3)

Table A1. List of specimens used in phylogenetic analysis. Sequences obtained from GenBank are listed with accession numbers. Sequences provided by M. Prous are indicated by 'MP'. Sequences that were newly obtained are indicated by their DNA sample number (e.g. NAPr_XXX).

Label	Catalog no.	Scientific name	Sex	Life stage	Distribution	Country	State/Province	Year collected	Collector	Identifier	Institution	COI	NaK	POL2	TPI
DEI-GISHym80477_Cladius-pectinicornis_l_Sweden_GB	DEI-GISHym80477	*Cladius pectinicornis*	l	larva	Holarctic	Sweden	Norrbottens Laen	2017	A. Liston & M. Prous	M. Prous	obtained from GenBank	MK624709	MK624791	MK624856	MK624893
DEI-GISHym80004_Dineura-militaris_f_Quebec_GB	DEI-GISHym80004	*Dineura militaris*	f	adult	Nearctic	Canada	Quebec	2012			obtained from GenBank	KY698157	KY698279	MK624850	KY698406
DEI-GISHym88536_Euura_spiraeae_f_Germany	DEI-GISHym88536	*Euura spiraeae*	f	adult	Palaearctic	Germany	Brandenburg	2017	A. Taeger		SDEI	MK624715	MK624797	MK624862	MK624897
DEI-GISHym21499_Euura_dispar_m_Sweden	DEI-GISHym21499	*Euura dispar*	m	adult	Palaearctic	Sweden	Torne Lappmark	2016	A. Liston & M. Prous		SDEI	MZ479419	MW939766	MW939876	MP
ZMUO.046539_Euura_leptocephalus_m_Finland	ZMUO.046539	*Euura leptocephalus*	m	adult	Holarctic	Finland	Lapland	2020	M. Mutanen	M. Prous	ZMUO	MP	MP	MP	MP
DEI-GISHym84184_Euura_clibrichella_m_Sweden	DEI-GISHym84184	*Euura clibrichella*	m	adult	Palaearctic	Sweden	Torne Lappmark	2016	A. Liston & M. Prous	M. Prous	SDEI	MK624670	MK624760	MK624813	MK624875
DEI-GISHym88516_Euura_obducta_f_Germany	DEI-GISHym88516	*Euura obducta*	f	adult	Holarctic	Germany	Brandenburg	2017	A. Taeger		SDEI	MZ479490	MW939773	MW939862	MP
DEI-GISHym83588_Euura_fahraei_l_Germany	DEI-GISHym83588	*Euura fahraei*		larva	Palaearctic	Germany	Brandenburg	2017	A.D. Liston	A. D. Liston	SDEI	MK624669	MK624759	MK624812	MK624874
ZMUO.046534_Euura_flavescens_m_Finland	ZMUO.046534	*Euura flavescens*	m	adult	Palaearctic	Finland	Lapland	2020	M. Mutanen	M. Prous	ZMUO	MP	MP	MP	MP
DEI-GISHym21330_Euura_weiffenbachiella_l_Sweden	DEI-GISHym21330	*Euura weiffenbachiella*		larva	Palaearctic	Sweden	Skane	2016	A.D. Liston	A. D. Liston	SDEI	MK624680	MK624768	MK624830	MK624883
DEI-GISHym80206_Euura_bohemani_m_Sweden	DEI-GISHym80206	*Euura bohemani*	m	adult	Palaearctic	Sweden	Torne Lappmark	2016	A. Liston & M. Prous	M. Prous	SDEI	KY698139	KY698264	MK624829	KY698389
DEI-GISHym84182_Euura_nigricornis_f_Germany	DEI-GISHym84182	*Euura nigricornis*	f	adult	Palaearctic	Germany	Brandenburg	2017	A.D. Liston	A. D. Liston	SDEI	MK624674	MK624763	MK624816	MK624878
DEI-GISHym80108_Euura_parvilabris_m_Sweden	DEI-GISHym80108	*Euura parvilabris*	m	adult	Palaearctic	Sweden	Torne Lappmark	2016	A. Liston & M. Prous	M. Prous	SDEI	MZ479465	MW939779	MW939853	MP
DEI-GISHym31247_Euura_myosotidis_m_Estonia	DEI-GISHym31247	*Euura myosotidis*	m	adult	Palaearctic	Estonia	Laanemaa	2015	A.D. Liston, M. Prous & A. Taeger	A. D. Liston	SDEI	KY698137	KY698263	MK624827	KY698390
DEI-GISHym88724_Euura_frenalis_m_Sweden	DEI-GISHym88724	*Euura frenalis*	m	adult	Palaearctic	Sweden	Torne Lappmark	2016	A. Liston & M. Prous	M. Prous	SDEI	MZ479542	MW939769	MW939877	MP
ZMUO.037168_Euura_amentorum_f_Finland	ZMUO.037168	*Euura amentorum*	f	adult	Holarctic	Finland		2018		A. D. Liston	ZMUO	MP	MP	MP	MP
ZMUO.058316_Euura_freyja_m_Finland	ZMUO.058316	*Euura freyja*	m	adult	Palaearctic	Finland	Lapland	2020		M. Prous	ZMUO	MP	MP	MP	MP
DEI-GISHym80261_Euura_humeralis_m_Germany	DEI-GISHym80261	*Euura humeralis*	m	adult	Palaearctic	Germany	Brandenburg	2017	A. Liston & M. Prous	M. Prous	SDEI	MK624681	MK624769	MK624831	MK624884

DEI-GISHym80073_Euura_berolinensis_l_Russia	DEI-GISHym80073	*Euura berolinensis*		larva	Palaearctic	Russia	Primorsky Krai	2016	K. Kramp, M. Prous & A. Taeger	M. Prous	SDEI	MP	MP	MP	MP
DEI-GISHym80072_Euura_ampla_l_Russia	DEI-GISHym80072	*Euura ampla*		larva	Palaearctic	Russia	Primorsky Krai	2016	K. Kramp, M. Prous & A. Taeger		SDEI	MP	MP	MP	MP
DEI-GISHym84189_Euura_variator_m_Sweden	DEI-GISHym84189	*Euura variator*	m	adult	Palaearctic	Sweden	Torne Lappmark	2016	A. Liston & M. Prous		SDEI	MK624671	MK624761	MK624814	MK624876
DEI-GISHym88661_Euura_ribesii_m_Germany	DEI-GISHym88661	*Euura ribesii*	m	adult	Palaearctic	Germany	Brandenburg	2017	A. Taeger		SDEI	MK624714	MK624796	MK624861	MK624896
DEI-GISHym80058_Euura_scutellata_m_Germany	DEI-GISHym80058	*Euura scutellata*	m	adult	Palaearctic	Germany	Brandenburg	2016	M. Prous	M. Prous	SDEI	KY698138	KY698265	MK624828	KY698391
ZMUO.045542_Euura_viduata_f_Finland	ZMUO.045542	*Euura viduata*	f	adult	Holarctic	Finland		2020	M. Mutanen	M. Prous	ZMUO	MP	MP	MP	MP
DEI-GISHym12523_Fagineura_spec._m_Russia	DEI-GISHym12523	*Fagineura spec.*	m	adult	Palaearctic	Russia	Primorsky Krai	2019	M. Prous	M. Prous	SDEI	MP	MP	MP	MP
tO9_Hemichroa-crocea_GB	tO9	*Hemichroa crocea*			Holarctic	Finland		1900			obtained from GenBank	KF936606	KF935901	KF936253	KF937152
DEI-GISHym80300_Hoplocampa-chrysorrhoea_f_Greece_GB	DEI-GISHym80300	*Hoplocampa chrysorrhoea*	f	adult	Palaearctic	Greece	Achaia	2017	SDEI Hym-group	M. Prous	obtained from GenBank	MK624717	MK624799	MK624864	MK624898
DEI-GISHym80228_Megadineura_grandis_m_Russia	DEI-GISHym80228	*Megadineura grandis*	m	adult	Palaearctic	Russia	Primorsky Krai	2016	K. Kramp, M. Prous & A. Taeger	M. Prous	SDEI	KY698132	KY698267	MK624824	KY698386
DEI-GISHym80015_Mesoneura_opaca_f_Morocco	DEI-GISHym80015	*Mesoneura opaca*	f	adult	Palaearctic	Morocco	Meknes-Tafilalet Region	2015	A. Liston & M. Prous	M. Prous	SDEI	KY698134	KY698258	MK624823	KY698384
DEI-GISHym86259_Nematus_spec._m_Russia	DEI-GISHym86259	*Nematus spec.*	m	adult	Palaearctic	Russia	Primorsky Krai	2016	K. Kramp, M. Prous & A. Taeger	M. Prous	SDEI	KY698141	KY698261	MK624832	KY698393
TUZ109010_Nematus_alniastri_f_Estonia	TUZ109010	*Nematus alniastri*	f	adult	Palaearctic	Estonia	Saaremaa	2017	V. Soon	A. D. Liston	TUZ	MK624747	MK624805	MK624870	MK624904
DEI-GISHym80332_Nematus_lucidus_m_Greece	DEI-GISHym80332	*Nematus lucidus*	m	adult	Palaearctic	Greece	Achaia	2017	SDEI Hym-group	M. Prous	SDEI	MK624685	MK624770	MK624835	MK624885
DEI-GISHym31229_Nematus_princeps_m_Estonia	DEI-GISHym31229	*Nematus princeps*	m	adult	Palaearctic	Estonia	Ida-Virumaa	2015	H. Vardal	M. Prous	NHRS	KX602591	KY698262	MK624833	KX602627
DEI-GISHym31044_Nematus_umbratus_f_Sweden	DEI-GISHym31044	*Nematus umbratus*	f	adult	Palaearctic	Sweden	Norrbottens Laen	2014	A. Liston & M. Prous	A. D. Liston	SDEI	MK624710	MK624792	MK624857	MK624894
DEI-GISHym80320_Pristiphora_abbreviata_m_Greece	DEI-GISHym80320	*Pristiphora abbreviata*	m	adult	Palaearctic	Greece	Achaia	2017	SDEI Hym-group	M. Prous	SDEI	MP	MP	MP	
DEI-GISHym80269_Pristiphora_biscalis_m_Germany	DEI-GISHym80269	*Pristiphora biscalis*	m	adult	Palaearctic	Germany	Brandenburg	2017	A. Liston & M. Prous	M. Prous	SDEI	MP	MP	MP	
DEI-GISHym80302_Pristiphora_biscalis_m_Greece	DEI-GISHym80302	*Pristiphora biscalis*	m	adult	Palaearctic	Greece	Achaia	2017	SDEI Hym-group	M. Prous	SDEI	MP	MP	MP	
DEI-GISHym80547_Pristiphora_biscalis_f_Greece	DEI-GISHym80547	*Pristiphora biscalis*	f	adult	Palaearctic	Greece	Achaia	2017	SDEI Hym-group	M. Prous	SDEI	MP	MP	MP	
DEI-GISHym88850_Pristiphora_biscalis_m_Bulgaria	DEI-GISHym88850	*Pristiphora biscalis*	m	adult	Palaearctic	Bulgaria	Varna	2018	A. Liston & M. Prous	M. Prous	SDEI	MP	MP	MP	
DEI-GISHym80720_Pristiphora_cadma_f_Russia	DEI-GISHym80720	*Pristiphora cadma*	f	adult	Holarctic	Russia	Primorsky Krai	2019	M. Prous	M. Prous	SDEI	MP	MP	MP	
TUZ615726_Pristiphora_cadma_f_Estonia	TUZ615726	*Pristiphora cadma*	f	adult	Holarctic	Estonia	Harjumaa	2010	M. Prous		TUZ	KX602583	KY698254	MP	KX602619

DEI-GISHym80158_Pristiphora_cincta_m_Sweden	DEI-GISHym80158	*Pristiphora cincta*	m	adult	Holarctic	Sweden	Torne Lappmark	2016	A. Liston & M. Prous	M. Prous	SDEI	KY698066	KY698224	MW939782	KY698329
DEI-GISHym80223_Pristiphora_condei_m_Russia	DEI-GISHym80223	*Pristiphora condei*	m	adult	Palaearctic	Russia	Primorskiy Kray	2016	K. Kramp, M. Prous & A. Taeger	M. Prous	SDEI	KY698117	KY698207		KY698373
DEI-GISHym11534_Pristiphora_conjugata_f_Germany	DEI-GISHym11534	*Pristiphora conjugata*	f	adult	Palaearctic	Germany	Bayern	2008	A.D. Liston	A. D. Liston	SDEI	KC975853	MP		KY698367
DEI-GISHym80258_Pristiphora_dedeara_m_Germany	DEI-GISHym80258	*Pristiphora dedeara*	m	adult	Palaearctic	Germany	Brandenburg	2017	A. Liston & M. Prous		SDEI	MF426918	MF426921	MK624822	MF426924
DEI-GISHym88800_Pristiphora_fausta_m_Bulgaria	DEI-GISHym88800	*Pristiphora fausta*	m	adult	Palaearctic	Bulgaria	Varna	2018	A. Liston & M. Prous	M. Prous	SDEI	MZ479651	MW939749	MW939865	MP
DEI-GISHym11596_Pristiphora_ferruginosa_f_Canada	DEI-GISHym11596	*Pristiphora ferruginosa*	f	adult	Nearctic	Canada	British Columbia	2002	T. Nyman	T. Nyman	SDEI	KC976044	MP	MP	
DEI-GISHym86207_Pristiphora_fulviceps_f_Russia	DEI-GISHym86207	*Pristiphora fulviceps*	f	adult	Palaearctic	Russia	Primorskiy Kray	2016	K. Kramp, M. Prous & A. Taeger	M. Prous	SDEI	KY698114	KY698198	MP	KY698371
DEI-GISHym20989_Pristiphora_geniculata_m_Estonia	DEI-GISHym20989	*Pristiphora geniculata*	m	adult	Palaearctic	Estonia	Ida-Virumaa	2015	M. Heidemaa	M. Prous	SDEI	KX602585	KY698209	MK624820	KX602616
DEI-GISHym31859_Pristiphora_helvetica_m_Austria	DEI-GISHym31859	*Pristiphora helvetica*	m	adult	Palaearctic	Austria	Tirol	2018	A.D. Liston	A. D. Liston	SDEI	MK624677	MK624765	MK624818	MK624880
DEI-GISHym88837_Pristiphora_insularis_m_Bulgaria	DEI-GISHym88837	*Pristiphora insularis*	m	adult	Holarctic	Bulgaria	Burgas	2018	A. Liston & M. Prous	M. Prous	SDEI	MZ479672	MW939776	MW939864	MP
DEI-GISHym11474_Pristiphora_litura_f_USA	DEI-GISHym11474	*Pristiphora litura*	f	adult	Nearctic	USA	Massachusetts (MA)	2003	T. Nyman	T. Nyman	SDEI	KC974654	MP	MP	
DEI-GISHym80697_Pristiphora_maesta_f_Russia	DEI-GISHym80697	*Pristiphora maesta*	f	adult	Palaearctic	Russia	Primorskiy Kray	2019	M. Prous	M. Prous	SDEI	MP	MP	MP	
DEI-GISHym80796_Pristiphora_maesta_m_Russia	DEI-GISHym80796	*Pristiphora maesta*	m	adult	Palaearctic	Russia	Primorskiy Kray	2019	M. Prous	M. Prous	SDEI	MP	MP	MP	
DEI-GISHym80808_Pristiphora_maesta_m_Russia	DEI-GISHym80808	*Pristiphora maesta*	m	adult	Palaearctic	Russia	Primorsky Krai	2019	M. Prous	M. Prous	SDEI	MP	MP	MP	
DEI-GISHym31040_Pristiphora_mollis_m_Sweden	DEI-GISHym31040	*Pristiphora mollis*	m	adult	Holarctic	Sweden	Norrbottens Laen	2014	A. Liston & M. Prous	M. Prous	SDEI	KX602587	KY698230	MK624821	KX602625
DEI-GISHym88772_Pristiphora_monogyniae_m_Bulgaria	DEI-GISHym88772	*Pristiphora monogyniae*	m	adult	Palaearctic	Bulgaria	Varna	2018	A. Liston & M. Prous	M. Prous	SDEI	MP	MP	MP	
DEI-GISHym80233_Pristiphora_prs006_m_Russia	DEI-GISHym80233	*Pristiphora prs006*	m	adult	Palaearctic	Russia	Primorskiy Kray	2016	K. Kramp, M. Prous & A. Taeger		SDEI	KY698112	KY698195		KY698369
DEI-GISHym83829_Pristiphora_prs006_f_Japan	DEI-GISHym83829	*Pristiphora prs006*	f	adult	Palaearctic	Japan	Nagano	2017	A. Taeger		SDEI	MP	MP	MP	
DEI-GISHym86131_Pristiphora_prs009_f_Russia	DEI-GISHym86131	*Pristiphora prs009*	f	adult	Palaearctic	Russia	Primorskiy Kray	2016	K. Kramp, M. Prous & A. Taeger	M. Prous	SDEI	KY698115	KY698197	MP	KY698370
DEI-GISHym15337_Pristiphora_punctifrons_f_Canada	DEI-GISHym15337	*Pristiphora punctifrons*	f	adult	Holarctic	Canada	Quebec	2012	CNC Hymenoptera Team		SDEI	KF642687	KY698212		KY698362
DEI-GISHym80257_Pristiphora_punctifrons_f_Germany	DEI-GISHym80257	*Pristiphora punctifrons*	f	adult	Holarctic	Germany	Brandenburg	2017	A. Liston & M. Prous	M. Prous	SDEI	MP	MP	MP	
DEI-GISHym88634_Pristiphora_testacea_f_Germany	DEI-GISHym88634	*Pristiphora testacea*	f	adult	Palaearctic	Germany	Brandenburg	2017	A. Taeger		SDEI	MP	MP	MP	
DEI-GISHym12006_Pristiphora_abietina_m_Estonia	DEI-GISHym12006	*Pristiphora abietina*	m	adult	Palaearctic	Estonia	Tartumaa	2007	M. Heidemaa	M. Prous	CMH	MP	MP	MP	MP

DEI-GISHym84251_Pristiphora_compressa_f_Finland	DEI-GISHym84251	*Pristiphora compressa*	f	adult	Palaearctic	Finland	Northern Ostrobothnia	2018	SDEI Hym-group	M. Prous	SDEI	MP	MP	MP		
ZMUO.033954_Pristiphora_decipiens_f_Finland	ZMUO.033954	*Pristiphora decipiens*	f	adult	Palaearctic	Finland		2018	M. Mutanen	M. Prous	ZMUO	MP	MP	MP		
DEI-GISHym12005_Pristiphora_gerula_m_Estonia	DEI-GISHym12005	*Pristiphora gerula*	m	adult	Palaearctic	Estonia	Tartumaa	2007	M. Heidemaa	M. Prous	CMH	MZ479587	MW939732	MW939881		
DEI-GISHym88365_Pristiphora_gerula_f_Germany	DEI-GISHym88365	*Pristiphora gerula*	f	adult	Palaearctic	Germany	Brandenburg	2017	A. Taeger		SDEI	MP	MP	MP		
DEI-GISHym84249_Pristiphora_pseudodecipiens_f_Finland	DEI-GISHym84249	*Pristiphora pseudodecipiens*	f	adult	Palaearctic	Finland	Northern Ostrobothnia	2018	A. Liston & M. Prous	M. Prous	SDEI	MP	MP	MP		
ZMUO.033777_Pristiphora_robusta_m_Finland	ZMUO.033777	*Pristiphora robusta*	m	adult	Palaearctic	Finland		2017	E S”derholm, M. Mutanen, M. Viitasaari	M. Prous	SDEI	MP	MP	MP		
DEI-GISHym11875_Pristiphora_saxesenii_f_Slovakia	DEI-GISHym11875	*Pristiphora saxesenii*	f	adult	Palaearctic	Slovakia		2005	A. Taeger	M. Prous	SDEI	KC974820	KY698235			MP
DEI-GISHym80732_Pristiphora_saxesenii_f_Russia	DEI-GISHym80732	*Pristiphora saxesenii*	f	adult	Palaearctic	Russia	Primorskiy Kray	2019	M. Prous	M. Prous	SDEI	MP	MP	MP		
DEI-GISHym80867_Pristiphora_saxesenii_m_Russia	DEI-GISHym80867	*Pristiphora saxesenii*	m	adult	Palaearctic	Russia	Primorsky Krai	2019	M. Prous	M. Prous	SDEI	MP	MP	MP		
DEI-GISHym80868_Pristiphora_saxesenii_m_Russia	DEI-GISHym80868	*Pristiphora saxesenii*	m	adult	Palaearctic	Russia	Primorsky Krai	2019	M. Prous	M. Prous	SDEI	MP	MP	MP		
DEI-GISHym84740_Pristiphora_alpestris_l_Germany	DEI-GISHym84740	*Pristiphora alpestris*		larva	Palaearctic	Germany	Berlin	2021	A.D. Liston	A. D. Liston	SDEI	MP	MP	MP		
DEI-GISHym80212_Pristiphora_pseudocoactula_m_Sweden	DEI-GISHym80212	*Pristiphora pseudocoactula*	m	adult	Holarctic	Sweden		2014	A. Taeger	M. Prous	SDEI	KY698105	KY698246			KY698337
DEI-GISHym11646_Pristiphora_borea_m_United_Kingdom	DEI-GISHym11646	*Pristiphora borea*	m	adult	Holarctic	United Kingdom	Scotland	2010	S. M. Blank, A. D. Liston & A. Taeger	M. Prous	SDEI	KC972848	MP	MP		
DEI-GISHym80148_Pristiphora_borea_m_Sweden	DEI-GISHym80148	*Pristiphora borea*	m	adult	Holarctic	Sweden	Torne Lappmark	2016	A. Liston & M. Prous	M. Prous	SDEI	KY698093	KY698241	MP		KY698348
DEI-GISHym80189_Pristiphora_borea_m_Sweden	DEI-GISHym80189	*Pristiphora borea*	m	adult	Holarctic	Sweden	Torne Lappmark	2016	A. Liston & M. Prous	M. Prous	SDEI	KY698092	KY698244	MP		KY698349
ZMUO.033281_Pristiphora_borea_f_Finland	ZMUO.033281	*Pristiphora borea*	f	adult	Holarctic	Finland		2017	Marko Mutanen, Nestori Mutanen, Anttoni Mutanen	M. Prous	ZMUO	MZ659994	MP	MP		MP
ZMUO.035412_Pristiphora_carinata_f_Finland	ZMUO.035412	*Pristiphora carinata*	f	adult	Holarctic	Finland		2018	Marko Mutanen, Nestori Mutanen		ZMUO	MP	MP	MP		MP
ZMUO.035355_Pristiphora_coactula_f_Finland	ZMUO.035355	*Pristiphora coactula*	f	adult	Holarctic	Finland		2018	Marko Mutanen, Nestori Mutanen	M. Prous	ZMUO	MZ630925	MP	MP		MP
ZMUO.035514_Pristiphora_coactula_f_Finland	ZMUO.035514	*Pristiphora coactula*	f	adult	Holarctic	Finland		2018	Marko Mutanen, Nestori Mutanen, Anttoni Mutanen	M. Prous	ZMUO	MZ630259	MP	MP		MP

ZMUO.041901_Pristiphora_coactula_m_Finland	ZMUO.041901	*Pristiphora coactula*	m	adult	Holarctic	Finland	Lapland	2020	M. Mutanen	M. Prous	ZMUO	MP	MP	MP	MP
DEI-GISHym31286_Pristiphora_groenblomi_f_Sweden	DEI-GISHym31286	*Pristiphora groenblomi*	f	adult	Holarctic	Sweden		2014	A. Taeger	M. Prous	SDEI	KY698096	KY698240		KY698340
DEI-GISHym80210_Pristiphora_groenblomi_m_Sweden	DEI-GISHym80210	*Pristiphora groenblomi*	m	adult	Holarctic	Sweden	Norrbottens Laen	2014	A. Liston & M. Prous	M. Prous	SDEI	KY698097	KY698239		KY698341
DEI-GISHym80321_Pristiphora_cretica_m_Greece	DEI-GISHym80321	*Pristiphora cretica*	m	adult	Palaearctic	Greece	Achaia	2017	SDEI Hym-group	M. Prous	SDEI	MT385400	MT385404	MT385408	MP
DEI-GISHym84170_Pristiphora_depressa_f_Bulgaria	DEI-GISHym84170	*Pristiphora depressa*	f	adult	Palaearctic	Bulgaria	Varna	2018	A. Liston & M. Prous	M. Prous	SDEI	MT385398	MT385402	MT385406	
DEI-GISHym83928_Pristiphora_krausi_f_Germany	DEI-GISHym83928	*Pristiphora krausi*	f	adult	Palaearctic	Germany	Sachsen-Anhalt	2019	23rd Symphyta Workshop	M. Prous	SDEI	MT385399	MT385403	MT385407	
DEI-GISHym80284_Pristiphora_melagonia_f_Greece	DEI-GISHym80284	*Pristiphora melagonia*	f	adult	Palaearctic	Greece	Achaia	2017	SDEI Hym-group		SDEI	MT385401	MT385405	MT385409	
DEI-GISHym80227_Pristiphora_prs005_f_Russia	DEI-GISHym80227	*Pristiphora prs005*	f	adult	Palaearctic	Russia	Primorskiy Kray	2016	K. Kramp, M. Prous & A. Taeger	M. Prous	SDEI	KY698126	KY698199		KY698319
DEI-GISHym80823_Pristiphora_prs005_m_Russia	DEI-GISHym80823	*Pristiphora prs005*	m	adult	Palaearctic	Russia	Primorsky Krai	2019	M. Prous	M. Prous	SDEI	MP	MP	MP	
DEI-GISHym80274_Pristiphora_prs008_l_Russia	DEI-GISHym80274	*Pristiphora prs008*		larva	Palaearctic	Russia	Primorsky Krai	2016	C. Schmidt		SDEI	MP	MP	MP	
DEI-GISHym86127_Pristiphora_prs008_f_Russia	DEI-GISHym86127	*Pristiphora prs008*	f	adult	Palaearctic	Russia	Primorskiy Kray	2016	K. Kramp, M. Prous & A. Taeger		SDEI	KY698113	KY698196		KY698320
ZMUO.041884_Pristiphora_subbifida_f_Finland	ZMUO.041884	*Pristiphora subbifida*	f	adult	Palaearctic	Finland	Alandia	2019	M. Mutanen, S. Haapala, M. Viitasaari	M. Prous	ZMUO	MP	MP	MP	MP
DEI-GISHym20946_Pristiphora_tetrica_m_Morocco	DEI-GISHym20946	*Pristiphora tetrica*	m	adult	Palaearctic	Morocco	Meknes-Tafilalet Region	2015	A. Liston & M. Prous	M. Prous	SDEI	KY698122	KY698202	MT385410	KY698315
DEI-GISHym12001_Pristiphora_glauca_m_France	DEI-GISHym12001	*Pristiphora glauca*	m	adult	Palaearctic	France	Midi-Pyrenees	2018	H. Savina	M. Prous	SDEI	MP	MP	MP	
DEI-GISHym83826_Pristiphora_glauca_f_Japan	DEI-GISHym83826	*Pristiphora glauca*	f	adult	Palaearctic	Japan	Nagano	2017	A. Taeger	M. Prous	SDEI	MP	MP	MP	
DEI-GISHym84986_Pristiphora_laricis_f_Japan	DEI-GISHym84986	*Pristiphora laricis*	f	adult	Palaearctic	Japan	Honshu	2016	A. Taeger	M. Prous	SDEI	KY698075	KY698231		KY698382
DEI-GISHym84268_Pristiphora_leucopodia_f_Finland	DEI-GISHym84268	*Pristiphora leucopodia*	f	adult	Palaearctic	Finland	Northern Ostrobothnia	2018	SDEI Hym-group	M. Prous	SDEI	MP	MP	MP	MP
DEI-GISHym80059_Pristiphora_nigriceps_m_Germany	DEI-GISHym80059	*Pristiphora nigriceps*	m	adult	Palaearctic	Germany	Brandenburg	2016	M. Prous	M. Prous	SDEI	KY698074	KY698234	MP	KY698381
DEI-GISHym84274_Pristiphora_nigriceps_m_Finland	DEI-GISHym84274	*Pristiphora nigriceps*	m	adult	Palaearctic	Finland	Northern Ostrobothnia	2018	SDEI Hym-group	M. Prous	SDEI	MP	MP	MP	
DEI-GISHym80219_Pristiphora_dasiphorae_l_Sweden	DEI-GISHym80219	*Pristiphora dasiphorae*		larva	Palaearctic	Sweden	Kalmar Laen	2013	A.D. Liston, M. Prous & A. Taeger	M. Prous	SDEI	KY698128	KY698257	MP	KY698379

DEI-GISHym80005_Pristiphora_malaisei_m_Sweden	DEI-GISHym80005	*Pristiphora malaisei*	m	adult	Palaearctic	Sweden	Kalmar Laen	2013	A.D. Liston, M. Prous & A. Taeger	M. Prous	SDEI	KX602589	KY698255	MP	KX602624
DEI-GISHym80112_Pristiphora_malaisei_m_Sweden	DEI-GISHym80112	*Pristiphora malaisei*	m	adult	Palaearctic	Sweden	Torne Lappmark	2016	A. Liston & M. Prous	M. Prous	SDEI	KY698127	KY698256	MW939852	KY698378
ZMUO.058126_Pristiphora_malaisei_l_Finland	ZMUO.058126	*Pristiphora malaisei*		larva	Palaearctic	Finland	Karelia borealis	2021	M. Mutanen, M. Prous, A. Liston	M. Prous	ZMUO	MP	MP	MP	MP
ZMUO.058132_Pristiphora_malaisei_l_Finland	ZMUO.058132	*Pristiphora malaisei*		larva	Palaearctic	Finland	Karelia borealis	2021	M. Mutanen, M. Prous, A. Liston	M. Prous	ZMUO	MP	MP	MP	MP
ZMUO.060609_Pristiphora_atripes_m_Finland	ZMUO.060609	*Pristiphora atripes*	m	adult	Palaearctic	Finland	Lapland	2021	M. Mutanen, M. Prous, A. Liston	M. Prous	ZMUO	MP	MP	MP	MP
ZMUO.045560_Pristiphora_kontuniemii_m_Finland	ZMUO.045560	*Pristiphora kontuniemii*	m	adult	Palaearctic	Finland		2020	M. Mutanen	M. Prous	ZMUO	MP	MP	MP	MP
DEI-GISHym12519_Pristiphora_micronematica_m_Russia	DEI-GISHym12519	*Pristiphora micronematica*	m	adult	Holarctic	Russia	Primorsky Krai	2019	M. Prous & S. Tuerk	M. Prous	SDEI	MP	MP	MP	
ZMUO.030827_Pristiphora_micronematica_m_Finland	ZMUO.030827	*Pristiphora micronematica*	m	adult	Holarctic	Finland		2017	M. Mutanen	M. Prous	ZMUO	MP	MP	MP	
DEI-GISHym80250_Pristiphora_reuteri_m_Sweden	DEI-GISHym80250	*Pristiphora reuteri*	m	adult	Palaearctic	Sweden	Norrbottens Laen	2014	A. Liston & M. Prous	M. Prous	SDEI	KY698087	MP	MP	KY698334
ZMUO.039194_Pristiphora_reuteri_l_Finland	ZMUO.039194	*Pristiphora reuteri*		larva	Palaearctic	Finland	Ostrobottnia ouluensis	2019	M. Mutanen	M. Prous	ZMUO	MP	MP	MP	MP
ZMUO.046515_Pristiphora_reuteri_f_Finland	ZMUO.046515	*Pristiphora reuteri*	f	adult	Palaearctic	Finland	Lapponia enontekiensis	2019	M. Mutanen	M. Mutanen	ZMUO	MP	MP	MP	MP
ZMUO.046510_Pristiphora_sermola_f_Finland	ZMUO.046510	*Pristiphora sermola*	f	adult	Holarctic	Finland	Lapland	2019	M. Mutanen	M. Prous	ZMUO	MP	MP	MP	MP
DEI-GISHym80051_Pristiphora_amphibola_m_Germany	DEI-GISHym80051	*Pristiphora amphibola*	m	adult	Palaearctic	Germany	Brandenburg	2016	A.D. Liston	M. Prous	SDEI	KY698078	KY698250	MP	KY698356
DEI-GISHym80061_Pristiphora_parva_m_Germany	DEI-GISHym80061	*Pristiphora parva*	m	adult	Palaearctic	Germany	Baden-W□rttemberg	2016	SDEI	M. Prous	SDEI	KY698079	KY698251	MP	KY698355
DEI-GISHym86164_Pristiphora_pallidiventris_m_Russia	DEI-GISHym86164	*Pristiphora pallidiventris*	m	adult	Holarctic	Russia	Primorskiy Kray	2016	K. Kramp, M. Prous & A. Taeger	M. Prous	SDEI	KY698108	KY698229	MP	KY698375
DEI-GISHym88341_Pristiphora_pallidiventris_f_Germany	DEI-GISHym88341	*Pristiphora pallidiventris*	f	adult	Holarctic	Germany	Brandenburg	2017	A. Taeger		SDEI	MP	MP	MP	
DEI-GISHym20791_Pristiphora_retusa_m_Sweden	DEI-GISHym20791	*Pristiphora retusa*	m	adult	Palaearctic	Sweden	Norrbottens Laen	2014	A. Liston & M. Prous	M. Prous	SDEI	KX602590	KY698205	MP	KX602623
DEI-GISHym84983_Pristiphora_ruficornis_group_f_Japan	DEI-GISHym84983	*Pristiphora ruficornis_group*	f	adult	Palaearctic	Japan	Nagano	2016	A. Taeger	M. Prous	SDEI	KY698054	KY698187		KY698307
DEI-GISHym31231_Pristiphora_albitibia_m_Estonia	DEI-GISHym31231	*Pristiphora albitibia*	m	adult	Palaearctic	Estonia	Ida-Virumaa	2015	M. Heidemaa	M. Prous	SDEI	KX602572	KY698189		KX602594
DEI-GISHym80357_Pristiphora_albitibia_f_Finland	DEI-GISHym80357	*Pristiphora albitibia*	f	adult	Palaearctic	Finland	Tavastia Proper	2017	V. Vikberg	V. Vikberg	SDEI	MF426916	MF426919		MF426922
DEI-GISHym84540_Pristiphora_astragali_f_Finland	DEI-GISHym84540	*Pristiphora astragali*	f	adult	Palaearctic	Finland	Lapland	2020	M. Mutanen, M. Prous, A. Liston	M. Prous & A. Liston	SDEI	MZ479477	MW939777	MW939849	

ZMUO.058050_Pristiphora_caraganae_m_Finland	ZMUO.058050	*Pristiphora caraganae*	m	adult	Palaearctic	Finland	Karelia australis	2021	M. Mutanen, M. Prous	M. Prous	ZMUO	MP	MP	MP	MP
DEI-GISHym31258_Pristiphora_aphantoneura_f_Estonia	DEI-GISHym31258	*Pristiphora aphantoneura*	f	adult	Palaearctic	Estonia	Viljandimaa	2015	A.D. Liston, M. Prous & A. Taeger	M. Prous	SDEI	KX602529	KY698177	MP	KX602604
DEI-GISHym20748_Pristiphora_beaumonti_l_Morocco	DEI-GISHym20748	*Pristiphora beaumonti*		larva	Palaearctic	Morocco	Marrakech-Tensift-El Haouz Region	2014	A. Liston & M. Prous	M. Prous	SDEI	KY698040	KY698178	MP	KY698301
DEI-GISHym80221_Pristiphora_bifida_f_Sweden	DEI-GISHym80221	*Pristiphora bifida*	f	adult	Palaearctic	Sweden		2016	A.D. Liston	M. Prous	SDEI	KY698048	KY698176		KY698296
DEI-GISHym31265_Pristiphora_confusa_m_Estonia	DEI-GISHym31265	*Pristiphora confusa*	m	adult	Palaearctic	Estonia	Parnumaa	2015	M. Heidemaa	M. Prous	SDEI	KX602551	KY698163	MK624819	KX602597
DEI-GISHym80067_Pristiphora_luteipes_l_Finland	DEI-GISHym80067	*Pristiphora luteipes*		larva	Palaearctic	Finland	Tavastia Proper	2016	V. Vikberg	V. Vikberg	SDEI	KY698034	KY698179	MP	KY698299
DEI-GISHym31311_Pristiphora_opaca_m_Sweden	DEI-GISHym31311	*Pristiphora opaca*	m	adult	Palaearctic	Sweden		2014	A. Taeger	M. Prous	SDEI	KX602552	KY698174	MK624808	KX602607
DEI-GISHym80191_Pristiphora_pusilla_f_Sweden	DEI-GISHym80191	*Pristiphora pusilla*	f	adult	Holarctic	Sweden	Torne Lappmark	2016	A. Liston & M. Prous	M. Prous	SDEI	KY698044	KY698168	MP	KY698286
DEI-GISHym80192_Pristiphora_pusilla_m_Sweden	DEI-GISHym80192	*Pristiphora pusilla*	m	adult	Holarctic	Sweden	Torne Lappmark	2016	A. Liston & M. Prous	M. Prous	SDEI	KY698046	KY698167	MP	KY698287
DEI-GISHym80147_Pristiphora_staudingeri_m_Sweden	DEI-GISHym80147	*Pristiphora staudingeri*	m	adult	Holarctic	Sweden	Torne Lappmark	2016	A. Liston & M. Prous	M. Prous	SDEI	KY698036	KY698165	MP	KY698298
DEI-GISHym80431_Pristiphora_staudingeri_m_Sweden	DEI-GISHym80431	*Pristiphora staudingeri*	m	adult	Holarctic	Sweden	Torne Lappmark	2017	A. Liston & M. Prous	M. Prous	SDEI	MP	MP	MP	
DEI-GISHym83656_Pristiphora_staudingeri_m_Sweden	DEI-GISHym83656	*Pristiphora staudingeri*	m	adult	Holarctic	Sweden	Torne Lappmark	2017	A. Liston & M. Prous	M. Prous	SDEI	MP	MP	MP	
ZMUO.037246_Pristiphora_staudingeri_f_Finland	ZMUO.037246	*Pristiphora staudingeri*	f	adult	Holarctic	Finland		2018	M. Mutanen, N. Mutanen, A. Mutanen	M. Prous	ZMUO	MP	MP	MP	MP
ZMUO.045122_Pristiphora_staudingeri_f_Finland	ZMUO.045122	*Pristiphora staudingeri*	f	adult	Holarctic	Finland	Lapland	2020	M. Mutanen	M. Prous	ZMUO	MP	MP	MP	MP
DEI-GISHym80017_Pristiphora_subopaca_m_Sweden	DEI-GISHym80017	*Pristiphora subopaca*	m	adult	Palaearctic	Sweden	Norrbottens Laen	2014	A. Liston & M. Prous	M. Prous	SDEI	KX602558	KY698172	MP	KX602609
DEI-GISHym80199_Pristiphora_subopaca_m_Sweden	DEI-GISHym80199	*Pristiphora subopaca*	m	adult	Palaearctic	Sweden	Torne Lappmark	2016	A. Liston & M. Prous	M. Prous	SDEI	KY698041	KY698170	MP	KY698292
DEI-GISHym80066_Pristiphora_appendiculata_l_Finland	DEI-GISHym80066	*Pristiphora appendiculata*		larva	Holarctic	Finland	Hame	2016	V. Vikberg	V. Vikberg	SDEI	KY698055	KY698194	MP	KY698312
ZMUO.037234_Pristiphora_appendiculata_m_Finland	ZMUO.037234	*Pristiphora appendiculata*	m	adult	Holarctic	Finland	Lapponia inarensis	2018	M. Mutanen, N. Mutanen, A. Mutanen	M. Prous	ZMUO	MP	MP	MP	MP
DEI-GISHym88374_Pristiphora_armata_m_Germany	DEI-GISHym88374	*Pristiphora armata*	m	adult	Palaearctic	Germany	Brandenburg	2017	A. Taeger		SDEI	MP	MP	MP	
DEI-GISHym88846_Pristiphora_armata_m_Bulgaria	DEI-GISHym88846	*Pristiphora armata*	m	adult	Palaearctic	Bulgaria	Burgas	2018	A. Liston & M. Prous	M. Prous	SDEI	MP	MP	MP	
DEI-GISHym80069_Pristiphora_leucopus_l_Sweden	DEI-GISHym80069	*Pristiphora leucopus*		larva	Palaearctic	Sweden	Oestergotland	2016	A. Liston & M. Prous	M. Prous	SDEI	KY698053	KY698186	MP	KY698306
DEI-GISHym31264_Pristiphora_melanocarpa_m_Estonia	DEI-GISHym31264	*Pristiphora melanocarpa*	m	adult	Holarctic	Estonia	Parnumaa	2015	M. Heidemaa	M. Prous	SDEI	KX602563	KY698182	MP	KX602611
DEI-GISHym83718_Pristiphora_melanocarpa_l_Sweden	DEI-GISHym83718	*Pristiphora melanocarpa*		larva	Holarctic	Sweden	Torne Lappmark	2017	A. Liston & M. Prous	M. Prous	SDEI	MP	MP	MP	

DEI-GISHym12595_Pristiphora_ruficornis_f_Finland	DEI-GISHym12595	*Pristiphora ruficornis*	f	adult	Palaearctic	Finland	Lapland	2020	M. Mutanen, M. Prous, A. Liston	M. Prous & A. Liston	SDEI	MP	MP	MP	
DEI-GISHym20987_Pristiphora_brevis_m_Estonia	DEI-GISHym20987	*Pristiphora brevis*	m	adult	Palaearctic	Estonia	Ida-Virumaa	2015	M. Heidemaa	M. Prous	SDEI	KY698062	KY698220	MP	KY698322
DEI-GISHym31261_Pristiphora_brevis_f_Estonia	DEI-GISHym31261	*Pristiphora brevis*	f	adult	Palaearctic	Estonia	Viljandimaa	2015	O. Lonnve	M. Prous	OLCO	KY698063	KY698221	MP	KY698321
ZMUO.032758_Pristiphora_brevis_m_Finland	ZMUO.032758	*Pristiphora brevis*	m	adult	Palaearctic	Finland		2017	Marko Mutanen		ZMUO	MZ656456	MP	MP	MP
ZMUO.032411_Pristiphora_rufipes_m_Finland	ZMUO.032411	*Pristiphora rufipes*	m	adult	Palaearctic	Finland		2017	Marko Mutanen	M. Prous	ZMUO	MZ656591	MP	MP	MP
ZMUO.032974_Pristiphora_rufipes_m_Finland	ZMUO.032974	*Pristiphora rufipes*	m	adult	Palaearctic	Finland		2017		M. Prous	ZMUO	MZ658578	MP	MP	MP
DEI-GISHym11428_Pristiphora_thalictri_m_United_Kingdom	DEI-GISHym11428	*Pristiphora thalictri*	m	adult	Palaearctic	United Kingdom	Scotland	2010	S. M. Blank, A. D. Liston & A. Taeger	A. D. Liston	SDEI	KC972652	MP	MP	
DEI-GISHym31030_Pristiphora_angulata_m_Sweden	DEI-GISHym31030	*Pristiphora angulata*	m	adult	Palaearctic	Sweden	Norrbottens Laen	2014	A. Liston & M. Prous	M. Prous	SDEI	KY698111	KY698227		KY698365
DEI-GISHym80701_Pristiphora_werzhutskii_f_Russia	DEI-GISHym80701	*Pristiphora werzhutskii*	f	adult	Palaearctic	Russia	Primorskiy Kray	2019	M. Prous	M. Prous	SDEI	MP	MP	MP	
NAPr_039_lena_m_Quebec	BIOUG11585-F03	*Pristiphora lena*	m	adult	Nearctic	Canada	Quebec	2013	Medo Toure	S.K. Monckton	BIOUG	NAPr_039	NAPr_039		NAPr_039
NAPr_047_sycophanta_m_Yukon		*Pristiphora sycophanta*	m	adult	Nearctic	Canada	Yukon	2018	S.K. Monckton	S.K. Monckton	PCYU	NAPr_047	NAPr_047	NAPr_047	NAPr_047
NAPr_050_frigida_m_Yukon		*Pristiphora frigida*	m	adult	Holarctic	Canada	Yukon	2018	S.K. Monckton	S.K. Monckton	PCYU	NAPr_050	NAPr_050	NAPr_050	NAPr_050
NAPr_051_margeta_f_Yukon		*Pristiphora margeta*	f	adult	Nearctic	Canada	Yukon	2018	S.K. Monckton	S.K. Monckton	PCYU	NAPr_051	NAPr_051	NAPr_051	NAPr_051
NAPr_092_litura_m_Ontario		*Pristiphora litura*	m	adult	Nearctic	Canada	Ontario	2019	S.K. Monckton	S.K. Monckton	PCYU	NAPr_092	NAPr_092	NAPr_092	NAPr_092
NAPr_107_serrula_f_Nova-Scotia	BIOUG19562-C04	*Pristiphora serrula*	f	adult	Nearctic	Canada	Nova Scotia	2014	B.McLean	S.K. Monckton	BIOUG	NAPr_107	NAPr_107		NAPr_107
NAPr_109_chlorea_f_Ontario	BIOUG08485-D05	*Pristiphora chlorea*	f	adult	Nearctic	Canada	Ontario	2013	L.Attard, K.Greenham	S.K. Monckton	BIOUG	NAPr_109	NAPr_109		NAPr_109
NAPr_110_chlorea_m_Ontario	BIOUG22289-H04	*Pristiphora chlorea*	m	adult	Nearctic	Canada	Ontario	2015	BIO Collections Staff	S.K. Monckton	BIOUG	NAPr_110	NAPr_110	NAPr_110	NAPr_110
NAPr_111_chlorea_m_Florida	10BBHYM-0743	*Pristiphora chlorea*	m	adult	Nearctic	USA	Florida	2010	Biobus 2010	S.K. Monckton	BIOUG	NAPr_111	NAPr_111	NAPr_111	NAPr_111
NAPr_112_lena_m_Haida-Gwaii	BIOUG22070-F07	*Pristiphora lena*	m	adult	Nearctic	Canada	British Columbia	2015	Stephen Querengesser	S.K. Monckton	BIOUG	NAPr_112		NAPr_112	NAPr_112
NAPr_113_leechi_f_Oregon		*Pristiphora leechi*	f	adult	Nearctic	USA	Oregon			S.K. Monckton	USNM	NAPr_113	NAPr_113	NAPr_113	NAPr_113
NAPr_115_appalachianum_f_Virginia		*Pristiphora appalachianum*	f	adult	Nearctic	USA	Virginia			S.K. Monckton	USNM	NAPr_115	NAPr_115		NAPr_115
NAPr_116_acidovalva_m_Quebec	BIOUG10223-D02	*Pristiphora acidovalva*	m	adult	Nearctic	Canada	Quebec	2013	F.Tremblay	S.K. Monckton	BIOUG		NAPr_116	NAPr_116	NAPr_116
NAPr_118_fructicola _Colorado	MTEC 018155	*Pristiphora fructicola*			Nearctic	USA	Colorado			S.K. Monckton	USNM	NAPr_118	NAPr_118	NAPr_118	NAPr_118
NAPr_121_flavipectus_f_Georgia	UGCA 027528	*Pristiphora flavipectus*	f	adult	Nearctic	USA	Georgia			S.K. Monckton	USNM	NAPr_121			NAPr_121
NAPr_122_maura_f_Ontario	BIOUG25703-G03	*Pristiphora maura*	f	adult	Nearctic	Canada	Yukon	2014	Mary Whitley	S.K. Monckton	BIOUG	NAPr_122	NAPr_122	NAPr_122	NAPr_122
NAPr_123_acidovalva_f_Ontario	BIOUG32796-E08	*Pristiphora acidovalva*	f	adult	Nearctic	Canada	Ontario	2014	CBG Collections Staff	S.K. Monckton	BIOUG		NAPr_123	NAPr_123	NAPr_123

NAPr_124_bivittata_USA		*Pristiphora bivittata*			Nearctic	USA					S.K. Monckton	USNM	NAPr_124	NAPr_124	NAPr_124		
NAPr_126_macnabi_Canada		*Pristiphora macnabi*			Nearctic	Canada					S.K. Monckton	LEMU	NAPr_126	NAPr_126	NAPr_126		
NAPr_152_lena_f_New-Mexico		*Pristiphora lena*	f	adult	Nearctic	USA	New Mexico				S.K. Monckton	USNM	NAPr_152	NAPr_152	NAPr_152	NAPr_152	
NAPr_153_sootryeni_f_Manitoba	BIOUG00998-F06	*Pristiphora sootryeni*	f	adult	Holarctic	Canada	Manitoba	2010	J Wang		S.K. Monckton	BIOUG	NAPr_153	NAPr_153	NAPr_153	NAPr_153	
NAPr_155_maura_f_Alberta	BIOUG08963-G07	*Pristiphora maura*	f	adult	Nearctic	Canada	Alberta	2012	BIOBus 2012		S.K. Monckton	BIOUG	NAPr_155	NAPr_155		NAPr_155	
NAPr_156_hucksena_f_BC		*Pristiphora hucksena*	f	adult	Nearctic	Canada	British Columbia				S.K. Monckton	RBCM	NAPr_156	NAPr_156			
NAPr_157_paloma_f_Kentucky		*Pristiphora paloma*	f	adult	Nearctic	USA	Kentucky				S.K. Monckton	USNM		NAPr_157	NAPr_157	NAPr_157	
NAPr_158_pusilla_m_BC	BIOUG19682-A05	*Pristiphora pusilla*	m	adult	Holarctic	Canada	British Columbia	2014	Jamie		S.K. Monckton	BIOUG		NAPr_158	NAPr_158	NAPr_158	
NAPr_160_siskiyouensis_f_Kentucky		*Pristiphora siskiyouensis*	f	adult	Nearctic	USA	Kentucky				S.K. Monckton	USNM	NAPr_160				
NAPr_168_siskiyouensis_m_Massachusetts	CSE3860	*Pristiphora siskiyouensis*	m	adult	Nearctic	USA	Massachusetts				S.K. Monckton	USNM	NAPr_168	NAPr_168	NAPr_168	NAPr_168	
NAPr_179_staudingeri_m_Nunavut		*Pristiphora staudingeri*	m	adult	Holarctic	Canada	Nunavut	2010	NBP field party		S.K. Monckton	LEMU	NAPr_179	NAPr_179	NAPr_179	NAPr_179	
NAPr_187_staudingeri_m_Yukon		*Pristiphora staudingeri*	m	adult	Holarctic	Canada	Yukon	2011	NBP field party		S.K. Monckton	LEMU	NAPr_187	NAPr_187	NAPr_187	NAPr_187	
NAPr_225_mollis_f_Quebec		*Pristiphora mollis*	f	adult	Holarctic	Canada	Quebec	2010	NBP field party		S.K. Monckton	LEMU	NAPr_225	NAPr_225	NAPr_225	NAPr_225	
NAPr_230_appendiculata_m_BC		*Pristiphora appendiculata*		adult	Holarctic	Canada	British Columbia				S.K. Monckton	RBCM	NAPr_230	NAPr_230	NAPr_230	NAPr_230	
NAPr_232_insularis_Canada		*Pristiphora insularis*		adult	Holarctic						S.K. Monckton	USNM		NAPr_232	NAPr_232	NAPr_232	
NAPr_233_melanocarpa_f_Labrador		*Pristiphora melanocarpa*	f	adult	Holarctic	Canada	Newfoundland and Labrador				S.K. Monckton	LEMU	NAPr_233		NAPr_233	NAPr_233	
NAPr_236_flavipectus_f_Virginia		*Pristiphora flavipectus*	f	adult	Nearctic	USA	Virginia	2018	D.R. Smith, O.S. Flint		S.K. Monckton	USNM	NAPr_236	NAPr_236	NAPr_236	NAPr_236	
NAPr_239_pallidiventris_f_Quebec	BIOUG10545-B07	*Pristiphora pallidiventris*	f	adult	Holarctic	Canada	Quebec	2013	F.Tremblay		S.K. Monckton	BIOUG			NAPr_239	NAPr_239	
NAPr_240_pallidiventris_f_Manitoba	BIOUG17865-A07	*Pristiphora pallidiventris*	f	adult	Holarctic	Canada	Manitoba	2014	D.Iles		S.K. Monckton	BIOUG	NAPr_240	NAPr_240	NAPr_240		
NAPr_241_pallidiventris_f_Kentucky		*Pristiphora pallidiventris*	f	adult	Holarctic	USA	Kentucky				S.K. Monckton	USNM	NAPr_241		NAPr_241	NAPr_241	
NAPr_242_cincta_m_Arkansas		*Pristiphora cincta*	m	adult	Holarctic	USA	Arkansas				S.K. Monckton	USNM		NAPr_242	NAPr_242	NAPr_242	
NAPr_244_abbreviata_f_Virginia		*Pristiphora abbreviata*	f	adult	Palaearctic	USA	Virginia				S.K. Monckton	USNM	NAPr_244	NAPr_244	NAPr_244	NAPr_244	
NAPr_245_mollis_Canada		*Pristiphora mollis*			Holarctic	Canada					S.K. Monckton	LEMU	NAPr_245		NAPr_245	NAPr_245	
NAPr_246_melanocarpa_Canada		*Pristiphora melanocarpa*			Holarctic	Canada					S.K. Monckton	LEMU	NAPr_246	NAPr_246	NAPr_246	NAPr_246	
NAPr_247_micronematica-gp-1_Canada		*Pristiphora micronematica_group_1*			Nearctic	Canada					S.K. Monckton	LEMU	NAPr_247		NAPr_247	NAPr_247	
NAPr_248_mollis_Canada		*Pristiphora mollis*			Holarctic	Canada					S.K. Monckton	LEMU	NAPr_248	NAPr_248	NAPr_248	NAPr_248	
NAPr_249_mollis_Canada		*Pristiphora mollis*			Holarctic	Canada					S.K. Monckton	LEMU	NAPr_249	NAPr_249	NAPr_249	NAPr_249	
NAPr_250_mollis_Canada		*Pristiphora mollis*			Holarctic	Canada					S.K. Monckton	LEMU	NAPr_250	NAPr_250	NAPr_250	NAPr_250	
NAPr_251_nigra_Canada	CCDB-34571 G10	*Pristiphora nigra*			Nearctic	Canada					S.K. Monckton	LEMU		NAPr_251		NAPr_251	

NAPr_252_nigra_Canada	CCDB-34571 H01	*Pristiphora nigra*			Nearctic	Canada					S.K. Monckton	LEMU				NAPr_252
NAPr_253_ferruginosa_Canada	DBUC 201200973 / 10BBCHY-0643*	*Pristiphora ferruginosa*			Nearctic	Canada	British Columbia				S.K. Monckton	DBUC	BOLD	NAPr_253		NAPr_253
NAPr_254_ferruginosa_Canada	DBUC 201200989 / DEI-GISHym11596*	*Pristiphora ferruginosa*			Nearctic	Canada	British Columbia				S.K. Monckton	DBUC	BOLD	NAPr_254		NAPr_254
NAPr_255_micronematica-gp-2_f_Ontario	BIOUG21912-E01	*Pristiphora micronematica_group_2*	f	adult	Nearctic	Canada	Ontario	2015	Jeramie Jenkins		S.K. Monckton	BIOUG	NAPr_255	NAPr_255	NAPr_255	NAPr_255
NAPr_256_micronematica-gp-3_m_Alberta	BIOUG05235-F08	*Pristiphora micronematica_group_3*	m	adult	Nearctic	Canada	Alberta	2012	BIOBus		S.K. Monckton	BIOUG	NAPr_256	NAPr_256	NAPr_256	NAPr_256

Table A2. Primers used for PCR and sequencing, including target locus, direction (F = forward; R = reverse), primer sequence, PCR annealing temperature, usage for PCR and/or sequencing, and reference.

Locus	Primer name	Direction	Sequence (5'–3')	PCR annealing temperature (°C)	Usage	Reference
COI	SymF4	F	AAATGATTATTYTCWACWAATCAYAA	50	PCR, seq	Prous et al. 2019
COI	A2590	R o	GCTCCTATTGATARWACATARTGRAAATG	49	PCR, seq	Normark et al. 1999
NaK	NaK_263F	F o	CTYAGCCAYGCRAARGCRAARGA	59	PCR, seq	Prous et al. 2017
NaK	NaK_809F	F i/o	GCWTTYTTCTCNACSAAYGCSGTNGARGG	55	seq	Prous et al. 2017
NaK	NaK_907Ri	R i/o	TGRATRAARTGRTGRATYTCYTTIGC	54	seq	Prous et al. 2017
NaK	NaK_1250Fv2	F	ATGTGGTTYGAYAAYCARATHATIGA	56	PCR, seq	Prous et al. 2019
NaK	NaK_1918R	R o	GATTTGGCAATNGCTTTGGCAGTDAT	59	PCR, seq	Prous et al. 2017
POL2	POL2_104Fv2	F	CGNATGTCNGTNACNGAYGGIGG	60	PCR, seq	Prous et al. 2019
POL2	POL2_797F	F	ATGTAYGGNTCNGCNAARAAYCARGA	58	PCR, seq	Prous et al. 2019
POL2	POL2_928R	R	GGCATNCCNGGCATRTCRTTRTCNAC	59	PCR, seq	Prous et al. 2019
POL2	POL2_1706F	F	TGGGAYGGNAARATGCCNCARCC	60	PCR, seq	Prous et al. 2019
POL2	POL2_1732R	R	GARAADATYTGYTTNCCNGTCCA	55	seq	Prous et al. 2019
POL2	POL2_2569R	R	TGNACCATNACNGAYTCCATAGCYTTDAT	60	PCR, seq	Prous et al. 2019
TPI	TPI_29Fi	F o	GYAAATTYTTYGTTGGNGGIAA	52	PCR, seq	Prous et al. 2016
TPI	TPI706R	R o	ACNATYTGTACRAARTCWGGYTT	52	PCR, seq	Prous et al. 2016
TPI	TPI 111Fb	F o	GGNAAYTGGAARATGAAYGG	56	PCR, seq	Bertone et al. 2008
TPI	TPI 275Ri	R o	GCCCANACNGGYTCRTAIGC	56	PCR, seq	Malm and Nyman 2015

Appendix B: Supplementary data (Chapter 4)

Table B1. Specimens sampled for hyRAD library capture, including those used to generate RAD probes (shaded rows) Specimens were assigned to eleven locations based on geographic proximity. Numbers of raw and filtered sequencing reads are indicated for 70 out of 72 specimens for which library preparation was successful. Populations used for DIYABC that differ from the originally-assigned locations are indicated in bold. Clusters inferred by fastStructure are provided as a Q-matrix, indicating proportional membership in each cluster, for each individual.

Sample no.	Collection	Country	Province /State	Locality	Latitude	Longitude	Date	Assigned location	Population for DIYABC	Raw reads	Filtered reads	Assigned DAPC cluster	Membership proportion by cluster # (fastStructure Q-matrix)						
													1	2	3	4	5	6	7
SKM.NAPr.095	PCYU	Canada	ON	Kawartha Highlands Provincial Park	44.67284	-78.34492	2019	-	-	-	-	-	-	-	-	-	-	-	-
SKM.NAPr.161	USNM	USA	OR	Corvallis	44.565	-123.262	2018	-	-	-	-	-	-	-	-	-	-	-	-
SKM.NAPr.165	USNM	USA	VA	Bull Run Mountain	38.867	-77.704	2017	-	-	-	-	-	-	-	-	-	-	-	-
SKM.NAPr.170	BIOUG	Canada	NT	Nahanni National Park Reserve	61.606	-125.758	2014	-	-	-	-	-	-	-	-	-	-	-	-
SKM.NAPr.217	LEMU	Canada	YT	Tombstone Territorial Park, North Fork Pass	64.59915	-138.30611	2011	-	-	-	-	-	-	-	-	-	-	-	-
PRC_C_129	CNC	USA	AK	Naknek, on tundra	58.728	-157.014	1952	AK/YT	AK/YT	3,995,696	3,640,042 (91.1%)	5	-	-	-	-	1.00	-	-
PRC_C_131	CNC	USA	AK	Naknek, on tundra	58.728	-157.014	1952	AK/YT	AK/YT	1,230,990	1,108,440 (90.0%)	1	0.96	-	-	0.04	-	-	-
PRC_C_133	CNC	USA	AK	Naknek, on tundra	58.728	-157.014	1952	AK/YT	AK/YT	2,235,020	2,014,998 (90.2%)	1	1.00	-	-	-	-	-	-
PRC_C_561	CNC	USA	AK	Naknek	58.728	-157.014	1952	AK/YT	AK/YT	2,896,620	2,606,298 (90.0%)	1	0.39	-	0.09	0.27	0.25	-	-
PRC_C_527	CNC	USA	AK	King Salmon, Naknek R.	58.688	-156.662	1952	AK/YT	AK/YT	5,164,040	4,601,222 (89.1%)	2	-	1.00	-	-	-	-	-
PRC_C_209	CNC	Canada	YT	Dawson	64.061	-139.432	1949	AK/YT	AK/YT	9,278,968	8,361,604 (90.1%)	1	0.32	-	0.11	0.23	0.34	-	-
PRC_C_036	CNC	Canada	YT	North Fork Crossing Mi.42 Peel Plt. Rd	64.467	-138.250	1962	AK/YT	AK/YT	2,570,976	2,319,910 (90.2%)	2	-	1.00	-	-	-	-	-
PRC_C_037	CNC	Canada	YT	North Fork Crossing Mi.42 Peel Plt. Rd	64.467	-138.250	1962	AK/YT	AK/YT	5,813,274	5,193,134 (89.3%)	1	0.87	-	-	-	0.13	-	-
PRC_C_412	CNC	Canada	YT	La Force L.	62.683	-132.333	1960	AK/YT	AK/YT	1,947,626	1,757,708 (90.2%)	5	-	-	-	-	1.00	-	-
PRC_C_413	CNC	Canada	YT	La Force L.	62.683	-132.333	1960	AK/YT	AK/YT	5,490,216	4,940,924 (90.0%)	5	-	-	-	-	1.00	-	-
PRC_C_276	CNC	Canada	BC	Nitinat R.	48.667	-124.850	1949	BC/AB	**WNA**	2,035,426	1,850,120 (90.9%)	4	-	-	-	1.00	-	-	-
PRC_C_274	CNC	Canada	BC	Langford	48.450	-123.505	1956	BC/AB	**WNA**	4,711,950	4,198,262 (89.1%)	4	-	-	-	1.00	-	-	-
PRC_C_246	CNC	Canada	BC	Robson	49.334	-117.695	1949	BC/AB	**WNA**	6,061,922	5,425,110 (89.5%)	4	-	-	-	1.00	-	-	-
PRC_C_231	CNC	Canada	AB	Whitehorn Lift L.Louise	51.454	-116.147	1962	BC/AB	**WNA**	2,892,784	2,641,914 (91.3%)	2	-	1.00	-	-	-	-	-
PRC_C_206	CNC	Canada	AB	Banff, Castle Junction [Eisenhower Jct.]	51.269	-115.918	1962	BC/AB	**WNA**	2,803,072	2,538,646 (90.6%)	2	-	1.00	-	-	-	-	-
PRC_C_481	CNC	Canada	AB	Banff, Castle Junction [Eisenhower Jct.]	51.269	-115.918	1962	BC/AB	**WNA**	6,546,376	5,865,536 (89.6%)	3	-	-	1.00	-	-	-	-

PRC_C_482	CNC	Canada	AB	Banff, Castle Junction [Eisenhower Jct.]	51.269	-115.918	1962	BC/AB	**WNA**	7,651,120	6,914,672 (90.4%)	3	-	-	1.00	-	-	-	-
PRC_C_483	CNC	Canada	AB	Banff, Castle Junction [Eisenhower Jct.]	51.269	-115.918	1962	BC/AB	**WNA**	5,469,238	4,886,520 (89.3%)	3	-	-	1.00	-	-	-	-
PRC_C_198	CNC	USA	CO	Corona Pass Boulder Co. Marshy Meadow at Timberline	39.936	-105.654	1961	COL	**WNA**	4,264,210	3,835,166 (89.9%)	2	-	1.00	-	-	-	-	-
PRC_C_016	CNC	USA	CO	Doolittle Ranch, Mt. Evans	39.675	-105.601	1961	COL	**WNA**	3,557,850	3,206,620 (90.1%)	2	-	1.00	-	-	-	-	-
PRC_C_571	CNC	USA	CO	Niwot Ridge nr Ward	40.055	-105.595	1961	COL	**WNA**	1,784,300	1,614,258 (90.5%)	2	-	1.00	-	-	-	-	-
PRC_C_589	CNC	USA	CO	Niwot Ridge nr Ward	40.055	-105.595	1961	COL	**WNA**	1,690,098	1,522,198 (90.1%)	2	-	1.00	-	-	-	-	-
PRC_C_261	CNC	USA	CO	Mt. Evans, Timberline	39.644	-105.593	1961	COL	**WNA**	3,287,366	2,909,816 (88.5%)	4	-	-	-	1.00	-	-	-
PRC_C_242	CNC	Canada	NT	Salmita Mines	64.083	-111.250	1953	NT/NU	NU/NT	5,006,892	4,538,422 (90.6%)	4	-	-	-	1.00	-	-	-
PRC_C_335	CNC	Canada	NT	Muskox L.	64.750	-108.167	1953	NT/NU	NU/NT	5,455,234	4,934,130 (90.4%)	2	-	1.00	-	-	-	-	-
PRC_C_336	CNC	Canada	NT	Muskox L.	64.750	-108.167	1953	NT/NU	NU/NT	6,152,440	5,557,592 (90.3%)	2	-	1.00	-	-	-	-	-
PRC_C_338	CNC	Canada	NT	Muskox L.	64.750	-108.167	1953	NT/NU	NU/NT	6,205,682	5,479,376 (88.3%)	5	-	-	-	-	1.00	-	-
PRC_C_343	CNC	Canada	NT	Muskox L.	64.750	-108.167	1953	NT/NU	NU/NT	2,840,396	2,553,430 (89.9%)	5	-	-	-	-	1.00	-	-
PRC_C_507	CNC	Canada	NU	Padlei [Padley]	61.933	-96.650	1950	NT/NU	NU/NT	4,299,604	3,919,734 (91.2%)	5	0.09	-	-	0.02	0.43	0.46	-
PRC_C_509	CNC	Canada	NU	Padlei [Padley]	61.933	-96.650	1950	NT/NU	NU/NT	1,185,678	1,081,218 (91.2%)	7	-	-	-	-	-	-	1.00
PRC_C_236	CNC	Canada	MB	Fort Churchill	58.756	-94.084	1952	NT/NU	NU/NT	6,340,810	5,570,046 (87.8%)	2	-	1.00	-	-	-	-	-
PRC_C_425	CNC	Canada	MB	Fort Churchill	58.756	-94.084	1952	NT/NU	NU/NT	9,971,540	8,948,006 (89.7%)	2	-	1.00	-	-	-	-	-
PRC_C_232	CNC	Canada	MB	Farnworth L. nr. Churchill	58.705	-94.051	1952	NT/NU	NU/NT	2,596,088	2,330,100 (89.8%)	5	-	-	-	-	-	1.00	-
PRC_C_266	CNC	Canada	ON	One Sided Lake	49.060	-93.895	1960	WGL	**ENA**	4,692,388	4,160,780 (88.7%)	6	-	-	-	1.00	-	-	-
PRC_C_547	CNC	Canada	ON	5mi E. Willard Lk	49.846	-93.871	1960	WGL	**ENA**	2,859,252	2,556,494 (89.4%)	7	-	-	-	-	-	-	1.00
PRC_U_236	USNM	USA	MI	Iron Co., Mich.	46.098	-88.334	1967	WGL	**ENA**	4,822,268	4,213,428 (87.4%)	6	-	-	-	1.00	-	-	-
PRC_U_237	USNM	USA	MI	Iron Co., Mich.	46.098	-88.334	1967	WGL	**ENA**	7,815,612	7,073,692 (90.5%)	6	-	-	-	1.00	-	-	-
PRC_C_451	CNC	Canada	ON	St. Lawrence Islands National Park	44.353	-75.955	1975	EON	**ENA**	5,823,736	5,272,512 (90.5%)	7	-	-	-	-	-	-	1.00
PRC_C_252	CNC	Canada	ON	S. March	45.356	-75.933	1945	EON	**ENA**	5,496,822	4,976,394 (90.5%)	7	-	-	-	-	-	-	1.00
PRC_C_248	CNC	Canada	ON	Rockport	44.379	-75.933	1959	EON	**ENA**	2,576,616	2,306,210 (89.5%)	7	0.03	-	-	-	-	-	0.97
PRC_C_050	CNC	Canada	ON	Mer Bleue	45.400	-75.500	1937	EON	**ENA**	6,086,766	5,436,688 (89.3%)	5	-	-	-	-	0.54	0.46	-
PRC_U_156	USNM	USA	VA	Smyth Co., Va.	36.836	-81.530	1979	EUS	**ENA**	2,388,204	2,146,378 (89.9%)	6	-	-	-	0.93	-	-	0.07
PRC_U_157	USNM	USA	VA	Giles Co., VA	37.309	-80.710	1978	EUS	**ENA**	2,094,312	1,901,046 (90.8%)	4	-	-	-	1.00	-	-	-
PRC_U_121	USNM	USA	VA	Mt. Lake, Va.	37.355	-80.538	1934	EUS	**ENA**	2,424,080	2,202,414 (90.9%)	7	-	-	-	-	-	-	1.00
PRC_U_120	USNM	USA	VA	Mt. Lake, Va.	37.355	-80.538	1935	EUS	**ENA**	3,906,542	3,519,948 (90.1%)	7	-	-	-	-	-	-	1.00
PRC_U_166	USNM	USA	VA	Louisa Co., 4 mi. S Cuckoo	37.899	-77.896	1985	EUS	**ENA**	1,694,458	1,531,104 (90.4%)	4	-	-	-	1.00	-	-	-

PRC_C_199	CNC	Canada	QC	Kangirsuk [Payne Bay]	60.025	-69.997	1958	UGV	UGV	2,602,788	2,349,142 (90.3%)	5	-	-	-	-	-	1.00	-
PRC_C_179	CNC	Canada	QC	Ft. Chimo	58.100	-68.400	1949	UGV	UGV	1,955,190	1,741,732 (89.1%)	5	-	0.49	-	-	-	0.51	-
PRC_C_174	CNC	Canada	QC	Ft. Chimo	58.100	-68.400	1954	UGV	UGV	3,892,042	3,493,830 (89.8%)	3	-	-	1.00	-	-	-	-
PRC_C_178	CNC	Canada	QC	Ft. Chimo	58.100	-68.400	1954	UGV	UGV	6,261,152	5,618,496 (89.7%)	5	-	-	-	-	-	1.00	-
PRC_C_249	CNC	Canada	LB	Okak Bay	57.433	-62.417	1954	UGV	UGV	2,536,090	2,240,416 (88.3%)	2	-	1.00	-	-	-	-	-
PRC_C_152	CNC	Canada	LB	Nutak	57.481	-61.834	1954	UGV	UGV	1,883,316	1,703,774 (90.5%)	5	-	-	-	-	-	1.00	-
PRC_C_083	CNC	Canada	LB	Cartwright	53.706	-57.020	1955	UGV	UGV	5,349,876	4,691,482 (87.7%)	5	-	-	-	-	-	1.00	-
PRC_C_277	CNC	Canada	QC	Mare-du-Sault	47.413	-71.196	1959	ATL	ATL	3,336,844	3,009,324 (90.2%)	6	-	-	-	1.00	-	-	-
PRC_C_211	CNC	Canada	QC	Saint-Joachims	47.06	-70.849	1954	ATL	-	0	-	6	0.04	-	-	0.96	-	-	-
PRC_C_183	CNC	Canada	QC	Parke Reserve Kam Co.	47.588	-69.507	1957	ATL	ATL	2,220,272	1,991,006 (89.7%)	7	-	-	-	-	-	-	1.00
PRC_C_592	CNC	Canada	NB	Charlotte Co.	45.227	-66.931	1951	ATL	ATL	11,892,622	10,477,802 (88.1%)	7	-	-	-	-	-	-	1.00
PRC_C_593	CNC	Canada	NB	Charlotte Co.	45.227	-66.931	1954	ATL	ATL	2,652,104	2,394,470 (90.3%)	5	-	-	-	-	-	1.00	-
PRC_C_245	CNC	Canada	NS	S. Milford	44.574	-65.400	1934	ATL	ATL	2,588,772	2,341,924 (90.5%)	5	-	-	-	-	-	1.00	-
PRC_C_479	CNC	Canada	NS	Lockeport	43.696	-65.111	1958	ATL	ATL	6,069,868	5,483,940 (90.3%)	5	-	-	-	-	-	1.00	-
PRC_C_480	CNC	Canada	NS	Lockeport	43.696	-65.111	1958	ATL	ATL	2,477,504	2,217,230 (89.5%)	2	-	1.00	-	-	-	-	-
PRC_U_174	USNM	Ireland		Upper Glenasmole, Co. DU.	53.233	-6.356	1927	EUR	EUR	6,615,096	5,993,978 (90.6%)	2	-	1.00	-	-	-	-	-
PRC_U_180	USNM	Ireland		Upper Dodder, Co. DU.	53.222	-6.339	1950	EUR	-	0	-	2	-	1.00	-	-	-	-	-
PRC_U_175	USNM	Ireland		Clara, Co. WI.	52.969	-6.255	1929	EUR	EUR	3,887,088	3,509,482 (90.3%)	2	-	1.00	-	-	-	-	-
PRC_C_259	CNC	Sweden		Riksgränsen	68.427	18.122	1951	EUR	EUR	4,899,820	4,402,438 (89.8%)	2	-	1.00	-	-	-	-	-
PRC_C_154	CNC	Sweden		Abisko	68.350	18.830	1951	EUR	EUR	3,861,892	3,441,474 (89.1%)	5	0.06	-	-	-	0.94	-	-
PRC_C_258	CNC	Sweden		Jebrenjokk	68.439	18.888	1951	EUR	EUR	8,521,022	7,647,332 (89.7%)	1	1.00	-	-	-	-	-	-
PRC_C_207	CNC	Sweden		Muodaslompolo	67.943	23.426	1951	EUR	EUR	6,558,348	5,783,114 (88.2%)	1	1.00	-	-	-	-	-	-
PRC_U_135	USNM	Korea		JIRISAN Hamyang Songjeon-li Munsu-sa	35.412	127.730	2005	KOR	KOR	6,275,490	5,656,244 (90.1%)	1	1.00	-	-	-	-	-	-
PRC_U_136	USNM	Korea		JIRISAN Hamyang Songjeon-li Munsu-sa	35.412	127.730	2005	KOR	KOR	10,657,928	9,539,796 (89.5%)	1	1.00	-	-	-	-	-	-
PRC_U_137	USNM	Korea		JIRISAN Hamyang Songjeon-li Munsu-sa	35.412	127.730	2005	KOR	KOR	6,967,730	6,119,588 (87.8%)	5	-	-	-	-	1.00	-	-
PRC_U_138	USNM	Korea		JIRISAN Hamyang Songjeon-li Munsu-sa	35.412	127.730	2005	KOR	KOR	2,539,800	2,289,408 (90.1%)	1	0.96	-	-	0.04	-	-	-

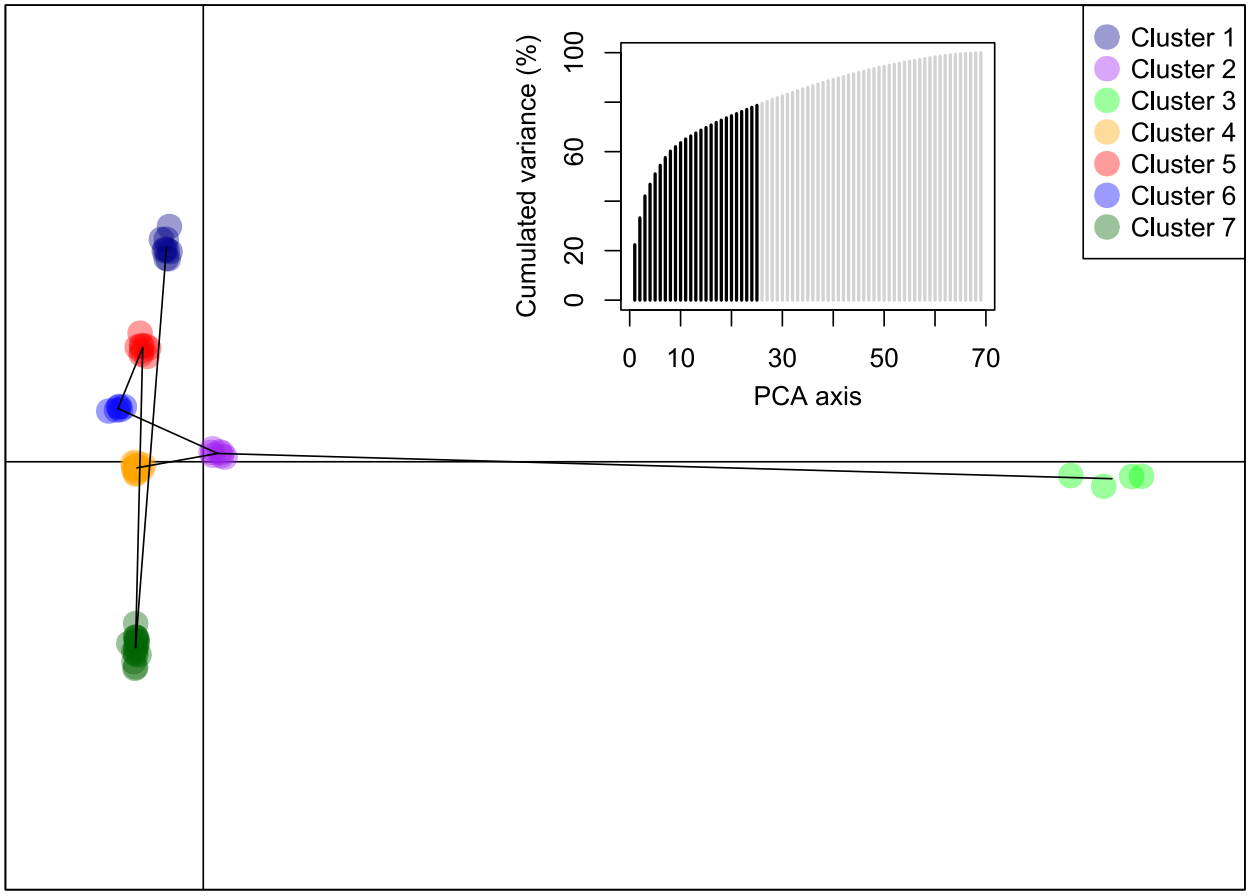

Figure B1. Results of discriminant analysis of principal components (DAPC) showing individual assignment to genetic clusters on two principal component axes. A minimum spanning tree based on squared genetic distances between groups is overlaid. Inset shows a bar plot of PCA eigenvalues retained during the dimension-reduction step of the DAPC analysis. Cluster numbers are arbitrary.

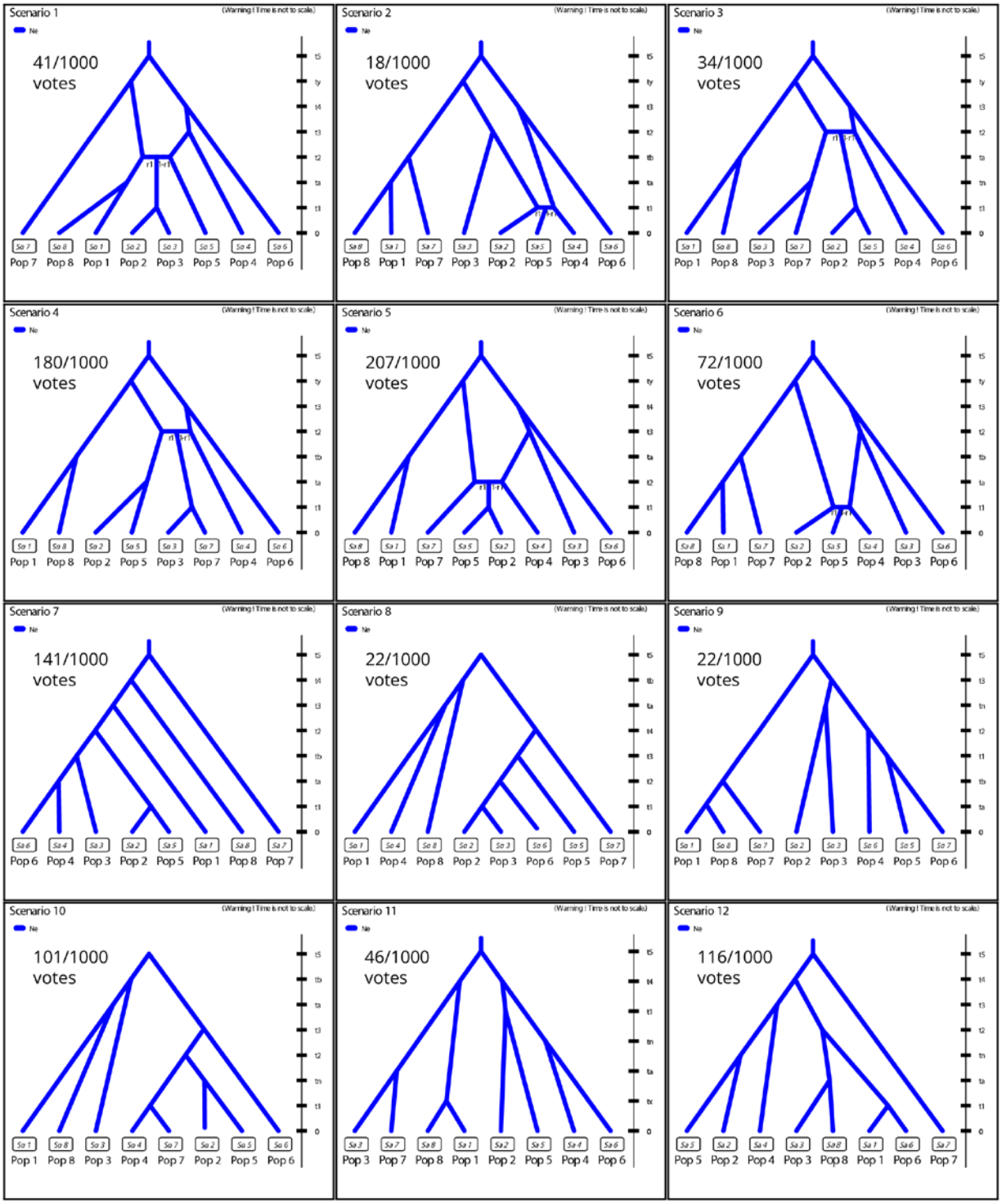

Figure B2. Scenarios used in first round of DIYABC analysis. A total of 48,000 datasets were simulated using uniform priors for population sizes (10-10,000 individuals), time parameters (10-100,000 years), and admixture rate (0.1-0.99). Random forest search was performed with 1000 trees. The number of votes for each scenario is noted. Scenario 5 was selected with a posterior probability of 0.98. Populations are numbered as follows: Pop 1 = AK/YT; Pop 2 = WNA; Pop 3 = NT/NU; Pop 4 = UGV; Pop 5 = ATL; Pop 6 = ENA; Pop 7 = EUR; Pop 8 = KOR.

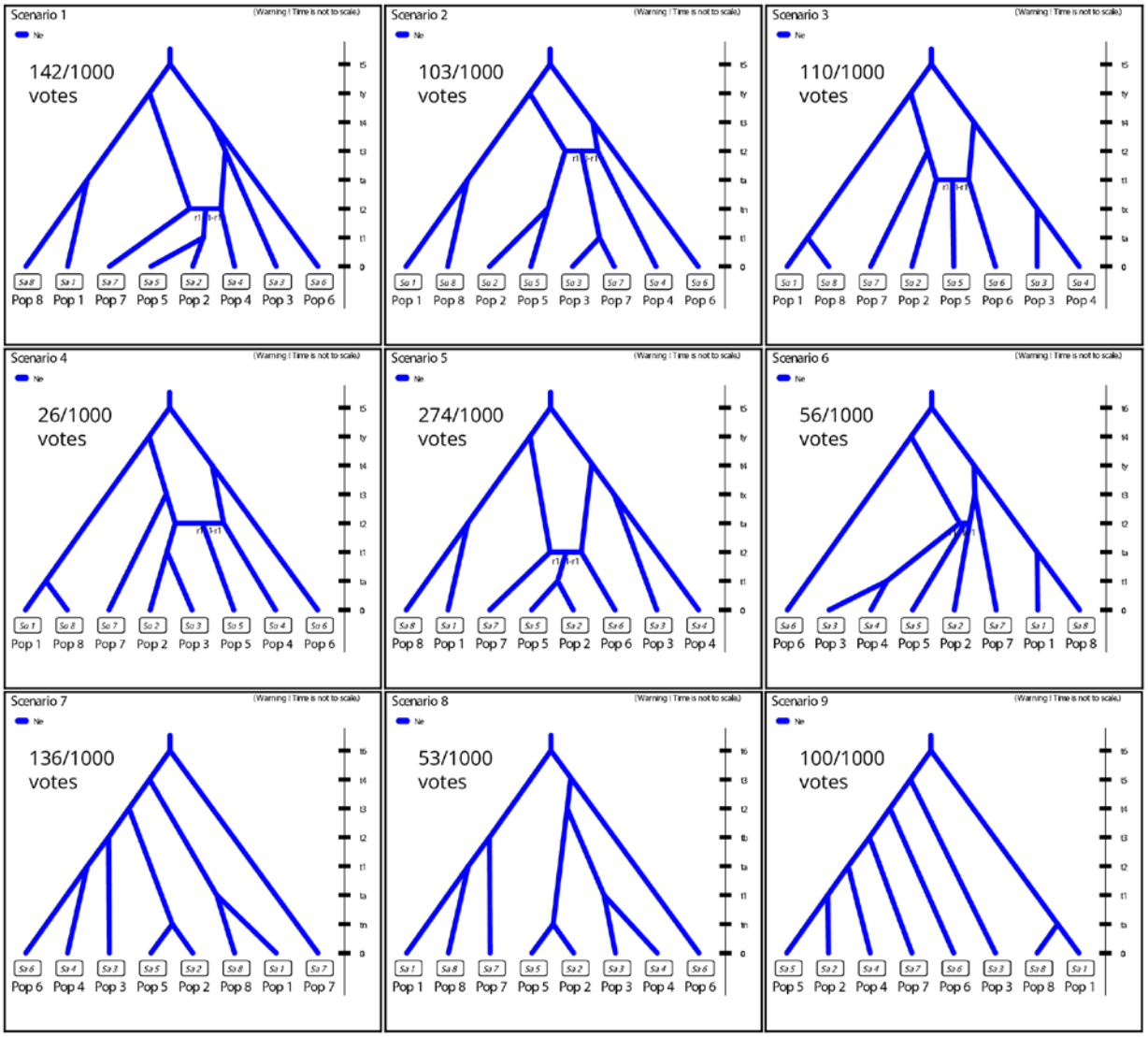

Figure B3. Scenarios used in second round of DIYABC analysis. A total of 36,000 datasets were simulated using uniform priors for population sizes (10-10,000 individuals), time parameters (10-100,000 years), and admixture rate (0.1-0.99). Random forest search was performed with 1000 trees. The number of votes for each scenario is noted. Scenario 5 was selected with a posterior probability of 0.916. Populations are numbered as follows: Pop 1 = AK/YT; Pop 2 = WNA; Pop 3 = NT/NU; Pop 4 = UGV; Pop 5 = ATL; Pop 6 = ENA; Pop 7 = EUR; Pop 8 = KOR.